MARTIN MARIETTA ENERGY SYSTEMS LIBRARIES

3 4456 0279976 4

ORNL/TM-10637

ornl

OAK RIDGE
NATIONAL
LABORATORY

MARTIN MARIETTA

A Review of Thermolysis Studies of Model Compounds Relevant to Processing of Coal

Marvin L. Poutsma

OAK RIDGE NATIONAL LABORATORY
CENTRAL RESEARCH LIBRARY
CIRCULATION SECTION
4500N ROOM 175
LIBRARY LOAN COPY
DO NOT TRANSFER TO ANOTHER PERSON
If you wish someone else to see this report, send in name with report and the library will arrange a loan.
ORNL-11a (6-97)

OPERATED BY
MARTIN MARIETTA ENERGY SYSTEMS, INC
FOR THE UNITED STATES
DEPARTMENT OF ENERGY

Printed in the United States of America. Available from
National Technical Information Service
U.S. Department of Commerce
5285 Port Royal Road, Springfield, Virginia 22161
NTIS price codes—Printed Copy: A11; Microfiche A01

This report was prepared as an account of work sponsored by an agency of the United States Government. Neither the United States Government nor any agency thereof, nor any of their employees, makes any warranty, express or implied, or assumes any legal liability or responsibility for the accuracy, completeness, or usefulness of any information, apparatus, product, or process disclosed, or represents that its use would not infringe privately owned rights. Reference herein to any specific commercial product, process, or service by trade name, trademark, manufacturer, or otherwise, does not necessarily constitute or imply its endorsement, recommendation, or favoring by the United States Government or any agency thereof. The views and opinions of authors expressed herein do not necessarily state or reflect those of the United States Government or any agency thereof.

ORNL/TM-10637

Chemistry Division

A REVIEW OF THERMOLYSIS STUDIES OF MODEL COMPOUNDS RELEVANT TO PROCESSING OF COAL

Marvin L. Poutsma

Date of Issue: November 1987

OAK RIDGE NATIONAL LABORATORY
Oak Ridge, Tennessee 37831
operated by
MARTIN MARIETTA ENERGY SYSTEMS, INC.
for the
U. S. DEPARTMENT OF ENERGY
under contract DE-AC05-84OR21400

MARTIN MARIETTA ENERGY SYSTEMS LIBRARIES

3 4456 0279976 4

TABLE OF CONTENTS

ABSTRACT..... 1
1. INTRODUCTION..... 2
1.1 STRUCTURE AND PROCESSING OF COAL..... 2
1.1.1 Structure of Coal..... 2
1.1.2 Thermal Behavior of Coal..... 3
1.1.3 Coal Conversion Processes..... 4
1.1.4 The Free-Radical Hypothesis..... 5
1.1.5 The Role of Model Compound Studies..... 6
1.2 SCOPE OF REVIEW..... 7
1.3 EXPERIMENTAL TECHNIQUES..... 8
1.4 SOME ELEMENTARY FREE-RADICAL STEPS..... 10
1.4.1 Bond Breaking..... 11
1.4.2 Bond Making..... 12
1.4.3 Hydrogen Transfer..... 12
1.4.4 Rearrangement..... 14
1.4.5 Chain Reactions..... 14
1.5 THERMOCHEMICAL KINETIC CONSIDERATIONS..... 15
2. ALKANES..... 17
2.1 THERMODYNAMICS..... 18
2.2 ETHANE..... 19
2.3 n-HEXANE..... 22
2.4 LARGER ALKANES..... 29
2.5 MOLECULAR DISPROPORTIONATION..... 30
3. AROMATIC HYDROCARBONS..... 31
3.1 BENZENE..... 32
3.2 POLYCYCLIC AROMATICS..... 36
4. ALKYLAROMATIC HYDROCARBONS..... 40
4.1 TOLUENE..... 40
4.1.1 Thermolysis..... 40
4.1.2 Added Hydrogen..... 49
4.2 OTHER METHYLATED AROMATICS..... 53
4.3 ETHYLBENZENE..... 54
4.4 LARGER ALKYLAROMATICS..... 61

5. TWO-ATOM LINKAGES 63
5.1 BIBENZYL 63
5.1.1 Gas-Phase Low-Temperature Regime 65
5.1.2 Gas-Phase High-Temperature Regime 70
5.1.3 Liquid-Phase Low-Temperature Regime 77
5.1.4 Added Hydrogen 85
5.2 OTHER 1,2-DIARYLETHANES 87
5.3 POLYPHENYLETHANES 90
5.4 METHYLATED BIBENZYLS 94
5.5 HETERO ATOM-CONTAINING TWO-ATOM LINKAGES 94
5.6 RELATIVE REACTIVITIES IN HYDROGEN ABSTRACTION BY BENZYL RADICAL 103
6. BIARYLS (ZERO-ATOM LINKAGES) 107
7. ONE-ATOM LINKAGES 110
7.1 DIPHENYLMETHANE 110
7.2 HETERO ATOM-CONTAINING ONE-ATOM LINKAGES 115
8. THREE-ATOM LINKAGES 118
8.1 1,3-DIPHENYLPROPANE 118
8.2 HETERO ATOM-CONTAINING THREE-ATOM LINKAGES 126
9. FOUR-ATOM LINKAGES 130
10. HYDROAROMATIC HYDROCARBONS 133
10.1 TETRALIN 133
10.1.1 Liquid-Phase Regime 133
10.1.2 Gas-Phase Regime 135
10.1.3 Added Hydrogen 139
10.1.4 Added Bibenzyl 140
10.1.5 Thermodynamics 141
10.1.6 Mechanisms 144
10.2 DIHYDRONAPHTHALENES 152
10.3 OTHER SIX-MEMBERED-RING HYDROAROMATICS 157
10.4 INDANE 158
10.5 BENZOCYCLOBUTENE AND DIMERS 160
10.6 HYDROGEN TRANSFER BETWEEN HYDROAROMATICS AND AROMATICS. 161
11. PHENOLS AND AROMATIC ETHERS 166
11.1 PHENOL 166

11.2 NAPHTHOLS..... 170
11.3 POLYHYDROXYAROMATICS..... 176
11.4 HOMOLYSIS OF KETONIC TAUTOMERS..... 180
11.5 CRESOLS AND ETHYLPHENOLS..... 181
11.6 ARYL ALKYL ETHERS..... 187
11.7 HYDROXY- AND METHOXYANISOLES..... 192
12. CARBONYL COMPOUNDS..... 197
12.1 DIARYL KETONES..... 197
12.2 ARYL ALKYL KETONES..... 198
12.3 BENZELDEHYDE..... 199
12.4 BENZYLIC ALCOHOLS..... 200
13. EFFECTS OF HYDROGEN SULFIDE..... 201
14. REFERENCES..... 204
15. FIGURE CAPTIONS AND FIGURES..... 219

A REVIEW OF THERMOLYSIS STUDIES OF MODEL COMPOUNDS RELEVANT TO PROCESSING OF COAL

Marvin L. Poutsma

ABSTRACT

The bond breaking, bond making, rearrangement, and hydrogen transfer reactions that occur in coal at ~350-1000°C largely involve transient free radicals as reactive intermediates. However, the structural complexity and heterogeneity of coal has hampered development of detailed reaction mechanisms at the molecular level. Studies of the thermolysis and hydrogenolysis of model compounds, chosen to represent individual structural units in coal, provide very useful input toward that goal. These are selectively and critically reviewed in this report.

Emphasis is placed on recent quantitative studies of product composition and kinetic behavior that have been carried out at low extents of conversion. The classes of organic structures covered are alkanes; aromatic hydrocarbons; alkylaromatics; α,ω-diphenylalkanes, $Ph(CH_2)_nPh$ (n = 0 - 4), and their analogs with a CH_2 group replaced by O, S, or NH; hydroaromatics; phenols, alkylphenols, and aryl ethers; and carbonyl compounds. Thermal behavior of pure model compounds is reviewed along with its perturbation by added hydroaromatics or molecular hydrogen. Structure-reactivity patterns within each class are illustrated whenever possible. Coverage is divided arbitrarily into a "low-temperature regime," ~300-450°C, which is dominated by studies in the liquid or dense supercritical state, and a "high-temperature regime," ~600-900°C, which is dominated by gas-phase studies.

Extensive use is made of the methodology of thermochemical kinetics. Several discrepancies between literature data or suggested mechanisms and predictions based on currently accepted thermochemistry of free radicals and kinetic expressions for prototypical elementary free radical reactions are pointed out. Inversely, certain mechanistic hypotheses offered herein require experimental evaluation.

1. INTRODUCTION

Coal provides a vast energy and materials resource. Burning of coal is a major contributor to electricity generation, and coke production is an integral part of the metallurgical industry. However, combustion of coal contributes to atmospheric pollution, and solid coal is obviously inconvenient for use as a transportation and residential heating fuel. Therefore, a large number of processes have been designed, developed, and, to varying extents, used over the last century to convert solid coal to higher valued, less polluting liquids and gases. Although these processes differ in design, all depend on the major chemical changes that occur when coal is heated above 350-400°C. The reactive intermediates responsible for most of the thermally induced reactions of coal are free radicals. Achieving detailed mechanistic descriptions of these reactions at the molecular level is severely hampered by the complex structure and heterogeneity of coal. Therefore the study of thermolysis of individual compounds that serve as models for key structural features in coal has proven to be a very useful research tool to improve understanding of the mechanisms of coal conversion. The purpose of this review is to outline recent research in this area.

1.1 STRUCTURE AND PROCESSING OF COAL

1.1.1 Structure of Coal[1,2,3a]

The dominant portion of coal consists of a cross-linked organic macromolecular network that is therefore nonvolatile and insoluble. Any process to convert coal to gaseous and liquid products must involve breaking of covalent bonds to disrupt this cross-linked backbone structure.

Coal is structurally extremely heterogeneous. Although macromolecular, it has no regularly repeating "monomer" units. Rather, its structure must be described statistically in terms of distributions of types of structural units and their modes of linkage. Structural considerations are further complicated by wide variations not only from one coal seam to another but also within a seam and even from one maceral to another within a given sample. In addition, inorganic mineral matter is

dispersed throughout the organic matrix and may play a catalytic role in coal processing.

The major building blocks in the network structure are polycyclic aromatic rings, their analogs containing O, S, and N heteroatoms, and partially hydrogenated derivatives of each. The aromatic rings are typically substituted with alkyl sidechains and phenolic hydroxyl groups. These aromatic building blocks are joined together into a three-dimensional network by short aliphatic linkages, some of which may themselves contain heteroatoms, especially oxygen. Although oversimplified, this brief picture of coal structure is sufficient to indicate the major types of model compounds that have been of interest for thermolysis studies.

1.1.2 Thermal Behavior of Coal[3b,3c,4,5]

Gradually increasing the temperature of coal leads first to loss of physisorbed materials held in the pore structure, largely water. Then at 350-400°C, chemical breakdown of the cross-linked structure begins. Fragments are formed which are of low enough molecular weight to be volatile at this temperature. These include water, carbon oxides, light hydrocarbon gases, and a condensable fraction known as "coal tar." By 500-550°C, evolution of tar is largely complete, although small amounts of lighter gases (especially hydrogen, methane, carbon monoxide, and water) continue to form up to at least 1000°C. The total weight loss to form volatiles under a controlled set of conditions, excluding the physisorbed water, is termed "volatile matter" in the proximate analysis of coals. It can range from virtually zero for anthracites to >50% for subbituminous coals and lignites and is a common indicator of coal rank. However, it is important to remember that this "volatile matter" is not present as such in the native coals but results from thermally induced bond-breaking reactions. Coal tar is an extremely complex mixture consisting typically of aromatic hydrocarbons and O- and N-heterocycles substituted with alkyl, especially methyl, and hydroxyl groups. Ring sizes range from benzene to 4- and 5-ring polycyclic aromatics and beyond. Tar from low-rank coals also contains complex aliphatic materials. To a zeroth-order approximation, the composition of tar reflects

the structure of the building blocks in coal itself, which are carved out of the network by breaking cross-links.

As volatiles are being released, major chemical changes occur simultaneously in the remaining solid until, at ~1000°C, a carbonaceous char or coke remains that is more highly cross-linked, more aromatic, and more refractory than the starting coal. For certain "caking" bituminous coals, the nonvolatile fraction goes through a "plastic" state in the 350-500°C range that is much more fluid than the original coal. The reduced viscosity allows achievement of the mutual orientation of aromatic rings that, after resolidification, results in the distinct anisotropic properties and mechanical strength of coke, as opposed to friable chars. The progression from coal to the plastic state to coke involves bond-making reactions which occur simultaneously with and subsequent to the bond-breaking reactions which are signaled by the evolution of volatiles.

The volatile fraction is typically more hydrogen-rich and the solid residue more hydrogen-poor than the native coal. In addition, if molecular hydrogen or a partially hydrogenated liquid coal product stream is supplied during heating, net incorporation of hydrogen into the coal products occurs. Thus hydrogen redistribution reactions are also a significant feature of the thermal chemistry of coal.

1.1.3 Coal Conversion Processes

The thermal reactivity of coal forms the basis of a variety of pyrolysis processes aimed at producing char as a solid fuel, coke for the metallurgical industry, coal tar as source of liquid fuels and organic chemical feedstocks, and gas for fuel and lighting. These can be subdivided into "low temperature pyrolysis" characterized by final temperatures of ~700°C, "high temperature pyrolysis" or "coking" characterized by final temperatures approaching 1000°C, and "flash pyrolysis" characterized by very rapid heating rates. Enumerating these further[3b,3d-h,4,5] is beyond our scope except to note that variations in process conditions take advantage of the fact that the yields and composition of the tar and the solid residue depend on the coal type and particle size, the time-temperature profile, the final temperature, the

pressure, and the configuration of the pyrolysis reactor. For example, the composition of the tar depends not only on the initial cleavage of fragments from the coal network but also on secondary reactions of these fragments as they pass through the heated bed of decomposing coal.

Hydropyrolysis processes[3b,5] take advantage of the fact that molecular hydrogen becomes chemically involved during thermal reactions of coal. Net hydrogen incorporation occurs as bonds break, and formation of new bonds is inhibited. As a result, yields of gas and tar are increased relative to the solid residue.

Liquefaction processes[3i,3j,6] are aimed at maximizing the yield of liquids that can serve as petroleum substitutes. A slurry of coal in a "solvent" is heated under hydrogen pressure at temperatures limited to ~450°C. This solvent is typically a partially hydrogenated fraction of the liquefied coal product which is then recycled and mixed with the feed coal. It plays an active chemical role ("hydrogen donor") by serving as a net source of hydrogen that is incorporated into the degrading coal and inhibits the bond formation ("retrograde reactions") that is characteristic of residue formation.

When the processing goal is liquid or gaseous synthetic fuels, the generally desirable chemical reactions are bond breaking to reduce molecular size, addition of hydrogen to increase the H : C ratio, and removal of hetero atoms; the undesirable reactions are bond formation (increase in molecular size) and aromatization (loss of hydrogen). Yet when the processing goal is coke or char, the general desirability of these chemical reactions is reversed. Knowledge concerning how each reaction depends on coal structure and may be manipulated by process conditions is thus clearly valuable.

Although the role of the thermal sensitivity of coal is less apparent in gasification[3k,3l] and combustion[3m,3n] processes, even here the initial degradation reactions of the coal, before reaction with oxygen and/or water begins, are largely thermal.

1.1.4 The Free-Radical Hypothesis

The most useful mechanistic framework in which to consider the thermal reactivity of coal and the processes based on it has been the

free-radical hypothesis.[7-9] In simplest terms, thermal activation causes breaking of covalent bonds in the network structure and generation of reactive, transient free radicals. These may then be "capped" by abstracting hydrogen. Given the breaking of enough bonds, stable fragments will be formed that have molecular weights low enough to be volatile and/or soluble. In pyrolysis, the source of hydrogen must be the coal itself; in hydropyrolysis, it may be hydrogen; and in liquefaction, it is largely the partially hydrogenated "donor solvent." On the other hand, if an appropriately reactive source of hydrogen is not immediately available, the reactive radicals undergo "condensation" reactions with themselves or other parts of the coal structure to form new bonds that are thermally more stable than those originally broken. The result is formation of char and coke.

1.1.5 The Role of Model Compound Studies

Because of the structural complexity of coal, understanding its thermal free-radical chemistry at the molecular level is a formidable challenge. One approach toward this goal is the study of thermolysis of model compounds of modest molecular size chosen to represent individual structural features of coal. The arsenal of tools of physical organic chemistry does allow detailed mechanistic description at this level of molecular complexity. A broad base of mechanistic understanding at the model compound level should then allow systematic extrapolation to the much more complex behavior of coal itself. It must be noted, of course, that such extrapolation is itself difficult because of the need to account for structure-reactivity relationships for each structural feature, interactions among individual structural features when present simultaneously, effects of restricted molecular mobility and diffusion in semi-solid decomposing coal, and effects of catalysis by mineral matter. Yet having definitive model compound data is the first prerequisite.

One of the earliest model compound studies targeted to coal conversion was reported in the 1950s by Depp, Stevens, and Neuworth,[10] who prepared the series of compounds **1** and **2** and determined the volatile products formed when they were heated slowly to 425°C in an open retort. Bond cleavage in the aliphatic linking groups was observed, and the

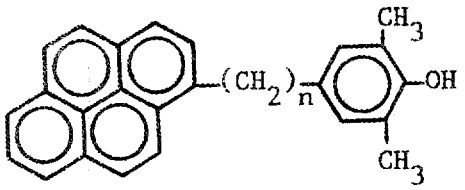

1

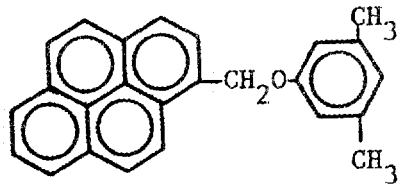

2

intermediacy of free radicals was correctly assigned. In the 1960s, Kölling's group[11] introduced the use of a second component to model the hydrogen donor solvent in liquefaction, specifically 1,2,3,4-tetrahydroquinoline. A number of more recent survey studies have been very important in establishing patterns of thermal reactivity and identifying candidates for subsequent more detailed mechanistic studies. Benjamin and coworkers[12] classified the thermal sensitivity at 400°C of over 50 model compounds as solutions in tetralin as a model hydrogen donor solvent. Complementary results were provided by the groups of Cronauer,[13] Kamiya,[14] and Whitehurst.[15]

The most comprehensive conceptual framework for experimental and thermochemical kinetic considerations of elementary free-radical reactions with probable relevance to coal conversion has been provided by Stein.[16,17] Gavalas[5] has also reviewed certain model compound studies with particular relevance to modeling coal pyrolysis.

1.2 SCOPE OF REVIEW

The recent growth in studies of model compounds for coal followed the resurgence of interest in coal-based synthetic fuels after the "energy crisis" of the early 1970s. Much new information has become available, especially in the first half of the 1980s. The purpose of this review is to summarize and evaluate recent studies of the thermolysis and hydrogenolysis of model compounds for coal, with particular emphasis on studies which have a quantitative mechanistic focus.

We first review briefly in Section 2 the thermal cracking of alkanes, which illustrates many of the key elementary radical steps involved in bond breaking and hydrogen transfer. We then review in Section 3 the thermolysis of unsubstituted aromatic hydrocarbons for

which the characteristic reaction is bond making to form biaryls. The thermal behavior of alkylaromatics covered in Section 4 introduces the important hydrodealkylation reaction. The locus of disruption of the network structure of coal is largely the aliphatic linkages between aromatic clusters, and therefore we give special attention to α,ω-diphenylalkanes, $Ph(CH_2)_nPh$, with n = 2 (Section 5), 0 (Section 6), 1 (Section 7), 3 (Section 8), and 4 (Section 9). In each case, the thermal behavior of the corresponding ethers, sulfides, and amines is also considered. Hydroaromatic structures, which are indigenous to coal and also play a key role as hydrogen donors in liquefaction processes, are covered in Section 10. The thermal reactivity afforded to aromatics by hydroxy and alkoxy substituents is reviewed in Section 11. Another class of O-containing structures, carbonyl compounds, is covered in Section 12.

For each class of model compound, we consider not only the thermal behavior of the pure substrates, but also the perturbations caused by model hydrogen donor solvents, especially tetralin, and by molecular hydrogen. Coal processing under reducing conditions generates hydrogen sulfide, both from hydrodesulfurization of organosulfur structures and from hydrogenation of pyrite mineral matter to pyrrhotite ($FeS_2 + H_2 \longrightarrow FeS + H_2S$). Modifying effects of hydrogen sulfide on thermolyses are reviewed briefly in Section 13.

Recent model compound studies have emphasized the temperature range of ~350-500°C, which is most relevant to liquefaction and the early stages of pyrolysis; we arbitrarily call this the "low-temperature regime." Studies at ~700-900°C are more relevant to interpreting the later stages of char formation, secondary reactions in tar generation, and flash pyrolysis; we call this the "high-temperature regime."

1.3 EXPERIMENTAL TECHNIQUES

Even the low-temperature regime exceeds the boiling points of most model compounds. Therefore, the most common apparatus in which to study the kinetics and product distributions of thermolysis of these materials as liquids has been metal autoclaves or sealed metal tubes used to contain the elevated vapor pressures involved. Enough substrate is

charged to occupy much of the available volume as liquid. Such static studies are limited to reaction times of at least several minutes by relatively slow heatup and cooldown, and kinetic studies often suffer from difficulties in assigning the time variable properly. With typically massive autoclaves, this problem is exacerbated, and there is a constant threat of catalysis by metal surfaces. It is therefore preferable to use small glass or quartz tubes which have the added advantage of allowing rigorous deoxygenation before sealing. Containing high vapor-pressure substrates can be accomplished by placing the sealed glass tube inside a sealed metal tube that contains some of the same substrate to balance the pressure differential across the fragile glass.

Static thermolysis of the same substrates as gases can be simply achieved by limiting the amount charged to the sealed tube. Static reactors connected to a pressure sensor are commonly used in gas-phase kinetic studies. Gas-phase studies are also commonly performed in flow reactors for which residence times are typically seconds rather than minutes or hours. Dilution with an inert carrier gas is a common means of introducing the substrate at a slow controlled rate. Care must be taken in kinetic studies to establish a constant temperature profile along the length of a flow reactor.

We will also encounter in the high-temperature regime several examples of two less traditional techniques. For Flash Vacuum Pyrolysis (FVP),[18] a substrate reservoir, an open heated tube, a cryogenic trap for collecting products, and a pumping source are placed in series. The temperature of the reservoir and the pumping speed are balanced to allow steady vaporization and passage of the substrate through the reactor tube at very low pressures; typically $\lesssim 1$ Pa. The combination of very short residence time and very few gas-phase collisions (long mean free path) with rapid downstream quenching has proven ideal for isolating initial thermolysis products which are themselves thermally labile. On the other hand, the FVP technique is not useful for kinetic studies because the time-temperature profile is ill-defined.

A modified high-temperature—low-pressure approach tailored to kinetic studies of unimolecular reactions is Very Low Pressure Pyrolysis (VLPP).[19] A heated flow cell is operated in the Knudsen diffusion regime

with an effusion orifice directed into the ionization source of a mass spectrometer. Initial decomposition products, even reactive radicals, survive because of the infrequency of gas-phase collisions and can be detected directly to derive rate constants. However, under these low-pressure conditions, unimolecular reactions are typically in the fall-off region, and rate constants are normally corrected to the high-pressure limit by applying an RRKM model to the data. Thus VLPP kinetic data at varying temperatures do not give an independent measure of both Arrhenius parameters A and E because assumptions about one or the other must be introduced into the modeling. Because coal conversion reactions typically occur under "concentrated" conditions, we will not explicitly discuss any of the fall-off data for unimolecular reactions of the model compounds considered.

The dominating experimental complication in the thermal chemistry under review is the tendency for initial products to be as reactive as the substrate or even more so. Hence, product distributions at even modest conversion levels are often seriously distorted by secondary reactions. Determining inherent product distributions then requires extrapolation of data on product analyses vs. reaction time back to zero time. The resulting demands on analytical sensitivity for minor products from reactions limited to very low conversions are often severe. Similarly, kinetics can be seriously perturbed if initial products interact with the substrate. Initial rates must then be derived from the initial slopes of product-vs.-time curves. This situation precludes determination of the kinetic order from the application of standard integrated rate forms to runs at a single concentration (or pressure) carried to several half-lives. Instead, runs must be made at widely differing initial concentrations and the kinetic order obtained from the slope of log-log plots of initial rate vs. concentration.

1.4 SOME ELEMENTARY FREE-RADICAL STEPS

The major types of thermal reactions to be modeled are bond breaking, bond making, hydrogen transfer, and skeletal rearrangement. Because free radical mechanisms dominate, we will briefly categorize some important elementary radical steps and establish some nomenclature by use

of structurally simple examples.

1.4.1 Bond Breaking

Breaking a covalent bond to form two radicals is termed "homolysis" and is characterized by a bond dissociation energy, D^o, defined as ΔH^o_{298}. Since the reverse reaction, radical-radical "combination" does not have an intrinsic potential energy barrier in the absence of major steric effects, D^o is a good approximation to E, the experimentally observed Arrhenius activation energy for homolysis (see Section 2.2 for a more detailed treatment). For the example in step 1, $E_1 \sim D^o(CH_3\text{-}CH_2CH_3) = 86$ kcal mol^{-1}.[20] The dependence of D^o on chemical structure will be an important aspect of our discussions.

$$CH_3CH_2CH_3 \longrightarrow CH_3\cdot + \cdot CH_2CH_3 \qquad E_1 \sim 86 \text{ kcal mol}^{-1} \qquad (1)$$

$$CH_3CH_2CH_2\cdot \longrightarrow CH_3\cdot + CH_2{=}CH_2 \qquad E_2 \sim 30 \text{ kcal mol}^{-1} \qquad (2)$$

It will be useful to have a guide for predicting the temperature range where reactivity can be expected if homolysis of the weakest bond in a compound is rate-controlling. If we use the approximation $E \sim D^o$, take $A \sim 10^{16}$ s^{-1}, as is typical for bond homolysis, and define "significant reactivity" as having a half-life of 1 h, then the following list can be compiled:

D^o (kcal mol^{-1})	Temperature (°C) for $t_{1/2} \sim 1$ h
50	281
60	392
70	503
80	614
90	725
100	836

A second important bond-breaking step is "β-scission" of a bond once removed from an existing radical center. This bond is considerably

weakened by the driving force provided by concurrent formation of a multiple bond. For the example in step 2, E_2 ~ 30 kcal mol^{-1},[21] only 35% of that for breaking of the analogous bond in step 1.

1.4.2 Bond Making

Radical-radical "combination," e.g., step -1, is, of course, a bond-making step. A second important member of this category is radical "addition" which is simply the microscopic reverse of "β-scission," e.g., step -2.

A common radical process is the formation of a new bond coupled with breaking an existing bond to an aromatic carbon. Although we will sometimes for simplicity depict such an ipso "aromatic displacement" reaction as a single event, it actually occurs in two steps: addition to form an alkylcyclohexadienyl radical intermediate (3) followed by its β-scission in the opposite sense or disproportionation with another radical.[22,23,24a] Step 3 is a typical example.

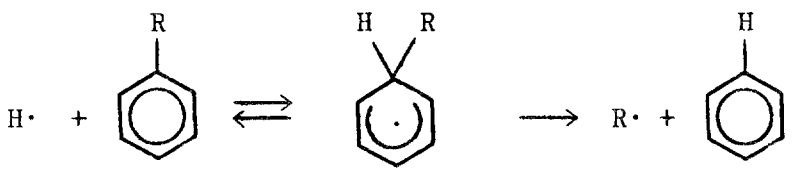

(3)

3

1.4.3 Hydrogen Transfer

Some of the hydrogen redistribution events we will encounter proceed through hydrogen atom as a discrete intermediate. More commonly however, hydrogen atom is transferred without becoming free. Considering that the donor and the acceptor of that hydrogen can each be either a spin-paired molecule or a radical, we can define four categories.

Transfer from a molecular donor to a radical acceptor constitutes the very familiar "hydrogen abstraction" step. The activation energy required is only a small fraction of D^o of the C-H bond being broken. For example, in step 4, E_4 ~ 12 kcal mol^{-1} [24b] whereas $D^o(H\text{-}C_2H_5)$ = 98 kcal mol^{-1}.[20]

$$CH_3\cdot + H\text{-}CH_2CH_3 \longrightarrow CH_3\text{-}H + \cdot CH_2CH_3 \qquad (4)$$

$$CH_3\cdot + H\text{-}CH_2CH_2\cdot \longrightarrow CH_3\text{-}H + CH_2{=}CH_2 \qquad (5)$$

A second familiar category is radical-radical "disproportionation" in which both the donor and acceptor are radicals, e.g., step 5. It is in a sense also a hydrogen abstraction but one with negligible activation energy. Except for tert-alkyl radicals, combination : disproportionation ratios exceed unity.[24b]

The remaining two categories are less familiar, and some of the specific examples to be discussed below have helped to establish them as significant elementary steps. If the donor is the β-hydrogen in a radical and the acceptor is an unsaturated molecule, there always exists a two-step possibility for hydrogen transfer: unimolecular β-scission of the radical to generate free hydrogen atom followed by its addition to the acceptor. However, there is growing evidence,[25] especially for cases involving highly stabilized cyclohexadienyl radicals, for the one-step bimolecular alternative illustrated by steps 6a and 6b. McMillen[26] has called this step "radical hydrogen transfer."

$$\cdot CH_2CH_2\text{-}H + CH_2{=}CHR \longrightarrow CH_2{=}CH_2 + H\text{-}CH_2\dot{C}HR \qquad (6a)$$

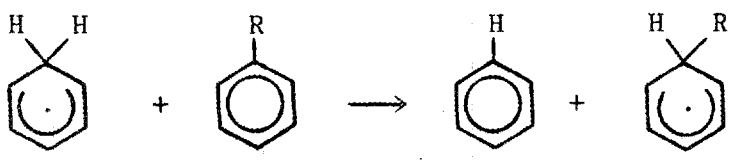

(6b)

Finally, there is the category in which both donor and acceptor are molecules, and hydrogen transfer generates a pair of radicals. In fact, it is simply the microscopic reverse of radical-radical disproportionation, e.g., step -5, and has been called "molecular disproportionation" by Stein.[16,27] Although this elementary process has only recently received much attention,[28] we will illustrate in Section 2.5 how its rate constant can be estimated quite accurately in simple cases.

1.4.4 Rearrangement[24c]

A large activation barrier is associated with 1,2-shifts of hydrogen or alkyl groups in radicals, and this potential mode of rearrangement is rarely observed. In contrast, 1,2-shifts of aryl groups, which proceed through spirocyclohexadienyl radical intermediates (**4**) as in step 7, are common. Another kinetically facile rearrangement pathway is a 1,5-shift

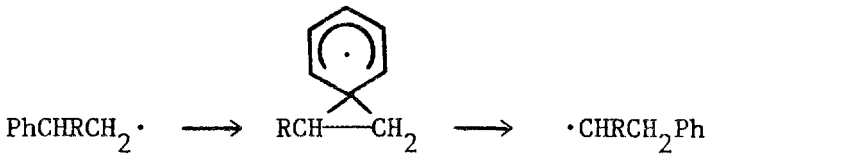

(7)

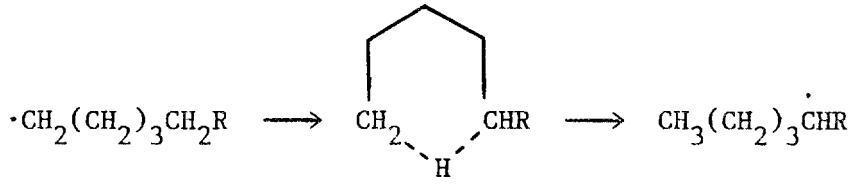

(8)

of hydrogen as in step 8; this is just an intramolecular hydrogen abstraction in which strain is minimized at the six-membered-ring transition state.

1.4.5 Chain Reactions

Elementary radical steps can be categorized as "initiating," "terminating," or "propagating," respectively, dependent on whether they achieve net production of radicals, net destruction of radicals, or conversion of one radical into another. If the sum of two or more propagating steps forms a cycle in which each of the radicals involved is produced and consumed in equal amounts, then a repeating chain can occur. The chain length is the number of propagating cycles that occurs for each radical formed in an initiating step (or, equivalently, destroyed in a terminating step). Homolysis and molecular disproportionation are initiating steps in the present context. Radical-radical combination and disproportionation are terminating steps. Hydrogen abstraction, radical hydrogen transfer, β-scission, addition, aromatic displacement, and intramolecular rearrangement are propagating steps.

For an individual model compound to react by a chain mechanism, it must be involved in both an initiation step and at least one propagation step, and radicals derived from it will control termination. However, for mixtures of compounds, these functions may be uncoupled. For example, a minor amount of an additive which contains a relatively weak bond may serve as an "initiator" for reactions of a major component by forming radicals by homolysis. Conversely, an additive which can be converted, often by hydrogen abstraction, to a relatively stable radical may function as an inhibitor because propagation rates are generally retarded much more by increasing radical stability than are termination rates. Remaining aware of the separable roles of various functional groups as stoichiometric reactants, initiators, and inhibitors when chain reactions are involved is critical for a polyfunctional material such as coal.

1.5 THERMOCHEMICAL KINETIC CONSIDERATIONS

Gas-phase radical reactions are particularly amenable to application of principles of thermochemical kinetics as outlined by Benson.[29] A principle that we will use frequently is that the Arrhenius parameters which describe the kinetics of any elementary step and those of its reverse are constrained by the overall thermochemistry by the well-known relationships:

$$\Delta H^{o}_{reaction} = E_{forward} - E_{reverse}$$

$$\Delta S^{o}_{reaction} = R\ln(A_{forward}/A_{reverse})$$

[Note the need for consistency in units for S and A for reactions other than first-order because thermochemical quantities for organics are usually tabulated for a standard state of 1 atm whereas rate constants are usually expressed in concentration units.] Therefore, knowing any two of the quantities in either equation allows calculation of the third. In another common situation, all three may be "known" from differing

sources and experimental methodologies, but application of these equations will show an inconsistency such that at least one must be in serious error.

The thermochemical quantities $\Delta H^o_{reaction}$ and $\Delta S^o_{reaction}$ are related to standard heats of formation and standard entropies by the relationships:

$$\Delta H^o_{reaction} = \Sigma\ \Delta H_f{}^o(\text{products}) - \Sigma\ \Delta H_f{}^o(\text{reactants})$$

$$\Delta S^o_{reaction} = \Sigma\ S^o(\text{products}) - \Sigma\ S^o(\text{reactants})$$

For most of the molecular reactants and products we will encounter, these parameters have been experimentally determined[30,31] or can be estimated with acceptable accuracy by group additivity methods.[29] Heats of formation of transient radicals are much more difficult to measure, but a growing data base does exist[20] and again can be extended to unknown cases by group additivity methods.[29] Standard entropies of radicals can often be estimated by statistical thermodynamic methods[29] with better accuracy than they can be measured; the major problem is assigning proper barriers to hindered internal rotations.

Since we will be considering reactions at temperatures much higher than 298 K, to be rigorous we must consider the temperature effects on thermochemical quantities:

$$\Delta H^o_T = \Delta H^o_{298} + \langle \Delta C_p{}^o \rangle (T - 298)$$

$$\Delta S^o_T = \Delta S^o_{298} + \langle \Delta C_p{}^o \rangle \ln(T/298)$$

Fortunately, heat capacity ($C_p{}^o$) values for radicals can be also estimated from statistical thermodynamic considerations.[29] Secondly, Arrhenius E and A parameters are, of course, not strictly temperature-independent and are therefore strictly valid only for the experimental temperature range used. In practice, these temperature effects typically introduce small uncertainties of a magnitude no greater than those in

much of the thermochemical data base. Therefore, we will often not consider them explicitly when our purpose is only to examine for "order-of-magnitude" consistency.

Finally, if we can estimate thermochemical parameters for transition states, then we can predict values of Arrhenius parameters by the relationships:

$$E = \Delta H^{\neq} + RT$$

$$A = (ekT/h)\exp(\Delta S^{\neq}/R)$$

This approach is especially useful for the A factor because entropies of transition state models can be estimated with useful accuracy or derived from analogous cases.[29]

We will consider reactions in the liquid as well as in the gas phase. We make the approximation that gas-phase rate constants and equilibrium constants for reactions involving carbon-centered radicals are transferable to reactions in relatively nonpolar hydrocarbon solvents.[32] Current molecular dynamics simulations of bimolecular atom transfer reactions suggest circumstances in dense solvents where $k_{solution}/k_{gas}$ may deviate significantly from unity.[33] Nevertheless, in the present circumstances, the transference of kinetic and thermodynamic data seems to be amply justified empirically. However, for radicals centered on hetero atoms, especially in hydrogen bonding solvents where specific complexation may occur, this is likely a poorer approximation.

2. ALKANES

Cracking of alkanes to form mixtures of smaller alkenes and alkanes serves as a useful vehicle to introduce several key elementary radical steps which we will encounter later in structurally more complex situations. In addition, certain coals contain nontrivial amounts of long-chain paraffinic material. The recognition by Rice[34-36] over 50 years ago that radical chains dominate thermal cracking represents one of the earliest triumphs of mechanistic organic chemistry. Considerable success has now been achieved in quantitative modeling of cracking to high

conversion by numerical integration of reaction networks containing literally hundreds of elementary radical steps to which rate constants in Arrhenius form have been assigned.[37-39,40a,40b] As conversion increases, the number of elementary steps which must be included increases steadily because primary products, especially alkenes, participate actively in secondary reactions. Thermolysis studies of alkanes also continue to provide fundamental kinetic and thermochemical information concerning alkyl radicals.

2.1 THERMODYNAMICS

Before considering mechanisms, we note an important generic thermodynamic feature of cracking reactions. Cracking of an alkane to an alkene and a smaller alkane is significantly endothermic. Hence, it becomes thermodynamically feasible only at temperatures high enough that the favorable entropy increase associated with converting one molecule to two or more dominates. To illustrate with one reaction channel (of several) for n-hexane (see Section 2.3), consider the thermochemical parameters at varying temperatures:[30]

$$\underline{n}\text{-}C_6H_{14} \longrightarrow C_3H_8 + C_3H_6$$

T (K)	ΔH^o (kcal mol^{-1})	ΔS^o (cal mol^{-1} K^{-1})	ΔG^o (kcal mol^{-1})	K (atm)
298	20.02	35.48	9.45	1.2×10^{-7}
600	19.42	34.14	-1.06	2.4
800	18.92	33.42	-7.82	1.4×10^{2}
1000	18.40	32.83	-14.43	1.4×10^{3}

Although ΔH^o and ΔS^o are each slightly temperature-dependent because $\Delta C_p^o \neq 0$, the dominant temperature effect arises from the role of T in the (ΔH - $T\Delta S$) term. At temperatures where $\Delta G^o \sim 0$, the situation can arise where alkenes formed by primary cracking are consumed in secondary reactions by addition to the alkane substrate to give products having more carbon atoms than the starting material. This was observed by Ford[41] during cracking of n-hexadecane at 350°C in the liquid phase where

reaction times of hours were required to achieve significant reaction. Although Zhou and Crynes[42] attributed the heavy products formed from n-dodecane at 350°C to radical coupling, the observation that these were formed only after an inhibition period gives more credence to a "re-addition" phenomenon in this example also.

2.2 ETHANE

We will use selected examples from the very large literature on thermolysis of alkanes to illustrate the important elementary steps in cracking. Gas-phase thermolysis of ethane at >500°C has been widely studied mechanistically[36,39] and is of major industrial importance as a source of ethylene feedstock. The major products are ethylene and hydrogen with lesser amounts of methane and n-butane. Although almost 50 elementary steps were included in a recent model[39] which is applicable to high conversions, six predominate at low conversion and illustrate the typical sequence of chain initiation by C-C homolysis, chain propagation by repetitive hydrogen abstraction and β-scission, and chain termination by coupling and disproportionation:

$$CH_3CH_3 \longrightarrow 2\ CH_3\cdot \tag{9}$$

$$CH_3\cdot + CH_3CH_3 \longrightarrow CH_4 + CH_3CH_2\cdot \tag{10}$$

$$CH_3CH_2\cdot \longrightarrow CH_2{=}CH_2 + H\cdot \tag{11}$$

$$H\cdot + CH_3CH_3 \longrightarrow H_2 + CH_3CH_2\cdot \tag{12}$$

$$2\ CH_3CH_2\cdot \longrightarrow CH_3CH_2CH_2CH_3 \tag{13}$$

$$2\ CH_3CH_2\cdot \longrightarrow CH_3CH_3 + CH_2{=}CH_2 \tag{14}$$

The initiating event is C-C homolysis in step 9. Since thermochemical parameters for methyl radical are available,[20,29] this reaction

serves as a paradigm for illustrating the relationships between kinetic and thermochemical data. Standard thermochemical data (Table 1) give:

$$\Delta H^{o}_{9,800} = \Delta H^{o}_{9,298} + \langle \Delta C_p{}^{o}{}_{9} \rangle (800 - 298) =$$

$$90.4 + 1.4 = 91.8 \text{ kcal mol}^{-1}$$

$$\Delta S^{o}_{9,800} = \Delta S^{o}_{9,298} + \langle \Delta C_p{}^{o}{}_{9} \rangle \ln(800/298) - \Delta nR\ln(800R') =$$

$$37.9 + 2.8 - 8.3 = 32.4 \text{ cal mol}^{-1} \text{ K}^{-1} \text{ (conc. units)}$$

Then taking methyl radical combination as an unactivated process with $k_{-9} = A_{-9} = 10^{10.3}$ $M^{-1}s^{-1}$,[40b,48] we can predict the Arrhenius parameters expected at 800 K, a temperature typical of existing kinetic data:

$$E_{9,800} = \Delta H^{o}_{9,800} - 800R/2 = 91.0 \text{ kcal mol}^{-1} \quad \text{(Reference 20)}$$

$$A_{9,800} = A_{-9}\exp(\Delta S^{o}_{9,800}/R) = 10^{17.4} \text{ s}^{-1}$$

Various experimental measurements[40b,48-50] give A values in the range $10^{16.3}$-$10^{16.9}$ s^{-1} and E values in the range 87.5-89.5 kcal mol^{-1}. This imperfect but very useful degree of correspondence is typical of the current status of thermochemical kinetics.

Methyl radicals formed in initiating step 9 abstract hydrogen from ethane in step 10 to form ethyl radical which enters the chain propagating cycle. Abstractions by methyl radical appear particularly prone to show non-Arrhenius behavior with expressions for k_{10} varying from $10^{8.5}\exp(-10{,}900/RT)$ $M^{-1}s^{-1}$ valid at <500 K to $10^{11.5}\exp(-20{,}900/RT)$ $M^{-1}s^{-1}$ valid at >1000 K.[40b]

In the first chain step, ethyl radical loses hydrogen atom by β-scission with $k_{11} = 10^{13.4}\exp(-38{,}400/RT)$ s^{-1}.[21] In the second, hydrogen atom regenerates ethyl radical by hydrogen abstraction from ethane with $k_{12} \sim 10^{11.3}\exp(-9{,}800/RT)$ $M^{-1}s^{-1}$.[39,40b]

Table 1. Thermochemical Parameters and Sources

Species	ΔH_f° (kcal mol^{-1})[a]	Ref.	S° (cal mol^{-1}K^{-1})[a]	Ref.	C_p° (cal mol^{-1}K^{-1})[b]	Ref.
H·	52.1	29	27.4	29	5.0 (300-1000)	29
H_2	0		31.2	30		
CH_3·	35.1	20	46.4	29	8.8 13.2 (800) 14.5 (1000)	29
C_2H_4	9.8 (800)	30	67.3 (800)	30		
C_2H_5·	25.9[c]	20				
C_2H_6	-20.2 -24.5 (800)	30	54.9 73.2 (800)	30	12.6 25.8 (800)	30
n-C_4H_{10}	-36.4 (800)	30	108.7 (800)	30		
C_6H_5·	78.6	20	69.4	29	18.8	29
$PhCH_2$·	47.8	20	75.3	29	25.4 45.6 (600) 54.0 (800) 59.9 (1000)	d
$PhCH_3$	12.0	30	76.6	30	24.9 47.2 (600) 63.3 (1000)	30
PhC_2H_3	35.2	30	82.5	30	29.4 52.1 (600)	30
$Ph\dot{C}HCH_3$	40.4	20	84.5	d		
$PhCH_2CH_2$·	53.2[c]	e				
PhC_2H_5	7.1	30	86.2	30	30.9 74.8 (1000)	30
Ph-Ph	43.5	30				
Ph_2CH_2	36.8	31				
t-PhCH=CHPh	55.5	31,43	108.3	d,44		
$Ph\dot{C}HCH_2Ph$	67.5	f	114.3	d,44		
$PhCH_2CH_2Ph$	34.2	45	114.5	d	49.4 91.3 (600) 108.3 (800) 120.1 (1000)	d
$Ph\dot{C}HCH_2CH_2Ph$	62.7	f				
$Ph(CH_2)_3Ph$	29.4	d	123.9	d	54.9 100.7 (600)	d

[a]At 298 K unless noted otherwise in parentheses (K). [b]At 300 K unless noted otherwise in parentheses (K). [c]Considerable recent evidence suggests that this value is ~2 kcal mol^{-1} too low; e.g., see refs. 21, 46, 47. [d]Group additivity (ref. 29). [e]Assumes $D^\circ(PhCH_2CH_2\text{-}H) = D^\circ(CH_3CH_2\text{-}H) = 98.2$ (ref. 20). [f]Assumes $D^\circ(Ph\underset{\underset{H}{|}}{C}H(CH_2)_nPh) = D^\circ(Ph\underset{\underset{H}{|}}{C}HCH_3) = 85.4$ (ref. 20).

At steady state, the rates of the two propagation steps must be equal so that:

$$[C_2H_5\cdot]/[H\cdot] = k_{12}[C_2H_6]/k_{11}$$

At typical conditions of 800 K and $[C_2H_6]$ = 50 kPa = 7.6×10^{-3} M, the rate constants listed above give $[C_2H_5\cdot]/[H\cdot] \sim (4.2 \times 10^8)(7.6 \times 10^{-3})/(8.1 \times 10^2) \sim 3900$. Thus termination will take place through the much more prevalent ethyl radical, with combination step 13 predominating over disproportionation step 14 by 7:1.[24b]

Note that the major products ethylene and hydrogen result from the repetitive chain sequence while the minor products methane and n-butane reflect the rates of initiation and termination, which must be equal at steady state.

2.3 n-HEXANE

For larger alkanes, the fundamental mechanistic pattern remains unchanged, but the number of elementary steps increases. Certain kinetic competitions among these steps, which are critical in establishing product distributions, will be illustrated by the example of n-hexane (5). Product distribution data[38,51-54] are given in Table 2. Detailed modeling has been carried out by Ebert and coworkers[38,55] and by Imbert and Marshall.[54] We will focus on initial behavior, except to note that olefinic products become involved as reactants already at very low conversions because they offer kinetically facile pathways to stabilized allylic radicals which then dominate termination.

Three different C-C bonds are now available for homolysis. Because of the stability order for radicals, tert > sec > prim > methyl, we would expect $k_{15a} \sim k_{15b} > k_{15c} > k_9$. Ebert and coworkers[55] estimated the total rate constant for homolytic initiation to be 2.2×10^{-7} s^{-1} at 500°C; Imbert and Marshall[54] estimated 1.2×10^{-6} s^{-1}. Yet the observed conversion[51] of 2% for a residence time of 24 s at 500°C and 101 kPa pressure corresponds to a formal first-order rate constant of

Table 2. Product Compositions from Thermolysis of n-Hexane

T (°C)	500	525	597	427	700
P (kPa)	100	13.4	100	13	13
Conversion (%)	2[a]	<2[b]		15	7
Product (Mol %)					
Hydrogen	1.1	1.7[c]	4	[d]	11.9
Methane	19.9	24.4	22	20.8	20.1
Ethylene	22.4	26.8	29	22.2	34.2
Ethane	14.9	11.5	11	13.8	2.9
Propylene	22.1	20.7	17	26.6	18.3
Propane	4.2	~0.8	2	1.4	trace
1-Butene	12.4	10.9	7	13.0	9.7
1-Pentene	2.9	3.2	5	2.2	2.9
Reference	51	54	53	38	52

[a]24 s residence time. [b]10 s reaction time. [c]Calculated by material balance. [d]Not determined.

$$\underset{\mathbf{5}}{CH_3CH_2CH_2CH_2CH_2CH_3} \longrightarrow CH_3CH_2CH_2\cdot + \cdot CH_2CH_2CH_3 \quad (15a)$$

$$\longrightarrow CH_3CH_2\cdot + \cdot CH_2CH_2CH_2CH_3 \quad (15b)$$

$$\longrightarrow CH_3\cdot + \cdot CH_2CH_2CH_2CH_2CH_3 \quad (15c)$$

$8.4 \times 10^{-4}\ s^{-1}$. This discrepancy is indicative of a chain length of ~1000.

To begin the chain, **5** is activated by hydrogen abstraction by a mixture of methyl, ethyl, and n-propyl radicals and hydrogen atom in a ratio indicated by the observed ratio of the corresponding paraffinic products. Typical rate constants for attack of methyl radical on sec C-H (k_{16a} or k_{16b}) and prim C-H bonds (k_{16c}) in alkanes are $10^{8.6}(-10{,}200/RT)$

$$R\cdot + \mathbf{5} \longrightarrow RH + \underset{\mathbf{8}}{CH_3CH_2\dot{C}HCH_2CH_2CH_3} \quad (16a)$$

$$\longrightarrow RH + \underset{\mathbf{7}}{CH_3\dot{C}HCH_2CH_2CH_2CH_3} \quad (16b)$$

$$\longrightarrow RH + \underset{\mathbf{6}}{\cdot CH_2CH_2CH_2CH_2CH_2CH_3} \quad (16c)$$

and $10^{8.4}\exp(-11{,}800/RT)\ M^{-1}s^{-1}$ per hydrogen, respectively (before upward curvature in Arrhenius plots begins; see Section 2.2).[24b] At 500°C, these correspond to selectivities, on a per hydrogen basis, of sec : prim ~ 4.5 : 1. A recent study of thermolysis of propane not only reproduced this sec : prim selectivity for methyl radical [$k_{sec}/k_{prim} = 10^{0.22}\exp(1730/RT)$ on a per hydrogen basis][56] but found experimentally indistinguishable selectivities for hydrogen atom and ethyl radical as well.

Whether formed by such hydrogen abstraction from the substrate, by β-scission of a larger radical, or by C-C homolysis of the substrate, every alkyl radical has available three potential decay routes:

(1) unimolecular β-scission; (2) bimolecular hydrogen abstraction from the substrate; and (3) if large enough, unimolecular intramolecular rearrangement by 1,5- (and, to a lesser extent, 1,4- and 1,6-) hydrogen shift. The dependencies of the relative rates of these three steps on radical structure, temperature, and substrate pressure determine the final product distribution.

The product distribution from **5** at 500°C and 101 kPa pressure was explained by Scheme I[51] where the numerical values indicate the partitioning of the carbon flow from 100 molecules of **5** which gave the best least-squares fit to the data. The <u>apparent</u> values of k_{16a}/k_{16c} and k_{16b}/k_{16c}, on a per hydrogen basis, were (38.6/6.3)(1.5) = 9.2 and (54.9/6.3)(1.5) = 13.1 [Imbert and Marshall[54] found 7.0 and 10.3 at 527°C]. This discrepancy from the "typical" value of 4.5 noted above for k_{sec}/k_{prim} results from the intervention of intramolecular rearrangement (Section 1.4.4). To consider the competition between intramolecular rearrangement and β-scission that is possible at the hexyl radical stage, we take rate constants estimated from the modeling study of Ebert and coworkers:[55] $k_{17a} \sim k_{17b} \sim k_{17c} \sim 10^{12.6}\exp(-27{,}900/RT)\ s^{-1}$; $k_{17d} \sim 10^{13.4}\exp(-31{,}500/RT)\ s^{-1}$; $k_{18a} \sim 10^{11.0}\exp(-13{,}700/RT)\ s^{-1}$; $k_{-18a} \sim 10^{11.1}\exp(-16{,}600/RT)\ s^{-1}$; $k_{18b} \sim 10^{11.0}\exp(-20{,}000/RT)\ s^{-1}$; and $k_{-18b} \sim 10^{11.1}\exp(-22{,}900/RT)\ s^{-1}$. Evaluated at 500°C, the relevant

$$\underset{\mathbf{7}}{CH_3CH_2CH_2CH_2\dot{C}HCH_3} \longrightarrow CH_3CH_2CH_2\cdot + CH_2{=}CHCH_3 \qquad (17b)$$

(18a) ~1,5H

$$\underset{\mathbf{6}}{\cdot CH_2CH_2CH_2CH_2CH_2CH_3} \longrightarrow CH_2{=}CH_2 + \cdot CH_2CH_2CH_2CH_3 \qquad (17a)$$

(18b) ~1,4H

$$\underset{\mathbf{8}}{CH_3CH_2CH_2\dot{C}HCH_2CH_3} \longrightarrow CH_3CH_2\cdot + CH_2{=}CHCH_2CH_3 \qquad (17c)$$

$$\longrightarrow CH_3CH_2CH_2CH{=}CH_2 + CH_3\cdot \qquad (17d)$$

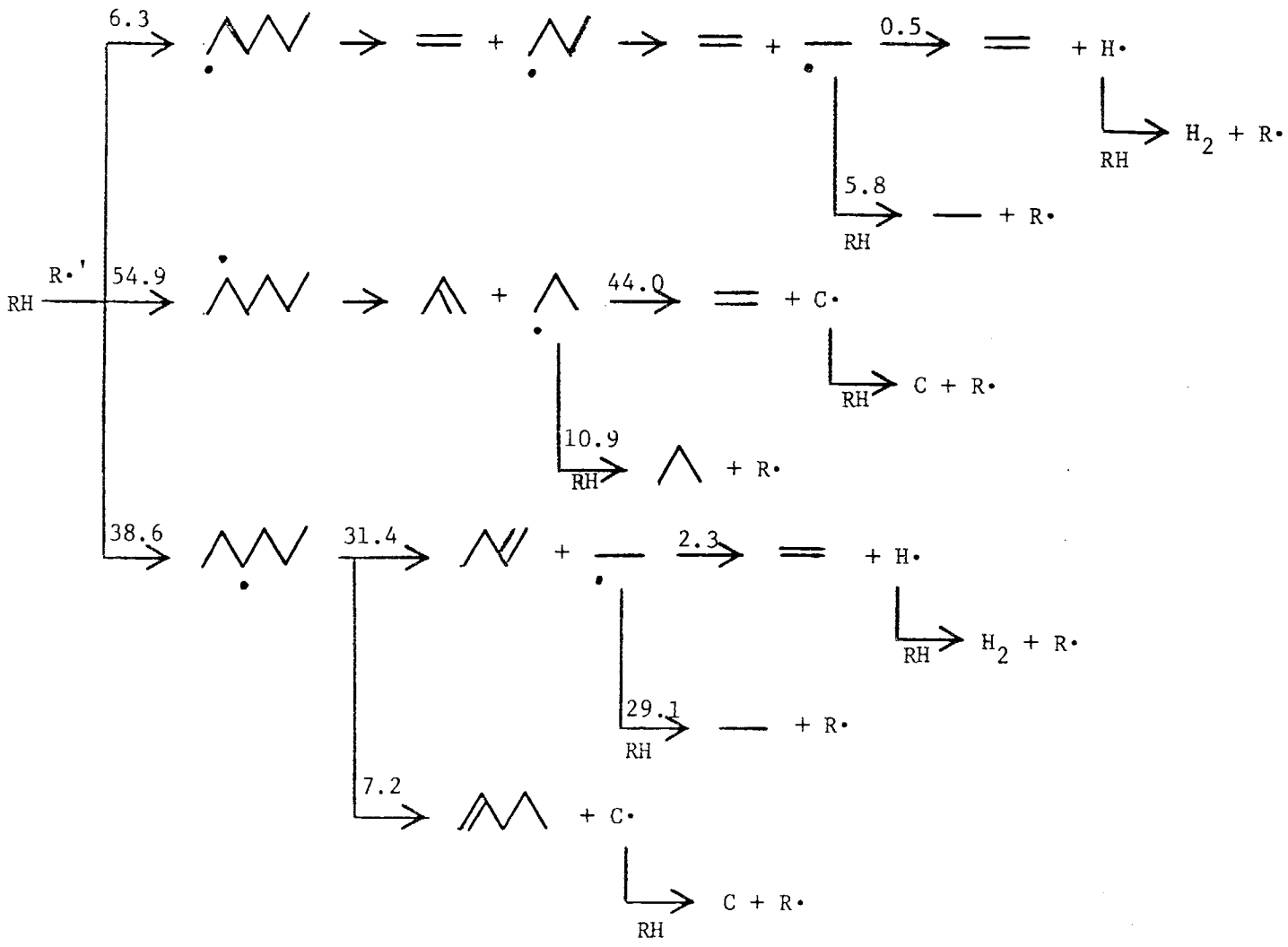

$R\cdot' = 51.2\ CH_3\cdot + 34.9\ C_2H_5\cdot + 10.9\ \underline{n}\text{-}C_3H_7\cdot + 2.8\ H\cdot$

SCHEME I

ratios for 1-hexyl radical (**6**) are $k_{1,5\text{-rearr}}/k_\beta = k_{18a}/k_{17a} \sim 260$ and $k_{1,4\text{-rearr}}/k_\beta = k_{18b}/k_{17a} \sim 4$; that for 2-hexyl radical (**7**) is $k_{1,5\text{-rearr}}/k_\beta = k_{-18a}/k_{17b} \sim 50$; and that for 3-hexyl radical (**8**) is $k_{1,4\text{-rearr}}/k_\beta = k_{-18b}/(k_{17c} + k_{17d}) \sim 0.5$. Thus, especially for the most facile 1,5-hydrogen shift ($k_{1,5\text{-rearr}}/k_{1,4\text{-rearr}} = k_{18a}/k_{18b} \sim 60$) which can interconvert **6** and **7**, rearrangement is much more rapid than β-scission. Thus the relative proportions in which the isomeric hexyl radicals contribute to product formation by β-scission are perturbed from the proportions in which they are initially formed in hydrogen abstraction step 16. Since the activation energy for β-scission is larger than that for intramolecular hydrogen shift, the importance of this perturbation will decrease with increasing temperature. In contrast, since both processes are unimolecular, their relative proportions are not dependent on the pressure of the substrate.

The second important competition in determining the product distribution is that between intermolecular hydrogen abstraction from the substrate and β-scission. Consider (Scheme I) this competition for the set of primary radicals 1-butyl, 1-propyl, and ethyl. The absence of n-butane product at 500°C and 101 kPa (Table 2) indicated that $k_{20a}[5]/k_{19a} \ll 1$; the ratio of propane : methane (after correction for step 17d) indicated that $k_{20b}[5]/k_{19b} = 0.25$; and the ratio of ethane : hydrogen indicated that $k_{20c}[5]/k_{19c} = 12.5$. Step 20 will be insensitive to the nature of R and we take $k_{20} \sim [10^{7.7}\exp(-10{,}300/RT)\ M^{-1}s^{-1}$ per sec-H][8 sec-H].[24b] In contrast, step 19 is sensitive to the structure of R, it becoming progressively

$$\cdot CH_2CH_2R \longrightarrow CH_2{=}CH_2 + R\cdot \qquad (19)$$

$$\cdot CH_2CH_2R + 5 \longrightarrow CH_3CH_2R + C_6H_{13}\cdot \qquad (20)$$

(a) $R = C_2H_5$; (b) $R = CH_3$; (c) $R = H$

more difficult to expel methyl radical and hydrogen atom compared with a prim radical such as ethyl. Earlier we noted $k_{19c} = k_{11} = 10^{13.4}\exp(-38{,}400/RT)\ s^{-1}$; the same analysis[21] recommended

$k_{19b} = 10^{13.1}\exp(-30,300/RT)\ s^{-1}$; k_{19a} has been given[24b] as $10^{13.6}\exp(-28,700/RT)\ s^{-1}$. Evaluated at 500°C and 101 kPa, these estimates give $k_{20a}[5]/k_{19a} \sim 0.03$, $k_{20b}[5]/k_{19b} \sim 0.23$, and $k_{20c}[5]/k_{19c} \sim 22$, in excellent agreement with the observed values noted above of <<1, 0.25, and 12.5, respectively.

The dependence of the rate of β-scission in step 19 on R in the order prim-R > CH_3 > H also rationalizes the fact that a radical such as 1-butyl preferentially expels ethyl radical to form ethylene rather than hydrogen atom to form 1-butene. The preference of **8** to expel ethyl radical over methyl radical by a factor of 4.4 at 500°C (Scheme I) [3.7 at 527°C[54]] reflects the same structural dependence. Note, however, that, although the activation energy for expelling hydrogen atom is some 10 kcal mol^{-1} larger than that for a prim alkyl radical, this increment is less than might have been anticipated from typical differences in C-H and C-C bond energies because expulsion of hydrogen atom has a notably lower intrinsic activation energy; i.e., the activation energy for exothermic addition of hydrogen atom to an olefin is typically 1-2 kcal mol^{-1}, whereas for addition of an alkyl radical, it is 7-8 kcal mol^{-1}.[21,24b,57,58]

Since the activation energy for β-scission is larger than that for intermolecular hydrogen abstraction, β-scission will be favored in the competition by increasing temperatures. When runs at the same pressure but different temperatures in Table 2 are compared, this effect can be seen most clearly in the increased yield of hydrogen at the expense of ethane and in the decreased yield of propane (Scheme I) at the higher temperature. Because of the functional form of the ratio $k_{20}[5]/k_{19}$, β-scission will be retarded by increasing the partial pressure of the substrate. For illustration, consider again the estimated ratio $k_{20a}[5]/k_{19a}$ which determines whether n-butane will be a product. Above we found this ratio to be ~0.03 at 500°C and [5] = 101 kPa ~ 1.6×10^{-2}M. Evaluated instead at 5 M, a condition which could in principle be achieved in supercritical **5**, this ratio would be ~8 and n-butane would be expected to be observed (see Section 2.4).

2.4 LARGER ALKANES

The considerations of temperature and pressure (concentration) effects, just illustrated for n-hexane, can be generalized to larger alkanes. When β-scission is much more facile than hydrogen abstraction (high temperatures and low pressures), radicals tend to break down all the way to methyl radical or hydrogen atom and only the latter participate in hydrogen abstraction from the substrate. This has generally been described as the Rice-Kossiakoff mechanism.[34] Each molecule of a linear paraffin, C_nH_{2n+2}, thus gives one molecule of a 1-olefin, C_mH_{2m} (m = 3 to n-1), several molecules of ethylene, and one molecule of methane or hydrogen. However, if the inverse kinetic extreme pertains (low temperatures and high pressures), the first radical formed by β-scission of the substrate-derived radical will undergo hydrogen abstraction rather than further β-scission. This has generally been described as the Fabuss-Smith-Satterfield mechanism.[59] Each molecule of linear paraffin thus gives one molecule of a 1-olefin, C_mH_{2m} (m = 2 to n-1), and one molecule of the corresponding paraffin, $C_{n-m}H_{2n-2m+2}$. Of course, these are simply two extremes of a single fundamental mechanism.

Under Fabuss-Smith-Satterfield conditions, substrate-derived radicals will also tend to abstract hydrogen from substrate competitively with their β-scission. Although such an intermolecular reaction as step 21, for example, does not achieve net cracking, it can alter product

$$\mathbf{6} + \mathbf{5} \longrightarrow \mathbf{5} + \mathbf{7} \qquad (21)$$

selectivities by interconverting the isomeric substrate-derived radicals just as intramolecular step 18a can. A difference is that product selectivity changes resulting from step 21 will be pressure- (concentration-) dependent, whereas those from step 18a will not. We will encounter this phenomenon explicitly in reactions of aralkanes in Sections 4.4, 9, and 10.1.6.

Although the data on cracking of alkanes is dominated by gas-phase examples, it appears that no major discontinuities in mechanism occur when heavy paraffins are cracked as liquids below their critical

points,[41,42] once it is realized that the Fabuss-Smith-Satterfield extreme is applicable. An instructive comparison can be made in this regard between product distributions from n-hexadecane at 350°C as a liquid[41] and at 502°C as a gas at 18 kPa.[40c] A recent proposal[60] that cracking of liquid n-hexadecane at ~400°C proceeded by a molecular rather than radical mechanism apparently arose from lack of recognition of the characteristics of this extreme of the mechanistic spectrum.

Cracking of branched alkanes involves no new mechanistic features other than the need to remember that tert radicals, which now become accessible, are still somewhat more stabilized than sec radicals. Kissin[61] has provided a recent example of thermolysis of large branched (isoprenoid) alkanes.

2.5 MOLECULAR DISPROPORTIONATION

As already noted, radical-radical encounters lead to combination and disproportionation with diffusion-controlled rates. Combination predominates except for tert radicals,[24b] but there appears to be a modest trend in which increasing temperature favors disproportionation.[62] Radical combination is the microscopic reverse of C-C homolysis, and considerable attention has been given to reconciling kinetic and thermodynamic information for the homolysis--combination equilibrium, as we have already illustrated in Section 2.2 for the ethane--methyl radical system in step 9. Much less attention has been given to a corresponding equilibrium involving radical disproportionation,[16] in which the "forward" reaction is a hydrogen atom transfer between an alkane and an olefin (a molecule-induced homolysis) to produce two alkyl radicals. Consider as an example step 22 (= step -14). Although such a radical-forming reaction has received comparatively little study until recently, we can, in fact, estimate its rate constant a priori. As a reference, we take the more familiar homolysis step 23 which also produces a pair of ethyl

$$CH_3CH_3 + CH_2{=}CH_2 \longrightarrow 2\ CH_3CH_2\cdot \qquad (22)$$

$$CH_3CH_2CH_2CH_3 \longrightarrow 2\ CH_3CH_2\cdot \qquad (23)$$

radicals. Without then even needing to know thermochemical properties of the ethyl radical, we can write (from Table 1 at 800 K for illustration):

$$R[\ln(A_{23}/A_{-23}) - \ln(A_{22}/A_{-22})] = \Delta S^{o}_{23} - \Delta S^{o}_{22} = S^{o}(C_2H_6) + S^{o}(C_2H_4) - S^{o}(C_4H_{10}) - R\ln(800R') = 23.5 \text{ cal mol}^{-1} \text{ K}^{-1}(\text{conc. units})$$

$$(E_{23} - E_{-23}) - (E_{22} - E_{-22}) = \Delta H^{o}_{23} - \Delta H^{o}_{22} = \Delta H_f{}^{o}(C_2H_6) + \Delta H_f{}^{o}(C_2H_4) - \Delta H_f{}^{o}(C_4H_{10}) = 21.7 \text{ kcal mol}^{-1}$$

We take $A_{-23} = 10^{10}$ $M^{-1}s^{-1}$.[21,24b,62] Since k_{dis}/k_{comb} for ethyl radical is 0.14,[24b] $A_{-22} = 10^{9.1}$ $M^{-1}s^{-1}$. Then with $A_{23} = 10^{16.4}$ s^{-1},[37,63] we can calculate $A_{22} = 10^{10.4}$ $M^{-1}s^{-1}$. Similarly, inserting $E_{23} = 82.1$ kcal mol^{-1} [37,63] and $E_{-23} = E_{-22} = 0$ leads to $E_{22} = 60.4$ kcal mol^{-1}. Thus $k_{22} \sim 10^{10.4}\exp(-60{,}400/RT)$ $M^{-1}s^{-1}$ compared with $k_{23} \sim 10^{16.4}\exp(-82{,}100/RT)$ s^{-1} so that $k_{22}/k_{23} \sim 10^{-6.0}\exp(21{,}700/RT)$ M^{-1}. On this basis, a mixture of ethylene and ethane at 800 K, 1 M in each, would be ~85% as effective in producing radicals as 1 M butane. Although this molecule-induced homolysis source of radicals is, of course, not important in the early stages of thermolysis of pure alkanes, we will encounter it later with certain unsaturated substrates.

3. AROMATIC HYDROCARBONS

Whereas the characteristic thermal reaction of alkanes is cracking to form smaller molecules, that of unsubstituted aromatic hydrocarbons is condensation to form larger biaryls with elimination of hydrogen. This reaction almost surely contributes to the formation of char and/or coke which occurs during high-temperature, hydrogen-poor treatments of coal. It has also been the subject of many model compound studies, but, compared with alkanes, details of mechanism remain clouded. We emphasize here a small subset of these studies which have focused on low-conversion behavior.

3.1 BENZENE

The prototype reaction is conversion of benzene (**9**) to biphenyl (**10**) and hydrogen. Data concerning its kinetics in the gas phase (reaction order and the importance of wall effects) are less than consistent.[64]

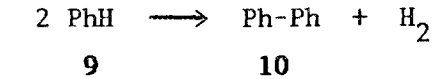

A study by Louw and Lucas[65] in a Pyrex stirred-tank flow reactor foreshadowed a more recent trend to couple experimental kinetic data with thermochemical kinetic estimates to formulate and test mechanisms. Conversion of **9** at 540°C and 33 kPa pressure was 0.2% after 100 s. The kinetic order over the pressure range 16-83 kPa was 1.7. Several observations were suggestive of radical intermediates: (1) inhibition by added propylene and by increased S/V ratio, an effect often diagnostic of quenching of hydrogen atoms at the wall; (2) acceleration by added formaldehyde, a possible source of hydrogen atom; and (3) H-D exchange between **9** and **9**-d_6 which occurred much more rapidly than net reaction. The authors considered possible elementary steps 24-29 and estimated their rate constants;[65] these estimates (shown below) are generally consistent with more recent experimental measurements that will be reviewed below. They considered both unimolecular C-H homolysis (step 24) and bimolecular molecular disproportionation (step 25) as initiating events and concluded that, because of the presence of only very strong bonds, the arene **9** represents an unusual example where both processes had comparable rates (at the reaction conditions of 540°C and [**9**] ~10^{-2} M). [Note for future reference that, if these estimates are correct, molecular disproportionation would dominate under lower-temperature, higher-pressure conditions, such as liquid-phase thermolysis of larger arenes, while unimolecular homolysis would dominate under the inverse conditions, such as those of Brooks and coworkers[66] (see below).] They considered hydrogen abstraction step 27 and homolytic aromatic substitution step 28 as the chain steps which formed products. Reversible step 26 was proposed to account for the rapid isotopic

$$\mathbf{9} \longrightarrow \underset{\mathbf{11}}{C_6H_5\cdot} + H\cdot \qquad (24)$$

$$k_{24} \sim 10^{16}\exp(-110{,}000/RT)\ s^{-1}$$

$$2\ \mathbf{9} \longrightarrow \underset{\mathbf{12}}{\text{[cyclohexadienyl radical, H, H]}} + \mathbf{11} \qquad (25)$$

$$k_{25} \sim 10^{11.5}\exp(-84{,}000/RT)\ M^{-1}s^{-1}$$

$$H\cdot + \mathbf{9} \rightleftharpoons \mathbf{12} \qquad (26)$$

$$k_{26} \sim 10^{10}\exp(-4{,}000/RT)\ M^{-1}s^{-1}$$
$$k_{-26} \sim 10^{13}\exp(-31{,}000/RT)\ s^{-1}$$

$$H\cdot + \mathbf{9} \longrightarrow H_2 + \mathbf{11} \qquad (27)$$

$$k_{27} \sim 10^{10}\exp(-13{,}000/RT)\ M^{-1}s^{-1}$$

$$\mathbf{11} + \mathbf{9} \underset{-a}{\overset{a}{\rightleftharpoons}} \text{[}C_6H_5\text{, H, cyclohexadienyl radical]} \xrightarrow{b} \mathbf{10} + H\cdot \qquad (28)$$

$$k_{28a} \sim 10^{10}\exp(-7{,}000/RT)\ M^{-1}s^{-1}$$
$$k_{-28a}/k_{28b} \sim 10^{1.7}\exp(-3{,}000/RT)$$
$$k_{28,eff} \sim 10^{8.3}\exp(-4{,}000/RT)\ M^{-1}s^{-1}$$

$$2\ \mathbf{12} \longrightarrow \mathbf{9} + \text{[cyclohexadiene]} \qquad (29)$$

$$\longrightarrow H_2 + \mathbf{9}$$
$$k_{29} \sim 10^{8}\ M^{-1}s^{-1}$$

exchange. Note that this hydrogen atom addition to **9** to give resonance-stabilized cyclohexadienyl radical (**12**), which is 25 kcal mol^{-1} exothermic,[20] was suggested to be kinetically much more favorable than hydrogen abstraction to give phenyl radical (**11**), which is 7 kcal mol^{-1} endothermic.[20] Hence, radical **12** was calculated to be more prevalent in the system than radical **11**. Although **12** was not considered to be kinetically competent to produce product **10** [this conclusion may merit re-examination[67]], it did therefore qualify as the most likely participant in termination reactions[68] such as step 29. Because of the suggested involvement of both steps 24 and 25 in initiation and of wall effects in termination, the authors did not attempt to deduce a unique

kinetic form but did conclude that their set of proposed steps and estimated rate constants led to a predicted rate three orders of magnitude slower than observed. Therefore, they finally concluded that steps 24 and 25 are, in fact, much too slow to rationalize the reactivity observed at 540°C and suggested that initiation actually involved a very efficient reaction of **9** with some unidentified trace contaminant. This suggestion was taken up more explicitly later by Stein,[69] who presented a convincing case that analogs of steps 24 and 25 could not explain the (much more rapid) rate of thermolysis of anthracene either (Section 3.2).

Somewhat later, Brooks and coworkers,[66] using a static silica reactor at lower pressures (1-7 kPa) and much higher temperatures (679-763°C) where step 24 should be favored over step 25 if the kinetic estimates of Louw and Lucas[65] are correct, observed a kinetic order of 1.5 and an overall rate constant of $10^{9.8}\exp(-53{,}800/RT)\ M^{-1/2}s^{-1}$. Extrapolated to 540°C, this expression predicts a rate more than an order of magnitude lower than that observed by Louw and Lucas. They proposed a somewhat different mechanism consisting of initiating step 24 and chain steps 27 and 28 but termination step 30; their estimated rate constants

$$2\ \mathbf{11} \longrightarrow \mathbf{10} \qquad (30)$$

of $k_{24} \sim 10^{15.7}\exp(-109{,}900/RT)\ s^{-1}$, $k_{28} \sim 10^{8.4}\exp(-5{,}000/RT)\ M^{-1}s^{-1}$, and $k_{30} \sim 10^{9.2}\ M^{-1}s^{-1}$ are not significantly different from those used by Louw and Lucas.[65] In the limit of long chains, the predictions are:

$$\text{Rate} = (k_{24}/k_{30})^{1/2}k_{28}[\mathbf{9}]^{3/2}$$

$$A_{exp} = (A_{24}/A_{30})^{1/2}A_{28} \sim 10^{11.7}\ M^{-1/2}s^{-1}$$

$$E_{exp} = 1/2\ E_{24} - 1/2\ E_{30} + E_{28} \sim 60\ \text{kcal mol}^{-1}$$

The modest agreement with experiment ($A = 10^{9.8}\ M^{-1/2}s^{-1}$ and $E = 53.8$ kcal mol^{-1}) may, however, be fortuitous because the apparently kinetically favorable step 26 was not included. If we do add it and

recognize that then step 29 would more probably dominate termination than step 30 (see above), we have the set of steps 24 and 26-29 for which, in the limit of long chains:

$$\text{Rate} = (k_{24}/k_{29})^{1/2}(k_{27}k_{-26}/k_{26})[\mathbf{9}]^{1/2}$$

$$A_{exp} = (A_{24}/A_{29})^{1/2}(A_{27}A_{-26}/A_{26}) \sim 10^{16.9}\ M^{1/2}s^{-1}$$

$$E_{exp} = 1/2\ E_{24} - 1/2\ E_{29} + E_{27} + E_{-26} - E_{26} \sim 95\ \text{kcal mol}^{-1}$$

These values are seriously inconsistent with experiment, and major questions of mechanistic interpretation thus remain for the dehydrogenative condensation of **9**. Heterogeneous wall effects may well be important to the final resolution of this problem.

In the temperature regime above 1000°C, cracking of **9** does begin and formation of acetylene, diacetylene, and hydrogen becomes the dominant reaction. Although this regime is of less relevance to coal chemistry, we nevertheless review some recent shock tube and Knudsen cell kinetic studies because they provide information on kinetics of some elementary steps discussed above. Literature disagreements and ambiguities regarding mechanistic details are at least as great here as at the lower temperatures characteristic of dehydrogenative condensation, and interpretation may well be confused by heterogeneous effects that result from soot product. The most recent studies[70-72] reach a consensus that the key steps in the mechanism are 24, 27, and 31. The values deduced for

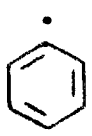

11

$$\longrightarrow \text{HC}\equiv\text{C-CH=CH-CH=CH}^{\bullet} \longrightarrow \text{HC}\equiv\text{C-CH=CH}^{\bullet} + \text{HC}\equiv\text{CH} \qquad (31)$$

$$\hookrightarrow \text{HC}\equiv\text{C-C}\equiv\text{CH} + \text{H}^{\bullet}$$

the C-H homolysis rate constant k_{24} are somewhat variable: $10^{17.3}\exp(-118{,}000/RT)\ s^{-1}$ (1900-2400 K);[70] $10^{13.8}\exp(-95{,}000/RT)\ s^{-1}$ (1630-1940 K);[71] and $10^{16.2}\exp(-107{,}900/RT)\ s^{-1}$.[72] However, considering the A-E compensation and allowing for temperature-dependent A factors, we

note that they compare favorably with expectations based on $D^o(C_6H_5\text{-}H) = 111$ kcal mol^{-1} [20] and with the estimates used in earlier, lower temperature studies[65,66] (see above). The rate constant for the hydrogen abstraction step 27 has been deduced as $10^{11.4}\exp(-16{,}000/RT)\ M^{-1}s^{-1}$ from shock tube results at 1900-2400 K,[70] compared with the earlier estimate[65] of $10^{10.0}\exp(-13{,}000/RT)\ M^{-1}s^{-1}$ (see above). Extrapolated downward, this expression gives $k_{27} = 2.5 \times 10^6\ M^{-1}s^{-1}$ at 700 K, not inconsistent with an upper limit of $<9 \times 10^6\ M^{-1}s^{-1}$ found by Nicovich and Ravishankara[73] in a lower-temperature, more direct study of reactions of hydrogen atom with **9**. The latter study focused on the hydrogen atom addition process and found $k_{26} = 10^{10.6}\exp(-4{,}300/RT)\ M^{-1}s^{-1}$ and $k_{-26} = 10^{13.1}\exp(-33{,}200/RT)\ s^{-1}$, again consistent with the earlier estimates[65] (see above). Ring cleavage of radical **11** (step 31) is poorly understood. It has been estimated to be >100 kcal mol^{-1} endothermic,[72] although others[71] suggest $k_{31} \sim 10^{15.2}\exp(-82{,}000/RT)\ s^{-1}$. Radical **12** may also undergo ring cleavage[72] or ring contraction to form methyl radical and cyclic C_5 products.[68]

If these general mechanistic formulations for **9** are correct, the branching between dehydrogenative coupling, which dominates in the lower temperature regime, and ring opening, which dominates in the higher, arises at the competition between steps 28 and 31. Taking the estimates of k_{28} from Louw and Lucas[65] and k_{31} from Rao and Skinner,[71] we have:

$$\text{Ring opening/Biphenyl formation} \sim 10^{6.9}\exp(-78{,}000/RT)[\mathbf{9}]^{-1}$$

This ratio is unity at, e.g., 1275°C and 1 kPa **9** or 1600°C and 100 kPa **9**. Available product data at high temperature is not sufficiently detailed to test this prediction.

3.2 POLYCYCLIC AROMATICS

In an early scoping study, Madison and Roberts[74] compared the amounts of heavy residue and gas formed from several polycyclic aromatics when heated as neat liquids at 475°C for 90 min in sealed glass ampoules. Little reactivity was observed for naphthalene, phenanthrene, pyrene, or fluoranthene. The minimum structural requirement needed for significant

thermal reactivity in this low-temperature regime appeared to be a linear 3-ring unit as in anthracene, benzo[a]anthracene, dibenzo[a,h]anthracene, and especially, naphthacene. Sharkey and coworkers[75] observed a generally similar reactivity order for liquid aromatics at 450°C: acenaphthylene >> 1-phenylnaphthalene > anthracene >> chrysene > pyrene ~ phenanthrene ~ naphthalene; mass spectral analyses confirmed the common formation of biaryls and hydrogen. Zander[76] recently reported the following conversions of polycyclic aromatics after they were heated at 430°C for 4 h in sealed tubes (unfortunately in the presence of a small amount of oxygen): naphthacene (99%) > benzo[a]anthracene (53%) $\gtrsim$ dibenzo[a,h]anthracene (50%) > benzo[e]pyrene (40%) $\gtrsim$ dibenzo[a,c]anthracene (36%) > perylene (30%) $\gtrsim$ benzo[g,h,i]perylene (27%) $\gtrsim$ picene (24%) $\gtrsim$ chrysene (20%) > benzo[a]pyrene (11%) $\gtrsim$ triphenylene (9%); an approximate correlation of reactivity with calculated Dewar localization energies was observed. Lewis and Edstrom[77] reported DTA studies of polycyclic aromatics at 10°C min^{-1} under flowing argon. In this open configuration, thermal condensation must compete with evaporation and only extremely reactive and/or high-boiling examples would be expected to form a carbonaceous residue. Herndon[78] has considered these data from a theoretical viewpoint. Note should be made of the particular carbonization and graphitization tendencies of aromatics, such as acenaphthylene,[81] which contain a 5-membered ring with a peripheral double bond.

Kinetic data often appears inconsistent. For example, whereas heating liquid anthracene at 500°C for 90 min resulted in >77% conversion to heavy residue, gaseous anthracene was virtually unaffected.[74] This behavior would suggest a kinetic order greater than unity. Indeed, Stein and coworkers[79] much more recently reported second-order kinetics for liquid anthracene (see below). Yet first-order behavior was reported under high applied pressure,[80] albeit with troublesome characteristics such as a significant induction period and Arrhenius parameters which varied widely with pressure.

Several product studies are available at high conversions. For example, the carbonization of naphthalene at 500°C and 9.3 MPa pressure for 50 h gave a pitch with a C : H ratio and molecular weight

distribution indicative of an average degree of condensation of 6.[82,83] However, quantitative regiochemical data at low conversions that would be more diagnostic of the initial reactions are sparse. The major binaphthyl formed from heating naphthalene at 500°C for only 1 h (~1% conversion) was the 2,2' isomer,[84] although both other isomers were detected. If binaphthyls result from step 32, in analogy to step 28 for

$$\mathrm{Ar}\cdot + \mathrm{Ar'H} \longrightarrow \mathrm{ArAr'H}\cdot \longrightarrow \mathrm{Ar\text{-}Ar'} + \mathrm{H}\cdot \qquad (32)$$

benzene, this regiochemistry does not correspond to predictions based on the expected position of highest reactivity for radical attack, namely, C-1.[78] Neat anthracene (**13**) at 350-470°C gave largely the unusual isomer 2,9'-bianthryl (**14**), whereas phenanthrene (**15**) gave eight isomeric coupling products in comparable amounts.[79] Regiochemistry may be

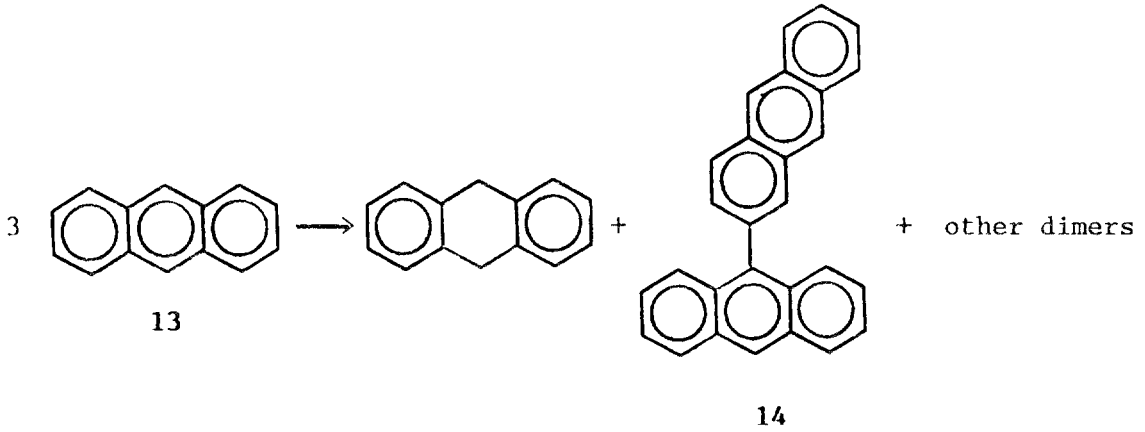

controlled by a tendency to form the least sterically crowded biaryls, a result which may be allowed because of reversibility in the first part of step 32.

Tricyclic arenes **15** and **13** showed very different kinetic behavior.[79] Disappearance of **15** showed a pseudo-first-order rate constant of $\sim 10^{8.6}\exp(-50{,}700/RT)\ s^{-1}$, was accelerated by added 9,10-dihydrophenanthrene (**16**), and gave similarly unselective formation of biphenanthryls in both the liquid and gas phase. Stein and

coworkers[79] tentatively suggested a chain homolytic arylation mechanism similar to that discussed in Section 3.1 for benzene:

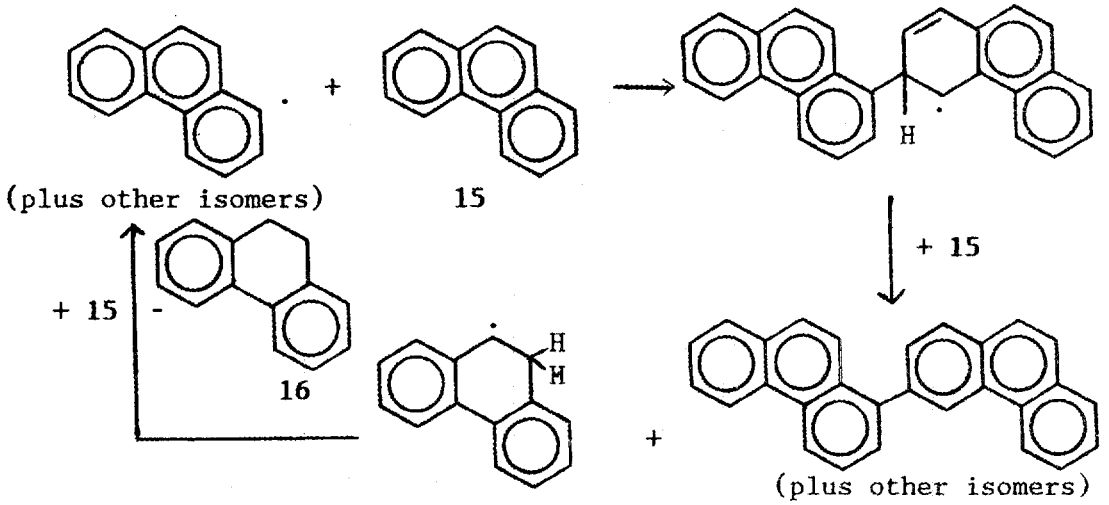

A difference is that they appeared to favor bimolecular radical hydrogen transfer over the intermediacy of free hydrogen atoms to rationalize the formation of dihydroaromatic **16** that occurs as the hydrogen-rich co-product, rather than hydrogen, at this low end of the temperature scale.[69] Based on their earlier thermochemical kinetic analysis of possible radical mechanisms for **13**,[69] they would also probably consider molecular disproportionation with **16** impurity as a likely initiation step:

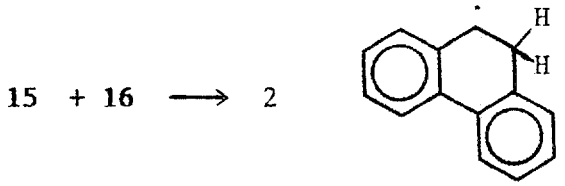

Surprisingly[69] different behavior was observed for liquid **13**.[79] The rate was much more rapid, was second-order with $k = 10^{8.0}\exp(-45{,}500/RT)\ M^{-1}s^{-1}$, and was not sensitive to radical-forming additives. In the presence of even such relatively inert arene additives as biphenyl, unsymmetrical anthrylarene adducts were formed competitively with bianthryls. Stein and coworkers[79] tentatively suggested the following mechanism:

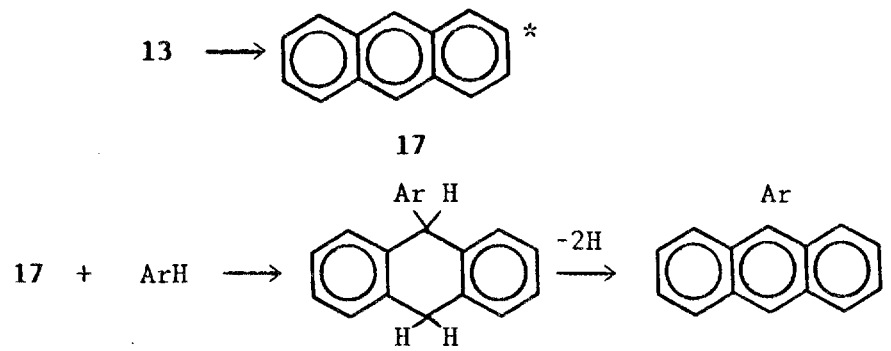

where **17** is some not fully identified activated or "excited" species and ArH is any arene, including anthracene.

At much higher temperatures, the characteristic unimolecular reaction of naphthalene is carbon scrambling without loss of molecular identity,[85,86] the details of which are beyond the scope of this review. Cypres and Bettens[87] described gas-phase thermolysis of phenanthrene at 850-900°C with 2 s residence time. Distinctive products, along with largely char and hydrogen, were naphthalene and fluorene. Isotopic labeling results suggested that the carbon atom lost in forming fluorene came largely from $C_{9(10)}$, while those lost in forming naphthalene came from both the central and outer rings. However, the reaction schemes presented are only representations of symmetry, not detailed mechanisms at the molecular level.

In the context of coal processing, it appears likely that homolytic arylation step 32 is an important contributor to char and/or coke formation. However, many questions remain concerning structure-reactivity relationships, the roles of other functional groups in coal as initiators and inhibitors, and alternate non-chain pathways.

4. ALKYLAROMATIC HYDROCARBONS

4.1 TOLUENE

4.1.1 Thermolysis

A ubiquitous product from thermal processing of coal is methane which likely arises largely from methyl substituents on the aromatic rings. The simplest compound with which to model this bond-breaking reaction is toluene (**18**) whose thermolysis, which requires temperatures in the high-temperature regime to proceed at a significant rate, has in

fact been a much studied problem in gas-phase kinetics. The seminal work was performed almost 40 years ago by Szwarc[88] who used a flow reactor at 738-864°C and 0.36-1.83 kPa pressure and limited conversions to <1% by using residence times typically <1 s. In a representative run, 0.107% decomposition of toluene was achieved at 796°C with a 0.286-s residence time. Reproducible first-order behavior was observed for carefully purified **18**, and rate constants were insensitive to the S/V ratio. The gaseous products were solely hydrogen and methane in a temperature-independent ratio of 60 : 40; approximately one mole of bibenzyl (**19**) was formed per mole of gas, and formation of benzene (**9**) was also observed. Steacie and coworkers[89] reported an average methane : **9** ratio of 0.91 under similar conditions. These products correspond to the stoichiometry:

$$\underset{\mathbf{18}}{(3 - x)\ PhCH_3} \longrightarrow \underset{\mathbf{19}}{PhCH_2CH_2Ph} + \underset{\mathbf{9}}{(1 - x)\ PhH} + x\ H_2 + (1 - x)\ CH_4$$

where x is the fraction of hydrogen in the gaseous products, 0.6 in Szwarc's data. Szwarc[88] interpreted the formation of hydrogen as indicative that the first step was C-H homolysis to produce hydrogen atom and benzyl radical (**20**) in step 33. Hydrogen abstraction by hydrogen atom would then produce hydrogen and another **20** in step 34. He proposed that hydrogen atom also effected methane formation competitively by one of two pathways: (1) homolytic aromatic displacement of methyl radical in step 35 followed by hydrogen abstraction in step 36; or (2) S_H2 displacement on the methyl group to form phenyl radical (**11**) in step 35a followed by hydrogen abstraction in step 36a. Finally, coupling step 37 was proposed to consume the radical **20** produced in steps 33, 34, and 36 (or 36a). The kinetic data were fitted to $k = 10^{13.3}\exp(-77{,}500/RT)\ s^{-1}$. Since the sequence of steps proposed does not constitute a chain, step 33 is rate-determining, and Szwarc identified the observed activation energy with $D^{o}(PhCH_2\text{-}H)$.

$$\mathbf{18} \longrightarrow \underset{\mathbf{20}}{PhCH_2\cdot} + H\cdot \qquad (33)$$

$$x\,H\cdot + x\,\mathbf{18} \longrightarrow x\,H_2 + x\,\mathbf{20} \qquad (34)$$

$$(1-x)\,H\cdot + (1-x)\,\mathbf{18} \longrightarrow (1-x)\,\mathbf{9} + (1-x)\,CH_3\cdot \qquad (35)$$

$$(1-x)\,CH_3\cdot + (1-x)\,\mathbf{18} \longrightarrow (1-x)\,CH_4 + (1-x)\,\mathbf{20} \qquad (36)$$

$$(1-x)\,H\cdot + (1-x)\,\mathbf{18} \longrightarrow (1-x)\,CH_4 + (1-x)\,\underset{\mathbf{11}}{Ph\cdot} \qquad (35a)$$

$$(1-x)\,\mathbf{11} + (1-x)\,\mathbf{18} \longrightarrow (1-x)\,\mathbf{9} + (1-x)\,\mathbf{20} \qquad (36a)$$

$$[1 + x + (1-x)]\,\mathbf{20} \longrightarrow \mathbf{19} \qquad (37)$$

Results from subsequent studies have required certain quantitative modifications and/or extensions of this reaction scheme, but the fundamental sequence of steps has stood the test of time. There is agreement that hydrogen and methane are the only gaseous products but some disagreement concerning their ratio and the derived value of x [$= k_{34}/(k_{34} + k_{35})$]. Similar to Szwarc who found $x = 0.60$,[88] Steacie and coworkers[89] found $x = 0.69$ over the somewhat higher temperature range 855-950°C; Takahasi[90] found $x = 0.64$-0.70 over the range 737-956°C; and Price[91] found $x = 0.65$-0.69 over the range 640-847°C. In each of these studies conducted in flow reactors, there was no significant temperature dependence of x. In contrast, using a static reactor with characteristic reaction times of minutes rather than fractions of a second and the correspondingly lower temperatures (647-697°C) needed to limit conversion, Brooks and coworkers[92] found both lower values of x and a temperature dependence which favored methane formation at higher temperatures: $x = 0.48$ at 680°C but only 0.22 extrapolated to 850°C, typical of the flow reactor studies. Although Brooks and coworkers had access to superior analytical techniques, this discrepancy remains puzzling because

the most current values of k_{34} and k_{35} (see below) confirm x values near 0.7 with a very small and opposite temperature dependence.

Later studies indicated that the heavier products are more complex than simply **19**. Most other workers[89,90,92,93] found comparable amounts of dimethylbiphenyls, but the isomer composition is unknown.[89,93] In addition, minor amounts of styrene,[89,92,93] stilbene,[92,93] phenanthrene,[92-94] anthracene,[89,94,95] and methyldiphenylmethanes[95] have been reported. Control experiments[89,95] suggest, however, that most, if not all, of these minor products result from secondary thermolysis of **19**.

There has been considerable variation in the Arrhenius parameters reported and in the degree to which the authors have associated them directly with step 33. In contrast to Szwarc's value[88] of $k = 10^{13.3}\exp(-77{,}500/RT)\ s^{-1}$ and assignment of $E_{exp} = D^{o}(PhCH_2\text{-}H)$, Steacie and coworkers[89] reported $k = 10^{15.8}\exp(-90{,}000/RT)\ s^{-1}$ for runs with 0.068-s residence time, but hesitated to identify these parameters with any single step because their calculated first-order rate constants increased with increasing residence time. Noting that the temperature ranges in these early studies[88,89] abutted but did not overlap, Takahasi[90] studied the entire range 737-953°C and reported some further evidence of a residence-time dependence of the rate constants.[91] His Arrhenius plot showed concave upward curvature, suggestive of activation energies ranging from ~75 kcal mol^{-1} at the low end of the temperature range to >90 kcal mol^{-1} at the high end. Therefore, the intervention of a second primary homolysis step at high temperatures, in competition with step 33, was suggested; the specific candidate, homolysis of an aromatic C-H bond, is, however, energetically unreasonable (see below). Price[91] combined his later results at 640-870°C with a reinterpretation of Takahasi's to obtain, after subtracting out a small heterogeneous component at low temperature, $k = 10^{14.8}\exp(-85{,}000/RT)\ s^{-1}$. Even more recently, noting the experimental difficulties which pertain to kinetic studies with very short residence times in flow systems,[96] Brooks and coworkers[92] carried out thermolyses in a static system (see above). They demonstrated modest autocatalysis of gas formation, which results from secondary reactions and which may rationalize the earlier reports[89-91] of

a residence time-dependence of the rate constants derived from flow-reactor studies. They obtained $k = 10^{16.0}\exp(-88{,}900/RT)\ s^{-1}$ from runs at 647-697°C, 4 kPa **18** in nitrogen diluent, and 4-min reaction time. Finally, most recently, Subba Rao and Skinner[97] have suggested $k_{33} = 10^{14.4}\exp(-83{,}000/RT)\ s^{-1}$ over the range 727-1527°C from modeling their direct resonance absorption spectroscopic measurements of deuterium atom formed during shock tube thermolyses of **18**-d_8.

We now consider steps 33-37 in more quantitative detail. Currently accepted thermochemical parameters (Table 1) lead to a prediction for C-H homolysis step 33 at 800°C, near the center of the various experimental temperature ranges, of:

$$E_{33,1073} = \Delta H^{o}_{33,298} + \langle\Delta C_p{}^{o}{}_{33}\rangle(1073 - 298) - 1073R/2$$

$$\sim 87.9 + 2.8 - 1.1 \sim 89.6 \text{ kcal mol}^{-1}$$

This prediction is in best agreement with the activation energy reported by Brooks and coworkers[92]: $k = 10^{16.0}\exp(-88{,}900/RT)\ s^{-1}$ at ~700°C. We can estimate from similar thermochemical data:

$$\Delta S^{o}_{33,1073} = \Delta S^{o}_{33,298} + \langle\Delta C_p{}^{o}{}_{33}\rangle\ln(1073/298) - R\ln(1073R')$$

$$\sim 26.1 + 4.5 - 8.9 \sim 21.7 \text{ cal mol}^{-1}\ K^{-1} \text{ (conc. units)}$$

$$(A_{33}/A_{-33})_{1073} = \exp(\Delta S^{o}_{33,1073}/R) \sim 10^{4.7}\ M$$

Brooks and coworkers' experimental A_{33} value then implies $A_{-33} \sim 10^{11.3}\ M^{-1}s^{-1}$. With regard to the possible incursion of alternative C-C homolysis step 38, which had often been suggested in earlier kinetic studies[89,99] as competitive with step 33, recent thermolysis studies at 900-1800°C and very low (~0.005-5 Pa) pressure in a Knudsen

$$\mathbf{18} \longrightarrow \mathbf{11} + CH_3\cdot \qquad (38)$$

cell with mass spectral detection[98] confirmed directly that the initial fragments from **18** under unimolecular conditions are **20** and hydrogen atom, not **11** and methyl radical. Step 33 was thus shown to be at least 200 times as important at 1000-1400°C as step 38. Homolysis step 33 is favored over step 38 by a $\Delta(\Delta H^o)$ factor of 13.8 kcal mol^{-1} (Table 1) which would contribute a factor of $\exp[\Delta(\Delta H^o)/RT] \sim 650$ to k_{33}/k_{38} at 1073 K (ignoring small heat capacity effects). On the other hand, step 33 suffers an entropy disadvantage of 13.1 cal mol^{-1} K^{-1} (Table 1) because formation of an atom is accompanied by less of an increase in entropy than that of a multi-atomic alkyl radical.[99] Not enough accurate thermochemical information is available to calculate the magnitude of the partially offsetting contributing of this entropy effect to k_{33}/k_{38}. However, a simpler illustration is instructive. Consider C-C homolysis of ethane to form two methyl radicals, which has $\Delta S^o_{298} = 37.3$ cal mol^{-1} K^{-1}, and C-H homolysis of methane to form methyl radical and hydrogen atom, which has $\Delta S^o_{298} = 29.0$ cal mol^{-1} K^{-1} (Table 1). This 8.3 cal mol^{-1} K^{-1} difference translates into $\exp[\Delta(\Delta S^o)/R] = (A_{39}/A_{-39})(A_{-40}/A_{40}) = 65$. Literature data[100] suggest

$$CH_3\text{-}CH_3 \longrightarrow 2\ CH_3\cdot \tag{39}$$

$$CH_3\text{-}H \longrightarrow CH_3\cdot + H\cdot \tag{40}$$

that methyl radical combines with hydrogen atom about 8 times faster than with itself, i.e., $A_{-40}/A_{-39} \sim 8$; then A_{39}/A_{40} must also be ~8. Thus C-C homolysis is favored over C-H homolysis in this example by almost an order of magnitude because of entropy alone. However, current data seem neither extensive nor accurate enough to draw conclusions how this partitioning of the entropy effect between homolysis and radical combination will occur in general.

Robaugh and Tsang[101] generated hydrogen atom from shock-tube thermolysis of hexamethylethane $[(CH_3)_3CC(CH_3)_3 \longrightarrow (CH_3)_3C\cdot \longrightarrow (CH_3)_2C{=}CH_2 + H\cdot]$ in the presence of excess **18** at 677-827°C and used the ratio of benzene : i-butene produced to determine $k_{34}/k_{35} = 10^{0.99}\exp(-3{,}100/RT)$. This expression gives x = 0.66 at 700°C

and 0.70 at 825°C, in good agreement with the values deduced from the products of thermolysis of **18**[88-91] except for that of Brooks and coworkers[92] (see above). By anchoring measurements to the known rate constant for reaction of hydrogen atom with methane, they were able to partition this ratio to give $k_{34} = 10^{11.1}\exp(-8,200/RT)\ M^{-1}s^{-1}$ and $k_{35} = 10^{10.1}\exp(-5,100/RT)\ M^{-1}s^{-1}$. Ravishankara and Nicovich (quoted in Reference 97) obtained the virtually identical value of $k_{34} = 10^{11.1}\exp(-8,400/RT)\ M^{-1}s^{-1}$ over the range 327-727°C by flash photolysis generation--resonance absorption detection studies of hydrogen atom [Subba Rao and Skinner[97] suggest non-Arrhenius behavior at higher temperatures]. For the corresponding hydrogen abstraction reaction from the sidechain of **18** by methyl radical, Cher and coworkwers[102] obtained $k_{36} = 10^{8.5}\exp(-9,500/RT)\ M^{-1}s^{-1}$; note the typically smaller A factor associated with hydrogen abstraction by a polyatomic radical rather than by an atom.

The Knudsen cell--mass spectrometric study[98] with **18** and **18**-α-^{13}C gave direct evidence that the methane-forming channel begins with aromatic displacement step 35 rather than S_H2 displacement step 35a and confirmed this conclusion reached earlier by Steacie and coworkers,[103] based on their observation that reaction of hydrogen atom, generated by co-thermolysis of a small amount of n-propylbenzene [$PhC_3H_7 \longrightarrow PhCH_2\cdot + CH_3CH_2\cdot \longrightarrow C_2H_4 + H\cdot$], with $PhCD_3$ gave PhH and CD_4 rather than PhD and CD_3H. The reasons for the disparate labeling results of Burr and coworkers[23,104] are not clear. Step 35 surely proceeds through an intermediate 6-methylcyclohexadienyl radical as already noted earlier in Section 1.4.2 (step 3). However, since expulsion of methyl radical rather than hydrogen atom is favored both enthalpically and entropically,[22] step 35 will be effectively unidirectional, and the initial hydrogen atom addition step is irreversible and rate-determining.

Subba Rao and Skinner[97] have demonstrated from the values of k_{33}, k_{34}, and k_{35} just discussed that steps 34 and 35 consume hydrogen atom rapidly enough to have prevented any serious complication from reversal of step 33 during typical flow kinetic experiments.

Finally, consider the reactions which consume radical **20** and the possible sources of the dimethylbiphenyls which accompany its dimer **19** as products. Two routes to the dimethylbiphenyls have been suggested. Several groups[89-91,99,103] have suggested that hydrogen abstraction from toluene might occur not only from the methyl group as in steps 34 and 36 but also <u>competitively</u> from the aromatic ring to generate methylphenyl radicals (**21**) which then couple to give homolytically stable dimethylbiphenyls. Abstraction from the ring suffers a relative enthalpy disadvantage of >20 kcal mol^{-1} [$D^o(PhCH_2\text{-}H)$ = 88 kcal mol^{-1}; $D^o(Ph\text{-}H)$ = 111 kcal mol^{-1}][20]. Although it is not known what fraction of this manifests itself in k_{34}/k_{41} and k_{36}/k_{41}, surely **20** would be generated in much greater quantities than **21** in any <u>direct</u> kinetic competition of step 41 with steps 34 and 36[101] However, we will see in Section 5.1.2 that coupling of **20** in step 37 will be significantly reversible in the temperature range where thermolysis of **18** proceeds at a convenient rate. Taking $k_{-37} \sim 10^{15.1}\exp(-61{,}400/RT)\ s^{-1}$ (Section 5.1.2), we can estimate the homolytic half-lives of **19** at 700, 800, and 900°C as 0.03, 0.002, and 0.0002 s, respectively. The fact that **19** could be observed at all in flow thermolyses with residence times of 0.1-1 s in this temperature range (see above) must indicate that much of it actually formed downstream from radical **20** which exited the heated zone.[99] Thus, step 42 might be significant in the heated zone even though [**20**] >> [**21**]. Also, bimolecular hydrogen abstraction equilibrium 43 must be considered.

$$H\cdot\ (CH_3\cdot)\ +\ \mathbf{18} \xrightarrow{?} H_2\ (CH_4)\ +\ \underset{\mathbf{21}}{\cdot C_6H_4CH_3} \qquad (41)$$

$$2\ \mathbf{21} \longrightarrow CH_3C_6H_4\text{-}C_6H_4CH_3 \qquad (42)$$

$$\mathbf{20}\ +\ \mathbf{18} \rightleftharpoons \mathbf{18}\ +\ \mathbf{21} \qquad (43)$$

Although clearly $K_{43} << 1$, it might also contribute to product formation if again **21** were continually siphoned off in irreversible step 42, whereas **20** accumulated because of the reversiblity of step 37. A second

suggestion[93,95] involves some coupling of **20** at ring positions (illustrated in step 37a for the p,p' isomer), a process known to occur to a

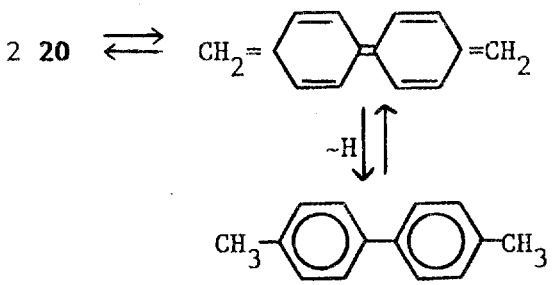

(37a)

minor extent at ambient temperatures.[105] Although the first step of such coupling is thermodynamically even less favorable (more reversible) than step 37, stable product formation might occur if the hydrogen shifts required to achieve aromatization of the initially formed methylenecyclohexadienes were rapid enough to compete with their C-C homolysis. These two routes might be distinguished if the isomeric composition of the dimethylbiphenyls were known because step 41 (or step 43), followed by step 42, should show little positional selectivity, whereas step 37a cannot produce the 3,3' isomer. There is, however, a further difficulty with both these hypotheses based on radical combination to the extent that they do not simply explain the observed preference for dimethylbiphenyls over methyldiphenylmethanes. If [**20**] >> [**21**] but **19** does not survive because of reversibility, then the next most favored routes statistically should be the unsymmetrical or cross combinations to form methyldiphenylmethanes, which should be reasonably stable under the thermolysis conditions (Section 7.1). Considering the dehydrogenative coupling of benzene (Section 3.1), we note a third possible route to the dimethylbiphenyls based on homolytic arylation of toluene by methylphenyl radicals:

$$\mathbf{21} + \mathbf{18} \longrightarrow CH_3C_6H_4\text{-}C_6H_4CH_3 + H\cdot$$

This possibility does not seem to have been considered.

At temperatures >1100°C, unimolecular ring-fragmentation reactions of benzyl radical, which are beyond the scope of this review, begin to occur.[98]

The thermal behavior of toluene just described provides a useful model to suggest that hydrodemethylation steps involving hydrogen atom and benzylic methyl groups on coal, analogous to step 35, are important in methane generation during pyrolysis of coal. However, the multifunctional character of coal provides other possible sources of hydrogen atom besides just analogs of benzylic C-H homolysis step 33; for example, we will see in Section 10 that β-scission of certain hydroaromatic radicals may be a source of hydrogen atom. Similarly, methyl radical will have a myriad of sources from which to abstract hydrogen, not just analogs of step 36. Finally, competitive conversion of benzylic methyl groups in coal to benzylic radicals will be mediated by a suite of radicals, not just methyl radical (step 36) and hydrogen atom (step 34).

4.1.2 Added Hydrogen

Addition of excess hydrogen considerably accelerates the decomposition of toluene (**18**) and increases the selectivity to form methane and benzene (**9**). For example, a mixture of 2.9 kPa **18**, 22.4 kPa hydrogen, and 14.7 kPa nitrogen exhibited a rate of conversion of **18** to methane of ~0.13 % min^{-1} at 553°C;[92] to achieve the same rate (to a more complex mixture of products) with the hydrogen replaced by additional nitrogen required 100°C higher temperature.[92] Hydrogenolysis of 2% **18** in hydrogen at atmospheric pressure was complete at ~835°C with a 10-s residence time with negligible formation of heavy products;[106,107] the thermal reaction under these conditions would have proceeded to only 10-15% conversion.[90]

Silsby and Sawyer[108] demonstrated that the rate law for hydrogenolysis was first-order in **18** and half-order in hydrogen for the range 700-950°C at atmospheric pressure with the partial pressure of hydrogen varied by a factor of 4, and this kinetic form has been confirmed in several subsequent flow studies at elevated hydrogen pressure.[109] Although there is some variation in Arrhenius parameters among the several studies, a master plot made by Benson and Shaw[23] of all the kinetic data over the range 460-960°C showed quite acceptable correlation with $k = 10^{11.1}\exp(-53{,}600/RT)\ M^{-1/2}s^{-1}$. The simplest set of reactions consistent with the observed kinetic form[23,108] is a chain (Scheme II) which combines reversible dissociation of hydrogen, displacement of

Scheme II:

$$H_2 \rightleftharpoons 2\ H\cdot \qquad (44)$$

$$H\cdot + \underset{\mathbf{18}}{PhCH_3} \longrightarrow \underset{\mathbf{9}}{PhH} + CH_3\cdot \qquad (35)$$

$$CH_3\cdot + H_2 \longrightarrow CH_4 + H\cdot \qquad (45)$$

methyl radical by hydrogen atom, and hydrogen abstraction by methyl radical from hydrogen; steady-state analysis gives:

$$\text{Rate} \sim k_{35}K_{44}^{1/2}[\mathbf{18}][H_2]^{1/2}$$

$$E_{exp} \sim E_{35} + 1/2\ \Delta H^{o}_{44}$$

$$A_{exp} \sim (A_{35})(A_{44}/A_{-44})^{1/2}\ .$$

Taking $K_{44,973} = 10^{4.0}\exp(-104{,}300/RT)$ M from standard data and $k_{35} = 10^{10.1}\exp(-5{,}100/RT)\ M^{-1}s^{-1}$,[101] we predict $E \sim 57.3$ kcal mol^{-1} and $A \sim 10^{12.1}\ M^{-1/2}s^{-1}$. This rather good agreement is strong circumstantial evidence that the mechanism is that of Scheme II or its kinetic equivalent.

On the other hand, several conclusions from the thermal reaction (Section 4.1.1) must be incorporated into the hydrogenolysis mechanism. Since $D^{o}(H\text{-}H)$ is 16 kcal mol^{-1} greater than $D^{o}(PhCH_2\text{-}H)$, step 44 is an unlikely chain initiation step compared with step 33.[23] Secondly, step 34 must be included because we have already seen that $k_{34} \gtrsim k_{35}$. Thirdly, we would expect methyl radical to abstract hydrogen more rapidly from **18** than from hydrogen ($k_{36} > k_{45}$). And finally, to provide escape routes for benzyl radicals (**20**) and allow a chain, we include the

Scheme III:

$$\mathbf{18} \rightleftharpoons \mathbf{20} + H\cdot \quad (33)$$

$$H\cdot + \mathbf{18} \rightleftharpoons H_2 + \mathbf{20} \quad (34)$$

$$H\cdot + \mathbf{18} \longrightarrow \mathbf{9} + CH_3\cdot \quad (35)$$

$$CH_3\cdot + \mathbf{18} \longrightarrow CH_4 + \mathbf{20} \quad (36)$$

$$CH_3\cdot + H_2 \longrightarrow CH_4 + H\cdot \quad (45)$$

reversals of steps 33 and 34. For this amplified Scheme III, steady-state analysis gives:

$$\text{Rate} \sim K_{33}^{1/2} K_{-34}^{1/2} k_{35} \alpha^{1/2} [\mathbf{18}][H_2]^{1/2}$$

$$\text{where } \alpha = \{k_{36}[\mathbf{18}] + k_{45}[H_2]\}/\{(k_{34} + k_{35})(k_{36}/k_{34})[\mathbf{18}] + k_{45}[H_2]\}$$

If $k_{36}[\mathbf{18}] \gg k_{45}[H_2]$, $\alpha \longrightarrow k_{34}/(k_{34} + k_{35}) = x$ ($x \gtrsim 1/2$; see above); for the reverse inequality, $\alpha \longrightarrow 1$; hence, the $\alpha^{1/2}$ term is only a small correction. But note then that $K_{33}K_{-34} = K_{44}$ and hence the rate expressions for Schemes II and III are indeed kinetically equivalent.

Scheme IV:

$$\mathbf{18} \longrightarrow \mathbf{20} + H\cdot \quad (33)$$

$$H\cdot + \mathbf{18} \rightleftharpoons H_2 + \mathbf{20} \quad (34)$$

$$H\cdot + \mathbf{18} \longrightarrow \mathbf{9} + CH_3\cdot \quad (35)$$

$$CH_3\cdot + \mathbf{18} \longrightarrow CH_4 + \mathbf{20} \quad (36)$$

$$CH_3\cdot + H_2 \longrightarrow CH_4 + H\cdot \quad (45)$$

$$2\,\mathbf{20} \longrightarrow \mathbf{19} \quad (37)$$

The most abundant radical in Scheme III is likely to be **20**. Not including its combination (step 37) as a chain termination step may be justified at temperatures high enough that step -37 is rapid compared with the overall reaction rate (see above). However, at the lower end of the temperature range which is effective for hydrogenolysis, this will no longer be true and Scheme IV should be considered. Steady-state analysis[92] now gives:

$$\text{Rate} \sim k_{-34}(k_{33}/k_{37})^{1/2}\beta[\mathbf{18}]^{1/2}[H_2]$$

$$\text{where } \beta = \{k_{36}[\mathbf{18}] + k_{45}[H_2]\}/\{(k_{34} + k_{35})(k_{36}/k_{35})[\mathbf{18}] + k_{45}(k_{34}/k_{35})[H_2]\}$$

where β is again near unity. Note that the kinetic form has now switched to half-order in **18** and first-order in hydrogen. This is indeed the approximate form observed by Brooks and coworkers[92] at a total pressure of 40 kPa over the range 535-570°C, which is lower than that of most other studies. For Scheme IV, $E_{exp} \sim E_{-34} + 1/2\ E_{33} - 1/2\ E_{37}$ and $A_{exp} \sim A_{-34}(A_{33}/A_{37})^{1/2}$. If we take $k_{33} = 10^{16.0}\exp(-88{,}900/RT)\ s^{-1}$,[92] $k_{37} \sim 10^{9.9}\ M^{-1}s^{-1}$ (Section 5.1.1), and $k_{-34} \sim 10^{10.6}\exp(-24{,}500/RT)\ M^{-1}s^{-1}$ [based on $k_{34} = 10^{11.1}\exp(-8{,}200/RT)\ M^{-1}s^{-1}$,[101] $\Delta H^{o}_{34,298} \sim -16.3$ kcal mol^{-1}, and $\Delta S^{o}_{34,298} \sim 2.5$ cal mol^{-1} K^{-1} (Table 1 and Section 4.1.1)], we predict $E \sim 69.0$ kcal mol^{-1} and $A \sim 10^{13.7}\ M^{-1/2}s^{-1}$, compared with experimental values[92] of $E = 58.8$ kcal mol^{-1} and $A = 10^{11.4}\ M^{-1/2}s^{-1}$. This much disagreement suggests that the details of the hydrogenolysis reaction at the lower end of its temperature range deserve further attention. The failure of rate constants calculated by Betts and coworkers[110] from their hydrogenolysis results at 10 MPa pressure and 540-660°C and those calculated from results by the same group[108] at atmospheric pressure and 700-950°C to define a single Arrhenius correlation also suggests a temperature-dependent mechanism.

4.2 OTHER METHYLATED AROMATICS

Szwarc's initial thermolysis study[88] included the isomeric xylenes as well as toluene. The products from m-xylene were parallel to those from toluene: $x = H_2/(H_2 + CH_4) = 0.6$ with 3,3'-dimethylbibenzyl (or possibly isomers) as the heavy product. The rate was unchanged, after correction for the statistical factor of 2 favoring the xylenes. The 3-fold rate acceleration observed for p-xylene, after statistical correction, corresponds to a decrease in E of 2.7 kcal mol^{-1}. This was attributed[88] to the hyperconjugative stabilization of a benzyl radical which is possible by a para, but not a meta, methyl substituent. Hydrogen and methane were again the gaseous products ($x = 0.65$), but the heavy product was largely a polymer that accumulated in the cold traps.[111] Szwarc[88] proposed that this difference resulted because p-methylbenzyl radical (**22**) can decay by disproportionation to form p-xylylene (**23**) which then polymerizes on cool surfaces:

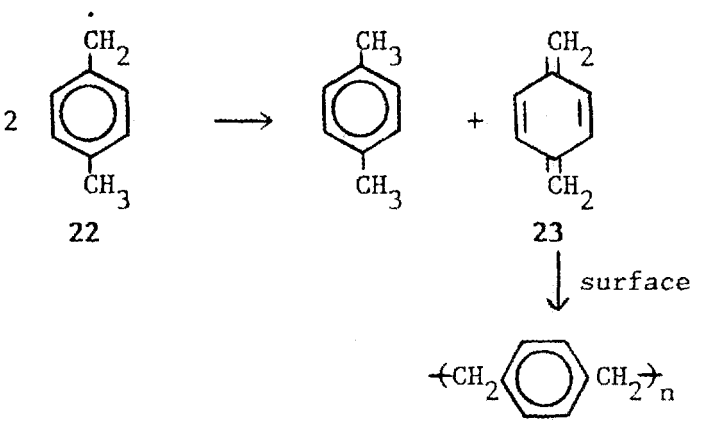

24

Schaefgen[111] demonstrated this disproportionation reaction by showing that the thermolysis of p,p'-dimethylbibenzyl (see Section 5.1) at 750°C, ~0.1 kPa, and 0.06 s residence time gave 15% conversion to p-xylene and poly-(p-xylylene) (**24**) as the major products. The formation of **23** from thermolysis of p-xylene, its "storage" as 2,2'-paracyclophane, and its surface-induced polymerization have become the basis of a commercial process.[112] Shull and Hixson demonstrated[109] that the hydrogenolysis of

mesitylene (555-700°C; 3-9-fold excess of hydrogen; 2.8-5.6 MPa total pressure) proceeded stepwise to give m-xylene, then toluene, and then benzene with relative rate constants, after statistical correction, of 1.4 : 1.15 : 1.0. Hence, we conclude that the thermolysis and hydrogenolysis behavior of polymethylbenzenes can be projected from that of toluene with only small rate enhancements which result from the stabilizing effects of methyl substituents on radicals.

Hydrodemethylation is more facile for methyl substituents on polycyclic aromatic rings. For example, the temperatures necessary for complete hydrodemethylation of toluene, 2-methylnaphthalene, and 1-methylnaphthalene in hydrogen (2% arene at atmospheric pressure) with a 10-s residence time[106] were ~835, ~780, and ~755°C, respectively. For the rate law associated with Scheme III, the increasing resonance stabilization of benzylic radicals in the order $PhCH_2\cdot$ < $2\text{-}NpCH_2\cdot$ < $1\text{-}NpCH_2\cdot$ (see Section 5.2) would be expected to enhance both K_{33} and K_{34} to similar extents such that the effect may largely cancel in the $(K_{33}K_{-34})^{1/2}$ term. However, k_{35} would also be expected to increase in accord with the observed reactivity order since the stabilization of benzocyclohexadienyl radicals falls in the same order: $C_6H_7\cdot$ < $2\text{-}C_{10}H_9\cdot$ < $1\text{-}C_{10}H_9\cdot$.[113]

4.3 ETHYLBENZENE

The number of alkyl sidechains, ArC_nH_{2n+1}, on the aromatic rings of coal decreases with increasing values of n. Nevertheless, it is instructive to consider the model behavior of alkylbenzenes with $n \geq 2$ because new steps occur which are not available to toluene. Szwarc[114] found that the temperature range appropriate for kinetic studies of thermolysis of gaseous ethylbenzene (**25**) was 550-700°C, over 100°C lower than that for toluene (**18**). The major products were hydrogen and styrene (**26**), with lesser amounts of C_2 hydrocarbons, methane, and bibenzyl (**19**). Rates were poorly reproducible. In contrast to the nonchain behavior of **18**, Szwarc proposed a chain reaction initiated by C-C homolysis in step 46. After hydrogen abstraction by methyl radical in step 47, repetition of steps 48 and 49 involving 1-phenylethyl radical

(27) constitutes a chain to produce hydrogen and **26** which is fully analogous to that for thermal dehydrogenation of ethane (Section 2.2).

$$\underset{\mathbf{25}}{PhCH_2CH_3} \longrightarrow \underset{\mathbf{20}}{PhCH_2\cdot} + CH_3\cdot \tag{46}$$

$$CH_3\cdot + \mathbf{25} \longrightarrow CH_4 + \underset{\mathbf{27}}{Ph\dot{C}HCH_3} \tag{47}$$

$$\mathbf{27} \longrightarrow \underset{\mathbf{26}}{PhCH{=}CH_2} + H\cdot \tag{48}$$

$$H\cdot + \mathbf{25} \longrightarrow H_2 + \mathbf{27} \tag{49}$$

$$H\cdot + \mathbf{25} \longrightarrow \underset{\mathbf{9}}{PhH} + \cdot CH_2CH_3 \tag{50}$$

$$CH_3CH_2\cdot + \mathbf{25} \longrightarrow CH_3CH_3 + \mathbf{27} \tag{51}$$

As for **18**,[88] Szwarc proposed that interaction of hydrogen atom with **25** involved competitive hydrogen abstraction (step 49) and aromatic displacement (step 50) reactions. Interpreting the relative abundances of hydrogen, C_2's, and methane in terms of steps 46-51 suggested a chain length of 15-25 and $y = k_{49}/(k_{49} + k_{50}) \sim 0.75$. The poor kinetic reproducibility discouraged any attempt to quantify k_{46} based on the amount of methane formed. Rather, this study was the first to use the now famous "toluene carrier technique" to measure rates of homolysis. We will return to results from this technique presently.

In a very recent study[115] with modern analytical methodology, the following initial product distribution at 648°C and ~10 kPa partial pressure of **25** in steam carrier at atmospheric pressure was derived by extrapolating results at 0.55-1.7 s residence time to zero conversion: styrene (**26**) (0.74 mol/mol ethylbenzene decomposed); hydrogen (0.66); benzene (**9**) (0.22); ethylene (0.18); methane (0.044); toluene (**18**) (0.044); and ethane (0.036). Note the stoichiometric equalities:

(hydrogen + ethane) ≃ **26**; **9** = (ethylene + ethane); and methane = **18**. These require the following elaborations of the Szwarc scheme: (1) adding step 52 to consume radical **20** formed in the initial homolysis; (2) adding step 11, in competition with step 51, to account for ethylene production; and (3) suggesting disproportionation step 53 to account for

$$\mathbf{20} + \mathbf{25} \longrightarrow \mathbf{18} + \mathbf{27} \qquad (52)$$

$$CH_3CH_2\cdot \longrightarrow CH_2{=}CH_2 + H\cdot \qquad (11)$$

$$2\ \mathbf{27} \longrightarrow \mathbf{25} + \mathbf{26} \qquad (53)$$

the small excess of styrene over (hydrogen + ethane). With these more accurate data, we can calculate the chain length as [**25** decomposed by radical attack (steps 47, 49, 50, 51, and 52)]/[**25** decomposed by homolysis (step 46)] = (1 - 0.044)/(0.044) = 22 and $y = (H_2)/(H_2 + \mathbf{9}) = 0.75$.

Ebert and coworkers[116] reported similar ratios of the two major pathways: $y = (\mathbf{26})/(\mathbf{26} + \mathbf{9}) = 0.82$ at 670°C and 2-3 ms residence time (7% conversion) and 0.76 at 720°C (20% conversion). However, at these non-zero conversions, the ratio of ethylene : **9** was greater than unity, 1.5 and 1.8, respectively; also, the **9** : **26** ratio was significantly temperature dependent, increasing from ~0.15 to ~0.5 over the broader range 600-800°C.

We now consider steps 46-53 in more quantitative detail. The "toluene carrier technique" to measure k_{46}[114] consisted of allowing **25** to decompose in the presence of a large excess of **18**, which is thermally stable at temperatures where **25** reacts. Under these conditions, the methyl radical formed in step 46 will abstract hydrogen largely from **18** (step 36) rather than from **25** (step 47). Thus the rate of formation of methane becomes a measure of k_{46}, and, in addition, the chain decomposition of **25** is inhibited. Values of k_{46} obtained in three toluene carrier studies[114,117,118] are given in Table 3; workers subsequent to Szwarc obtained considerably larger A and E values, at least partly because of better correction for residual reversal of step 46. Also given in

Table 3. Kinetic Studies of Homolysis of Ethylbenzene

($PhCH_2CH_3 \longrightarrow PhCH_2\cdot + CH_3\cdot$; step 46)

T(°C)	Method	log A (s^{-1})	E (kcal mol^{-1})	k^a_{1000K} (s^{-1})	Ref.
615-745	Toluene carrier; 2-5 mol% in $PhCH_3$ at 0.9-2.1 kPa; $d(CH_4)/dt$	13.0	63.2	0.15	114
603-723	Aniline carrier; $PhNH_2$ at 1.2-2.1 kPa; $d(CH_4)/dt$	14.6	70.1	0.19	119
633-737	Toluene carrier; 0.8-5 mol% in $PhCH_3$ at ~1.6 kPa; $d(CH_4)/dt$, corrected for reverse reaction	14.7	69.2	0.38	118
637-816	Toluene carrier; ~1 mol% in $PhCH_3$ at 2.7-4.8 kPa; $d(CH_4)/dt$, corrected for decomposition of $PhCH_3$	14.7	70.1	0.24	117
715-910	VLPP; E from $\Delta H°$; A from RRKM model; ~0.015 Pa	15.85	74.7	0.33	100,121
780-960	VLPP; same data treatment; ~0.15 Pa	15.3	72.7	0.26	122
600-670	5.1-17.2 kPa in steam at 100 kPa; 0.55-1.7 s contact time; $d(PhCH_3)/dt$, which constitutes 4.4 mol% of total products	15.7	74.5	0.26	115
1027-1527	Shock tube; density gradient detection; 1-2 mol% in Kr at 9-75 kPa; RRKM model to k^∞	15.95	74.7	0.42	120

[a]Rate constant at 1000 K calculated from Arrhenius parameters listed.

Table 3 are values of k_{46} from an aniline carrier study[119] and from Davis's study[115] of neat **25** in which k_{46} was derived from the rate of formation of **18**, i.e., the sum of steps 46 and 52. Finally, Table 3 includes a recent value deduced from a shock tube study at much higher temperatures.[20] A "grand average," excluding Szwarc's data, gives $A_{46} \sim 10^{15.1}\ s^{-1}$ and $E_{46} \sim 71.7$ kcal mol^{-1}.

Thermochemical data in Table 1 lead to a prediction at 700°C, near the center of the various experimental ranges, of:

$$E_{46,973} = \Delta H^{o}_{46,298} + \langle \Delta C_p{}^{o}{}_{46} \rangle (973 - 298) - 973R/2$$

$$\sim 75.8 \text{ kcal mol}^{-1}$$

Similarly, based on $\Delta S^{o}_{46,973} = 28.5$ cal mol^{-1} K^{-1} (conc. units), $A_{46}/A_{-46} = 1.7 \times 10^{6}$ M. If $A_{-46} \sim 10^{9.5}$-$10^{10}\ M^{-1}s^{-1}$, A_{46} is then predicted to be $10^{15.7}$-$10^{16.2}\ s^{-1}$. Hence, the more recent kinetic values[115,120] correspond more closely to thermochemical predictions. Two VLPP studies[100,121,122] are also included in Table 3, although as usual the A and E values assigned are not independent. In each case E was assigned with thermochemical formalisms and heats of formation slightly different from those currently accepted, and hence these studies could also be consistent with slightly larger A and E values.

The branching between the (**26** + hydrogen) pathway and the (**9** + C_2's) pathway is determined by k_{49}/k_{50}, the ratio of hydrogen abstraction to <u>ipso</u> addition in attack of hydrogen atom on **25**. We would expect this ratio to be slightly larger than the analogous ratio for **18**, k_{34}/k_{35}, because the extra methyl group in **25** will stabilize the benzylic radical formed by abstraction but not the cyclohexadienyl radical formed by addition. The slightly larger value of y observed for **25**, compared with that of x for **18**, is in accord with this expectation. Ebert's indication[116] that y decreased with increasing temperature corresponds with Brooks' similar indication[92] for x. However, as pointed out in Section 4.1.1, the associated implication that $E_{add} > E_{abstr}$ for attack of hydrogen atom on alkylaromatics deserves further attention in light of other indications of the reverse inequality.[101]

The ethylene : ethane ratio depends on the ratio $k_{11}/(k_{51}[25])$. If we take $k_{11} = 10^{13.4}\exp(-38{,}400/RT)\ s^{-1}$,[21] $k_{51} \sim 10^{8.0}\exp(-8{,}000/RT)\ M^{-1}s^{-1}$ [taken equal to the estimate for the corresponding reaction of 2-phenylethyl radical with 1,4-diphenylbutane[123]], T = 650°C, and [**25**] = 10 kPa = 1.3×10^{-3} M, then $k_{11}/(k_{51}[25]) \sim (2.0 \times 10^{4})/(1.3 \times 10^{6})(1.3 \times 10^{-3}) \sim 12$. At these conditions, Davis[115] observed ethylene/ethane = 5, well within the error limits of the estimation procedure.

Ebert and coworkers[116] carried out detailed computer modeling of the thermolysis of **25** based on numerical integration of a reaction network similar to steps 46-53 but with a number of significant differences. Although their data is similar to that of Davis[115] and they were able to model it well, a number of their individual steps and assigned rate constants are questionable. They explained the formation of (**26** + hydrogen) by steps 46-49 as above. However, they assigned $k_{48} \sim 10^{14.9}\exp(-30{,}000/RT)\ s^{-1}$; this appears incorrect because step 48 is ~47 kcal mol^{-1} endothermic (Table 1). To explain the formation of (**9** + C_2's), they suggested that radical **27** disappears not only by step 48, but also by step 48a. However, there is little precedent for

$$\underset{\mathbf{27}}{PhCH\dot{C}H_3} \xrightarrow{?} \underset{\mathbf{11}}{Ph\cdot} + CH_2{=}CH_2 \qquad (48a)$$

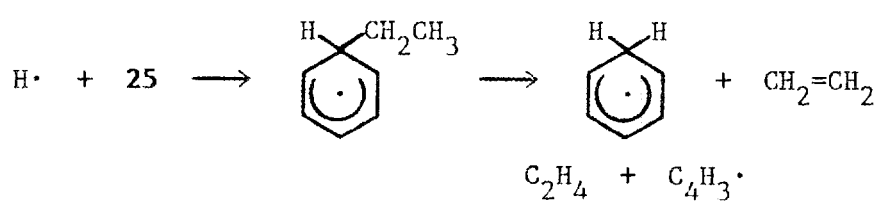

(50a)

$$\mathbf{25} \longrightarrow \mathbf{11} + \cdot CH_2CH_3 \qquad (46a)$$

such an α-scission. They did not consider step 50 as the source of **9**, in spite of the accumulated evidence for hydrodealkylation (see Section 4.1), but proposed instead that addition of hydrogen atom to **25**

followed sequence 50a to rationalize their observation that the ethylene : **9** ratio exceeded unity at high temperatures. Although disintegrations of cyclohexadienyl radical at high temperatures have indeed been suggested,[72] the unusual proposed elimination of ethylene leading to it has no good precedents. Finally, to rationalize overall rates at >750°C, they suggested that homolysis step 46a began to operate and assigned $k_{46a} \sim 10^{16.0}\exp(-83{,}000/RT)\ s^{-1}$. However, this value of E_{46a} is incompatible with $D^{o}(Ph\text{-}C_2H_5) \gtrsim 97.4$ kcal mol^{-1} (Table 1). A more likely source of added initiation at higher temperatures is homolysis of the α-C-H bond for which $D^{o} = 85.4$ kcal mol^{-1} (Table 1).

In his original formulation of the mechanism, Szwarc[114] allowed for the possibility that hydrogen abstraction from ethylbenzene in step 49 (and step 47) might produce some of the less stable 2-phenylethyl radical (**28**) as well as 1-phenylethyl radical (**27**). If ~1/2 of their difference in stability [$\Delta(\Delta H_f^{o}) = 12.8$ kcal mol^{-1}] is manifested in the transition states for abstraction,[123] then production of **28** by direct abstraction will be trivial ($k_{49a}/k_{49} \sim 0.03$ at 650°C). A second possible source of **28**, equilibrium 54, would be significant only if it competed successfully

$$H\cdot + 25 \longrightarrow H_2 + \underset{\mathbf{27}}{Ph\dot{C}HCH_3} \qquad (49)$$

$$H\cdot + 25 \longrightarrow H_2 + \underset{\mathbf{28}}{PhCH_2CH_2\cdot} \qquad (49a)$$

$$27 + 25 \rightleftharpoons 25 + 28 \qquad (54)$$

with decay of **27** in step 48. Step 48 has $\Delta H^{o}_{48} \sim 46.9$ kcal mol^{-1} and $\Delta S^{o}_{48} \sim 25.4$ cal mol^{-1} K^{-1} (Table 1). We estimate $k_{-48} \sim 10^{10.3}\exp(-1{,}600/RT)\ M^{-1}s^{-1}$, based on rate constants of $10^{10.3}\exp(-2{,}100/RT)$, $10^{9.8}\exp(-1{,}200/RT)$, and $10^{10.6}\exp(-1{,}700/RT)\ M^{-1}s^{-1}$ for addition of hydrogen atom to ethylene,[124,125] propylene,[21] and isobutene,[21] respectively. From these estimates we have $k_{48} \sim 10^{14.5}\exp(-48{,}500/RT)\ s^{-1}$. We take

$k_{54} \sim 10^{8.6}\exp(-21{,}900/RT)\ M^{-1}s^{-1}$, the same as that estimated[123] for reaction between 1,4-diphenyl-1-butyl radical and the prim hydrogens in ethylbenzene. Then at 650°C and [**25**] = 10 kPa ~ 1.3×10^{-3} M, $k_{48}/(k_{54}[\mathbf{25}]) \sim (1.0 \times 10^{3})/(2.6 \times 10^{3})(1.3 \times 10^{-3}) \sim 300$. So again there is no reason to assign a major role to **28**.

4.4 LARGER ALKYLAROMATICS

The relative rate constants for homolysis of the C_α-C_β bond at 700°C for the series ethylbenzene, n-propylbenzene, and n-butylbenzene, taken from an aniline carrier study by Estaban and coworkers[119], were 1 : 4.5 : 4.1, respectively, an order reflective of the stability order

$$ArCH_2R \longrightarrow ArCH_2\cdot + \cdot R$$

expected for radical R· : $CH_3\cdot < C_2H_5\cdot \sim n\text{-}C_3H_7\cdot$. The corresponding relative rate constants at 700°C for the series ethylbenzene, i-propylbenzene, and t-butylbenzene, taken from a VLPP study by Robaugh

$$ArCR'_2CH_3 \longrightarrow ArCR'_2\cdot + \cdot CH_3$$

and Stein,[122] were 1 : 6.8 : 28.3, an order reflective of the cumulative stabilizing effects of added methyl substituents at the benzylic radical center.

The longer the sidechain in n-alkylbenzenes becomes, the more the thermal behavior can be considered that of n-alkanes (Section 2) perturbed by the phenyl substituent rather than of toluene perturbed by an alkyl substituent. For example, Rebick[40c] has provided a rather complete product distribution for thermolysis of n-butylbenzene at 595°C, 47 kPa, and 5.5 s residence time, conditions which achieved 21.9% conversion. There is evidence for product formation pathways which involve β-scission reactions of all four radicals which can be formed by hydrogen abstraction. The production of styrene (57.1 mol/100 mol cracked) and much of the ethylene and ethane (28.8 plus 41.4 = 70.2 mol/100 mol) can be ascribed to β-scission of the benzylic radical at C-1. The production of allylbenzene (listed, presumably in error, as "alkylbenzene";

5.3 mol/100 mol; probably quite susceptible to secondary reactions) and methane (15.5 mol/100 mol) would arise from the secondary radical at C-2. Propylene (19.7 mol/100 mol) and toluene (19.8 mol/100 mol) are diagnostic of the secondary radical at C-3. Finally, the primary radical at C-4 would contribute to the ethylene yield and be the primary source of ethylbenzene (4.5 mol/100 mol). This product distribution suggests the following reasonable ratio of involvement of the isomeric radicals in product formation:

$$\underset{3.6}{\text{Ph-CH}_2}\text{—}\underset{1.0}{\text{CH}_2}\text{—}\underset{1.3}{\text{CH}_2}\text{—}\underset{0.4}{\text{CH}_3}$$

Rebick attributed the small amount of benzene formed (2.3 mol/100 mol) to β-scission of 2-phenylethyl radical (**28**)(see Section 5.1.2). However, in light of the active competition between hydrogen abstraction and <u>ipso</u> ring addition by hydrogen atom, which we have already seen for toluene (Section 4.1.1) and ethylbenzene (Section 4.3), it may be more reasonable to ascribe benzene as a hydrodealkylation product. The extent of hydrodealkylation would be expected to decrease in relative importance with increasing length of the alkyl sidechain because (1) hydrogen atom will increasingly tend to abstract because of the increasing number of C-H bonds available; and (2) hydrogen atom will carry less and less of the overall chain, compared with methyl, ethyl, and benzyl radicals, as the number of possibilities for β-scission increases.

For higher-boiling alkylbenzenes with much longer sidechains, data is available under liquid-phase conditions in the low-temperature, long-residence-time regime. Results for 1-phenylpentadecane[126,127] are typical. Heating for 30 min at 375°C gave 6.9% conversion to a mixture of alkanes, alkenes, phenylalkanes, and phenylalkenes generally reminiscent of the cracking of <u>n</u>-hexadecane according to the Fabuss-Smith-Satterfield mechanistic extreme (Section 2.4). However, two particular product pairs stood out above the others: some 35% of the initial products consisted of a mixture of toluene and 1-tetradecene while 13% consisted of a mixture of tridecane and styrene. The latter pair is

simply rationalized by noting that abstraction of hydrogen with kinetic selectivity would be expected to favor the stabilized benzylic radical at C-1 whose β-scission is then destined to give styrene and 1-tridecyl radical. However, the former, even more dominant pair cannot be so simply rationalized because formation of its precursor radical at C-3 would not be kinetically favored compared with any of the other twelve possible secondary radicals. On the other hand, this radical, once formed, indeed has the most favorable β-scission decay pathway because only it can expel the stabilized benzyl radical. The observed product selectivity therefore likely indicates that, under these dense, low-temperature conditions, intermolecular interconversion of the various secondary radicals by hydrogen abstraction from substrate is highly competitive with their decay by β-scission (see Section 2.4). In the extreme where the various secondary radicals were fully equilibrated by this route before β-scission occurred, product selectivity would be determined by the relative stabilities of the various transition states for β-scission. Since β-scission is highly endothermic, the Hammond postulate suggests a transition state with much of the radical character on the departing radical. Clearly, then, the most favored <u>transition state</u> is the one derived from the radical at C-3, the only one in which the stabilized benzyl radical is being expelled.

5. TWO-ATOM LINKAGES

5.1 BIBENZYL

The likely locus of bond breaking within the cross-linked backbone of coal is the aliphatic linkages between aromatic rings. The simplest models for these are the α,ω-diphenylalkanes, $Ph(CH_2)_nPh$ (n = 1, 2, 3, ...), and their analogs containing hetero atoms. Focusing first on C-C homolysis as a bond-breaking mode, we have compiled in Table 4 estimates of D^o for the weakest C-C bond in each of the early members of this series and derived estimates of the half-lives for homolysis at 450°C and 850°C. The thermally most labile bond occurs in bibenzyl (**19**; n = 2) because only in this case can both radicals formed be resonance-stabilized by the adjacent phenyl ring. The magnitudes of the estimated half-lives show why bibenzyl, as a model for dimethylene

Table 4. Dependence of Half-Lives for Homolysis on Bond Dissociation Energies

Compound	$D°(kcal\ mol^{-1})^a$	Estimated $t_{\frac{1}{2}}$ for Homolysis[b]	
		450°C	850°C
Ph-Ph	113.7	5×10^{10} yr	11 days
Ph-CH_2Ph	89.6	3×10^{3} yr	20 s
PhCH_2-CH_2Ph	61.4	4 min	60 μs
PhCH_2-CH_2CH_2Ph	71.6	4 days	6 ms

[a]From Table 1 for indicated C-C bond. [b]Assuming $A = 10^{16}\ s^{-1}$ and $E = D°$.

linkages, has received more recent attention as a model compound for coal processing than any other.

5.1.1 Gas-Phase Low-Temperature Regime

Poutsma[128] reported that the major products of thermolysis of **19** at 400°C and 54 kPa pressure, limited to very low conversions to minimize complications from secondary reactions, were toluene (**18**; 53 mol%), 1,2,3,4-tetraphenylbutane (**29**; both diastereoisomers; 18%), 1,2,3-triphenylpropane (**30**; 18%), and trans-stilbene (**31**; 10%) (column 1, Table 5). Under similar conditions at higher pressure (660 kPa of **19** diluted 1 : 1 with biphenyl), Petrocelli and Klein[129] later reported similar proportions of **18** and **31** (73 and 18 mol%) as well as three minor products: diphenylmethane (**32**; 4%), benzene (**9**; 3.5%), and phenanthrene (**15**; 2%). However, their analytical procedures apparently did not detect the heavier materials (the values above are normalized to 100% for observed products). This has been a common experimental difficulty, and only the detection of dehydrodimers **29** and **30**[44,128] has allowed a satisfying rationalization of products based on expected radical behavior.

Product composition depended strongly on the extent of conversion[128] because of very rapid secondary decomposition of primary product **29** to form **31** and regenerate **19** and of **30** to form **31** and **18**. Even at only 1-2% conversion, the relative amount of **31** was already somewhat increased and that of **29** decreased compared with the inherent primary products at zero conversion. Reaction mixtures examined at high conversions were dominated by **18** and **31**, at which point the primary products are thus seriously disguised.

In contrast with the behavior of ethane (Section 2.2) and ethylbenzene (Section 4.3) at higher temperatures, the primary products from **19** do not indicate a long chain reaction. The key elementary steps are (1) C-C homolysis in step 55 to produce benzyl radical **20**; (2) hydrogen abstraction from **19** by **20** in step 56 to produce **18** and 1,2-diphenylethyl radical (**33**); and (3) interaction of the radicals by combination steps 57a and 58a to give **30** and **29**, and, to a lesser extent, by disproportionation steps 57b and 58b to give some **31** as a primary product. The

Table 5. Product Compositions from Thermolysis of Bibenzyl at 400°C

Time (min)	15	15	15	60
Phase	Gas (54 kPa)	Liquid	Liquid	Liquid
Conversion (%)	1.7	1.4	--	7.5
Product (mol %)				
Toluene	53.0	56.1	56	58
1,2,3,4-Tetraphenylbutane	17.5	20.9	23	8
1,2,3-Triphenylpropane	17.7	2.1	2	1.5
Stilbene	9.6	9.9	9	17
1,1-Diphenylethane	1.1	10.5	10	10
Benzene	1.2	0.6		0.9
Ethylbenzene				1.0
Diphenylmethane				0.8
Phenanthrene				0.9
Hydrogen				1.7
Methane				0.08
Reference	128	128	44[a]	44[a]

[a]Product values estimated visually from published Figures.

occurrence of product **30** indicates that not all of radical **20** is captured by hydrogen abstraction in step 56 but some survives for coupling with radical **33** in step 57a. The observed smooth increase in the ratio **29** : **30** with increasing pressure of **19**[128] results because increasing concentration of **19** enhances decay of radical **20** by step 56 and thus fewer remain to enter step 57. Gibian and Corley[130] found the combination : disproportionation ratio k_{58a}/k_{58b} for radical **33**,

$$\underset{\mathbf{19}}{PhCH_2CH_2Ph} \longrightarrow 2\ \underset{\mathbf{20}}{PhCH_2\cdot} \tag{55}$$

$$\mathbf{20} + \mathbf{19} \longrightarrow \underset{\mathbf{18}}{PhCH_3} + \underset{\mathbf{33}}{PhC\dot{H}CH_2Ph} \tag{56}$$

$$\mathbf{20} + \mathbf{33} \longrightarrow \underset{\mathbf{30}}{PhCH_2CHPhCH_2Ph} \tag{57a}$$

$$\mathbf{20} + \mathbf{33} \longrightarrow \mathbf{18} + \underset{\mathbf{31}}{PhCH{=}CHPh} \tag{57b}$$

$$2\ \mathbf{33} \longrightarrow \underset{\mathbf{29}}{PhCH_2CHPhCHPhCH_2Ph} \tag{58a}$$

$$2\ \mathbf{33} \longrightarrow \mathbf{19} + \mathbf{31} \tag{58b}$$

generated independently to be 9 : 1 at 118°C. For historical perspective, note that steps 55 and 56 were clearly recognized in 1951 by Horrex and Miles,[131] but their explanation of product formation was somewhat confused by lack of consideration of combination steps 57a and 58a.

The independence of conversion level on initial pressure (21-421 kPa at 366°C and 54-462 kPa at 401°C) showed that the disappearance of **19** is first-order. However, deriving the rate constant for C-C homolysis, k_{55}, from the overall rate of disappearance requires attention to two related complications. First, **19** disappears not only by homolysis step 55, but also by decomposition induced by hydrogen abstraction step 56. The

fraction of total disappearance attributable to homolysis can, however, be extracted from the product data. For example, for the particular conditions shown in column 1 of Table 5, the ratio of products containing C_7 fragments to those containing C_{14} fragments indicated that only 36% of the total disappearance of **19** resulted from homolysis. Second, some fraction of the homolytic events would be experimentally invisible if any recombination of **20** occurred via step -55. If we make the simplifying approximation that the radical-radical reactions all occur with the same rate constant ($k_{-55} = k_{58} = k_{57}/2 = k_t$; see Section 5.1.2), then the quantity "product **29** : product **30** : 'reformed' **19**" will have a binomial expansion dependence on the ratio of steady-state concentrations of radicals **33** and **20**. Thus the data in column 1 of Table 5 (**29** : **30** = 17.5 : 17.7) imply a **33** : **20** ratio of (2)(17.5)/(17.7) = 1.98 and suggest that "reformation of **19**" was barely significant ($[(17.7)/(2)(17.5)^{1/2}]^2$ = 4.5 mol%) under these conditions. However, as we will see in Section 5.1.2, reversibility may become dominant at lower pressures and/or higher temperatures.

The most common experimental approach to deal with these complications and to determine k_{55} has been a carrier technique (Section 4.3) in which an added hydrogen donor captures benzyl radicals, both to prevent their recombination and to protect **19** from induced decomposition. The prototypical carrier in the low-temperature regime has been tetralin (**34**) (Section 10.1), in which case steps 56-58 are largely replaced by steps 59 and 60, and the rate of formation of **18**, the only significant

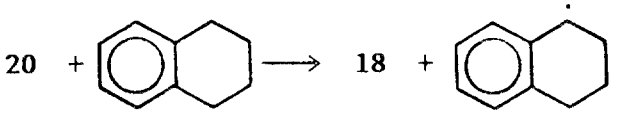

20 + **34** ⟶ **18** + **35** (59)

2 **35** ⟶ Products not involving **19** (60)

product from **19**, becomes a direct indicator of k_{55}. Bockrath and coworkers[132] have measured the relative rates of hydrogen abstraction from **34** and **19** by **20** to be 4.78 : 1 at 170°C (Section 5.6). If this

selectivity results entirely from a ΔE term, the factor favoring **34** will be attenuated to 2.8 at 400°C.

Using a 2.85-fold molar excess of **34** at ~13 kPa total pressure, Sato and coworkers[133] observed first-order disappearance of **19** and >85% selectivity to **18**, and they found $k_{55} = 10^{14.8}\exp(-60{,}400/RT)\ s^{-1}$ over the range 358-451°C. Using a 10-fold excess of **34** at 50-1000 kPa, Stein and coworkers[134] found $k_{55} = 10^{15.3}\exp(-62{,}300/RT)\ s^{-1}$ over the range 375-475°C, independent of conversion and pressure. These very similar Arrhenius correlations are shown in Figure 1 (for clarity without the experimental points). At the midpoint of the experimental range (415°C), the k_{55} values from these independent studies differ by only 36%. Two similar "one-point" values of k_{55} from thermolysis of neat gaseous **19**, derived by correction of the total conversion level for the percentage of homolysis based on the product data,[128] are also plotted in Figure 1. In contrast, using a 1 : 1 ratio of **19** and biphenyl in the gas phase at ~1.5 MPa with no added hydrogen donor solvent, Petrocelli and Klein[129] found $k_{55} = 10^{10.2}\exp(-45{,}300/RT)\ s^{-1}$ based on formation of **18** and $k_{total} = 10^{10.5}\exp(-46{,}200/RT)\ s^{-1}$ based on total disappearance of **19** (Figure 1).

A choice among these significantly different Arrhenius parameters can be made from available thermochemical information. We examine at 415°C (688 K) an average of the Sato[133] and Stein[134] correlations, i.e., $A_{55} = 10^{15.1}\ s^{-1}$ and $E_{55} = 61.4$ kcal mol^{-1}. From kinetic input then (see Section 2.2):

$$D^{o}(\mathbf{19}) = \Delta H^{o}_{55,298} = E_{55,688} - \langle\Delta C_p{}^{o}{}_{55}\rangle(688 - 298) + 688R/2$$

$$\sim 61.4 - 0.3 + 0.7 \sim 61.8 \text{ kcal mol}^{-1}$$

From separate thermochemical input (Table 1):

$$D^{o}(\mathbf{19}) \sim 61.4 \text{ kcal mol}^{-1}$$

If we take $A_{-55} \sim k_{-55} \sim 10^{9.9}\ M^{-1}s^{-1}$, equal to the gas-phase value for the similarly stabilized allyl radical,[135] then the kinetic data lead to:

$$\Delta S^{o}_{55,298} = R\ln(A_{55}/A_{-55}) - \langle\Delta C_p{}^{o}{}_{55}\rangle\ln(688/298)$$

$$\sim 23.2 \text{ cal mol}^{-1} \text{ K}^{-1} \text{ (conc. units)}$$

From thermochemical input:

$$\Delta S^{o}_{55,298} \sim 36.1 - R\ln(298R') \sim 28.1 \text{ cal mol}^{-1} \text{ K}^{-1}$$

Within the cumulative uncertainties of such estimates, the Sato-Stein gas-phase kinetic data in the low-temperature regime are thus in good agreement with the best available thermochemical parameters for radical **20**. However, the "low A-low E" values of Petrocelli and Klein,[129] which lead to D^{o}(**19**) = 45.7 kcal mol^{-1} and $\Delta S^{o}_{55,298}$ = 0.8 cal mol^{-1} K^{-1}, are not.

5.1.2 Gas-Phase High-Temperature Regime

VLPP studies of **19** at 613-732°C and <0.01 Pa have been reported by Stein's group.[134] Typical values of k_{55}, based on an RRKM model with $A_{55} = 10^{15.3}$ s^{-1}, were 7.35 s^{-1} at 660°C and 46 s^{-1} at 715°C. Extrapolation from the low-temperature Sato-Stein correlation (Figure 1) gives 4.6 s^{-1} and 29 s^{-1}, respectively. Hence, by this low-pressure approach, C-C homolysis of **19** seems to remain kinetically well behaved into the high-temperature regime.

Zeldes and Livingston[136] carried out thermolysis of **19** in excess supercritical toluene (**18**) at 590-620°C, 13.8-20.7 MPa pressure, and ~1 s residence time in a quartz flow cell positioned within an ESR cavity. At very high ratios of **18** : **19** (>85 : 1), the observed ESR spectrum was dominated by benzyl radical (**20**), and the decomposition rate of **19** was very much suppressed compared with that in an inert diluent such as benzene. These observations suggested[136] that equilibrium 56 was shifted to the left by the large excess of **18** and hence that **20** accumulated to the point that equilibrium was also attained in step 55. Under such conditions, an ESR spin assay for **20** combined with the known feed concentration of **19** gave $K_{55,878}$ = [**20**]^2/[**19**] = 0.75 x 10^{-10} M. This experimental K_{55} value and the already estimated temperature-independent

value of k_{-55} can be combined to give $k_{55,878} = (K_{55,878})(k_{-55}) \sim (0.75 \times 10^{-10}\ M)(10^{9.9}\ M^{-1}s^{-1}) \sim 0.6\ s^{-1}$ (Figure 1); the Sato-Stein correlation gives the same value. Hence, by this high-pressure ESR approach, C-C homolysis again seems kinetically well behaved at high temperatures.

When the ESR-monitored thermolysis was carried out in benzene instead of **18** as solvent, the dominant radical observed[137] was 1,2-diphenylethyl (**33**), equilibrium 56 now lying to the right. With feed compositions containing both **18** and **19** in ratios of 2.5-7, both radicals **20** and **33** were observed simultanously, and $K_{56,833}$ could be measured directly from the four necessary concentrations to be [**33**][**18**]/[**20**][**19**] = 10. If step 56 is isoentropic, this K_{56} value corresponds to $\Delta H^{o}_{56,833} = -3.8$ kcal mol^{-1}, a value quite reasonable for the difference in stability between a <u>prim</u> and <u>sec</u> benzylic radical.[20]

Low-conversion product and kinetic data from studies in traditional flow reactors at high temperatures are more sparse and less detailed than in the low-temperature regime. A product distribution at 573°C with nitrogen carrier at atmospheric pressure and low conversion (3.5%) obtained by Duprez and coworkers[138] is listed in column 1 of Table 6. Column 2 shows analogous data at higher temperature (690°C) and higher conversion (39%). Data at 540°C and moderate conversion from Klabunde[139] and at 700°C and high conversion from Sweeting and Wilshire[140] are also listed in Table 6. Finally, the last column shows much earlier data from Horrex and Miles[131] which, while naturally less quantitative, were historically very suggestive. The analytical procedures used in all these studies would probably not have detected heavier products such as **29** and **30**, had they been formed. Nevertheless, the cumulative data clearly reveal the emergence of a new high-temperature reaction 61--unsymmetrical cracking of **19** to form benzene (**9**) and styrene (**26**)--in

$$\underset{\mathbf{19}}{PhCH_2CH_2Ph} \longrightarrow \underset{\mathbf{9}}{PhH} + \underset{\mathbf{26}}{PhCH{=}CH_2} \qquad (61)$$

addition to formation of **18** and **31**. Kinetic studies at high temperature that only follow the disappearance of **19** will need to be corrected for

Table 6. Product Compositions from Thermolysis of Bibenzyl at High Temperatures in the Gas Phase

Temperature (°C)	573	690	540	700	630-770
Pressure (kPa)	<100	<100	<100	<100	~0.01
Conversion (%)	3.5	39	30	97	0.4-15
Product (mol %)[a]					
Toluene	37	31	37	46	~40
Stilbene	3	8	14	6	~20
Benzene	23	27	8	17	~20
Styrene	25	22	12	11	~20
Phenanthrene	1	6	4	16	b
Diphenylmethane	3	1		0.5	
Reference	138	138	139	140	131

[a]Product compositions normalized to 100%; deficiencies in totals in each column represent trace of unidentified products. [b]Not detected.

the modest proportion of this additional reaction. Similarly, when extrapolating to expected behavior of dimethylene linkages in coal, we would need to consider this unsymmetrical cracking pathway as a source of C_2-substituents in light products under, for example, flash pyrolysis conditions, whereas only methyl substituents would be expected under "low-temperaure pyrolysis" conditions.

In their early study at 630-790°C and 10 Pa, Horrex and Miles[131] found $k = 10^{9.3}\exp(-48{,}000/RT)\ s^{-1}$, based on formation of **18**. They noted, however, that this A factor seemed "low" for a bond dissociation process; current understanding of A factors some 35 years later strongly reinforces this concern. Klabunde[139] found $k = 10^{10.8}\exp(-46{,}600/RT)\ s^{-1}$, based on disappearance of **19** over the range 500-620°C and an unspecified but probably higher pressure. These two Arrhenius expressions are also plotted in Figure 1 along with an extrapolation of the Sato-Stein correlation. Klabunde's correlation intersects that of Sato and Stein at 510°C, but his rate constants are lower at higher temperatures, as indicated by the 15 kcal mol^{-1} lower derived activation energy. Horrex and Miles[131] found a similarly low E but still lower rate constants as indicated by a derived A factor 30-fold lower than Klabunde's. In summary, data from these "traditional" kinetic studies at high temperature deviate seriously both from an extrapolation of the Sato-Stein low-temperature correlation and from data from the "non-traditional" VLPP[134] and ESR[136] approaches.

The factor which causes this disagreement, as already hinted in Section 5.1.1, appears to be significant reversibility of homolysis. Applying the steady-state approximation and again using the simplifying assumption that radicals **20** and **33** interact statistically with a single rate constant k_t leads to:

$$[\mathbf{20}]/[\mathbf{33}] \sim (2k_{55}^{1/2}k_t^{1/2})/(k_{56}[\mathbf{19}]^{1/2})$$

The fraction, F, of benzyl radicals which decay by reversal (step -55), compared with the sum of all its decay pathways (steps -55, 56, and 57), can then be expressed as:

$$F = (2k_{55}^{1/2}k_t^{1/2})^2/(2k_{55}^{1/2}k_t^{1/2} + k_{56}[\mathbf{19}]^{1/2})^2$$

We take $k_{55} = 10^{15.1}\exp(-61{,}400/RT)\ s^{-1}$ and $k_t \sim 10^{9.9}\ M^{-1}s^{-1}$ (Section 5.1.1). To estimate k_{56}, we take Stein's reassignment[44] of the Arrhenius parameters from Jackson and O'Neill's data[141] for the (**20** + **18**) identity reaction and adjust E_{56} downward to account for net exothermicity[123] to obtain $k_{56} \sim 10^{8.6}\exp(-14{,}200/RT)\ M^{-1}s^{-1}$. [A recent measurement[142] of the rate constant for hydrogen abstraction from m- or p-xylene by the 2-allylbenzyl radical (Section 5.6) gave $10^{7.6}\exp(-13{,}400/RT)\ M^{-1}s^{-1}$ per methyl group; however, intrusion of tunneling[142,143] may have caused both A and E to be somewhat low.] Insertion of these estimates at 400°C and fairly dilute gas (50 kPa = 9×10^{-3} M) gives F ~ 0.18. This estimate compares favorably with the estimate of F ~ 0.045 made in Section 5.1.1 for these conditions based on the experimentally observed **29** : **30** product ratio. However, F will clearly increase with decreasing [**19**], and, even more importantly, with increasing temperature because the rate constant with the highest activation energy, k_{55}, dominates the numerator. Thus, a parallel estimate at 700°C and 10 Pa (1.6×10^{-6} M), the middle of Horrex and Miles' experimental range,[131] gives F = 0.999. That is, under these conditions, we estimate that only 0.1% of the actual homolytic events leads to observable disappearance of **19**. The experimental result to be expected is then indeed values of k_{55} which are low and values of E_{55} which are also low because F increases with increasing temperature. Klabunde,[139] in fact, noted this problem of reversibility, based on his observation that conversion to **18** was increased some 4-fold by added tetralin; however, he did not note the magnitude of the problem nor its effect on E_{obsd}. [Arguments based on reversibility alone will not reconcile the Petrocelli-Klein data[129] and the Klabunde data[139] (Figure 1) because the former authors obtained lower values of k_{55} at higher pressures.]

Note that the VLPP approach[134] was designed to avoid the complication of reversal of homolysis while the ESR approach[136] was in fact based on purposely establishing the homolysis-combination equilibrium. Measuring k_{55} at high temperatures by "traditional" techniques would require

very much higher pressures of very good hydrogen donors or some labeling technique which breaks the symmetry of **19** and makes step -55 visible. In fact, Louw and Bunk[144] have recently described just such a labeling approach. They heated **19** at 571-610°C in flowing nitrogen carrier gas in the presence of a 5-fold excess of $(\underline{p}\text{-}CH_3C_6H_4CH_2)_2$. Since the methyl substituent will, if anything, slightly accelerate C-C homolysis (Section 4.2), these reaction conditions would be expected to create a steady-state ratio of $\underline{p}\text{-}CH_3C_6H_4CH_2\cdot$: **20** >> 1. Thus, whenever **20** is formed in step 55, it would be more likely to combine with $\underline{p}\text{-}CH_3C_6H_4CH_2\cdot$ than with itself; the rate of formation of the cross-over product, $\underline{p}\text{-}CH_3C_6H_4CH_2CH_2C_6H_5$ could then be used as a measure of k_{55}. Although the data were neither extensive nor precise enough to establish an Arrhenius correlation, they were consistent with $k_{55} = 10^{15}\exp(-60{,}500/RT)\ s^{-1}$ (Figure 1). Thus we conclude that C-C homolysis is kinetically well behaved over the entire temperature range 350-725°C <u>if</u> reversibility is properly considered.

Now we return to the high-temperature unsymmetrical cracking reaction 61. Three possible mechanisms were laid out already by Horrex and Miles,[131] but the limited thermochemical kinetic data base available to them made choices difficult. A similar formulation was considered later by Duprez and coworkers.[138] In these three hypotheses, the breaking of the sp^2-sp^3 C-C bond in **19** occurs by direct homolysis, by β-scission in derived radical **33**, or by <u>ipso</u> aromatic displacement by hydrogen atom.

Consider first the common suggestion[139,140] of direct homolysis step 55a to form phenyl (**11**) and 2-phenylethyl radical (**28**). We estimate $D^o(Ph\text{-}CH_2CH_2Ph) \gtrsim 97.6$ kcal mol^{-1} (Table 1), some 36 kcal mol^{-1} less favorable than $D^o(PhCH_2\text{-}CH_2Ph)$. Even at 700°C, this difference translates into a rate difference $k_{55}/k_{55a} \sim 10^8$, and step 55a can be eliminated from consideration. In fact, the second most favorable homolytic decomposition pathway for **19** must be step 55b for which $D^o \sim 85.4$ kcal mol^{-1} (cf. Sections 4.1 and 4.3).

The second hypothesis depends on β-scission of radical **33** to form **26** and radical **11** as shown in step 62; alternation with step 63 would then form the usual β-scission--hydrogen abstraction chain. However, Stein[44] has suggested that the preferred β-scission mode for **33** is loss of

$$\underset{\mathbf{19}}{PhCH_2CH_2Ph} \longrightarrow \underset{\mathbf{11}}{Ph\cdot} + \underset{\mathbf{28}}{\cdot CH_2CH_2Ph} \qquad (55a)$$

$$\longrightarrow \underset{\mathbf{33}}{PhC\dot{H}CH_2Ph} + H\cdot \qquad (55b)$$

hydrogen atom in step 62a rather than loss of **11**. We estimate $\Delta H^o_{62a,298} \sim 40.1$ kcal mol^{-1} < $\Delta H^o_{62,298} \sim 46.3$ kcal mol^{-1} (Table 1). In addition to this enthalpy advantage for step 62a, the inherent activation

$$\underset{\mathbf{33}}{PhC\dot{H}CH_2Ph} \longrightarrow \underset{\mathbf{26}}{PhCH{=}CH_2} + \underset{\mathbf{11}}{Ph\cdot} \qquad (62)$$

$$\mathbf{11} + \underset{\mathbf{19}}{PhCH_2CH_2Ph} \longrightarrow \underset{\mathbf{9}}{PhH} + \mathbf{33} \qquad (63)$$

$$\mathbf{33} \longrightarrow \underset{\mathbf{31}}{PhCH{=}CHPh} + H\cdot \qquad (62a)$$

energy advantage for expulsion of hydrogen atom (Section 2.3) will favor it still further. Step 62 does have an overall entropy advantage of ~16.2 cal mol^{-1} K^{-1} (Table 1). However, examination of available data[24b,44] for similar β-scission--addition reactions suggests that the smaller entropy increase associated with expulsion of an atom will be reflected largely in $A_{-62a} > A_{-62}$ rather that in $A_{62a} < A_{62}$. Hence, we conclude that $k_{62a} > k_{62}$; Stein[44] estimated the disparity to be >10^3 at 400°C; on the same basis at 700°C it would still be >60.

The third hypothesis invokes hydrogen atom, generated in steps such as 62a, to effect a homolytic aromatic hydrodealkylation reaction as shown in step 64. Radical **28** would then be converted to **26** by β-scission (step 65a) and/or disproportionation (step 65c) or, at lower temperatures, to **25** by hydrogen abstraction (step 65b). A concern with operation of step 64 arises from the potential competition from hydrogen abstraction step 64a. The observation that hydrogen is not a significant product,[131,139] under conditions where **9** is, would demand $k_{64} >> k_{64a}$.

$$\mathbf{19} + H\cdot \longrightarrow \mathbf{9} + \underset{\mathbf{28}}{PhCH_2CH_2\cdot} \qquad (64)$$

$$\mathbf{28} \xrightarrow{} \mathbf{26} + H\cdot \qquad (65a)$$

$$\mathbf{28} \xrightarrow{RH} \underset{\mathbf{25}}{PhCH_2CH_3} + R\cdot \qquad (65b)$$

$$\mathbf{28} \xrightarrow{R\cdot} \mathbf{26} \text{ and/or } \mathbf{25} \qquad (65c)$$

$$\mathbf{19} + H\cdot \longrightarrow \mathbf{33} + H_2 \qquad (64a)$$

Yet for the closely analogous example of ethylbenzene (Section 4.3), we saw $k_{50} < k_{49}$. More information is therefore necessary to decide whether this third hypothesis represents the correct mechanism for the unsymmetrical cracking pathway observed at high temperature.

5.1.3 Liquid-Phase Low-Temperature Regime

Liquid-phase thermolyses of neat **19** are, of course, limited to the region below its critical temperature, estimated to be ~513°C.[44] Product distributions from parallel studies[44,128,145] at 400°C and very low (1.5%) conversion are shown in columns 2 and 3 of Table 5. Comparison with the gas-phase product data in column 1 reveals two major effects of the phase change, both of which can be shown to result from the much different concentrations of **19**.[128] As a continuation of the trend seen in the gas phase of increasing **29** : **30** ratio with increasing pressure, **30** has become insignificant in the neat liquid. Essentially all of radical **20** is captured in step 56 and combination step 57a can be ignored. Secondly, the skeletally rearranged 1,1-diphenylethane (**36**) has become a significant product. To account for it, we add steps 66 and 67 [along with steps 55, 56, and 58], which constitute a chain, albeit with a chain length less than unity under these conditions. Step 66 to form

$$\underset{\mathbf{33}}{\dot{\mathrm{PhCHCH_2Ph}}} \rightleftharpoons \underset{\mathbf{37}}{\mathrm{Ph_2CHCH_2}\cdot} \qquad (66)$$

$$\mathbf{37} + \underset{\mathbf{19}}{\mathrm{PhCH_2CH_2Ph}} \longrightarrow \underset{\mathbf{36}}{\mathrm{Ph_2CHCH_3}} + \mathbf{33} \qquad (67)$$

2,2-diphenylethyl radical (**37**) is an example of a 1,2-aryl shift, one of the few facile radical rearrangements[24c] (Section 1.4.4). Its exothermic reversal, step -66, has been observed[146] at lower temperatures. Applying the steady-state approximation to the three radicals involved and ignoring step 57 gives:

$$d[\mathbf{36}]/dt \sim \{k_{66}k_{67}(k_{55}/k_{58})^{1/2}[\mathbf{19}]^{3/2}\}/\{k_{-66} + k_{67}[\mathbf{19}]\}$$

$$d[\mathbf{18}]/dt \sim 2k_{55}[\mathbf{19}]$$

$$[\mathbf{36}]/[\mathbf{18}] \sim \{k_{66}k_{67}[\mathbf{19}]^{1/2}\}/\{2k_{55}{}^{1/2}k_{58}{}^{1/2}(k_{-66} + k_{67}[\mathbf{19}])\}$$

For the ratio **36** : **18** to increase with increasing [**19**] as observed, the inequality $k_{-66} \gg k_{67}[\mathbf{19}]$ must pertain; i.e., the phenyl shift step 66 must be highly reversible with hydrogen abstraction step 67 being rate-limiting. This is quite reasonable because step 66, which converts a <u>sec</u>-benzylic radical to a <u>prim</u> unstabilized one, is endothermic by ~14 kcal mol^{-1}. Miller and Stein[44] have made thermochemical kinetic estimates of all the relevant liquid-phase rate constants based on their rate data (k_{55}), similar hydrogen abstractions (analogs of k_{67}), Hamilton and Fischer's data[147] for the classic neophyl rearrangement (analogs of k_{66} and k_{-66}), and literature background (k_{58}). Introducing these expressions [$k_{55} \sim 10^{15.9}\exp(-65{,}000/RT)\ s^{-1}$; $k_{58} \sim 10^{9.5}\ M^{-1}s^{-1}$; $k_{66} \sim 10^{13}\exp(-23{,}500/RT)\ s^{-1}$; $k_{-66} \sim 10^{13}\exp(-9{,}000/RT)\ s^{-1}$; and $k_{67} \sim 10^{8.6}\exp(-7{,}900/RT)\ M^{-1}s^{-1}$] at 400°C and [**19**] ~ 4 M (neat liquid) indeed gives the needed inequality:

$$k_{-66} \sim 1.2 \times 10^{10}\ s^{-1} \gg k_{67}[\mathbf{19}] \sim 4.5 \times 10^{6}\ s^{-1}$$

and further predicts **36** : **18** ~ 0.16 compared with the experimental value of 0.18 (Table 5). Applying the same equations at [**19**] = 50 kPa = 9.1×10^{-3} M predicts **36** : **18** ~ 0.008 compared with the experimental gas-phase value of 0.021 (Table 5). [The gas-phase estimate involves further approximations because it is no longer legitimate to ignore step 57, and gas-phase values of k_{55} and k_{58} may differ slightly (see below).] It is thus clear that the significant differences in product distribution as a function of phase[128] result directly from changes in concentration rather than from any fundamental changes in reaction mechanism or from specific solvation effects.

Data at 7.5% conversion shown in column 4 of Table 5 exemplify the same pattern of secondary reactions seen in the gas phase, predominantly the conversion of **29** to **31**. Miller and Stein[44] have successfully modeled their product evolution curves to high conversions by numerical integration of a reaction network including steps 55, 56, 58, 66, and 67 and their reversals. Secondary reactions are, as already noted, dominated by the lability of **29** which reaches its maximum concentration already at only 5% conversion. A measurement by the tetralin carrier technique of the rate constant for homolysis of its weakest central C-C bond gave $k_{-58} = 7.8 \times 10^{-5}\ s^{-1}$ at 350°C compared with $k_{55} = 1.4 \times 10^{-7}\ s^{-1}$ (see below). This 550-fold enhancement reflects the added stability of a <u>sec</u> benzylic radical and possibly some steric acceleration (Section 5.4). Operation of step -58 reinjects radicals **33** into the system, part of which continually bleed off to form **31** by disproportionation which is effectively irreversible. However, the kinetic simulations revealed a second route for conversion of **29** to **31**, the induced β-scission chain consisting of steps 68 and 69, which is actively competitive with homolysis via step -58.

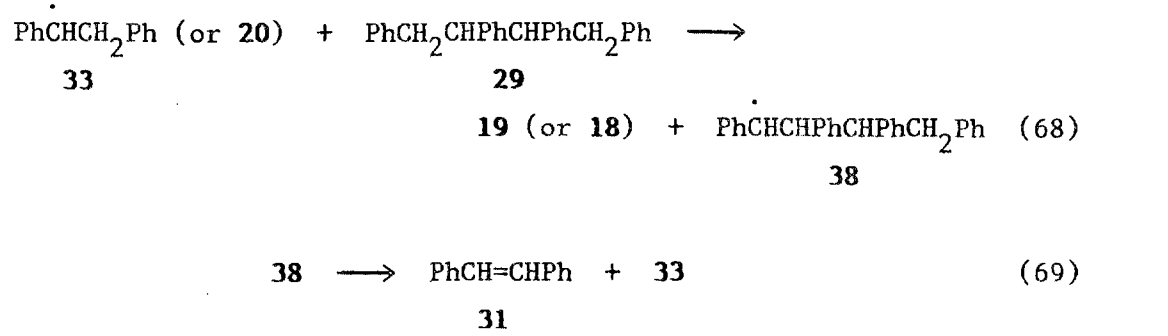

$$\underset{\mathbf{33}}{\mathrm{Ph\dot{C}HCH_2Ph}}\ (\text{or } \mathbf{20}) + \underset{\mathbf{29}}{\mathrm{PhCH_2CHPhCHPhCH_2Ph}} \longrightarrow \mathbf{19}\ (\text{or } \mathbf{18}) + \underset{\mathbf{38}}{\mathrm{Ph\dot{C}HCHPhCHPhCH_2Ph}} \quad (68)$$

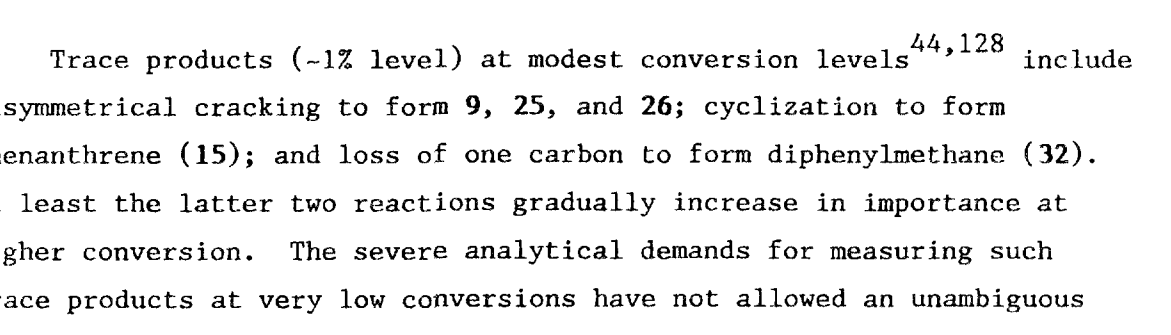

$$\mathbf{38} \longrightarrow \underset{\mathbf{31}}{\mathrm{PhCH{=}CHPh}} + \mathbf{33} \quad (69)$$

Trace products (~1% level) at modest conversion levels[44,128] include unsymmetrical cracking to form **9**, **25**, and **26**; cyclization to form phenanthrene (**15**); and loss of one carbon to form diphenylmethane (**32**). At least the latter two reactions gradually increase in importance at higher conversion. The severe analytical demands for measuring such trace products at very low conversions have not allowed an unambiguous decision whether they are truly primary products. Possible pathways for the unsymmetrical cracking have been discussed in Section 5.1.2 in connection with higher-temperature, gas-phase conditions where this process becomes more prominent. Cyclization remains a trace process at low conversions at high temperatures as well and becomes significant only under forcing high-conversion conditions (Table 6). Such cyclization in coal would represent a retrograde reaction since a potentially labile dimethylene linkage is converted to a stable polycyclic aromatic ring. Selectivity to **15** is higher from **19** than from parallel thermolysis of stilbene (**31**);[129] hence, **31** does not appear to be an intermediate. Recent studies[148] indicate that the initial cyclization product is actually 9,10-dihydrophenanthrene (**16**), and thermochemical kinetic analyses[148] of possible modes of cyclization suggest the following route involving a 1,4-hydrogen shift:

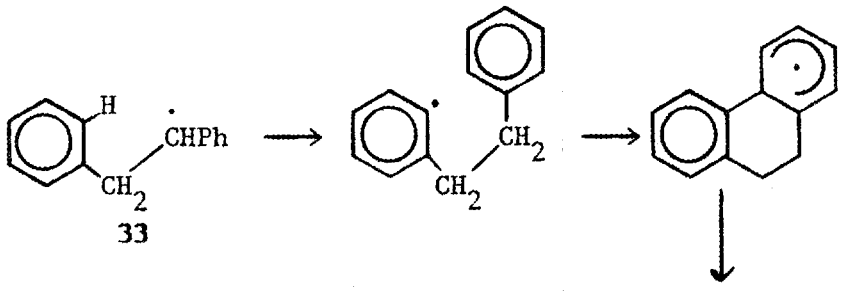

$$H\cdot + \mathbf{16} \longrightarrow \mathbf{15} + H_2$$

Secondary homolysis of rearrangement product **36** could be a source of **32** at high conversion. However, its measured rate of disappearance at 401°C and 274 kPa was less than 1/50 that of **19** (Section 5.3), apparently too slow to account for much **32** at low conversions. Additional evidence is needed concerning the fate of the "missing carbon" since not enough methane was found to balance **32** (Table 5).

Several authors have used the tetralin carrier technique to determine k_{55} in the liquid phase. At the same time, these conditions constitute a very useful model for liquefaction in hydrogen donor solvents. Before discussing these data, we note Benjamin's observation[149] that thermolysis of $PhCD_2CD_2Ph$ in tetralin led to H-D exchange with tetralin at a rate considerably faster than net consumption of **19**-d_4. Hence, a more precise version of the discussion in Section 5.1.1 of the competition between steps 56 and 59 can be given. The extensive H-D exchange indicates that radicals **33** and **35** must extensively equilibrate by hydrogen abstraction step 70, regardless of the exact kinetic competition involved in their formation in steps 56 and

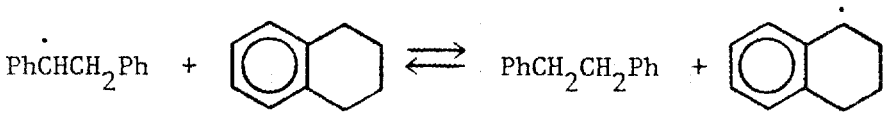

(70)

33 **34** **19** **35**

59. However, the excess of **34** compared with **19** and the special stability of **35** (among <u>sec</u>-benzylic radicals) lead to a steady-state ratio of

35 : **33** >> 1. Hence, **19** is "protected" from induced decomposition, not because **33** is never formed, but because the majority of structure-insensitive radical-radical decay events involve the more prevalent **35**.

An important implication for thermal reactions of coal that can be drawn from the rapidity of such H-D exchange (and several other examples to be considered later) is that the myriad of radical structures possible in coal can always potentially equilibrate by means of hydrogen abstraction for which step 70 is a realistic model. Thus, the most easily formed radical in a multifunctional molecule or mixture need not necessarily be the one through which the bulk of the chemistry occurs. We have already seen one example of this phenomenon in a model system in the regiochemistry of cracking of 1-phenylpentadecane (Section 4.4), and others will be seen later in the regiochemistry of cracking of 1,4-diphenylbutane (Section 9) and the mechanism of ring contraction of tetralin (Section 10.1.6).

Arrhenius parameters from 4 tetralin carrier studies[133,134,150,151] (and one study in neat **19**[152]) are compared in Table 7 and the correlation lines are plotted in Figure 2, along with Stein's gas-phase correlation for comparison. The excellent agreement between Stein's liquid-phase data[134] and that of McMillen and coworkers[151] and the sensible relationship between these and Stein's gas-phase data (see below) lead us to accept the parameters $A_{55} = 10^{16.6}\ s^{-1}$ and $E_{55} = 66.6$ kcal mol^{-1}. The reasons why Sato's rate constant values[133] are typically 3-fold lower and Cronauer and coworkers' values[150] are typically somewhat higher with a "low" E are not apparent. Identical extents of conversion of **19** after 9 h at 400°C were observed in tetralin and in its 1,1,4,4-d_4, 2,2,3,3-d_4, and d_{12} analogues,[153] a result consistent with no participation of tetralin in rate-controlling homolysis. The rate of disappearance of **19** was also unaffected by replacing tetralin with tetralin-phenol mixtures.[154,155]

Focusing on the experimental values from which these Arrhenius parameters were derived, we note that the ratio k_{55}(liquid tetralin)/k_{55}(gas) was somewhat less than unity to an extent which increased with decreasing temperature, e.g., 0.75 at 450°C and 0.5 at 375°C.[134] This trend translates into a 5.2 kcal mol^{-1} increase in E_{55}

Table 7. Kinetic Studies of Homolysis of Bibenzyl in Liquid Tetralin

($PhCH_2CH_2Ph \longrightarrow 2\ PhCH_2\cdot$; step 55)

T (°C)	log A (s^{-1})	E (kcal mol^{-1})	Source (Ref.)
350-440	16.6	66.8	Stein (134)[a]
---	16.4	66.3	McMillen (151)
380-440	15.4	64.6	Sato (133)[b]
400-475	10.9	48.1	Cronauer (150)[c]
337-400	15.5	63	Brower (152)[d]

[a]This group had earlier reported (ref. 145) log A = 16 and E = 64.8 over the range 325-425°C. [b]Ref. 133 reports log A = 14.4 and E = 61.5 over the range 380-460°C; the values reported here are derived by omitting the data point which lies above T_c for tetralin (444°C). [c]Combined data from runs in tetralin and mesitylene. [d]Neat bibenzyl at 6.7 MPa in absence of tetralin; k based on $d(PhCH_3)/dt$.

from the gas to the liquid phase and an almost offsetting increase in A_{55}. In dodecahydrotriphenylene as the hydrogen donor solvent, the depression from gas-phase rates was somewhat larger, e.g., k_{55}(liquid dodecahydrotriphenylene)/k_{55}(gas) at 375°C was 0.3; correspondingly, the Arrhenius parameters were still larger ($A_{55} = 10^{16.9}$ s^{-1} and $E_{55} = 68.4$ kcal mol^{-1}). Noting that this solvent should be more viscous than tetralin, Stein[134] suggested that the depression in k_{55} in the liquid phase results from a cage effect whose importance, i.e., the fraction of benzyl radical pairs which recombine before diffusive separation, increases with increasing solvent viscosity at a given temperature and with decreasing temperature for a given solvent. Each of these responses is that expected from known radical cage behavior.[24d] The net result of such a cage effect is a measured k_{55} for production of <u>kinetically free</u> benzyl radicals which falls off slightly more steeply with decreasing temperature than in the gas phase. This in turn leads to a derived E_{55} which is slightly larger than anticipated from the inherent bond dissociation energy.

Brower[152] reported a volume of activation based on formation of **18** from neat **19** of $\Delta V^{\neq} = 31$ mL mol^{-1} at 395°C over the range 7-93 MPa pressure. This large positive value is consistent with a rate-determining dissociation although its exact interpretation in terms of operation of a cage effect was not clear.

Stock[156] carried out individual thermolyses of **19** in liquid tetralin at 400°C for 4 h in the presence of phenyl benzyl sulfide, anthraquinone, naphthacene, phenol, and benzoic acid. The failure of any of these additives to accelerate or inhibit the reaction attests to its nonchain character; [although the rearrangement sequence, steps 66 and 67, is a chain, it accounts for only a small fraction of the total consumption of **19**]. Similarly, Yao and Kamiya[154] found phenol and quinoline to be ineffective as catalysts at 450°C. Even in such an unusual medium as a mixture of water and zinc metal (to generate "nascent hydrogen"), the 33% conversion to **18** observed after 1 h at 445°C[157] compares favorably with the 45% predicted from the Stein-McMillen correlation in tetralin. Such indifference to solvent polarity and polar catalysts is confirmatory of radical mechanisms.

5.1.4 Added Hydrogen

Whereas thermolysis of **19** in hydrogen donor solvents simplifies the product composition and directs it toward **18** by inhibiting induced decomposition, added molecular hydrogen at high pressures introduces a new reaction, formation of an equimolar mixture of benzene (**9**) and ethylbenzene (**25**) in an amount linearly dependent on the hydrogen pressure. This behavior, illustrated in Table 8 by the data of Vernon,[158] is reminiscent of the hydrodealkylation of toluene discussed in Section 4.1. Vernon[158] proposed that hydrogen abstraction step 71 becomes competitive with steps 56 and 59 for capture of radical **20** and that the hydrogen atoms so formed then enter a chain cycle consisting of step 64, already discussed in Section 5.1.2, and step 72. [To be rigorous, one of course needs to consider all possible hydrogen atom transfers among **19**, **34**, and hydrogen and their derived radicals.]

$$\underset{\mathbf{20}}{PhCH_2\cdot} + \mathbf{19\ (34)} \longrightarrow \underset{\mathbf{18}}{PhCH_3} + \mathbf{33\ (35)} \qquad (56 \text{ or } 59)$$

$$\mathbf{20} + H_2 \longrightarrow \mathbf{18} + H\cdot \qquad (71)$$

$$\underset{\mathbf{19}}{PhCH_2CH_2Ph} + H\cdot \longrightarrow \underset{\mathbf{9}}{PhH} + \underset{\mathbf{28}}{PhCH_2CH_2\cdot} \qquad (64)$$

$$\mathbf{28} + H_2 \longrightarrow \underset{\mathbf{25}}{PhCH_2CH_3} + H\cdot \qquad (72)$$

Although step 71 will be much less favored than step 59 enthalpically because of the strong bond in hydrogen, Vernon[158] proposed that a more favorable A factor might overcome much of this disadvantage. To model step 59 [note that $k_{59} > k_{56}$[132]], we start with its analog, step 56, for which we have already estimated $k_{56} \sim 10^{8.6}\exp(-14{,}200/RT)\ M^{-1}s^{-1}$ (Section 5.1.2), and adjust by Bockrath's relative rates[132] (Section 5.6) to give $k_{59} \sim 10^{8.6}\exp(-12{,}900/RT)\ M^{-1}s^{-1}$. We estimate $\Delta H^{o}_{71,298} \sim 16.3$ kcal mol^{-1} and $\Delta S^{o}_{71,298} \sim -2.5$ cal mol^{-1} K^{-1} (Table 1).

Table 8. Product Compositions from Thermolysis of Bibenzyl at 450°C for 30 min with Various Sources of Hydrogen[a]

Feed Composition				
Bibenzyl	Neat	0.42[b]	0.42[b]	Neat
Tetralin	--	0.58[b]	0.58[b]	--
Hydrogen	--		11 MPa[c]	11 MPa
Conversion (%)	68.5	45	57	79.5
Product (mol %)				
Toluene	61.5	97.9	72.9	47
Stilbene	29.3	--	--	--
Benzene	2.1	0.3	14.7	38
Ethylbenzene	1.2	1.8	12.4	15[d]
Phenanthrene	3.5	--	--	--
Others ($>C_{14}$)[e]	2.2	--	--	--

[a]Ref. 158. [b]Molar fraction of liquid feed. [c]Molar ratio of hydrogen charged:tetralin = 18.4. [d]Some secondary hydrocracking of ethylbenzene may have occurred. [e]Calculated as C_{21}.

A value of $k_{-71} = k_{34} = 10^{11.1}\exp(-8{,}400/RT)\ M^{-1}s^{-1}$ has been reported (Section 4.1.1).[97] Then $E_{71} \sim 24.7$ kcal mol^{-1} and $A_{71} \sim 10^{10.6}\ M^{-1}s^{-1}$ so that $k_{71}/k_{59} \sim 10^{2.0}\exp(-11{,}800/RT)$. Thus, hydrogen abstraction from hydrogen at 450°C appears kinetically unfavorable compared with that from tetralin (**34**) at an equal concentration by a factor of ~37-fold. However, since Vernon's experiments above the critical temperature of **34** were probably single-phase, the full 18-fold molar excess of hydrogen charged would have been available to counterbalance the k_{71}/k_{59} ratio. Further, one would expect the less stabilized radical **28** to be inherently less selective in choosing between **34** and hydrogen.

Burr and Javeri[159] described gas-phase thermolyses of **19** at 600-800°C with hydrogen carrier at atmospheric pressure and invoked a similar hydrodealkylation to account for **9**, **25**, and **26** among the products, along with **18**. However, comparison of their **9** : **18** ratio at 600°C in the presence of hydrogen (0.69) with that of Duprez[138] at 573°C in the absence of hydrogen (0.63; Table 6) does not indicate a large perturbation by the added hydrogen. Thus, in the absence of parallel control experiments in an inert carrier, it is not rigorously demonstrated that hydrogen became chemically involved at these much lower pressures. The reported overall activation energy of only 12 kcal mol^{-1} is difficult to reconcile with the proposed (or any) chain sequence since initiation by step 55 must introduce a term involving k_{55} to at least the one-half power into the rate expression and therefore lead to $E_{exp} > 1/2\ E_{55} \sim 31$ kcal mol^{-1}.

Virk[160] proposed nonradical, concerted processes for formation of **18** from thermolysis of **19** in tetralin and for the unsymmetric cleavage in the presence of hydrogen. However, Stein's thermochemical kinetic analysis[161] showed that these routes must be too slow by several orders of magnitude to contribute to the chemistry under discussion.

5.2 OTHER 1,2-DIARYLETHANES

The homolytic half-life of **19**, >20 h at 400°C, is long on the time scale of coal liquefaction, and several workers have therefore suggested that dimethylene linkages cannot be a significant site for thermal bond breaking in coal. This argument is incorrect because the typical

aromatic unit at the terminus of such a linkage will be polycyclic. Therefore, a more correct model is the set of 1,2-diarylethanes, $ArCH_2CH_2Ar'$, where Ar and Ar' are varied among the range of polycyclic aryl groups present in coal. Although experimental thermolysis data for such compounds is sparse, reliable extrapolations can be made from the now well understood behavior of **19** to $ArCH_2CH_2Ar'$ because the perturbation will be dominated by ΔRE, the added increment in benzylic resonance energy in going from $PhCH_2\cdot$ to $ArCH_2\cdot$. Values of ΔRE can be assigned with reasonable accuracy based on studies of the relative reactivity of methylarenes in hydrogen abstraction reactions,[162] recent VLPP data for homolysis of ethylarenes ($ArCH_2$-CH_3),[121,122] and molecular orbital calculations.[121,162a,163,164] These are listed in Table 9 for some typical polycyclic aromatic systems. Reasoning that E for homolysis of $ArCH_2CH_2Ar'$ will be reduced from that for **19** by a factor of ($\Delta RE_{Ar} + \Delta RE_{Ar'}$) but that the A factor will not change, we can estimate homolytic half-lives. For example, a dimethylene linkage between the 1-position of naphthalene and the 1-position of pyrene is thus predicted to have a homolytic half-life at 400°C of only 4 minutes. Additional predicted half-lives at 400°C, in the range of several minutes to several seconds (Table 9), are clearly significant in the context of coal liquefaction.

The data that is available support these predictions. In a direct comparison to a study of **19** in the same laboratory, Sato[165] found homolysis of 1,2-bis(1-naphthyl)ethane (**38**) in liquid tetralin at 300-400°C to have the same A factor but a 5 kcal mol^{-1} lower E value. This gives ΔRE(**39**) = 2.5 kcal mol^{-1}, compared with the prediction of

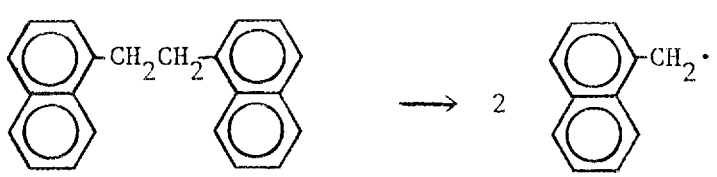

38 **39**

2.9 kcal mol^{-1} in Table 9. Acceleration of the disappearance of 1-(2-naphthyl)-2-phenylethane at 400°C in tetralin compared with **19** was

Table 9. Relative Resonance Energies of Arylmethyl Radicals and Predicted Homolytic Half-Lives of 1,2-Diarylethanes

Ar	$\Delta RE(ArCH_2\cdot)$[a,b] (kcal mol^{-1})	Predicted $t_{\frac{1}{2}}$ at 400°C for Homolysis of $ArCH_2CH_2Ar$[c]
Phenyl	0	26 h[d]
1-Naphthyl	2.9	20 min
2-Naphthyl	1.4	3.2 h
9-Phenanthrenyl	2.5	37 min
1-Anthryl	4.6	1.6 min
9-Anthryl	7.8	0.8 s
1-Pyrenyl	5.1	45 s
1-Perylenyl	5.6	22 s

[a]Enhancement in resonance energy of $ArCH_2\cdot$ compared with $PhCH_2\cdot$. [b]Estimated from eqn. 2 in ref. 121 with A = 14.21 and B = 17.14. [c]Assume $E(ArCH_2CH_2Ar) = E(PhCH_2CH_2Ph) - 2(\Delta RE)$. [d]From the Stein-McMillen correlation in tetralin (see text).

noted but not quantified.[12] Sato[165] reported significant decomposition of 1,2-bis(9-anthryl)ethane already at 300°C.

Thermolysis of **38** in tetralin at 450°C with 11 MPa added hydrogen was also much more rapid than that of **19**,[158] but the very high conversion reported (99%) does not allow quantitation of the extent of acceleration. In contrast with **19**, the presence of high-pressure hydrogen induced essentially no hydrodealkylation of **38**.[158] This may indicate that the added stability of radical **39**, compared with **20**, makes the competition between hydrogen abstraction from hydrogen and tetralin even less favorable for the former.

5.3 POLYPHENYLETHANES

Other known substitution patterns for dimethylene linkages in coal are the 1,1,2-triarylethane cross-linking group, for which the simplest model is 1,1,2-triphenylethane (**40**), and the 1,1-diarylalkane group, for which 1,1-diphenylethane (**36**) serves as a model; [the latter is considered here because the sp^3-sp^3 bond breaks most easily; in the context of breaking the coal network, it is better classified as a one-atom linkage (see Section 7)]. We examine here the thermolysis of **40**, **36**, and 1,1,2,2-tetraphenylethane (**41**), with ethylbenzene (**25**) as the initial reference point. Homolysis of **25** (Section 4.3) is much too slow at 400°C to be directly measurable, but we take $k_{46} \sim 10^{15.8}\exp(-74{,}600/RT)\ s^{-1}$ from Table 3. A VLPP study of **36**[166] gave $k_{73} = 10^{15.5}\exp(-67{,}600/RT)\ s^{-1}$. Recent liquid-phase tetralin carrier studies of **40** and **41**[167] gave $k_{74} = 10^{16.2}\exp(-57{,}800/RT)\ s^{-1}$ over the range 320-380°C and $k_{75} = 10^{15.9}\exp(-47{,}500/RT)\ s^{-1}$ over the range 200-277°C. These rate constants are compared in Table 10 in terms of half-life for homolysis at 400°C; to put the gas-phase values for **19**, **25**, and **36** and the liquid-phase values for **40** and **41** on a common gas-phase basis, we have arbitrarily increased k_{74} and k_{75} by 50% to correct for a probable small cage effect in the liquid studies,[167] as seen for **19** (Section 5.1.3). Even in the absence of aromatic rings more stabilizing than phenyl, the C-C bond in a 1,1,2-triarylethane unit is thus highly reactive at 400°C. In another confirmatory case, Benjamin and

Table 10. Rate Constants for Homolysis of Polyphenylethanes

Process	$k(s^{-1})$	$k_{400°C}(s^{-1})^a$	$t_{\frac{1}{2}}$, 400°C[a]
$PhCH_2CH_3$ ---> $PhCH_2\cdot$ + $CH_3\cdot$	$10^{15.8}$ exp(-74,600/RT)[a,b]	3.7×10^{-9}	5.9 yr
Ph_2CHCH_3 ---> $Ph_2CH\cdot$ + $CH_3\cdot$	$10^{15.5}$ exp(-67,600/RT)[a,c]	3.5×10^{-7}	28 days
$PhCH_2CH_2Ph$ ---> 2 $PhCH_2\cdot$	$10^{15.1}$ exp(-61,400/RT)[a,d]	1.4×10^{-5}	15 h
Ph_2CHCH_2Ph ---> $Ph_2CH\cdot$ + $PhCH_2\cdot$	$10^{16.2}$ exp(-57,800/RT)[e]	4.0×10^{-3} [e]	4.5 min[e]
$Ph_2CHCHPh_2$ ---> 2 $Ph_2CH\cdot$	$10^{15.9}$ exp(-47,500/RT)[e]	4.5[e]	0.2 s[e]

[a]Gas phase. [b]From Table 3. [c]Ref. 166. [d]Sato-Stein correlation; see text. [e]Ref. 167; in liquid tetralin; calculated k increased by 50% to account for probable small cage effect.

$$\underset{\mathbf{25}}{PhCH_2CH_3} \longrightarrow \underset{\mathbf{20}}{PhCH_2\cdot} + \cdot CH_3 \qquad (46)$$

$$\underset{\mathbf{19}}{PhCH_2CH_2Ph} \longrightarrow 2\ \mathbf{20} \qquad (55)$$

$$\underset{\mathbf{36}}{Ph_2CHCH_3} \longrightarrow \underset{\mathbf{42}}{Ph_2CH\cdot} + \cdot CH_3 \qquad (73)$$

$$\underset{\mathbf{40}}{Ph_2CHCH_2Ph} \longrightarrow \mathbf{42} + \mathbf{20} \qquad (74)$$

$$\underset{\mathbf{41}}{Ph_2CHCHPh_2} \longrightarrow 2\ \mathbf{42} \qquad (75)$$

coworkers[12] reported 99% decomposition of 1,2-diphenyl-1-p-tolylethane after 60 min at 400°C in tetralin.

Note first the enhancement in homolysis rate at 400°C from substituting a phenyl group onto a methyl group. In going from CH_3CH_2Ph to $PhCH_2CH_2Ph$ (k_{55}/k_{46}), it is 3,800; in going from CH_3CHPh_2 to $PhCH_2CHPh_2$ (k_{74}/k_{73}), it is 11,400. Next consider the enhancement from substituting a second phenyl group onto a carbon already containing one. In going from $PhCH_2CH_3$ to Ph_2CHCH_3 (k_{73}/k_{46}), it is 95; in going from $PhCH_2CH_2Ph$ to Ph_2CHCH_2Ph (k_{74}/k_{55}), it is 285; in going from $PhCH_2CHPh_2$ to $Ph_2CHCHPh_2$ (k_{75}/k_{74}), it is 1125. The larger enhancements in the first set than in the second reflect the now well-recognized fact that the resonance energy of diphenylmethyl radical (**42**) is less than twice that of benzyl radical. This attenuation in resonance energy results largely from the steric restrictions to placing both phenyl rings in the coplanar arrangement optimum for maximum overlap with the 2p orbital on the benzylic carbon. In polycyclic analogues of **42** for which this conformation is more nearly achieved already in a radical precursor, greater resonance stabilization can occur.[166] This is demonstrated by a comparison of D^o in Ph_2CH-H (80.9 kcal mol^{-1} [168]) with that in

9,10-dihydroanthracene (75.3 kcal mol^{-1} [20]). Hence, structural units in coal such as:

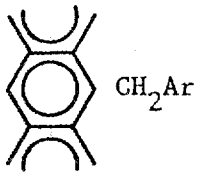

would be even more labile than predicted from the noncyclic model **40**.

The steady increase in rate enhancement which results from adding a phenyl group <u>within</u> each set above, as the "constant" carbon becomes progressively more phenylated, seems to result from steric destabilization of the ground state. A thermochemical kinetic analysis of **40** and **41**, each compared with its all-aliphatic parent (2-methylbutane and 2,3-dimethylbutane), led Stein[167] to conclude that the magnitude of such steric acceleration of homolysis for **41** was more than 10-fold at 300°C.

Livingston and coworkers[137] were able to observe radical **42** by ESR during thermolysis of flowing solutions of **41** in benzene or in benzene-diphenylmethane at temperatures (425°C) considerably less than needed to produce observable concentrations of radical **20** from **19**. By feeding a solution of diphenylmethane in benzene with added di-<u>t</u>-butyl peroxide as a radical source, Stein[167] established equilibrium 75 at

$$C_4H_9OOC_4H_9 \xrightarrow[\text{fast}]{\text{very}} 2\ C_4H_9O\cdot \quad \text{and/or} \quad CH_3COCH_3 + CH_3\cdot$$

$$C_4H_9O\cdot\ (CH_3\cdot) + Ph_2CH_2 \xrightarrow[\text{fast}]{\text{very}} C_4H_9OH\ (CH_4) + \underset{\mathbf{42}}{Ph_2CH\cdot}$$

$$\mathbf{41} \rightleftharpoons 2\ \mathbf{42} \qquad (75)$$

~375°C and found, from ESR assay for **42**:

$$K_{75} = 10^{6.7}\exp(-47{,}200/RT)\ M.$$

Note the consistency between the kinetic and thermodynamic information:[167]

$$\Delta H^{o}_{75,648} = 47.2 - E_{75,510} = 47.5 \text{ kcal mol}^{-1}$$

as expected for $E_{-75} \sim 0$.

5.4 METHYLATED BIBENZYLS

The central C-C bond in diarylethanes would also be further weakened by alkyl substituents at the benzylic carbons, both for electronic and steric reasons.[169] The temperatures necessary to achieve a half-life of 1 h in tetralin solution for the following structures are indicative of the significant magnitude of this effect:

$PhCH_2$-CH_2Ph	$t_{1/2}$ = 1 h at 444°C	(Reference 134,151)
$PhCH(CH_3)$-$CH(CH_3)Ph$	$t_{1/2}$ = 1 h at 365°C	(Reference 169)
$PhC(CH_3)_2$-$C(CH_3)_2Ph$	$t_{1/2}$ = 1 h at 233°C	(Reference 169)

Structures with the second substitution pattern might be expected in coal if hydroaromatic units are joined at their benzylic carbons as in, for example, 1,1'-bitetralyl (**43**) (cf. Reference 170).

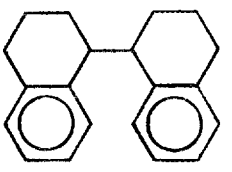

43

5.5 HETERO ATOM-CONTAINING TWO-ATOM LINKAGES

The compounds $PhCH_2XPh$ with X = O, S, or NH, which serve to model two-atom linkages containing a hetero atom, are each thermally more labile than bibenzyl (**19**). Elkobiasi and Hickinbottom[171] observed cleavage products, toluene (**18**) and phenol (**45**), and rearranged products,

o- and p-benzylphenol, from heating neat liquid benzyl phenyl ether (**44**) (X = O) for long periods at 250-270°C. Added 2-naphthol and quinoline were benzylated and hydroxyphenylated. These products suggest benzyl (**20**) and phenoxy (**46**) radicals as reactive intermediates, but the quantitative data were not detailed enough to calculate a material balance. Schlosberg and coworkers[172] observed ~40% conversion of liquid **44** after it was heated for 1 min at 375°C, but again a material balance is not available because of the formation of many unidentified heavy products. The molar ratio of observed products **45** : **18** : **19** ~ 72 : 26 : 2 suggests a greater loss of benzyl fragments to heavier products than of phenoxy fragments. Both benzylphenols and phenyl tolyl ether were noted as rearrangement products. Ozawa and coworkers[173] heated gaseous **44** at 400-500°C in the presence of heptane and hydrogen diluents. The major light products were **45**, **18**, and **19** in a molar ratio of ~60 : 20 : 20, which does represent a balance between benzyl and phenoxy fragments. In all these cases[171-3] however, the primary hydrogen-depleted products which must accompany the formation of **18** and **45** were not identified. [Of course, compared with **19**, ether **44** has no structural analog of stilbene to fill this role.]

Brucker and Kölling[11] reported clean formation of cleavage products **18** and **45** in equimolar amounts when **44** was heated in excess 1,2,3,4-tetrahydroquinoline at 300-350°C, a result analogous to the selective formation of **18** from **19** observed in hydrogen donor solvents. However, more recent studies have revealed that significant amounts of additional products, especially rearranged ones, persisted even in hydrogen donor solvents. Using a 9,10-dihydrophenanthrene medium at 300°C, Meyer and coworkers[174] observed 36-80% conversion in 20-40 min; 21-26% of the **44** consumed isomerized to benzylphenols (o : p = 2) while the remaining gave **18** and **45** in 75-65% and 82-95% selectivity, respectively. Diphenylmethane and various benzylated aromatics, detected by NMR, were also found. In a tetralin--1-methylnaphthalene--H_2 medium at 320°C, Kamiya and coworkers[14] observed 30% conversion in 30 min; 40% of the **44** consumed isomerized to benzylphenols while the remaining gave **18** and **45** in 92% and 83% selectivity, respectively. After 30 min at 400°C, the corresponding values were 100% conversion, 17% isomerization,

and 86% and 80% selectivity to the cleavage products.[154] King and Stock[156] also described the formation largely of **18** and **45**, along with small amounts of benzylphenols and diphenylmethane, from runs in tetralin at 350°C. Sato and Yamakawa[155] reported the major products formed in tetralin at 300°C to be **18** and **45** and the minor products to be benzophenone, benzhydrol, diphenylmethane, and benzylphenols. In contrast, Schlosberg and coworkers[172] described the major isomerization product formed in tetralin or tetrahydroquinoline after 1 min at 375°C to be phenyl tolyl ether rather than benzylphenol.

These product patterns are qualitatively consistent with C-O homolysis in step 76a followed by radical capture by hydrogen abstraction from tetralin in steps 59 and 77a. The benzylphenols probably represent radical coupling at ring carbons (step 78), at least in part in the cage. This difference from the behavior of **19**, from which methyldiphenylmethanes are only minor products,[105] may result from the known greater tendency of radical **46**, compared with **20**, to couple at ring carbons.[175] The minor products containing the Ph_2CH- unit probably result from a 1,2-phenyl shift from O to C in radical **47** in step 80, analogous to step 66 for the all-carbon analog (Sections 5.1.3 and 11.6).

To ascertain whether the rate of thermolysis of **44** is quantitatively consistent with homolysis step 76a being rate-determining, we compare the available tetralin-carrier kinetic data (all in the liquid phase) with thermochemically based predictions of D^o for the C-O bond. Sato and Yamakawa[155] found $k = 10^{15.2}\exp(-53{,}200/RT)\ s^{-1}$ for disappearance of **44** in tetralin at 260-320°C. Yao and Kamiya's data[154] give $k = 10^{13.4}\exp(-46{,}900/RT)\ s^{-1}$ in tetralin--1-methylnaphthalene--H_2 at 320-350°C. Stein[145] reported $k = 3.0 \times 10^{-5}\ s^{-1}$ at 300°C in tetralin. These results are compiled in Table 11 along with several other "one-point" rate constants that we have calculated from single conversion-time observations, with first-order behavior assumed. The agreement among different research groups, especially between the two temperature-effect studies,[154,155] is rather poor. For a direct comparison to the behavior of **19** in the liquid phase, we <u>assume</u> $A_{76a} = 10^{16.6}\ s^{-1}$, as for **19**, and calculate the corresponding E_{estd} values for each experimental rate constant listed in Table 11. The

results from the six separate research groups for four separate solvent systems then cluster closely to E_{76a} = 56.0 kcal mol^{-1}, a reduction of ~10.5 kcal mol^{-1} from E_{55} for **19** in the liquid phase.

		$PhCH_2XPh$	$\longrightarrow$	$PhCH_2\cdot$	+	$PhX\cdot$
(a)	(X = O)	**44**		**20**		**46**
(b)	(X = S)	**48**				**50**
(c)	(X = NH)	**53**				**56**

(76)

20 + 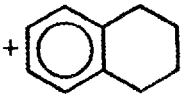 $\longrightarrow$ $PhCH_3$ + 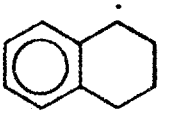

34 **18** **35**

(59)

	$PhX\cdot$	+	**34**	$\longrightarrow$	$PhXH$	+ **35**
(a)	**46**				**45**	
(b)	**50**				**49**	
(c)	**56**				**54**	

(77)

20 + **46** $\longrightarrow$

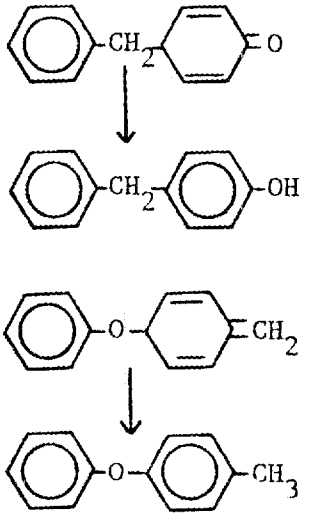

(78)

		$PhCH_2XPh$	+	$R\cdot$	$\longrightarrow$	$Ph\dot{C}HXPh$	+ RH
(a)	(X = O)	**44**				**47**	
(b)	(X = S)	**48**				**51**	

(79)

$$PhCHXPh \longrightarrow Ph_2\dot{C}HX \longrightarrow \longrightarrow \quad (80)$$

Table 11. Rate Data for Disappearance of Phenyl Benzyl Ether in Hydrogen Donor Solvents

T(°C)	Solvent system	$10^6 k(s^{-1})$	$E_{estd}(kcal\ mol^{-1})^a$	Ref.
260	Tetralin	0.23[b,c]	56.7	155
280	Tetralin	1.42[b,c]	56.7	155
300	Tetralin	7.82[b,c]	56.8	155
300	Tetrahydroquinoline	37[d,e]	55.1	11
300	Tetralin	30[b]	55.3	145
300	Dihydronaphthalene	370[d]	52.5	174
320	Tetralin	36.5[b,c]	57.0	155
320	Tetralin-Methylnaphthalene-H_2	139[b,f]	55.4	154
320	Tetralin-Methylnaphthalene-H_2	210[d]	54.9	14
340	Tetralin-Methylnaphthalene-H_2	519[b,f]	55.8	154
350	Tetrahydroquinoline	97[d,e]	58.8	11
350	Tetralin	670[d]	56.4	156
350	Tetralin-Methylnaphthalene-H_2	952[b,f]	55.9	154

[a]Based k and assumed $A = 10^{16.6}\ s^{-1}$. [b]Reported first-order rate constant. [c]These four values gave $k = 10^{15.2} \exp(-53{,}200/RT)\ s^{-1}$. [d]Calculated first-order rate constant from a single reported conversion-time data point. [e]These two values, based on rather high conversions, gave the unreasonable $k = 10^{0.8} \exp(-13{,}700/RT)\ s^{-1}$. [f]These three values gave $k = 10^{13.4} \exp(-46{,}900/RT)\ s^{-1}$.

One approach to estimating D^o values for $PhCH_2XPh$ is shown in Table 12 as "Method 1." We begin with currently accepted values of $D^o(CH_3CH_2\text{-}XCH_3)$ where the order is $CH_2\text{-}CH_2 \sim CH_2\text{-}O \gtrsim CH_2\text{-}NH > CH_2\text{-}S$. These will be altered unequally in going to $PhCH_2XPh$ because the value of $RE(PhX\cdot)$ depends on X. The required RE values are estimated in Table 12 as the difference between $D^o(CH_3X\text{-}H)$ and $D^o(PhX\text{-}H)$. Then we can estimate $D^o(PhCH_2\text{-}XPh)$ as shown in the last column of Table 12. [Note that radical "stabilities" based on X-H bond strengths are not necessarily identical to those based on X-C bond strengths.[176]] A second estimation procedure is shown in Table 12 as "Method 2." Here we use the definition $D^o(PhCH_2\text{-}XPh) = \Delta H_f{}^o(PhX\cdot) + \Delta H_f{}^o(PhCH_2{}^\cdot) - \Delta H_f{}^o(PhCH_2XPh)$. Group additivity methods must be used to estimate the last term because experimental data are not available. The agreement between the two estimation methods is well within their error limits for X = CH_2, O, and NH but is poorer for X = S.

Thermochemistry thus predicts a decrease in E for homolysis in going from **19** to ether **44** of ~8.5 kcal mol^{-1} in the gas phase compared with the "observed" liquid-phase value (Table 11) of ~10.5 kcal mol^{-1}. We judge this to be acceptable agreement, considering the scatter in the data and the approximations involved in estimating D^o. The conclusion that C-O homolysis is the rate-controlling step in the thermolysis of **44** is further strengthened by the observation[156] that the rate was unaffected by added benzyl phenyl sulfide, 9,10-anthraquinone, or naphthacene and was only very moderately accelerated by added phenol[14,155] or benzoic acid at high concentrations. Analogies for modest acceleration of homolyses which produce O-centered radicals in hydrogen bonding solvents are known.[177]

Data for benzyl phenyl sulfide (**48**) (X = S) are more limited. Heating **48** at 270°C for 96 h in the nondonor solvent isoquinoline[178] gave toluene (**18**) (25%), bibenzyl (**19**) (30%), and stilbene (**31**) (15%), products reasonably derived from radical **20**, along with thiophenol (**49**) (41%), reasonably derived from thiophenoxy radical (**50**). Under conditions of complete consumption of neat **48** (400°C for 30 min), Alnajjar and Franz[179] found **18**, **49**, diphenylmethane (**32**), diphenyl disulfide (**52**), triphenylmethane, diphenyl sulfide,

Table 12. Estimation of $D^\circ(PhCH_2\text{-}XPh)$[a]

Method 1

X	Inherent C-X Bond Strength		RE(PhX·)			$D^\circ(PhCH_2\text{-}XPh)$[c]
	Standard	D° [b]	Standards	D° [b]	RE(PhX·)	
CH_2	$CH_3CH_2\text{-}CH_2CH_3$	82.2	$CH_3CH_2\text{-}H$	98.2	10.2	61.8
			$PhCH_2\text{-}H$	88.0		
O	$CH_3CH_2\text{-}OCH_3$	81.8	$CH_3O\text{-}H$	104.4	17.9	53.9
			PhO-H	86.5		
S	$CH_3CH_2\text{-}SCH_3$	73.3	$CH_3S\text{-}H$	90.7	7.4	55.7
			PhS-H	83.3		
NH	$CH_3CH_2\text{-}NHCH_3$	79.8	$CH_3NH\text{-}H$	100.0	12.0	57.6
			PhNH-H	88.0		

Method 2

X	$\Delta H_f^\circ(PhCH_2XPh)$[d]	$\Delta H_f^\circ(PhX\cdot)$[b]	$D^\circ(PhCH_2\text{-}XPh)$[e]
CH_2	34.2[f]	47.8	61.4
O	6.5	11.4	52.7
S	51.1	54.9	51.6
NH	46.3	56.7	58.2

[a]All values in kcal mol^{-1} at 298 K. [b]All values from ref. 20. [c]$D^\circ(PhCH_2\text{-}XPh) = D^\circ(CH_3CH_2\text{-}XCH_3) - RE(PhX\cdot) - RE(PhCH_2\cdot)$. [d]Estimated by group additivity from parameters in ref. 29. [e]$D^\circ(PhCH_2\text{-}XPh) = \Delta H_f^\circ(PhCH_2\cdot) + \Delta H_f^\circ(PhX\cdot) - \Delta H_f^\circ(PhCH_2XPh)$. [f]See Table 1.

2-phenylbenzothiophene, and 2,3-diphenylbenzothiophene. Key steps in their proposed reaction scheme, which should be especially important in the early stages of reaction, were 76b, 79b, and 80b. Note again the proposal of a 1,2-phenyl shift as a decay route for radical **51**. Under FVP conditions (800°C, ~1 Pa), gaseous **48** gave an equimolar mixture of **19** and **52**[180] by what appears to be homolysis followed by symmetrical radical combinations to form more stable products. Ignasiak and Strauss[181] observed the formation of **18** and **49** in a ratio of 1 : 0.86 when **48** was heated in excess tetralin at 388°C; diphenyl sulfide and **32** were formed in smaller amounts. Under similar conditions, Panvelker and coworkers[182] also found **18** but noted benzene rather than **49** as the second major product, behavior suggestive of a secondary desulfurization process. Thermolysis in the gas phase at 500°C for ~10 s (>98% conversion) in the presence of benzene diluent gave **18** > **31** ~ **52** ~ **49** > **19**; an excess of added tetralin and dihydroanthracene lowered conversion to 92% and sharply increased the amounts of **18** and **49** (1 : 0.75) while lowering those of **52**, **31**, and **19**.[183] Panvelker and coworkers[182] reported a 3-fold increase in the rate of disappearance of **48** in tetralin-mesitylene solvent at 350°C on adding 10-14 MPa hydrogen. This increase is much larger than that observed under similar conditions for **19** (Section 5.1.4). It probably results from a hydrodethiolation step such as 81, but no product data were reported for the hydrogen-perturbed system.

$$\mathbf{48} + H_2 \longrightarrow PhCH_2SH + \mathbf{9} \qquad (81)$$

Kinetic data for disappearance of sulfide **48** are also more limited than for ether **44**. Stein[145] found $k = 1.04 \times 10^{-5}\ s^{-1}$ in tetralin at 300°C. Panvelker and coworkers[182] found $k = 10^{14.7}\exp(-51{,}700/RT)\ s^{-1}$ in mesitylene-tetralin (11 : 1) over the small range of 345-365°C and $k = 10^{13.9}\exp(-49{,}200/RT)\ s^{-1}$ in tetrahydroquinoline. This "solvent effect" in terms of rate constants at 350°C is only 20%; thus, the presence of a nucleophilic nitrogen atom in the latter solvent has not induced an added ionic pathway. Converted to a "liquid-phase $A = 10^{16.6}\ s^{-1}$ standard" (see above), these measurements lead to

E_{76b} = 56.6, 57.1, and 56.8 kcal mol^{-1}, respectively, for an average ~1 kcal mol^{-1} greater than that for ether **44** (cf. Table 11). In terms of thermochemical comparison, this experimental value would suggest that "Method 1" in Table 12 is preferable to "Method 2" for X = S.

Abraham and Klein[184] observed the formation of toluene (**18**), aniline (**54**), and benzalaniline (**55**) in a molar ratio of ~5 : 6 : 2, along with minor amounts of **19**, **32**, o-benzylaniline, and heavier products, when neat benzyl phenyl amine (**53**) (X = NH) was heated at 386°C. In tetralin, **18** and **54** were the major products, although some **55** persisted. King and Stock[156] also observed formation of **18** and **54** from heating **53** in tetralin at 400°C. Stein[145] reported $k = 4.4 \times 10^{-5}\ s^{-1}$ for disappearance in tetralin solvent at 375°C. Abraham and Klein[184] reported $2.7 \times 10^{-4}\ s^{-1}$ at 386°C. King and Stock's data at 400°C[156] allow calculation of "one-point" rate constants of $1.5 \times 10^{-4}\ s^{-1}$ in tetralin and $3.3 \times 10^{-4}\ s^{-1}$ in diphenylmethane--tetralin-d_{12}. Again converted to the "$A = 10^{16.6}\ s^{-1}$ standard" (see above), these rate constants correspond to E_{76c} = 62.1, 60.8, 62.9, and 61.8 kcal mol^{-1}. While they thus appear consistent with expectations for step 76c (Table 12), King and Stock[156] noted accelerating effects of several additives on the thermolysis of this amine which were much greater than for other members of the $PhCH_2XPh$ series: 12-fold by equimolar 1-naphthol; 9-fold by equimolar benzoic acid; 2.6-fold by 1/8 the molar amount of naphthacene; and 6-fold by 1/8 the molar amount of sulfide **48** (or, more likely, its decomposition products). Abraham and Klein[184] reported that the rate of disappearance of **53** in tetralin was only 1/7 that without the hydrogen donor solvent, a decrease much larger than expected from simply elimination of induced decomposition to form **55**. These effects deserve further attention because they serve as hints of competing, possibly ionic, pathways.

In summary, the available liquid-phase, hydrogen-donor-carrier kinetic data for homolysis of the the series $PhCH_2XPh$, forced to a common A value of $10^{16.6}\ s^{-1}$, give E values of 66.6, 62, 57, and 56 kcal mol^{-1} for X = CH_2, NH, S, and O, respectively. This order correlates with the order of bond strengths estimated in Table 12. The consistent offset of $E > D^{o}$ presumably reflects the same factors explored in Section 5.1.3 for the small difference between liquid-phase and gas-phase Arrhenius

parameters for **19**. In more concrete terms, this spread in E_{76} values corresponds at 400°C to relative rates of 1 : 30 : 1300 : 2800 and half-lives for homolysis of about 20 h, 40 min, 55 s, and 25 s for X = CH_2, NH, S, and O, respectively.

Thermolyses of 1-naphthylmethyl phenyl ether[185] and 1-naphthyl benzyl ether[186] each gave products consistent with a radical mechanism, but the results do not add significant new mechanistic detail.

5.6 RELATIVE REACTIVITIES IN HYDROGEN ABSTRACTION BY BENZYL RADICAL

Because of the prominent role played by benzylic radicals in the thermal chemistry of two-atom linkages and of other linking units as well (Sections 7-10), recent studies have been conducted, typically at temperatures in the 150-200°C range, of the relative rates at which benzylic radicals abstract hydrogen from various donors. Bockrath and coworkers[132] produced benzyl radical (**20**) from thermolysis of dibenzyl mercury at 170°C in the presence of various donors and used deuterium atom abstraction from triphenylsilane-d as the internal reference point. Representative relative rates of abstraction, on a per hydrogen basis, are listed in Table 13. Franz and coworkers[142] produced a ring-substituted example, 2-allylbenzyl radical (**57**), from thermolysis of its

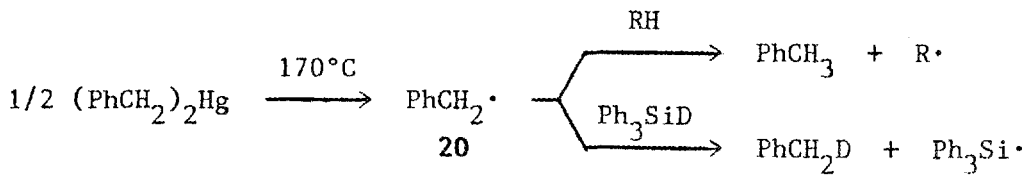

azo precursor at 160°C and used its intramolecular cyclization to 2-indanylmethyl radical (**58**) (Section 10.1.6) as the "radical clock".[187] Representative results are also listed in Table 13. The agreement between the two studies is satisfactory and confirms the contention[142] that the 2-allyl substituent does not significantly perturb the inherent benzyl radical selectivity.

The relative rate sequence mesitylene (or m-xylene) : bibenzyl : diphenylmethane : triphenylmethane = 1 : 4.5 : 21 : 91 reflects the added stability as a primary benzylic radical becomes progressively secondary,

Table 13. Relative Rates of Hydrogen Atom Transfer to Benzylic Radicals

Donor	$k_{rel}^{170°C}$(per H)[a]	$k_{rel}^{160°C}$(per H)[b]
Mesitylene	0.05	
m-Xylene		0.05
Diphenylmethane	0.96	0.93
Triphenylmethane	4.3	
Bibenzyl	0.21	0.23
1,3-Diphenylpropane	0.30	
1-Methylnaphthalene	0.18	
1-Ethylnaphthalene	0.46	
Indane	0.50	
Tetralin	1.00[c]	1.00[c]
9,10-Dihydrophenanthrene	1.5	1.9
4,5-Dihydropyrene	3.6	
1,2-Dihydronaphthalene	3.3	
Fluorene	7.9	12
9,10-Dihydroanthracene	33	41
5,6,7,8-Tetrahydroquinoline	1.4	
Phenol		5.6
1-Naphthol		73[d]
Benzenethiol		6×10^4

[a]Benzyl radical; Ref. 132. [b]o-Allylbenzyl radical; Ref. 142. [c]Assigned for each column. [d]Ref. 188.

doubly benzylic, and triply benzylic. Locking a benzylic carbon with a given substitution pattern into a five- or six-membered ring leads to an enhanced rate; e.g., bibenzyl : indane : tetralin = 1 : 2.3 : 4.4. This increase results at least in part from a more favorable entropy of activation because the resonance-stabilizing overlap between the developing p-orbital at the radical center and the adjacent π-system can occur in the cyclic case without the need to freeze out an internal

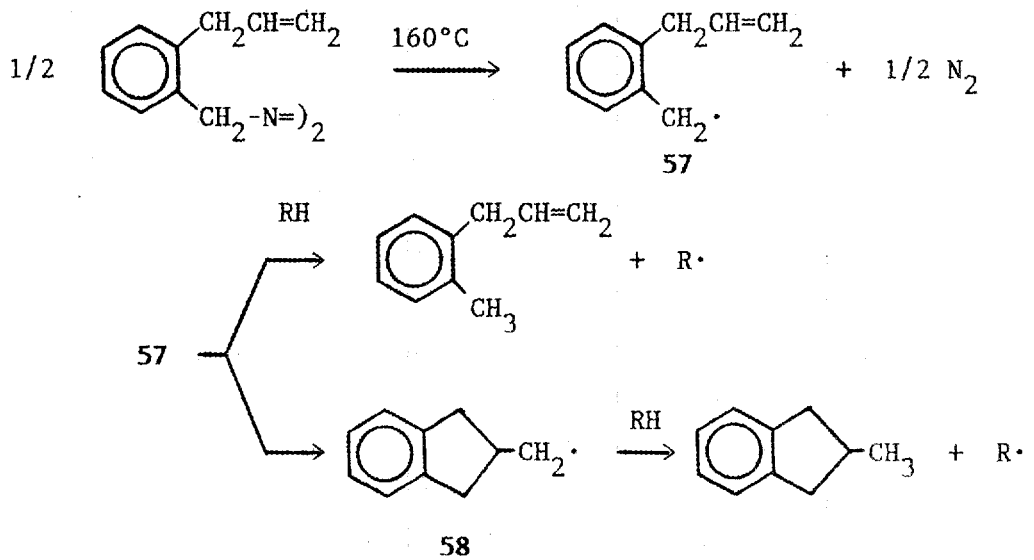

rotation. The ring effect is even more dramatic for the comparison diphenylmethane : fluorene : 9,10-dihydroanthracene (1 : 10 : 36) because steric inhibition of resonance is reduced in the cyclic examples (Section 5.3). Replacing the phenyl ring by a larger aromatic ring system leads to the expected increase in reactivity (Section 5.2); e.g., mesitylene : 1-methylnaphthalene = 1 : 3.8 and tetralin : 9,10-dihydrophenanthrene : 4,5-dihydropyrene = 1 : 1.7 : 3.7. The interplay of these factors leads to the following order of reactivity for hydrogen abstraction from the most commonly studied model donor solvents (on a per hydrogen basis): 9,10-dihydroanthracene >> 1,2-dihydronaphthalene > 4,5-dihydropyrene > 9,10-dihydrophenanthrene > tetralin.

The relative rates in Table 13 can be converted to ΔE values, if it is assumed that the A factors are all similar, and then compared with differences in C-H bond energies.[20] For the mesitylene--1-methylnaphthalene pair, $\Delta E \sim RT\ln(k'/k) \sim 1.2$ kcal mol^{-1} while $\Delta D^{o} \sim 2.9$ kcal mol^{-1}; for the mesitylene--diphenylmethane pair, $\Delta E \sim 2.7$ kcal mol^{-1} while $\Delta D^{o} \sim 4$ kcal mol^{-1}; for the mesitylene--9,10-dihydroanthracene pair, $\Delta E \sim 5.8$ kcal mol^{-1} while $\Delta D^{o} \sim 12.7$ kcal mol^{-1}. Thus, approximately one-half the difference in C-H bond strengths is manifested at the transition state for abstraction, a fully reasonable result for hydrogen transfer between centers of similar electronegativity.[24e] In contrast, the high hydrogen atom donor abilities of phenol and thiophenol cannot be rationalized from bond strength effects alone but reflect the well-known occurrence of stabilizing polar effects in hydrogen transfer between centers of differing electronegativity.[24e] For example, the ΔE, as defined above, for the mesitylene--thiophenol pair is 12 kcal mol^{-1}, over twice ΔD^{o}.

Franz and coworkers[142] assigned absolute rate constants for reaction of **57** with m-xylene, p-xylene, diphenylmethane, and fluorene on the basis of an assignment of the rate constant for cyclization which was itself derived[187] from a series of straightforward, but nonetheless indirect, rate comparisons ultimately anchored to the self-combination reaction of **20**. These Arrhenius expressions offer one approach to estimating the degree to which the relative rates of hydrogen abstraction at 160-170°C will be compressed in going to the 400°C range. For example, the 240-fold difference between fluorene and m-xylene at 160°C would be reduced to 75-fold at 400°C on this basis. However, this procedure must be viewed with some caution based on indications[142,143] that there may be a significant tunneling contribution to hydrogen atom transfer even at 160-170°C, such that Arrhenius plots would be curved.

A relevant high-temperature gas-phase relative rate study is that of Fixari and le Perchec,[189] who produced **20** from thermolysis of dibenzyl sulfone at 500°C in the presence of various donors and used coupling of **20** as the internal reference point. The relative rates of hydrogen

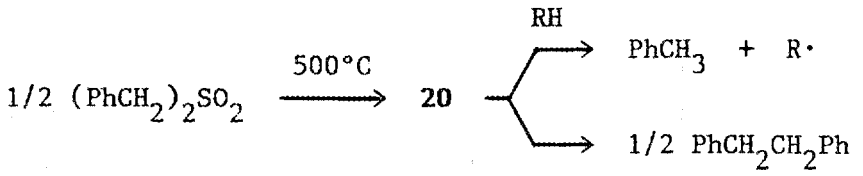

abstraction fell in the order: 9,10-dihydroanthracene > 1,2-dihydronaphthalene > tetralin ~ 9,10-dihydrophenanthrene > 1-methylnaphthalene > t-butylbenzene. This order is generally consistent with the lower temperature data, but a more quantitative comparison is not possible because the ratio of hydrogen abstraction : radical combination contains a dependence on the concentration of **20** which need not have been the same from case to case.

6. BIARYLS (ZERO-ATOM LINKAGES)

Compared with bibenzyl (Section 5), biphenyl (**10**) is very stable. Gaumann and Rayroux[190] reported that liquid **10**, containing 2% diphenylmethane impurity, decomposed very slowly at 472°C (~2 mol% h^{-1}) to give benzene (**9**), terphenyls (**59**), quaterphenyls (**60**), and hydrogen according to the stoichiometry:

$$\underset{\mathbf{10}}{\text{Ph-Ph}} \longrightarrow 0.53\ \underset{\mathbf{9}}{\text{PhH}} + 0.25\ \underset{\mathbf{59}}{\text{Ph-C}_6\text{H}_4\text{-Ph}} + 0.18\ \underset{\mathbf{60}}{\text{Ph-C}_6\text{H}_4\text{-C}_6\text{H}_4\text{-Ph}} + 0.04\ \text{H}_2 \qquad (82)$$

where the isomer ratio for **59** was o : m : p = 11 : 50 : 38 and for **60** was o,o' : o,m' : o,p' : m,m' : m,p' : p,p' = 1 : 12 : 7 : 29 : 39 : 12. With the assumption of first-order behavior, the rate constant was $10^{14}\exp(-66{,}000/RT)\ s^{-1}$ over the range 438-472°C. The authors recognized that this value of E, compared with the much larger (updated) values of $D^o(C_6H_5\text{-}C_6H_5) = 113.7$ kcal mol^{-1} (Table 4) and $D^o(C_6H_5C_6H_4\text{-}H) \sim D^o(C_6H_5\text{-}H) = 111$ kcal mol^{-1},[20] is strongly suggestive of chain behavior. Combining various literature suggestions[65,190,191] with current knowledge of the behavior of aryl radicals and hydrogen atom

(Sections 3.1, 4.1.2, and 5.1.4) allows writing the following hypothetical chain, in which each of the species hydrogen atom, phenyl radical (**11**), and biphenylyl radical (**61**) is allowed to interact with **10** by abstracting hydrogen, displacing aromatic hydrogen, or displacing **11**:

$$0.04\ H\cdot + 0.04\ \mathbf{10} \longrightarrow 0.04\ H_2 + 0.04\ \underset{\mathbf{61}}{Ph\text{-}C_6H_4\cdot} \quad (83)$$

$$(0.39 - x)\ H\cdot + (0.39 - x)\ \mathbf{10} \longrightarrow (0.39 - x)\ \mathbf{9} + (0.39 - x)\ \underset{\mathbf{11}}{Ph\cdot} \quad (84)$$

$$(0.14 + x)\ \mathbf{11} + (0.14 + x)\ \mathbf{10} \longrightarrow (0.14 + x)\ \mathbf{9} + (0.14 + x)\ \mathbf{61} \quad (85)$$

$$(0.25 - x)\ \mathbf{11} + (0.25 - x)\ \mathbf{10} \longrightarrow (0.25 - x)\ \mathbf{59} + (0.25 - x)\ H\cdot \quad (86)$$

$$0.18\ \mathbf{61} + 0.18\ \mathbf{10} \longrightarrow 0.18\ \mathbf{60} + 0.18\ H\cdot \quad (87)$$

$$x\ \mathbf{61} + x\ \mathbf{10} \longrightarrow x\ \mathbf{59} + x\ \mathbf{11} \quad (88)$$

Addition of these steps for x in the range 0-0.25 will produce the observed stoichiometry 82. However, if we assume that initiation involves homolysis of the weakest bond(s) in **10** and take its rate constant as $\sim 10^{16}\exp(-111{,}000/RT)\ s^{-1}$ based on the D^o values above, the unreasonable chain length of $\sim 10^{11}$ would be required to produce the observed rate of ~2 mol% h^{-1}. Although the chain pictured may thus rationalize the observed products, the source of initiation remains unknown, as in the thermolysis of benzene itself (Section 3.1).

Lutz[191] observed formation of **9**, **59** (o : m : p = 1 : 62 : 37), and hydrogen from thermolysis of highly purified, gaseous **10** at temperatures as low as 400°C, although the rate was extremely slow (~0.001 mol% h^{-1}). No **60** was detected; rather a "polyphenyl" residue formed on the surface of the glass reaction vessel. The typical stoichiometry was:

$$\mathbf{10} \longrightarrow 0.68\ \mathbf{9} + 0.23\ \mathbf{59} + 0.63/n\ \langle C_6H_{3.9}\rangle_n + 0.05\ H_2$$

Effects of S/V on rate suggested that reaction occurred totally on the vessel surface and that there was no true homogeneous component. When the charge of **10** used was large enough to exceed the saturation vapor pressure of 1 MPa, such that a distinct liquid phase appeared, the thermolysis rate was modestly accelerated.

Fields and Meyerson[192] observed 1.2% conversion of **10** in nitrogen carrier in 7.5 s at 700°C to give **59**, **60**, and quinquephenyl in a ratio of 1.16 : 1.00 : 0.02; **9** was also formed but not quantified. These authors suggested mechanisms involving formal additions and eliminations proceeding through cyclohexadienes as discrete intermediates, but radical displacements proceeding through cyclohexadienyl radicals again seem more likely, especially at these higher temperatures.

The sensitivity of **10** towards radical-initiated hydrogenolysis appears more directly relevant to coal conversion than are these slow thermal conversions. We have seen (Table 8) that addition of high-pressure hydrogen during thermolysis of bibenzyl (**19**) in tetralin induced the hydrodealkylation pathway that gives benzene (**9**) and ethylbenzene (**25**) as a significant, although still minor, competitor to the homolysis pathway that gives toluene (**18**). In that same series of thermolyses carried out at 450°C for 30 min, Vernon[158] demonstrated that **10** in tetralin was inert unless both **19**, as a thermal source of radicals, and high-pressure hydrogen, as a specific source of hydrogen atom, were present. Under those conditions, however, **10** was efficiently cleaved to form **9**. Since these conditions are a realistic model for typical liquefaction processes, hydrogenolysis of diaryl linkages can be anticipated as a bond-breaking process. In the presence of hydrogen and good hydrogen donors, the set of steps 83-88 almost surely collapses to the simple chain consisting of steps 84 and 89 because step 89 will supersede steps 85 and 86 and equilibrium 83 will be shifted to the left. From the relative amounts of **9** and **25** produced, it can be deduced that step 84 occurred ~1/3 as fast as step 64. Of course, the overall rate of each is the product of the rate constant for ipso addition of hydrogen atom and

$$\underset{}{H\cdot} + \underset{\mathbf{10}}{Ph\text{-}Ph} \longrightarrow \underset{\mathbf{9}}{PhH} + \underset{\mathbf{11}}{Ph\cdot} \qquad (84)$$

$$\mathbf{11} + H_2 \longrightarrow \mathbf{9} + H\cdot \qquad (89)$$

$$H\cdot + \underset{\mathbf{19}}{PhCH_2CH_2Ph} \longrightarrow \mathbf{9} + PhCH_2CH_2\cdot \qquad (64)$$

the fraction of the resulting cyclohexadienyl radical which proceeds on to product rather than reverting to starting materials. While the hydrogenolysis of **10** is thus actually somewhat slower than that of **19**, it appears more dramatic because the "thermal background" for **10** is so small.

An intramolecular version of the dehydrogenative condensation of benzene (Section 3.1) applied to larger biaryls of appropriate constitution would give polycyclic aromatics, e.g., the conversion of 1,1'-binaphthyl to perylene:

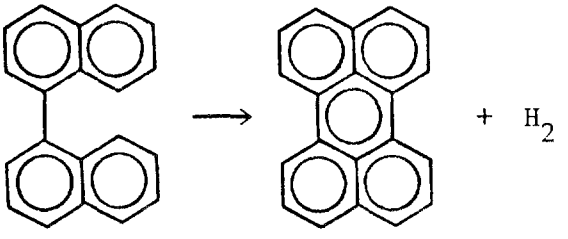

Stein and Senthilnathan[67] have recently reported that such dehydrogenative cyclizations are catalyzed by hydrogen donors, behavior suggestive that cyclohexadienyl rather than aryl radicals may be involved in the intramolecular C-C bond formation step.

7. ONE-ATOM LINKAGES

7.1 DIPHENYLMETHANE

Diphenylmethane (**32**), the simplest model for one-carbon linkages, is also much more stable thermally than bibenzyl (Section 5). In the low-temperature regime, it is experimentally stable: $t_{1/2} > 9000$ h at 400°C in tetralin solvent.[151] In the high-temperature regime, a VLPP

study at 750-975°C by Rossi, McMillen, and Golden[168] showed that C-C homolysis (step 90) and C-H homolysis (step 91) occurred competitively

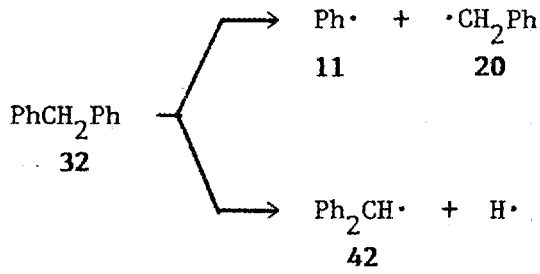

(90)

(91)

under unimolecular conditions. Starting with analyses which assigned $A_{90} = A_{91} = 10^{15.3}\ s^{-1}$, the authors derived $k_{90} = 10^{15.3}\exp(-82{,}300/RT)\ s^{-1}$ and $k_{91} = 10^{15.3}\exp(-81{,}400/RT)\ s^{-1}$. These Arrhenius expressions were then used to derive $\Delta H_f^{o}(\mathbf{42}) = 69.0$ kcal mol^{-1} [Stein[193] found 68.0 kcal mol^{-1} from a VLPP study of C-C fission in 1,1-diphenylethane; see Section 5.3], $D^{o}(Ph_2CH\text{-}H) = 81.4$ kcal mol^{-1}, and $D^{o}(PhCH_2\text{-}Ph) = 86.7$ kcal mol^{-1}. The unusually large difference between the latter value and E_{90} reflects a large negative estimated $\langle\Delta C_p^{o}{}_{90}\rangle$. We note, however, that this analysis began with a value of $\Delta H_f^{o}(\mathbf{32}) = 39.7$ kcal mol^{-1}, estimated from group additivity, whereas the selected value[31] from experimental data is 36.8 kcal mol^{-1}; this difference of 2.9 kcal mol^{-1} corresponds to the difference between $D^{o}(PhCH_2\text{-}Ph)$ given here and that listed in Table 4.

Sweeting and Wilshire[140] had much earlier observed ~2% conversion of **32** in nitrogen carrier after 8-24 s at 700°C. This flow-system behavior corresponds to $k = 0.8\text{-}2.5 \times 10^{-3}\ s^{-1}$ whereas the VLPP results[168] predict $1.7 \times 10^{-3}\ s^{-1}$ for the sum of C-C and C-H homolysis. The good agreement suggests that homolysis is rate-controlling in the high-temperature, low-pressure regime. In contrast, Petrocelli and Klein[129] derived much lower Arrhenius parameters [$k = 10^{12.7}\exp(-66{,}000/RT)\ s^{-1}$] from static thermolyses in biphenyl diluent at still lower temperatures (550-600°C) and much higher pressures (1.8-6.2 MPa). This expression corresponds to $k = 1.5 \times 10^{-5}\ s^{-1}$ at 550°C, some 20-fold greater than that extrapolated from the VLPP results.[168] While this discrepancy might suggest the

occurrence of a chain reaction at higher concentrations, there is no direct evidence, and a fully consistent kinetic picture is not available.

In spite of the kinetic differences, the products reported in the two gas-phase studies were identical: benzene (**9**), toluene (**18**), and fluorene (**62**) in a ratio (1.0 : 1.3 : 1.1[140] and ~1 : 1 : 1[129]) which constitutes a stoichiometric balance. Note that these represent both a cracking and a retrograde reaction. One speculative hypothesis to rationalize these products by a nonchain sequence consists of steps 90 and 92-96:

$$\underset{\mathbf{32}}{PhCH_2Ph} \longrightarrow \underset{\mathbf{11}}{Ph\cdot} + \underset{\mathbf{20}}{\cdot CH_2Ph} \qquad (90)$$

$$\mathbf{11} + \mathbf{32} \longrightarrow \underset{\mathbf{9}}{PhH} + \underset{\mathbf{42}}{Ph_2CH\cdot} \qquad (92)$$

$$\mathbf{20} + \mathbf{32} \longrightarrow \underset{\mathbf{18}}{PhCH_3} + \mathbf{42} \qquad (93)$$

42 ⟷ 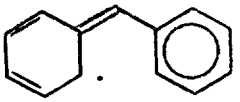 ⟶ 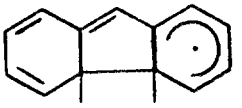 (94)

63

63 + **42** ⟶ 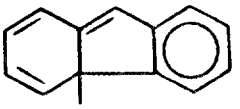 + **32** (95)

64

64 ⟶ 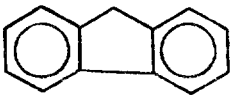 (96)

62

---

2 **32** ⟶ **9** + **18** + **62**

However, this sequence does not allow for competitive C-H homolysis

(step 91). The major expected fate of hydrogen atom would be formation of hydrogen by abstraction from the doubly benzylic position (step 97).

$$H\cdot + \mathbf{32} \rightleftharpoons H_2 + \mathbf{42} \qquad (97)$$

Yet, hydrogen was not reported, nor would its formation be consistent with the stoichiometry among **9**, **18**, and **62**. A second hypothesis, which would avoid formation of hydrogen as a major product, would be a chain sequence consisting of steps 98, 93, 94, and 96, for which steps 90 and

$$\mathbf{63} + \mathbf{32} \longrightarrow \mathbf{64} + \mathbf{9} + \mathbf{20} \qquad (98)$$

$$\mathbf{20} + \mathbf{32} \longrightarrow \mathbf{18} + \mathbf{42} \qquad (93)$$

$$\mathbf{42} \longrightarrow \mathbf{63} \qquad (94)$$

$$\mathbf{64} \longrightarrow \mathbf{62} \qquad (96)$$

$$2\ \mathbf{32} \longrightarrow \mathbf{9} + \mathbf{18} + \mathbf{62}$$

91 only serve as initiating events. Step 98 is a radical hydrogen transfer from the cyclohexadienyl radical **63** to to the ipso position of **32** to effect a homolytic aromatic displacement to form **9** and radical **20** without proceeding through free hydrogen atom (Section 1.4.3 and below). Clearly, more work is needed to clarify the high-temperature reactivity of **32**.

Thermolysis of **32** is markedly accelerated by added hydrogen or sources of hydrogen atom. As for biphenyl (Section 6), cracking by hydrogenolysis rather than homolysis then appears to have the more significant implications for coal processing. Yao and Kamiya[14,154] reported 1.7% conversion to produce hydrodealkylation products **9** and **18** in a tetralin--1-methylnaphthalene mixture under 3.6 MPa hydrogen after 30 min at 450°C, a temperature where steps 90 and 91 would have 1% conversion times of ~1 yr. Intermediacy of hydrogen atom in chain steps

99 and 71 is likely. Although step 97 would again be expected to be

$$\underset{}{H\cdot} + \underset{\mathbf{32}}{PhCH_2Ph} \longrightarrow \underset{\mathbf{9}}{PhH} + \underset{\mathbf{20}}{PhCH_2\cdot} \qquad (99)$$

$$\mathbf{20} + H_2 \longrightarrow \underset{\mathbf{18}}{PhCH_3} + H\cdot \qquad (71)$$

highly competitive with step 99, it may well be effectively reversible in the presence of excess hydrogen.

Whereas Allen and Gavalas[194] found negligible conversion of **32** in tetralin after 30 min at 400°C, slow but steadily increasing hydrogenolysis to form **9** and **18** occurred in 1,2-dihydronaphthalene (**65**) solvent and reached 0.75% conversion in 30 min. The source of radicals was proposed to be molecular disproportionation of **65** in step 100 (see Section 10.2). The disappearance of **32** was fit by numerical integration of a kinetic model with rate constants estimated for the key steps 99-102. The assigned value of k_{99}, $\sim 10^{11.3}\exp(-11{,}000/RT)\ M^{-1}s^{-1}$, is, however,

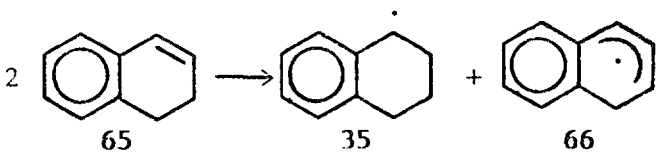

(100)

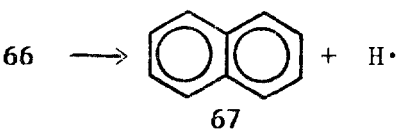

(101)

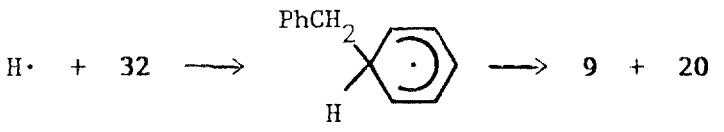

(99)

$$\mathbf{20} + RH \longrightarrow \mathbf{18} + R\cdot \qquad (102)$$

troublesomely different from that of k_{35}, $10^{10.1}\exp(-5{,}100/RT)\ M^{-1}s^{-1}$ (Section 4.1.1), for the very similar process involving hydrodealkylation

of toluene. In this proposed model, the reason for more efficient hydrogenolysis of **32** in **65** than in tetralin is the greater ease of ejection of hydrogen atom from radical **66** (step 101) than from radical **35** (Section 10.2). The fact that $k_{99}/k_{97} < 1$ is again immaterial here because radical **42** formed in step 97 can be restored to **32** by hydrogen abstraction from **65** and because hydrogen was indeed a major product formed simultaneously from **65**. The analogous hydrogenolysis of bis(1-naphthyl)methane under these conditions to form naphthalene and 1-methylnaphthalene was more rapid than that of **32** and was even more extensively modeled by Allen and Gavalas.[194]

McMillen and coworkers[26] have also described the hydrogenolysis of **32** in hydroaromatic solvents and concluded that, in appropriate cases, hydrogen atom need not be a free intermediate, as in steps 101 and 99, but that radical hydrogen transfer may occur from cyclohexadienyl radicals to the <u>ipso</u> position of **32**, analogous to hypothesized step 98.

7.2 HETERO ATOM-CONTAINING ONE-ATOM LINKAGES

There are numerous reports of the thermal stability of diphenyl ether (**68**) in hydrogen donor solvents in the low-temperature regime.[14,151,154,186,194-196] No decomposition of diphenyl sulfide (**69**) in tetralin was observed after $\gtrsim$1.5 h at 394°C[181] nor even under FVP conditions at 900°C.[180] Hence, the low reactivity of diphenylmethane (**32**) carries over to these PhYPh (Y = O, S) analogues. The decreases in D^{o}(Ph-YPh) in going from Y = CH_2 to O and S (see estimates in Table 14), just as in the $PhCH_2$-XPh series (Table 12), should translate to somewhat greater thermal reactivity of **68** and **69** compared with **32**, but the absolute values are still too large to lead to significant rates at 400-500°C, a conclusion consistent with observation. Reactivity at higher temperature is anticipated but has not been explored in any detail.

Kamiya and coworkers[197] treated several diaryl ethers in tetralin with high-pressure hydrogen at 430°C. Conversion of **68** after 5 h was only 3%, but it increased for ethers with larger aryl groups such that phenyl 9-anthryl ether was totally consumed under these conditions. The pseudo-first-order rate constants for disappearance of a series of phenyl

Table 14. Estimation of $D^\circ(Ph\text{-}YPh)$[a]

Y	$\Delta H_f^\circ(PhYPh)$[b]	$\Delta H_f^\circ(PhY\cdot)$[c]	$D^\circ(Ph\text{-}YPh)$[d,e]	$D^\circ(X\text{-}H)$
CH_2	36.8	47.8	89.6 (86.7)[f]	83.8[g,h] (81.4)[f]
O	11.9	11.4	78.1	i
S	55.3	54.9	78.2	i
NH	54.2	56.7	81.1	j

[a]All values in kcal mol^{-1} at 298 K. [b]Ref. 31. [c]Ref. 20. [d]$D^\circ(Ph\text{-}YPh) = \Delta H_f^\circ(PhY\cdot) + \Delta H_f^\circ(Ph\cdot) - \Delta H_f^\circ(PhYPh)$. [e]$\Delta H_f^\circ(Ph\cdot) = 78.6$; ref. 20. [f]Based on group additivity estimate of $\Delta H_f^\circ(Ph_2CH_2)$; see text and ref. 168. [g]$D^\circ(Ph_2CH\text{-}H) = \Delta H_f^\circ(Ph_2CH\cdot) + \Delta H_f^\circ(H\cdot) - \Delta H_f^\circ(Ph_2CH_2)$. [h]$\Delta H_f^\circ(Ph_2CH\cdot) = 68.5$; ref. 168 and 193. [i]Not applicable. [j]No value for $\Delta H_f^\circ(Ph_2N\cdot)$ available.

aryl ethers as a function of the aryl group increased in the order phenyl < 4-biphenylyl < 2-naphthyl < 1-naphthyl < 9-phenanthryl << 9-anthryl. Similarly for a series of 2-naphthyl aryl ethers, reactivity increased in the order 2-naphthyl < 1-naphthyl < 9-phenanthryl. The yields of product phenols (and presumably the corresponding arenes) were ~60% with 40% unidentified materials. The oxygen was preferentially retained with the "less activating" ring; e.g., phenyl 9-phenanthryl ether gave phenol and 9-phenanthrol in a ratio of 6.5 : 1. Because π-aryloxy radicals will profit more than will σ-aryl radicals from resonance stabilization by aromatic rings which offer more possibility for delocalization than phenyl, direct C-O homolysis of PhOAr (step 103) should produce preferentially Ph• and ArO•. On the other hand, if C-O cleavage occurs by homolytic aromatic displacement (step 104), the attack

$$\mathrm{PhOAr} \longrightarrow \mathrm{Ph}\bullet + \bullet\mathrm{OAr} \qquad (103)$$

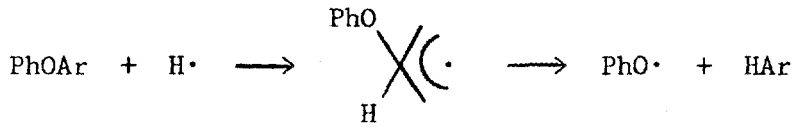

(104)

of hydrogen atom or its equivalent should occur preferentially on the ring which gives the more delocalized cyclohexadienyl radical intermediate. The observed regiochemistry thus corresponds to aromatic displacement, not homolysis. Additional confirmation of the displacement mechanism comes from the observation[197] that the rate of ether cleavage depended on the nature of the hydrogen donor solvent in the order 9,10-dihydroanthracene > tetralin > 1-methylnaphthalene. The relative degree of involvement of free hydrogen atom and radical hydrogen transfer from solvent-derived radicals (see Section 7.1) remains unclear. Finally, the observed activation energy of 36 kcal mol^{-1} for conversion of bis(2-naphthyl) ether in tetralin is, of course, much too low to correspond to direct homolysis.

The reason for the modest acceleration of the cleavage of diaryl ethers (as well as other ethers) in donor solvents by added phenols

remains a subject of debate. Yao and Kamiya[154] and King and Stock[156] suggested a stabilization of aryloxy radicals by hydrogen bonding to phenols, while Miller and coworkers[198] have recently suggested involvement of single electron transfer processes.

Medepalli and Kao[199] heated ether **68** at 550-600°C under high-pressure hydrogen and observed very complex reaction mixtures, including light gases such as carbon dioxide and methane, after only 30 min at 550°C. However, at the shortest reaction times, the primary products appeared to be not only benzene (**9**) and phenol (**45**) but also a lesser amount of dibenzofuran (**71**). The authors[199] suggested initiation by C-O homolysis but also noted an increase in rate with increasing ratios of hydrogen : **68**. Again a hydrogenolysis route is implicated. Note that the (unknown) route to form **71** cannot be analogous to hypothetical step 94 discussed in Section 7.1 for the formally analogous dehydrocyclization

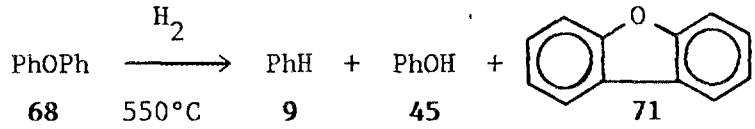

of diphenylmethane to fluorene because of the absence of abstractable hydrogen atoms in **68**.

Kamiya's group[14,154] treated all the members of the PhYPh series in a tetralin--1-methylnaphthalene mixture with high-pressure hydrogen at 450°C for 30 min. Compared with a conversion of 1.7% for **32** (Y = CH_2) (see Section 7.1), the conversions for **68** (Y = O), **69** (Y = S), and **70** (Y = NH) were 0, 10.7%, and 8.2%, respectively. The product from **69** was benzene in 183% yield; i.e., further hydrogenolysis of intermediate benzenethiol apparently occurred rapidly. Amine **70** gave benzene in modest yield and a trace of aniline.

8. THREE-ATOM LINKAGES

8.1 1,3-DIPHENYLPROPANE

The half-life for homolysis of the C-C bond in 1,3-diphenylpropane (**72**) (step 105) at 400°C should be ~3500 h according to the estimation procedure outlined in Table 4. Yet the observed half-life for **72** in

tetralin at 400°C was only ~1 h,[12,200] a value even less than the observed half-life of bibenzyl (**19**).[12] Hence, the thermal stability of three-atom linkages must not be controlled simply by C-C bond strength, and such linkages in coal must also be considered as possible bond-breaking sites in the low-temperature regime. A similar kinetic disparity occurred in the gas phase at 550°C where a predicted half-life for homolysis of ~12 min can be compared with an observed conversion of 15% in only 10-20 s.[140] The first hypothesis to explain the enhanced reactivity over that predicted from homolysis, as suggested already by Sweeting and Wilshire,[140] is a chain consisting of hydrogen abstraction step 106 and β-scission step 107 which leads to the observed products toluene (**18**) and styrene (**26**) through benzyl (**20**) and 1,3-diphenyl-1-propyl (**73**) radicals. Step 106 is analogous to step 56 which occurs during thermolysis of **19**; however, we have seen (Section 5.1.1) that step 62, the analog of step 107, is not operative

$$\underset{\mathbf{72}}{PhCH_2CH_2CH_2Ph} \longrightarrow \underset{\mathbf{20}}{PhCH_2\cdot} + \cdot CH_2CH_2Ph \qquad (105)$$

$$\mathbf{20} + \mathbf{72} \longrightarrow \underset{\mathbf{18}}{PhCH_3} + \underset{\mathbf{73}}{Ph\dot{C}HCH_2CH_2Ph} \qquad (106)$$

$$\mathbf{73} \longrightarrow \underset{\mathbf{26}}{PhCH{=}CH_2} + \mathbf{20} \qquad (107)$$

$$2\ \mathbf{20} \longrightarrow \underset{\mathbf{19}}{PhCH_2CH_2Ph} \qquad (-55)$$

for **19** in the low-temperature regime. Later, Virk[160,201] suggested an alternate hypothesis: a unimolecular symmetry-allowed retroene reaction:

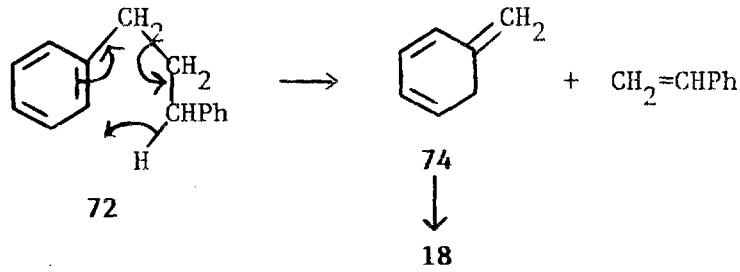

which, after rapid aromatization of methylenecyclohexadiene **74**, would also give the observed products. Such retroene processes were well documented for certain olefins and acetylenes[202] but not for aromatics.

Recent work by Poutsma amd Dyer[123] and Gilbert and Gajewski[203] has resolved this issue in favor of the radical chain hypothesis for thermolysis of **72** and has indicated why **19** behaves differently. The initial products from neat **72** in either the liquid or gas phase at 335-425°C are indeed **18** and **26** in equimolar amounts. [Secondary products derived from **26** will be discussed below.] Four mechanistically discriminating probes were applied: kinetic order, Arrhenius parameters, deuterium labeling, and effects of additives.

The extent of conversion of **72** at a given time and temperature was much less in the gas phase than in the liquid, behavior diagnostic of a kinetic order greater than one. Initial rates were determined at 365°C for the neat liquid (3.65 M), for solutions in biphenyl (1.70-0.14 M), and for the neat gas at varying pressures (0.058-0.0034 M). A plot of log (initial rate) vs. log (concentration) over this 10^3 variation in concentration was linear with a slope indicating a kinetic order of 1.59.[123] In the parallel study over the ranges of 0.2-3.8 M and 335-380°C,[203] the slopes were between 1.51 and 1.60. Relevant kinetic data for **72** and its ether analogs (see Section 8.2) are collected in Table 15. Although clearly incompatible with the unimolecular retroene hypothesis, this observed 3/2-order is consistent with the radical chain hypothesis <u>if</u> k_{106}[**72**] << k_{107}; then [**20**] >> [**73**] to maintain equal rates for the two chain steps and chain termination will take place predominantly by coupling of the more prevalent benzyl radical (step -55). In

Table 15. Kinetic Parameters for Thermolysis of Compounds with Three-Atom Linkages

Compound	Kinetic Order	log A[a]	E (kcal mol^{-1})	k_{rel} [a,b]	Ref.
$PhCH_2CH_2CH_2Ph$	1.59	13.1	52.3	1.9[c]	123
	1.55	12.5	51.4	1.0[c,d,e]	203
$PhCH_2OCH_2Ph$	1.43	12.6	48.0	19.6[e]	203
$PhCH_2CH_2OPh$	1.21	12.3	50.3	1.5[e]	203

[a]Units are M^{1-n} s^{-1} where n is the kinetic order; these were given in ref. 203, presumably mistakenly, as s^{-1}. [b]At 350°C. [c]Same substrate; different study. [d]Assigned. [e]Different substrates; same study.

this extreme the full steady-state rate expression[123] simplifies to:

$$-d(\mathbf{72})/dt \sim (k_{105}/k_{-55})^{1/2} k_{106} [\mathbf{72}]^{3/2}$$

Thermochemical kinetic estimates[123] gave $k_{106} \sim 10^{8.6} \exp(-14{,}200/RT)\ M^{-1}s^{-1}$ (see Section 5.1.2 for discussion of analogous step 56) and $k_{107} \sim 10^{14.8} \exp(-27{,}300/RT)\ s^{-1}$. This estimate for E_{107} arose from an estimate of $\Delta H^{o}_{107} \sim 20.7$ kcal mol^{-1} (Table 1) and an inherent barrier of ~7.0 kcal mol^{-1} estimated from the propagation step in styrene polymerization. [The slight change from the original reference results from a slight change in the current estimate of benzylic resonance energy.[20]] Over the concentration range 0.0034-3.65 M at 365°C, these estimates lead to $k_{106}[\mathbf{72}]/k_{107} \sim 0.00007$-$0.07$, and the required inequality for observation of 3/2-order kinetics is indeed met. Note that it is the possibility of expelling the stabilized benzyl radical in β-scission step 107, compared with the need to expel the unstabilized phenyl radical or hydrogen atom in the homologous β-scission steps 62 and 62a (see Section 5.1.2), that has opened up this chain thermolysis route for **72**, whereas an analogous route for **19** is closed in the low-temperature regime.

The Arrhenius parameters determined for initial thermolysis of neat liquid **72** were $A = 10^{13.1}\ M^{-1/2}s^{-1}$ and $E = 52.3$ kcal mol^{-1} over the range 343-425°C .[123] The values in the parallel study[203] were $A = 10^{12.5}\ M^{-1/2}s^{-1}$ [the units in reference 203 were given, presumably mistakenly, as s^{-1}] and $E = 51.4$ kcal mol^{-1} over the range 335-380°C. For the 3/2-order rate expression above, $E_{exp} = 1/2\ E_{105} - 1/2\ E_{-55} + E_{106}$. Inserting the various estimates we have already discussed [$E_{105} \sim D^{o}(\mathbf{72}) \sim 71.6$ kcal mol^{-1}; $E_{-55} \sim 0$; and $E_{106} \sim 14.2$ kcal mol^{-1}] leads to $E_{estd} \sim 50.0$ kcal mol^{-1}. Agreement between experiment and estimate is excellent. Estimation of the barrier for the retroene process is more problematical, but ~59 kcal mol^{-1} has been suggested.[123]

A characteristic feature of the retroene mechanism is transfer of hydrogen from the α position of **72** onto the aromatic ring of the toluene product. In fact, the aromatic ring of the toluene formed from

thermolysis of **72**-1,1,3,3-d_4 in the liquid phase contained <0.025 deuterium atoms.[123] This result sets an upper limit on participation of the retroene route of 5%. A small enrichment of protium in the α position of the toluene product suggested that hydrogen abstraction by radical **20** was not restricted to the α position of **72** (step 106) but that step 106a competed to a small extent. However, since radical **75**, like radical **33**, has no kinetically accessible β-scission decay route available, it presumably is continuously converted back to its isomer **73** by bimolecular hydrogen abstraction in step 108. [A minor possibility of 1,2-phenyl

$$\mathbf{20} + \mathbf{72} \longrightarrow \mathbf{18} + \underset{\mathbf{75}}{PhCH_2\dot{C}HCH_2Ph} \qquad (106a)$$

$$\mathbf{75} + \mathbf{72} \longrightarrow \mathbf{72} + \mathbf{73} \qquad (108)$$

shift in **75** followed by β-scission would be invisible in the absence of carbon labeling.] In Section 9 we will see chemical consequences of a step analogous to 108.

The modest acceleration of the thermolysis of **72** by added sources of radicals such as benzyl phenyl sulfide[156,200] or the corresponding ether **44**[203] is further evidence in favor of the radical chain hypothesis. For example, addition of 5 mol% **44** to neat **72** increased the initial rate at 350°C by a factor of 4.4.

At higher conversion levels, product mixtures became more complex because of secondary reactions of styrene (**26**) which formed, among other

$$\underset{\mathbf{73}}{Ph\dot{C}HCH_2CH_2Ph} + \underset{\mathbf{26}}{PhCH{=}CH_2} \longrightarrow PhCH_2CH_2CHPhCH_2\dot{C}HPh \xrightarrow{RH} \underset{\mathbf{76}}{PhCH_2CH_2CHPhCH_2CH_2Ph}$$

products, ethylbenzene and 1,3,5-triphenylpentane (**76**).[123] The latter is presumably formed by addition of radical **73** to **26**, followed by hydrogen abstraction. This secondary reaction dramatizes the fact that cracking is only moderately preferred thermodynamically over addition in this low-temperature regime (Section 2.1). For example, at 350°C, the overall reaction 109 has an estimated equilibrium constant of only ~0.5 M. By the same reasoning, a certain extent of addition of **72** to product **26** to give **76** is thermodynamically allowed.

$$\mathbf{72} \rightleftharpoons \mathbf{18} + \mathbf{26} \qquad (109)$$

ΔH^{o}_{298} ~ 17.8 kcal mol^{-1} (Table 1)

ΔS^{o}_{298} ~ 35.2 cal mol^{-1} K^{-1} (Table 1)

$\langle \Delta C_p^{o} \rangle$ ~ -1.0 cal mol^{-1} K^{-1} (ref. 123)

ΔG^{o}_{623} ~ 17.5 - (623)(0.0345) ~ -4.0 kcal mol^{-1}

K_{623} ~ 25 atm ~ 0.5 M

Replacement of inert diluents such as biphenyl with tetralin (**34**) did not significantly affect the rate of thermolysis of **72** in the liquid phase.[123] Surely there must be active competition for consumption of radical **20** between step 106 to form radical **73** and step 59 to form radical **35** since **34** is known (see Section 5.6) to be the better hydrogen atom donor. However, as we will see in Section 10.1.6, radical **35** has no efficient, productive unimolecular decay route [its β-scission lacks the entropy advantage of step 107], and it can simply be converted back to **73** by step 110. Thus, the tetralin carrier technique is <u>not</u> effective in inhibiting efficient chain reactions at these elevated temperatures. Similarly, various phenols were ineffective as inhibitors at 350°C,[204] again presumably because phenoxy radicals at elevated temperatures are effective hydrogen abstraction agents and are not destined only to couple and terminate chains as they normally are at ambient temperatures. The

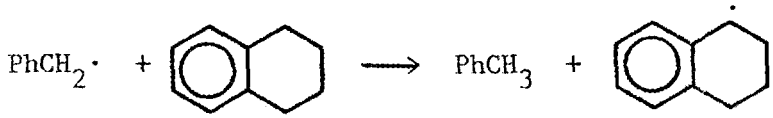

(59)

20 **34** **35**

$$\mathbf{35} + PhCH_2CH_2CH_2Ph \longrightarrow \mathbf{34} + PhCHCH_2CH_2Ph \qquad (110)$$

72 **73**

implication for coal processing is that chain reactions of the type which occurs for **72** can still proceed efficiently even in the presence of hydrogen donor solvents.

At complete consumption in tetralin at 400°C, the products from **72** included toluene, ethylbenzene, and 1- and 2-methylnaphthalenes (**77** and its isomer) in a ratio of 0.56 : 0.32 : 0.12.[205] Experiments with **72**-1-^{14}C and **72**-2-^{14}C revealed that the methyl group in **77** was derived from the central carbon of **72**. At partial conversion, 1- and 2-(2-phenylethyl)tetralins were detected; mechanistically these can be viewed as analogs of adduct **76**. Hence, the key steps in the most economical route[156] appear to be:

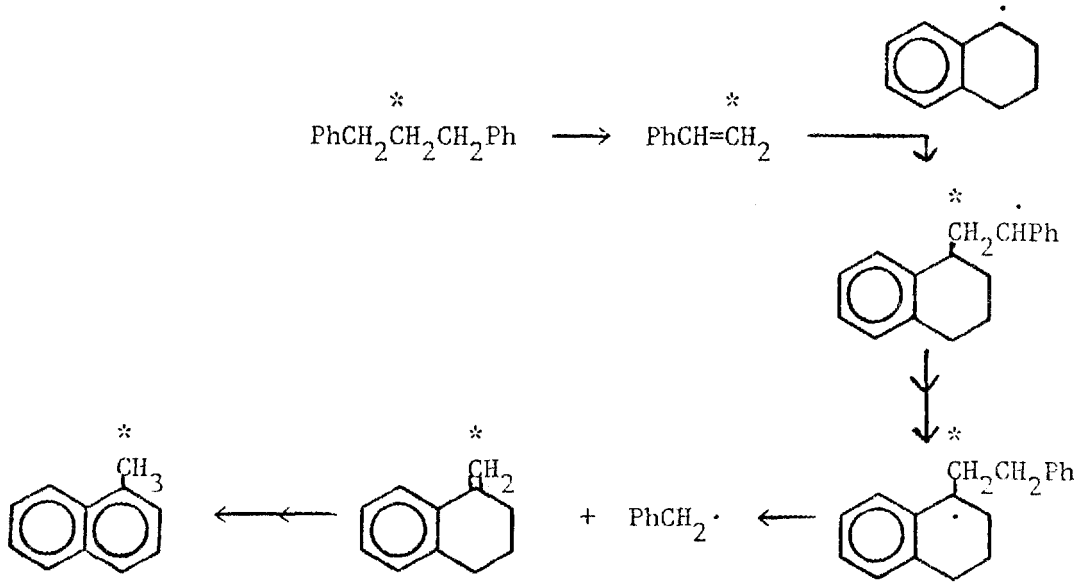

77

8.2 HETERO ATOM-CONTAINING THREE-ATOM LINKAGES

The strength of the C-O bond in dibenzyl ether (**78**) (step 111) should be greater than that in benzyl phenyl ether (**44**) [D^o(**44**) ~ 54 kcal mol^{-1}; Table 12] by the relatively large increment corresponding to RE(PhO·), ~18 kcal mol^{-1} [$D^o(CH_3O\text{-}H) - D^o(PhO\text{-}H)$ = 104.4 - 86.5][20]. Yet numerous studies of thermolysis of ether **78** in hydrogen donor solvents[11,13,14,154,156,182,186,195] have revealed a reactivity greater than that of its all-carbon analog **72** and approaching that of ether **44**. For example, Panvelker and coworkers[182] reported 10% conversion of **78** as a 1% solution in tetralin-dodecane after 30 min at 375°C. However, members of this same group[13] had earlier reported ~25% conversion of **78** as a 40% solution in tetralin after 30 min at only 350°C. Although data in each paper was formulated by assumed first-order kinetics, this comparison is suggestive of an order greater than unity. The dominant products in hydrogen donor solvents at moderate conversions were toluene (**18**) and benzaldehyde (**79**)[13,14,154,156,182,186,195] with evidence for a slower secondary decarbonylation of **79** to form benzene (Section 12.3). Similar product patterns were observed for the neat ether as a liquid[203,206,207] or gas.[203]

These observations of reactivity greater than that predicted from D^o ~ 72 kcal mol^{-1}, of a kinetic order probably greater than unity, of acceleration by additives with weak bonds,[156,204] and of simple cracking products suggest a chain decomposition pathway via steps 112 and 113, which is fully analogous to that for the comparable hydrocarbon **72**.

$$\underset{\mathbf{78}}{PhCH_2OCH_2Ph} \longrightarrow \underset{\mathbf{20}}{PhCH_2\cdot} + \cdot OCH_2Ph \qquad (111)$$

$$\mathbf{20} + \mathbf{78} \longrightarrow \underset{\mathbf{18}}{PhCH_3} + \underset{\mathbf{80}}{PhC\overset{\cdot}{H}OCH_2Ph} \qquad (112)$$

$$\mathbf{80} \longrightarrow \underset{\mathbf{79}}{PhCH{=}O} + \mathbf{20} \qquad (113)$$

Mechanistic confirmation comes from the work of Gilbert and Gajewski,[203] who observed an average reaction order of 1.43 at 310-350°C (Table 15) and Arrhenius parameters of $A = 10^{12.6}\ s^{-1}$ [again the units given do not correspond to the reaction order observed] and $E = 48.0$ kcal mol^{-1}. Parallel to our earlier discussion for **72**, the ~3/2 order indicates that the overall kinetic barrier in the chain again lies in the hydrogen abstraction step 112. Dissecting $E_{exp} = 1/2\ E_{111} - 1/2\ E_{-55} + E_{112}$ leads to $E_{112} \sim 48 - 0 - 36 \sim 12$ kcal mol^{-1}. This value, slightly lower than that deduced in the same way for step 106, is quite reasonable since an adjacent oxygen is expected to moderately enhance hydrogen abstraction. Further insight into the chain dynamics comes from the ESR-monitored thermolysis studies of Livingston and Zeldes.[206] Under conditions of active thermolysis (452-497°C at ~1 s residence time), the only radical observed was **20**, consistent with the inequality $k_{112}[\mathbf{78}] \ll k_{113}$ and therefore [**20**] >> [**80**] to achieve a steady state. A chain length of ~140 for neat **78** was determined at 452°C and 20.7 MPa pressure. Radical **80** was produced independently at much lower temperatures (105-155°C) by photolysis of di-t-butyl peroxide in a solution of **78** in benzene, and its β-scission was observed directly by ESR assay for both radicals **80** and **20**. The derived activation energy, $E_{113} = 15.5$ kcal mol^{-1}, is much less than our previous estimate of $E_{107} \sim 27.7$ kcal mol^{-1} for β-scission of the all-carbon analog **73** (Section 8.1). This lowering of the barrier for β-scission presumably reflects the more favorable overall enthalpy that results from the greater difference in stability between double and single bonds for C-O than for C-C systems. The prototypical illustration of this difference for cases where the heats of formation are well known is shown below:

$$CH_3O\cdot \longrightarrow CH_2{=}O + H\cdot$$

$$\Delta H^{o}_{298} = 20.2 \text{ kcal mol}^{-1}$$

$$CH_3CH_2\cdot \longrightarrow CH_2{=}CH_2 + H\cdot$$

$$\Delta H^{o}_{298} = 38.7 \text{ kcal mol}^{-1}$$

Klein and coworkers[208] determined the ratio $[d_1/(d_0 + d_1)]$ for the toluene formed from thermolysis of **78** in tetralin-d_{12} at 400°C and low conversions as a function of the **78** : tetralin ratio. As the latter ratio decreased and approached zero, the former increased and approached one. This result is consistent with the radical chain mechanism in which **20** abstracts hydrogen competitively from tetralin and **78**, but it is inconsistent with a retroene mechanism from which the toluene product would be unlabeled. In summary, the thermolysis of ether **78** seems fully analogous mechanistically to that of hydrocarbon analog **72**.

The isomeric phenyl 2-phenylethyl ether (**81**) as a neat liquid cracked to form phenol (**45**) and styrene (**26**) at a rate some 10-fold slower than **78** and comparable to that of the all-carbon analog **72**. Gilbert and Gajewski's kinetic data[203] for **81** (Table 15) were similar to those for **78** and **72**, except that the kinetic order was 1.2 rather than the "ideal" 1.5. Reaction was again accelerated by additives with weak bonds.[204] They proposed that a chain decomposition occurred for this ether as well, with the modification that some cross-termination (step 118) occurred with a resultant lowering of the kinetic order.

$$\underset{\mathbf{81}}{PhOCH_2CH_2Ph} \longrightarrow \underset{\mathbf{46}}{PhO\cdot} + \cdot CH_2CH_2Ph \qquad (114)$$

$$\mathbf{46} + \mathbf{81} \longrightarrow \underset{\mathbf{45}}{PhOH} + \underset{\mathbf{82}}{PhOCH_2\dot{C}HPh} \qquad (115)$$

$$\mathbf{82} \longrightarrow \underset{\mathbf{26}}{PhCH{=}CH_2} + \mathbf{46} \qquad (116)$$

$$2\ \mathbf{46} \xrightarrow{k_t} \text{Nonradical products} \qquad (117)$$

$$\mathbf{46} + \mathbf{82} \longrightarrow \qquad (118)$$

This might indeed occur either if phenoxy radical coupling (step 117) were inefficient or if the inequality $k_{115}[\mathbf{81}] \ll k_{116}$ were no longer true in this case. The former circumstance might hold if the

cyclohexadienone structures formed by phenoxy radical combination dissociate more rapidly than they aromatize (cf. Section 11.2). The latter might hold if k_{115} is enhanced compared with k_{106} and k_{112} by polar contributions to the hydrogen abstraction transition states. Klein and Virk[209] observed a very similar kinetic order of 1.16 but slightly lower Arrhenius parameters of $A = 10^{11.1}$ [there is ambiguity in both References 203 and 209 in that the units for A do not conform to the magnitude of the reaction order] and $E = 45.0$ kcal mol^{-1} than did Gilbert and Gajewski[203] ($A = 10^{12.3}$ and $E = 50.3$ kcal mol^{-1}). This group[209] estimated the Arrhenius parameters for the ideal radical chain with only cross-termination to be $A \sim 10^{14}$ s^{-1} and $E \sim 55$ kcal mol^{-1}, and the rather poor correspondence between experiment and prediction led them to propose again a retroene route. They also cited the failure of tetralin to inhibit the reaction as evidence against a chain; however, as we have seen in Section 8.1, this is not a reliable criterion. Isotopic labeling data is needed to decide whether the mechanism for **81** is indeed parallel to that of analogs **72** and **78** or whether an authentic example of a retroene reaction involving an aromatic ring has finally emerged because of the extra stability associated with forming an intermediate cyclohexadienone rather than methylenecyclohexadiene.

The other members of the $PhCH_2ZCH_2Ph$ series (Z = S and NH) are also thermally labile, but the products are more complex than those from **78** (Z = O) and the mechanisms have not been clearly elucidated. Heating dibenzyl sulfide (**83**) in tetralin for several hours at 388°C gave toluene and bibenzyl in a 7 : 1 ratio;[181] the sulfur apparently was eliminated largely as hydrogen sulfide. In the gas phase with benzene diluent at 500°C and ~10 s residence time,[183] conversion was 92% and the detected products were stilbene > toluene > bibenzyl > toluenethiol > diphenyl disulfide. Polymeric product was noted and thiobenzaldehyde (**84**), known to be very prone to polymerization, was suggested as a possible precursor. Addition of hydrogen donor solvents in the gas phase increased the relative amounts of toluene and toluenethiol and lowered those of stilbene and bibenzyl. Although not enough information is available to construct a detailed mechanism, the presence of benzyl radicals can be clearly inferred. It was also suggested[183] that radical **85** was probably

formed by hydrogen abstraction from **83** and that it might disappear by β-scission to give the unstable **84** and by cyclization to give ultimately 2-phenylisobenzothiophene (**86**), which was a ubiquitous trace product.

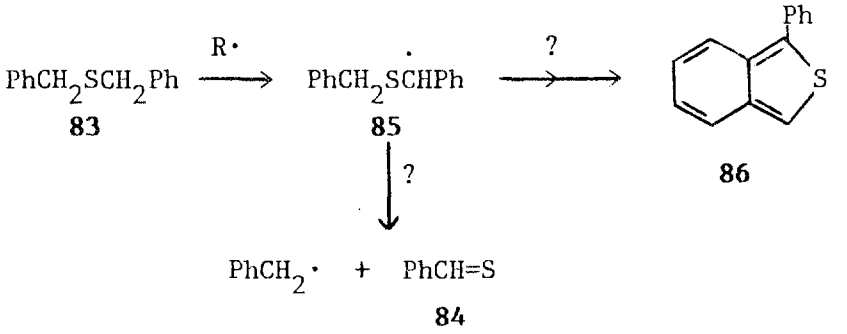

Badr and coworkers[210] heated dibenzyl amine at reflux (≲300°C) for five days and observed the formation of stilbene, bibenzyl, toluene, benzaldehyde (the mixture was exposed to air during heating), and ammonia. These products again suggest the formation of benzyl radicals, which indeed could be trapped by added naphthalene, and C-N homolysis was proposed as the initial step. King and Stock[156] found that this amine in tetralin was 60% consumed after 10 min at 350°C; thus it was considerably more reactive than the corresponding ether **78** which was only 22% consumed after 10 min at 50°C higher temperature. Therefore, a chain process which amplifies the effects of initial homolysis is strongly implied. The major product was toluene with smaller amounts of bibenzyl and benzyl amine; this amine product, which may have been a secondary hydrogen transfer product from benzaldehyde imine, was itself rapidly converted under the reaction conditions to toluene and bibenzyl.

9. FOUR-ATOM LINKAGES

Simple extension of steps 105-107 for 1,3-diphenylpropane to the next higher homolog, 1,4-diphenylbutane (**87**), would predict operation of a chain based on formation and β-scission of the most stable radical, 1,4-diphenyl-1-butyl (**88**), to produce an equimolar mixture of styrene (**26**) and ethylbenzene (**25**). In fact, the initial products from thermolysis of liquid **87** at 400°C included not only **25** and **26**, but also an equimolar mixture of toluene (**18**) and allylbenzene (**89**).[123] The ratio of

the two competing cracking pathways, extrapolated to zero conversion and expressed as the ratio of **18** : **25**, was 0.8 at 400°C and 1.6 at 365°C. The toluene-producing pathway might have resulted either from incursion of a retroene component or from formation and β-scission of the less stable 1,4-diphenyl-2-butyl radical (**90**). The retroene hypothesis can be dismissed because the toluene produced from thermolysis of **87**-2,2,3,3-d_4 in tetralin at 400-425°C was unlabeled.[211] Conversely, the observed acceleration by added benzyl phenyl sulfide[156] supports a radical chain reaction.

The minimum radical chain to account for the observed products must include initiation step 119 and the interwoven propagation steps 120-125.

$$\underset{\mathbf{87}}{PhCH_2CH_2CH_2CH_2Ph} \longrightarrow \underset{\mathbf{20}}{PhCH_2\cdot} + \cdot CH_2CH_2CH_2Ph \qquad (119)$$

$$\mathbf{20} + \mathbf{87} \longrightarrow \underset{\mathbf{18}}{PhCH_3} + \underset{\mathbf{88}}{PhC\overset{\cdot}{H}CH_2CH_2CH_2Ph} \qquad (120)$$

$$\mathbf{20} + \mathbf{87} \longrightarrow \mathbf{18} + \underset{\mathbf{90}}{PhCH_2C\overset{\cdot}{H}CH_2CH_2Ph} \qquad (121)$$

$$\mathbf{88} \longrightarrow \underset{\mathbf{26}}{PhCH{=}CH_2} + \underset{\mathbf{28}}{PhCH_2CH_2\cdot} \qquad (122)$$

$$\mathbf{90} \longrightarrow \underset{\mathbf{89}}{PhCH_2CH{=}CH_2} + \mathbf{20} \qquad (123)$$

$$\mathbf{28} + \mathbf{87} \longrightarrow \underset{\mathbf{25}}{PhCH_2CH_3} + \mathbf{88} \qquad (124)$$

$$\mathbf{28} + \mathbf{87} \longrightarrow \mathbf{25} + \mathbf{90} \qquad (125)$$

Substrate **87** is activated by hydrogen abstraction both by benzyl radical (**20**) in steps 120 and 121 and by 2-phenylethyl radical (**28**) in steps 124 and 125. In each case, formation of the more stable benzylic radical **88** should be kinetically preferred compared with **90**. Because **88** is destined in step 122 to lead to the ethylbenzene-styrene pathway, the latter is predicted to be dominant. Hence, even this set of six steps cannot rationalize the result that the ratio of **18** : **25** from liquid **87** was almost unity at 400°C and exceeded it at 365°C. Nor can it rationalize the observation[123] that this ratio of the two cracking pathways was concentration dependent, decreasing at 400°C in a nonlinear fashion from 0.8 for the neat liquid (~3.2 M) to 0.185 for the dilute gas (105 kPa; 1.8×10^{-2} M). This concentration dependence could be modeled, however, by adding reversible step 126 (Sections 2.3, 4.4, 8.1, and 10.1.6), which

$$\mathbf{88} + \mathbf{87} \longrightarrow \mathbf{87} + \mathbf{90} \qquad (126)$$

provides an interconversion route for radicals **88** and **90**, not by intramolecular 1,2-hydrogen shift, but by intermolecular hydrogen abstraction from substrate **87**. Steady-state analysis of this network showed that:

$$[\mathbf{18}]/[\mathbf{25}] = \{(k_{125})/(k_{124} + k_{125}) + (k_{126}/k_{122})[\mathbf{87}]\}/ \{(k_{120})/(k_{120} + k_{121}) + (k_{-126}/k_{123})[\mathbf{87}]\}$$

At infinite dilution where step 126 would not occur because of a vanishing concentration of **87**, the selectivity between the two pathways (~0.17) would be determined by the hydrogen abstraction selectivities, particularly by the $(k_{125})/(k_{124} + k_{125})$ term associated with radical **28**. Inversely, at infinite concentration of **87** (a condition not quite fulfilled kinetically by the neat liquid), radicals **88** and **90** would be fully equilibrated before β-scission, and the selectivity would be determined by the term $K_{126}(k_{123}/k_{122})$. Thermochemical kinetic estimates[123] suggested $K_{126} \sim 0.0036$ and $k_{123}/k_{122} \sim 320$ at 400°C; thus, these terms almost exactly counterbalance to give the observed

selectivity near unity. In more pictorial terms, benzylic radical **88** is more stable but also has the larger barrier for β-scission since it must expel unstabilized radical **28**, whereas less stable **90** can expel the more stable **20**.

While the initial selectivity between the two cracking pathways is thus sensibly explained, the observed[123] dependence of selectivity on conversion level, the auto-acceleration behavior, and the overall kinetic order dependences have not yet been fully unraveled and suggest even further complexity of mechanism which is induced by accumulating reaction products.

10. HYDROAROMATIC HYDROCARBONS

10.1 TETRALIN

Just as bibenzyl has become the prototypical model compound for thermally labile aliphatic linkages in coal, tetralin (**34**) has become the major representative of hydroaromatic structures in coal and liquefaction solvents. In fact, systematic studies of coal liquefaction itself are very commonly performed in **34** as a stand-in for recycled hydrogen donor solvents.

10.1.1 Liquid-Phase Regime

The onset of reactivity occurs near 400°C. Quantitative data for liquid **34** at low conversions from several groups[133,212-214] are compared in Table 16. [Data from a study with potentially catalytic γ-alumina as a reactor packing is not included.[215]] The dominant initial reaction at 400°C is ring contraction to form 1-methylindane (**91**) at a rate of ~0.35% h^{-1}. After high conversion at 500°C, isomer **91** was 20-fold more prevalent that 2-methylindane.[84] The second most prevalent reaction is dehydrogenation to form naphthalene (**67**) and hydrogen (not **67** and decalin[212,215]); data on its rate show much more variation among the studies. A third (trace) reaction is ring-opening hydrodealkylation to form n-butylbenzene (**92**). Table 16 also includes data[212,214] at 450°C, above the critical temperature of **34** (~427°C[215]), but still under comparably dense conditions because of high applied pressure. In the context of coal liquefaction, dehydrogenation of hydroaromatics is a

Table 16. Product Compositions from Thermolysis of Dense Tetralin in Metal Autoclaves

T(°C)	Conditions	Initial rate of formation (% h^{-1})[a]				Ref.
		1-Methyl-indane	Naphthalene	n-Butylbenzene	Others	
	NO ADDED REAGENTS					
400	Liquid; autogenous pressure	0.4	≲0.04	b		212
400	Liquid; 10.3 MPa applied pressure	0.34	0.17			214
400	Liquid; 10 MPa N_2 pressure	0.26	0.07[c]	0.01		213
420	Liquid; autogenous pressure	0.48	0.03	0.01		133
450	Supercritical; 4.3 M	3.5	~0.5[d]	b	e	212
450	Supercritical; 10.3 MPa applied pressure	3.8	0.73		f	214
	ADDED HYDROGEN					
400	Liquid; 10 MPa H_2 pressure	0.25	0.07[c]	0.09		213
450	Supercritical; 10 MPa H_2 pressure	5.0	1.1	2.0		213
450	Supercritical; 13 MPa H_2 pressure	5.7	1.3			216
450	Supercritical; 3.4 MPa H_2 pressure	2.4(?)[g]	1.4	1.8[h]		154
450	Supercritical; 3.5 MPa H_2 pressure[i]	2.8	0.7	2.0		217

[a]From stated initial rate constants (refs. 213 and 214) or estimated from product-time data. [b]Detected in small amounts but not quantified. [c]Value under H_2 pressure; yield said not to depend on atmosphere. [d]Increased with increasing reaction time. [e]Traces of indane and PhR (R = CH_3, C_2H_5, n-C_3H_7). [f]Traces of indane and PhR (R = H, CH_3, C_2H_5). [g]Said to be decalin; however, this is commonly confused with 1-methylindane in GC analyses. [h]"Alkylbenzenes." [i]Tetralin:biphenyl = 7:3.

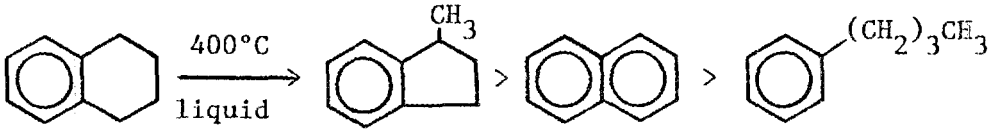

34 **91** **67** **92**

desirable mode of hydrogen donation by the solvent because the aromatized product can be rehydrogenated elsewhere in the process for recycle. In contrast, ring contraction and ring opening of hydroaromatics are not desirable to the extent they are "irreversible" in a processing sense.

The most detailed kinetic data are from Mallinson and coworkers,[214] who modeled the formation of **91** and **67** as parallel first-order reactions.[213,214] The initial **91** : **67** ratio was very temperature-sensitive, increasing from 2.0 at 400°C to 5.3 at 450°C; Hooper and coworkers[212] described a similar trend. Conversion of the kinetic data at two temperatures[214] to Arrhenius form gives rate constants for formation of **91** and **67** of $10^{9.2}\exp(-46{,}900/RT)\ s^{-1}$ and $10^{2.8}\exp(-27{,}900/RT)\ s^{-1}$, respectively. Coupling the observation of such an unusually low A factor for formation of **67** with Hooper's observation[212] of autocatalytic behavior suggests some unrecognized mechanistic complexity in the formation of **67** which clouds recognition of the true kinetic form and temperature effect.

10.1.2 Gas-Phase Regime

Low-conversion product data from gas-phase runs[218-226] are compiled in Table 17. [Data from studies[227,228] at conversions too high to allow conclusions about initial products are not included.] Over the entire temperature range of 400-750°C, the dominant initial reaction is dehydrogenation to form **67** rather than the ring contraction to form **91** which dominates in the liquid phase (except for one case[218] which we consider further below). Also in contrast with liquid-phase studies, not only **67** but also 1,2-dihydronaphthalene (**65**) (but not the 1,4-isomer) is commonly detected. In all cases where data on product composition vs. reaction time is available,[219,222,224,225] the initial dehydrogenation product proved to be **65**, which subsequently, and more rapidly, was converted to **67**.

Table 17. Product Compositions from Thermolysis of Gaseous Tetralin

T(°C)	400	500	500	575	620	700	725	730[a]	~737[b]	~750[c]
P(kPa)	0.46	<100	640	152[d]	~4	<100	52	52	0.01[b]	0.04
Reactor	Static, quartz	Static	Flow, SS[e]	Flow, pyrex	Flow	Flow, silica	Flow, quartz	Flow, SS[e,f]	Flow[b]	Static, pyrex[c]
Added gas; kPa	Ar; 215	None	N_2; 8 x 10^4	He; 101[d]	He; 101	N_2; 101	N_2; 101	H_2O; 101	None	SiF_4; 0.7
t(s)	3.6 x 10^4	--	--	6	--	~1	0.5	0.09[a]	--	--
Conversion (%)	3.5	5	"few"	4	24	25	16	17[a]	6	2-10
Product (mol %)[g]										
1,2-Dihydro-naphthalene	40[h]	16		84	51	7	63	59	55	16
Naphthalene	60	40	83	16	11	49	17	17	10	1
1-Methylindane	i	14[j]	10			1[j]				
Indene		7				13	8	12	5	3
Benzocyclobutene		0.4				0.2			6	56
Styrene		5	(4)[k]		22	2	6	8	10	8
Ethylbenzene		7	(4)[k]		12	10	2			
Others		10	2		4	17	4	4	13	18[l]
Reference	219	220	221	222	223	220	225	224	226	218

[a]Product compositions reported as function of conversion with exact T and t not specified; 0.09 s at 730°C achieved the 17% conversion at which the composition shown was calculated. [b]FVP conditions. [c]Laser-sensitized with SiF_4 absorbing pulses from CO_2 laser; estimated peak pulse temperature. [d]Calculated from reported concentration of 2.15 x 10^{-5} mol cm^{-3}; yet reactor had no back-pressure control. [e]Stainless steel. [f]Sulfur-poisoned. [g]Normalized to 100% for products reported; does not include C_1-C_3 products where reported. [h]No 1,4-isomer. [i]Specifically reported as absent. [j]Reported as 2-methylindane. [k]Not distinguished. [l]2-Allyltoluene.

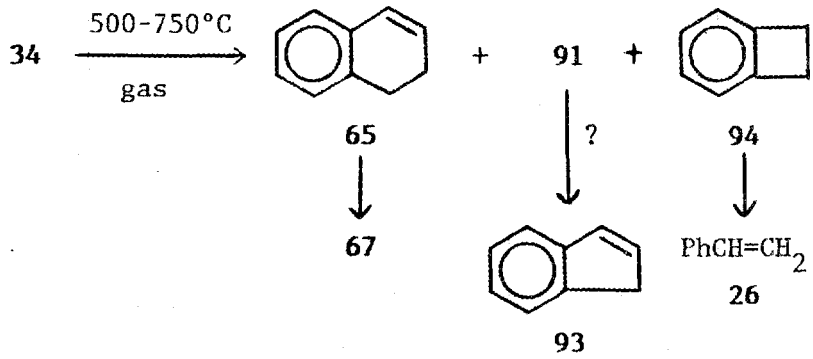

The nature of the other gas-phase products reported is more variable among the studies. At the lowest temperature (400°C), Gangwer[219] found only **65** and **67** at very low **34** pressure (465 Pa) but noted the onset of formation of **91** at higher (unspecified) pressures. Penninger[221] reported that the **91** : **67** ratio at 500°C increased with increasing tetralin partial pressure (0.4-4.1 MPa; 0.06-0.6 M) and actually exceeded unity above 4 MPa (see below). A continuation of this trend into the liquid phase (>1 M) would rationalize the dominance of ring contraction displayed in Table 16. Loudon[220] also reported ring contraction as the second most prevalent process at 500°C (although the product was assigned, probably in error, as 2-methylindane). However, at >575°C, **91** is no longer reported; rather indene (**93**) is the major ring-contracted product. While upward curvature in amount-vs.-time plots for **93**[218,220,224,225] suggests a precursor and while mechanistic considerations suggest that **91** could qualify as such, explicit experimental evidence is not available.

The third gas-phase product class consists of molecules which have lost two carbon atoms: benzocyclobutene (**94**), styrene (**26**), and ethylbenzene (**25**). Some **26** may be formed as a secondary product from **94** by a known unimolecular conversion (Section 10.5). However, the labeling patterns observed in the **26** formed from **34**-1,1,4,4-d_4[218] and **34**-1-^{14}C[228] suggest that it has other precursors as well.

If we divide the products generically into the three classes of dehydrogenation, ring contraction, and C_2-loss, then no major effect of temperature on product distribution is evident at the only pressure (near

100 kPa) where such a comparison can be made from the data in Table 17. However, this tentative conclusion may need to be modified when the source of secondary products such as **25**, **26**, and **93** becomes clearer.

Kinetic information for gas-phase thermolysis is sparse. Noting a dependence of rate on the history of the quartz vessel used, Gangwer and coworkers[219] assigned the successive dehydrogenation steps at 400°C as totally heterogeneous. They assigned a zero-order dependence on **34** (i.e., surface site saturation), but the data presented (<5% conversion at a single **34** pressure) do not seem to warrant a choice of kinetic order. In contrast, Takahashi and Ogino[222] reported no effect of the S/V ratio at 575°C and modeled dehydrogenation as homogeneous, consecutive, irreversible first-order reactions:

$$\mathbf{34} \xrightarrow[-H_2]{(a)} \mathbf{65} \xrightarrow[-H_2]{(b)} \mathbf{67} \qquad (127)$$

Temperature dependence studies gave $k_{127a} = 10^{17.7}(\exp{-77,000/RT})\ s^{-1}$ and $k_{127b} = 10^{10.6}\exp(-47,000/RT)\ s^{-1}$. Although the absolute values of these rate constants are not widely different ($k_{127b}/k_{127a} = 8$ at 545°C), such a large difference in A factors for formally similar stoichiometries again suggests a disguised complexity for the mechanism of dehydrogenation. Penninger[221] presented kinetic data for formation of individual products at 500°C as log rate-vs.-log [**34**] plots over the range 0.06-0.6 M (0.4-4 MPa partial pressure). The slope (kinetic order) for **67** (~0.75) was much less than that for **91** (~1.9).

Trushkova and coworkers[223] reported a further kinetic complication in studies at 620-680°C: an inhibition period whose length decreased with increasing temperature and with small additions of allene. Such behavior is suggestive of radical chain reactions with an initiation step involving unsaturated products. The activation energies for disappearance of **34**, after the inhibition period, were 51 and 39 kcal mol^{-1}, without and with allene, respectively.

In an effort to circumvent heterogeneous effects[213,219,222,224] and the suspicion that dehydrogenation in particular might be wall-catalyzed,

Bergman and coworkers[218] carried out laser-powered, SiF_4-sensitized thermolyses of **34** at >650°C and very low partial pressure (40 Pa). Energy from a pulsed carbon dioxide laser at 1027.4 cm^{-1}, where **34** is transparent, is absorbed by a 15-fold excess of silicon tetrafluoride, and **34** is heated by gas-phase energy transfer from silicon tetrafluoride while the reactor walls remain cool. Each laser pulse generates a short temperature pulse centered on the laser beam. The dependence of product distribution on the estimated peak temperature and the number of pulses revealed three primary products: **94** in a relative amount (~60% at ~700°C) greater than in any other study (Table 17); 2-allyltoluene (**95**) (~20%) which was not reported in other studies; and **65** (~10%). There may also have been a minor primary channel to form **26**, but it arose mainly

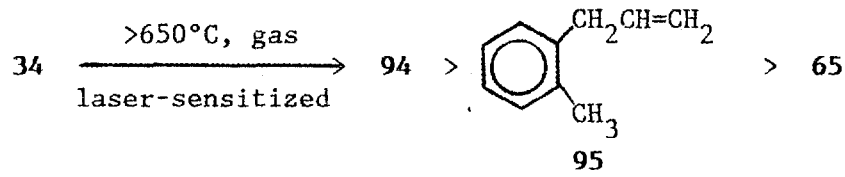

from secondary decomposition of **94** (Section 10.5); secondary reaction of **65** gave **67**. The relative amount of dehydrogenation was indeed lowered under these "wall-free" conditions but not eliminated. Deuterium labeling experiments showed that most, if not all, of the formation of **65** involved intermolecular steps rather than concerted cis-1,2-elimination of hydrogen. At the other experimental extreme of FVP, in which wall effects have every opportunity to reveal themselves, Trahanovsky[226] did find relatively more dehydrogenation, in accord with other studies at higher pressures,[220,224,225] but formation of **94** and **26** still persisted. In summary, no clear resolution to the question of the importance of wall effects has emerged.

10.1.3 Added Hydrogen

The major effect of added hydrogen on the initial product distribution from thermolysis of liquid and dense supercritical **34** is marked acceleration of formation of **92** (lower section of Table 16). There is

less effect on formation of **91** and possibly a slight suppression of **67**.[213] The aromatic hydrodealkylation reaction to form **92**, analogous to

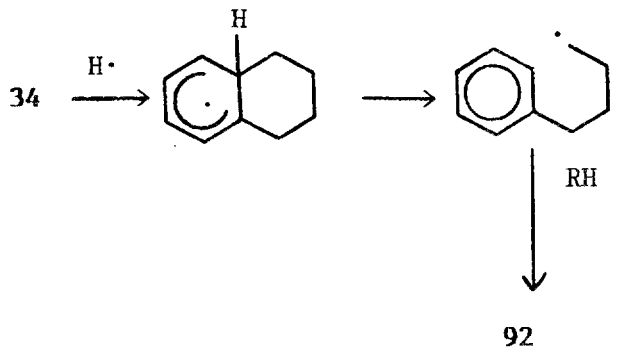

the formation of benzene and ethylbenzene from bibenzyl (Section 5.1.4), presumably is again diagnostic of the presence of hydrogen atom. Penninger[221] presented log rate-vs.-log [**34**] plots for individual products at 500°C over a concentration range of 0.012-0.64 M (see above and Table 17). On changing from nitrogen to hydrogen (8 MPa; 1.2 M), formation of **67** was slightly depressed while that of **91**, **92**, and C_2-benzenes was accelerated to varying extents. At large hydrogen : **34** ratios, the hydrogen-dependent rates of formation of **91** and **92**, after subtraction of the amounts of these products formed under nitrogen, could be fit to the forms $k[\mathbf{34}][H_2]^{1/2}$ and $k[\mathbf{34}][H_2]^{3/2}$, respectively.[221,229] In more concrete terms at a specific concentration of **34** (0.1 M; 640 kPa), the ratio of **67** : **91** : **92** : PhC_2 changed from 83 : 10 : 2 : 4 under nitrogen to 41 : 23 : 18 : 18 under hydrogen. Penninger assigned dissociation-recombination of hydrogen at the reactor wall as the controlling initiation-termination event.

10.1.4 Added Bibenzyl

We discussed in Sections 5.1.1 and 5.1.3 the use of the tetralin carrier technique to measure the homolysis rate of bibenzyl (**19**) based on the rate of formation of toluene (**18**). Having now considered the thermolysis of pure **34**, we return to consider explicitly the effects of added **19** as a radical source.

Sato and coworkers[133] reported a ratio of **67** : **18** = 0.44 from low-conversion decomposition of **19** in excess liquid **34** at 420°C, after correcting for the small amount of **67** formed from **34** alone under identical conditions. Analogously, Benjamin[230] reported **67** : **18** = 0.55 at 400°C and Cronauer and coworkers[150] reported 0.49 at 450°C; these two values are upper limits because they do not contain any correction for **67** formed from **34** alone. Sato and coworkers[133] reported a lower value of 0.33 from similar runs in the gas phase. Note that values of 0.50 and 0.25 would be anticipated for this ratio for the idealized stoichiometries:

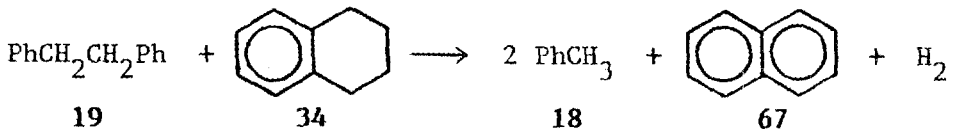

19 + 1/2 **34** ⟶ 2 **18** + 1/2 **67**

In addition to accelerating the formation of **67** in this reaction in which **19** is stoichiometrically involved, added **19** <u>also</u> accelerates the ring contraction to **91**.[133,150,213] This result suggests that isomerization proceeds by a chain mechanism which can be initiated by benzyl radicals (Section 10.1.6).

Accelerating effects of added **19** on the thermolysis of **34** in the presence of added hydrogen have also been reported. The rates of formation of **67** and **91** at 450°C and ~12 MPa hydrogen increased from 1.3 % h^{-1} and 5.7 % h^{-1}, respectively, to 6.6 % h^{-1} and 16.4 % h^{-1}, respectively, on adding 15 mol% **19**;[216] the incremental **67** : **18** ratio was 0.33. The rates of formation of **67** and **91** from a mixture of **34** and biphenyl (73 : 27) at 450°C under 3.45 MPa hydrogen were 0.7 % h^{-1} and 2.8 % h^{-1}, respectively, while those from a mixture of **34** and **19** (76 : 24) were 14.2 % h^{-1} and 11.3 % h^{-1}, respectively.[217]

10.1.5 <u>Thermodynamics</u>

Estimated equilibrium constants for various reactions of **34** in the low-temperature (450°C) and high-temperature regimes (727°C) are shown in Table 18. In Section 8.1 we discussed the cracking of

Table 18. Estimated Thermochemistry of Reactions of Tetralin

Reaction	ΔH°_{298} (kcal mol^{-1})	ΔS°_{298} (cal mol^{-1}K^{-1})	ΔG°_{723} [a] (kcal mol^{-1})	K_{723}	ΔG°_{1000} [a] (kcal mol^{-1})	K_{1000}
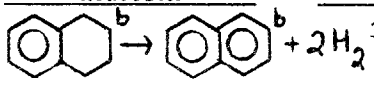	30.1	54.4	-9.2	6×10^2 atm^2 0.2 M^2	-24.3	2×10^5 atm^2 30 M^2
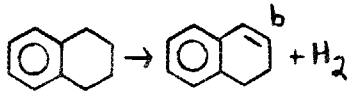	28.3	28.2	7.9	4×10^{-3} atm 7×10^{-5} M	0.1	1 atm 1×10^{-2} M
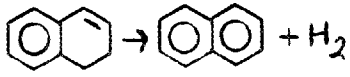	1.8	26.2	-17.1	1.5×10^5 atm 2.5×10^3 M	-24.4	2.2×10^5 atm 2.6×10^3 M
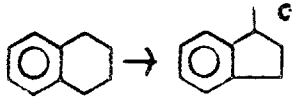	3.2	3.2	0.9	0.5	0	1
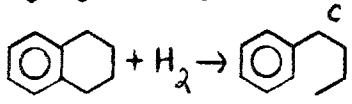	-8.9	-13.2	0.6	0.6 atm^{-1} 38 M^{-1}	4.3	0.1 atm^{-1} 9 M^{-1}
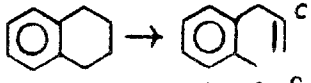	20.2	14.7	9.6	1×10^{-3}	5.5	6×10^{-2}
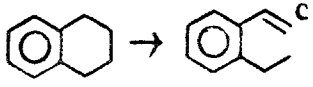	17.1	12.2	8.3	3×10^{-3}	4.9	8×10^{-2}

[a] $G^\circ_T \simeq \Delta H^\circ_{298} - T(\Delta S^\circ_{298})$; no corrections made for $\langle C_p^\circ \rangle$ terms which are small and tend to cancel. [b] Thermochemical properties from ref. 231. [c] Thermochemical properties from group additivity estimates (ref. 29).

1,3-diphenylpropane to form toluene plus styrene and noted how the unfavorable ΔH^{o} is offset at $\gtrsim$250°C by the favorable ΔS^{o} associated with forming two molecules of product. In contrast, analogous cracking pathways which would convert **34** to 2-allyltoluene (**95**) or 2-ethylstyrene (**96**) enjoy much less entropy gain because they are intramolecular. At 450°C, K ~ 0.001-0.003, and cracking products could be significant only at trivial conversion levels; even at 727°C, their formation is still thermodynamically quite constrained (K ~ 0.1). Hence, the failure to find this product class is not surprising. The singular observation[218] of **95** during laser-powered thermolysis at high temperatures may well have been near the equilibrium limit.

Complete dehydrogenation to form naphthalene (**67**) is thermodynamically favorable over most of the range of experimental conditions. However, to the extent that it is mechanistically constrained to proceed through 1,2-dihydronaphthalene (**65**) as an intermediate, thermodynamic limitations appear here as well, especially for the low-temperature, dense-**34** regime. For example, for 5 M **34** in a closed supercritical system at 450°C (typical conditions of Table 16), the equilibrium constant shown in Table 18 predicts a <u>maximum</u> ratio of **65** : **34** of only ~0.004; as additional hydrogen accumulates during subsequent formation of **67**, this ratio must, of course, decrease even further. The corresponding maximum ratios for gaseous **34** initially at 100 kPa and 450°C and initially at 10 kPa and 727°C are ~0.06 and ~11, respectively. [All these values are, of course, approximations to the extent that non-ideal behavior intervenes.] Thus the observation that **65** accumulates as an intermediate in high-temperature, gas-phase runs (Table 17) but not in low-temperature, dense runs (Table 16) can be a direct consequence of thermodynamics, not necessarily of some fundamental difference in mechanism.

In contrast to these restrained reactions, the equilibrium constant for ring contraction to 1-methylindane (**91**) is near unity. In fact, thermal reversion of ^{14}C-labeled **91** to **34** has been demonstrated at 400°C.[84] Hydrogenolysis to form <u>n</u>-butylbenzene (**92**) is also thermodynamically allowed if sufficient hydrogen is supplied.

10.1.6 Mechanisms

All mechanistic proposals in the literature for the ring contraction to form **91** have involved radical intermediates, and its acceleration by added bibenzyl supports the occurrence of a short chain. Three different radicals have been suggested as the species from which the skeletal rearrangement originates: 1-tetralyl (**35**) via β-scission to form 2-vinylphenylethyl radical (**98**) followed by re-addition to form 1-indanylmethyl radical (**97**) in sequence 128;[7] 4-phenyl-1-butyl (**99**) via sequence 129;[229] and 2-tetralyl (**100**) via 1,2-aryl shift 130.[232] Sequence 128 does not conform to the labeling pattern observed in the **91**

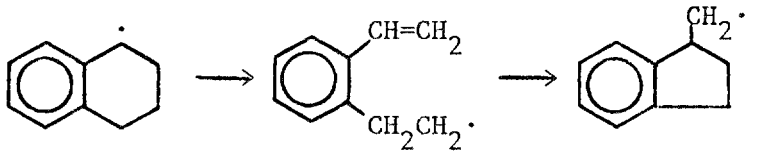

35 **98** **97** (128)

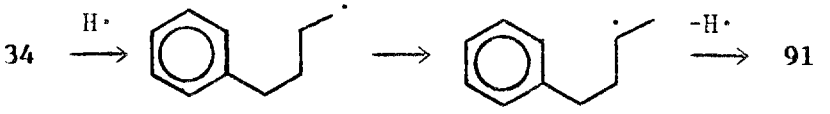

99 (129)

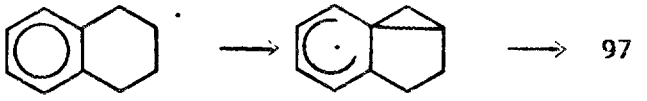

100 (130)

produced by thermolysis of **34**-1-^{13}C at 500°C,[84] which indicated predominant loss of the C_1-C_{8a} connectivity, not of the C_2-C_3 connectivity characteristic of sequence 128. Sequence 129 is unlikely because it demands a 1,2-hydrogen shift;[24c] in addition, its obligatory dependence on hydrogen atom suggests, contrary to observation, that the formation of **91** should respond to reaction conditions similarly to that of **92**. In contrast, we have already discussed a direct analogy for sequence 130 in the conversion of bibenzyl to 1,1-diphenylethane (Section 5.1.3). A series of detailed product studies by Franz and coworkers,[232,233] in

which the radicals 1-tetralyl (**35**), 2-tetralyl (**100**), 1-indanylmethyl (**97**), 2-indanylmethyl (**58**), 2-methyl-1-indanyl, and 1-methyl-2-indanyl were generated individually at 327-627°C and 3 Pa from their respective t-butyl perester precursors, gave strong support for sequence 130 as the favored ring contraction route, at least at temperatures <500°C.

More recently, Franz and coworkers[187,234] have assigned rate constants in Arrhenius form to the 1,2-phenyl shift, β-scission, and addition reactions which connect the various $C_{10}H_{11}\cdot$ radicals by measuring the temperature dependences (100-200°C range) of the relative rates of these intramolecular transformations compared with hydrogen abstraction from tri-n-butylstannane, the rates of the latter now being known on an absolute basis for generic classes of carbon-centered radicals. We have constructed in Figure 3 a free-energy profile of the connections among the relevant radicals at 400°C, based on these rate constants, converted to $\Delta G^{\neq}$, and on Franz's group additivity estimates[234] of ΔH_f^{o} and S^{o} of the various radicals. If one enters this system by abstracting H-2 of **34** to form radical **100**, rearrangement by 1,2-phenyl shift to form radical **97**, which contains the 1-methylindane skeleton, is indeed indicated by Figure 3 to be some 150-fold more rapid than rearrangement by ring opening to form radical **57** followed by reclosure to radical **58**, which contains the 2-methylindane skeleton. However, if one enters via the more stable 1-tetralyl radical (**35**), as would be the predominant case for any kinetically controlled hydrogen abstraction from **34**, consideration of Figure 3 indicates sequence 128 as the favored rearrangement pathway. The resolution to this apparent anomaly most probably lies in the facile interconversion of radicals **35** and **100** via bimolecular hydrogen abstraction reactions with **34**, fully analogous to the situation we have already encountered with 1,4-diphenylbutane (Section 9). We estimate $k_{131} \sim 10^{9.2}\exp(-20{,}100/RT)\ M^{-1}s^{-1}$,[123] which

$$\mathbf{35} + \mathbf{34} \rightleftharpoons \mathbf{34} + \mathbf{100} \qquad (131)$$

corresponds for liquid **34** (~5 M) to a $\Delta G^{\neq}_{673} \sim 30.1$ kcal mol^{-1} on the scale of Figure 3. Indeed, then, this bimolecular route allows

conversion of **35** to **100** (and thence to **97**) with a lower free energy barrier than for unimolecular ring-opening to **98** (~35.6 kcal mol^{-1}). However, this analysis predicts that scheme 128 should become operative at the much lower concentrations of **34** characteristic of gas-phase conditions, under which some **91** is still formed.

Rearrangement via sequence 130 is also supported by evidence that formation of **91** has a higher kinetic order in **34** than dehydrogenation.[221,235] Were the rearrangement sequence:

$$\mathbf{34} \xrightarrow{R_i} \mathbf{35}$$

$$\mathbf{35} \longrightarrow \mathbf{97} \qquad (128)$$

$$\mathbf{97} + \mathbf{34} \longrightarrow \mathbf{91} + \mathbf{35} \qquad (132)$$

$$2\ \mathbf{34} \xrightarrow{k_t} \text{Non-radical products}$$

for which $k_{128} < k_{132}[\mathbf{34}]$ even for gas-phase **34** [$k_{128} \sim (1/2)(kT/h)\exp(-35{,}600/RT)\ s^{-1} \sim 19\ s^{-1}$ at 400°C (Figure 3); $k_{132} \sim 10^{8.3}\exp(-8{,}000/RT)\ M^{-1}s^{-1} \sim 5 \times 10^5\ M^{-1}s^{-1}$ [123]], the steady-state expression for formation of **91** would have the form:

$$d[\mathbf{91}]/dt = f\{(R_i/k_t)^{1/2}\}k_{128}$$

i.e., it would have no further kinetic dependence on [**34**] than that arising from the $R_i^{1/2}$ term. However, if step 128 were replaced by steps 131 and 130, then the occurrence of step 131 allows added kinetic dependence on [**34**].

Mechanistic proposals in the literature for the formation of **65**, and subsequently of **67**, fall into three categories: wall-catalyzed,[219] concerted,[220] and radical. In most studies, a heterogeneous component has been neither rigorously demonstrated nor eliminated, although the persistence of some dehydrogenation even under the laser-powered

conditions[218] suggests at least some homogeneous component. The isotopic labeling results in that study[218] did not support a concerted loss of hydrogen but were consistent with intermolecular radical pathways. All proposals involving radicals begin with **35** but differ in the mode of hydrogen atom loss: direct expulsion (step 133),[218,224] which creates the possibility of a chain involving hydrogen atom as a carrier, or disproportionation (step 134),[230,233] which cannot propagate a chain.

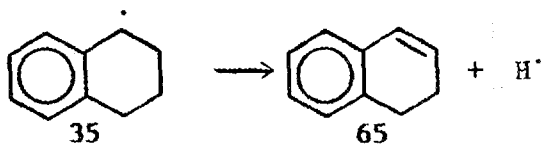

(133)

$$2\ \mathbf{35} \longrightarrow \mathbf{34} + \mathbf{65} \qquad (134)$$

[Although each interaction of two **35** radicals gives more combination than disproportionation (k_{comb}/k_{dis} = 12 at 150°C with a small tendency to decrease with increasing temperature[236]), combination will be reversible at >400°C because of the homolytic instability of 1,1'-bitetralyl (Section 5.4)[170]]. Two lines of argument suggest that disproportionation dominates at the low-temperature, dense-phase end of the experimental range. First, β-scission of **35** would be expected to expel a carbon-centered radical (step 128) in preference to hydrogen atom (Section 2.3). Yet we have just seen that step 128 is not an active process under these conditions because, were it to occur, it would lead to **91** with a labeling pattern opposite to that observed[84] (Figure 3). Secondly, we estimate $k_{133} \sim 10^{13.6}\exp(-41{,}000/RT)\ s^{-1}$, in analogy with Miller and Stein's value[44] for 1,2-diphenylethyl radical and $k_{134} \sim 0.1k_t \sim 10^9\ M^{-1}s^{-1}$. We then calculate the steady-state level of **35** needed to sustain the observed rate of dehydrogenation by each route. The route which leads to the <u>lower</u> calculated radical level will be the one more likely to occur. To sustain a rate of ~0.1 % h^{-1} in liquid **34** at 400°C (Table 16) by the β-scission route would require [**35**] ~ 7 x 10^{-7} M but, by the disproportionation route, only ~ 4 x 10^{-8} M. In contrast, to sustain the observed rate of 25 % s^{-1} with 50 kPa **34** at 725°C[225] would require [**35**] ~ 3.8 x 10^{-8} M and

~ 1.2 x 10^{-6} M, respectively. Hence, β-scission may occur in the high-temperature, gas-phase regime.

Once at **65**, from which further hydrogen abstraction can give radical **66**, a similar competition arises between steps 135 and 136:

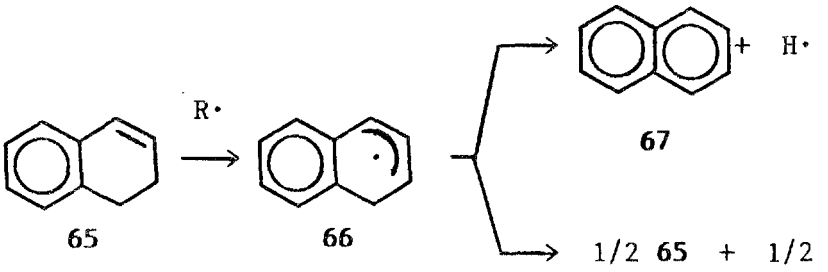

(135)

(136)

However, the energetics of expulsion of hydrogen atom are now much more favorable (Section 10.2) because of the aromatic stability of product **67**, and β-scission may well predominate under all conditions.

When mixtures of aralkanes and **34**-d_{12} were heated, H-D exchange between the benzylic carbons occurred.[149,237,238] The extents of exchange after 1 h at 400°C for 1 : 1 mixtures of **34**-d_{12} and 1-phenylpropane (10%), diphenylmethane (28%), and 5,12-dihydronaphthacene (43%) increased as the C-H bond energies decreased.[237] Exchange was accelerated by materials which generate radicals, such as bibenzyl[149] and benzyl phenyl sulfide,[237,238] but not by acids or bases.[237] Thus exchange almost surely occurs by the radical chain sequence:

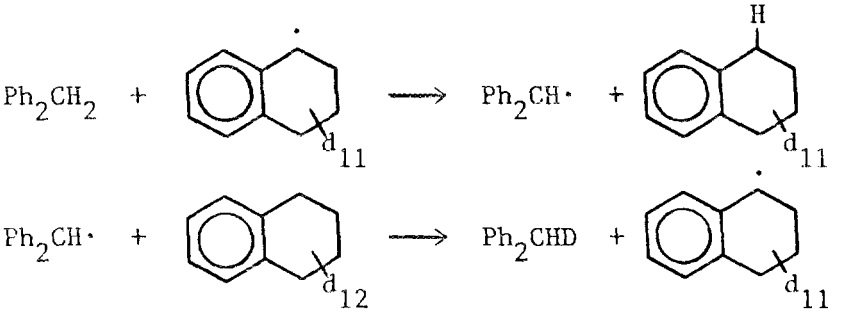

which functioned smoothly at 400°C even in the absence of added initiators.

Granted then that rearrangement to **91** occurs via a short radical chain, that dehydrogenation also occurs at least in part from radical **35**, and that H-D exchange is a radical process, what is the radical source? Bergman and coworkers [218] proposed that all three primary products under laser-powered, high-temperature, low-pressure conditions arose from 1,6-diradical **101**, which was formed in step 137 by rate-limiting homolysis of the C_1-C_2 bond, clearly the weakest bond in **34**. Because benzylic radicals are slightly less stable than allylic radicals with the same substitution pattern,[20] we take the rate constant for homolysis of vinylcyclohexane, $10^{16.0}\exp(-73{,}900/RT)\ s^{-1}$,[239] as an upper limit for k_{137}. [A somewhat lower estimate of $D^o(C_1\text{-}C_2)$ in **34**[218] was based on a value for the benzylic resonance energy somewhat larger than currently accepted.[20,29]] The derived $t_{1/2,137} \gtrsim 1$ s at 727°C is not incompatible with observations[218] of overall disappearance of **34**. The formation of 2-allyltoluene (**95**), which could arise from intramolecular disproportionation in step 138, is especially suggestive of the presence of **101**. Benzocyclobutene (**94**) could arise via competitive loss of ethylene in step 139 followed by ring closure of o-xylylene (**102**). However, in light of the energetics of β-scission processes (Section 2.3), it seems improbable that expulsion of hydrogen atom from **101** in step 140, proposed as the route to **65**, could compete effectively with expulsion of **102** which may be considered an "especially stable benzylic radical" (see below for estimates of k_{138} and k_{139}). Thus, C_1-C_2 homolysis may well rationalize the ring-opening and C_2-loss reactions at high temperatures but not necessarily non-chain dehydrogenation.

The upper limit for k_{137} estimated above predicts a C_1-C_2 homolysis rate at 450°C of $\lesssim$0.2 % h^{-1}. The experimental value for total consumption of **34** under dense-phase conditions, largely by ring contraction to **91** (Table 16), was ~4 % h^{-1}, 20 times greater. King and Stock[237] estimated a lower C_1-C_2 homolysis rate at 400°C of ~0.02 % h^{-1}, from slightly different thermochemical assumptions, whereas H-D exchange with diphenylmethane occurred at a rate of 28 % h^{-1}, 1400 times greater. Such differences might be made up by appropriate chain lengths <u>if</u> biradical

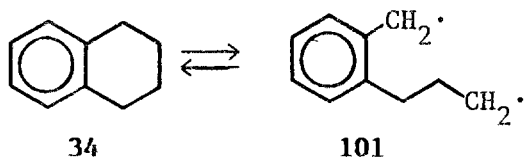

(137)

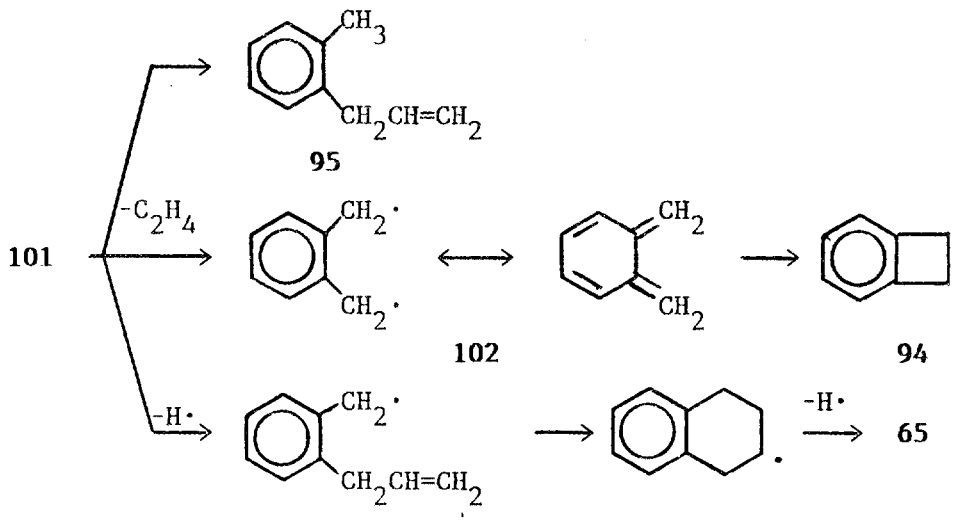

(138)

(139)

(140)

101 served as an initiator by being converted to a mono-radical. However, steps 138 and 139 just discussed for intramolecular decay of **101** do not produce radicals but rather spin-paired products. Bergman and coworkers[218] estimated $k_{138} \sim 10^{12}\exp(-1{,}000/RT)\ s^{-1}$ and $k_{139} \sim 10^{13.5}\exp(-6{,}000/RT)\ s^{-1}$ from known behavior of other 1,6-diradicals (presumably some ring closure to reform **34** also occurs). The most reasonable intermolecular decay pathway would be step 141,

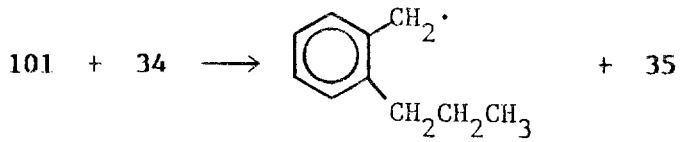

(141)

hydrogen abstraction from **34** by the unstabilized prim radical center, for which we estimate $k_{141} \sim 10^{8.3}\exp(-8{,}000/RT)\ M^{-1}s^{-1}$.[123] At 450°C in 5 M **34**, these estimates lead to values for k_{138}, k_{139}, and $k_{141}[\mathbf{34}]$ of 5×10^{11}, 5×10^{11}, and $4 \times 10^{6}\ s^{-1}$, respectively. At 727°C and 100 kPa **34**, they are 8×10^{11}, 1.5×10^{12}, and $4 \times 10^{4}\ s^{-1}$, respectively.

Thus, only an infinitesimal fraction of **101** would produce the mono-radicals needed to initiate chains, and C_1-C_2 homolysis does not therefore appear to offer an effective "radical source." Homolysis of other C-C bonds in **34** has been suggested,[225,240] but they will be considerably stronger and offer no relief from the fundamental problem that biradicals are not likely chain initiation sources.

The weakest bond which could break to produce monoradicals directly, as suggested by Penninger[221] and by Bergman and coworkers[218], is the C_1-H bond, but its homolysis in step 142 must be much slower than C_1-C_2

$$\mathbf{34} \longrightarrow \mathbf{35} + H\cdot \qquad (142)$$

homolysis in step 137. [The estimate by Bergman and coworkers[218] that C_1-C_2 and C_1-H homolysis will have similar ΔG^o values at ~1000°C is only indirectly relevant to the relative rates of homolysis because the more favorable ΔS^o term for the latter is not expected to be reflected in a larger A value for the latter homolysis as much as in a larger A value for the reverse of the former.] We estimate $k_{142} \sim 10^{16}\exp(-85{,}000/RT)\ s^{-1}$ (see Section 4.1.1),[20,29] which corresponds to a predicted time for 1% homolysis at 450° of almost 2 yr. We therefore conclude that, even though much of the low-temperature thermal chemistry of **34** involves radical chains, the initial source of radicals remains unknown. A corollary conclusion is that trace impurities or initial products may, in fact, be crucial to the bulk of the observed chemistry. Trushkova and coworkers[223,241] have also noted the thermochemical difficulty in forming radicals directly from **34** and have proposed that chain initiation occurs by bimolecular molecular disproportionation involving olefinic products formed during an inhibition period. King and Stock[237] made a similar suggestion. Hooper and coworkers[212] interpreted their low-conversion data at <400°C to indicate that formation of **91** did not commence until some dehydrogenation had occurred; however, their specific inference that the key "initiating product" was hydrogen is unlikely, since it was based on the improbable sequence 129 for rearrangement. We will consider in Section 10.2 a possible

bimolecular initiation route involving **65**. Experimental data is needed at very low conversions with very highly purified **34**.

10.2 DIHYDRONAPHTHALENES

Gill and Hawkins[242] determined the rate of disproportionation of 1,2-dihydronaphthalene (**65**) in various solvents at 300°C to form tetralin (**34**) and naphthalene (**67**) in a 1 : 1 ratio. The second-order rate constant in 1-chloronaphthalene solvent was $k = 10^{9.8}\exp(-37{,}000/RT)\ M^{-1}s^{-1}$ over the range 290-317°C; it varied only 35% in changing the solvent from n-dodecane to DMF. A concerted ($\sigma_{2s} + \sigma_{2s} + \pi_{2s}$) hydrogen transfer mechanism was proposed:

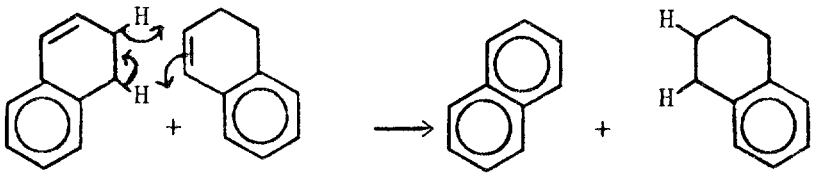

65 **65** **67** **34**

However, Heesing and Müllers[243] found that the deuterium distribution in the products formed from cis- and trans-1,2-dideuterio-**65** did not conform to the predictions of the concerted mechanism but was considerably scrambled. They proposed that the initial interaction was a molecular disproportionation[16] to produce 1-tetralyl radical (**35**) and 1,4-dihydro-1-naphthyl radical (**66**), which then disproportionated by the other possible mode to give the observed products:

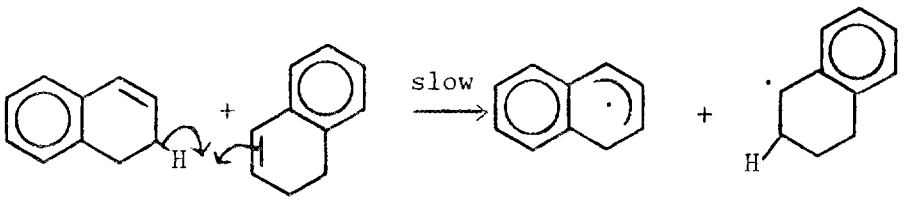

(143)

65 **65** **66** **35**

fast

67 + **34**

That the initial step involves breaking the C_2-H bond was supported by the observation[153] of a significant kinetic isotope effect (2.3) at 290°C for **65**-d_{10} but not for **65**-1,1,3-d_3.

King and Stock[244] also described rapid disproportionation of **65** (36% conversion of the neat liquid after 2 h at 300°C; 64% after 5 min at 400°C) but noted the formation of a 15-20% excess of **67** over **34**. In more extensive kinetic data for neat **65** and for mixtures diluted with **34** and biphenyl at 350-400°C and quite high conversions, Allen and Gavalas[245] observed that rates fell off with dilution somewhat less rapidly than expected for second-order behavior. The ratio of **67** : **34** was again typically 1.15-1.20, and hydrogen was found in amounts corresponding to this stoichiometric excess of **67** over **34**. These authors proposed that step 143 was the initiation event of a chain, and the kinetics were modeled by numerical integration of a set of some 10 propagation steps. Omitting those involving secondary reactions of **34** and those involving a minor amount of radical **100**, we note that the key steps in the proposed chain at low conversion were:

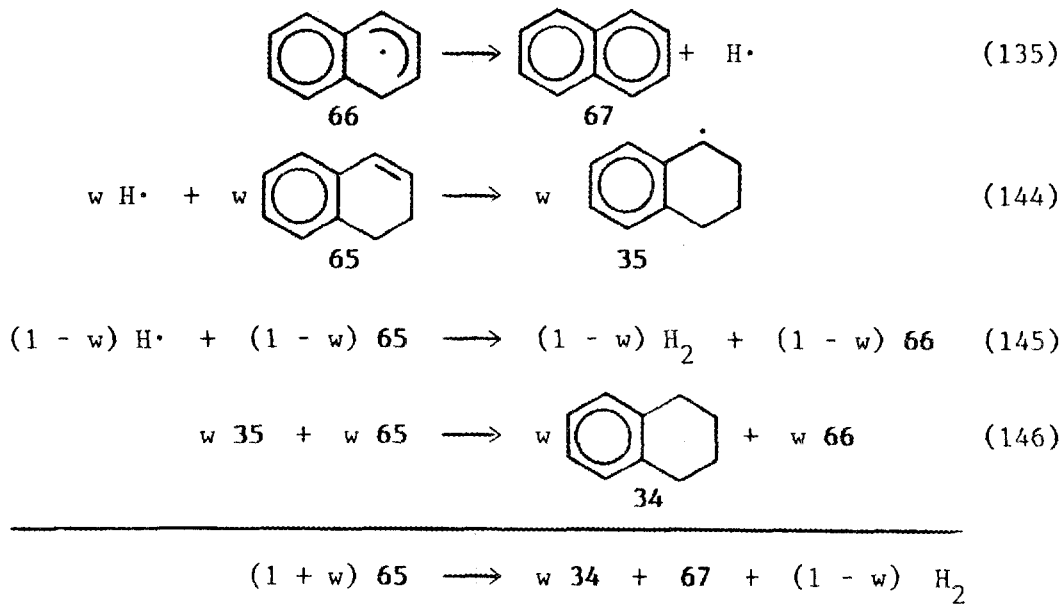

The difference from the Hessing-Müllers non-chain mechanism[243] is that **66** was proposed to efficiently expel hydrogen atom (step 135) which could then react with **65** both by addition (step 144) and hydrogen abstraction (step 145). The presence of hydrogen atom was also signaled by the

production of some n-butylbenzene when **34** was the solvent.[246] Exothermic hydrogen abstraction from **65** by **35** (step 146) would then complete the chain. Allen and Gavalas[245] assigned $k_{143} \sim 10^{8.0}\exp(-38{,}000/RT)\ M^{-1}s^{-1}$; $k_{135} \sim 10^{14.5}\exp(-27{,}000/RT)\ s^{-1}$; $k_{144} \sim 10^{11.0}\exp(-3{,}000/RT)\ M^{-1}s^{-1}$; $k_{145} \sim 10^{10.0}\exp(-3{,}000/RT)\ M^{-1}s^{-1}$; and $k_{146} \sim 10^{7.0}\exp(-9{,}000/RT)\ M^{-1}s^{-1}$ by a combination of thermochemical kinetic estimates and data fitting. The critical ratio in determining the **67** : **34** product ratio is $k_{144}/(k_{144} + k_{145}) = w$; if hydrogen atom largely adds to **65** (w ---> 1), **67** : **34** ---> 1; if it largely abstracts (w ---> 0), **67** : **34** ---> ∞. No effect of the concentration of **65** on the **67** : **34** ratio was observed; this result is consistent with the model in which steps 144 and 145 are of the same kinetic order in **65**. No temperature effect on this ratio was observed either; this demanded the assignment $E_{144} = E_{145}$. The derived value of w was 0.91. In contrast, McMillen and coworkers[26] reported a gradual increase in **67** : **34** from 1.2 to 1.4 with decreasing [**65**] over the range [**65**] = 2-30 mol% in biphenyl at 385°C. They therefore made a further modification of the chain by suggesting that the net result of steps 135 and 144 could be achieved not only by these steps occurring successively, but also by a single bimolecular radical hydrogen transfer, step 147. Their steady-state analysis of product data led to a best fit

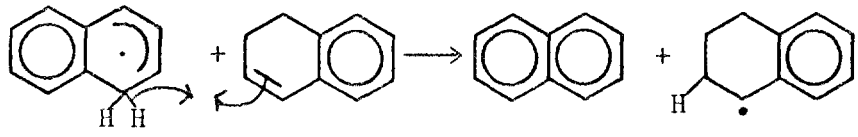

66 **65** **67** **35** (147)

for $k_{147}/k_{135} = 1.08\ M^{-1}$; i.e., direct expulsion of hydrogen atom and bimolecular hydrogen transfer were of equal importance at [**65**] ~ 1 M . With this modification, they concluded w = 0.68.

Although there is now general agreement that disproportionation of **65** involves a chain, certain of the details thus remain unclear. Of particular interest is the chain length as a function of conditions; i.e., what fraction of the total rate[242] results directly from the initial molecular disproportionation step 143? Allen and Gavalas[245] found 38.3% conversion of neat **65** after 5 min at 350°C. If we take neat

65 as ~5.5 M, the Gill-Hawkins rate constant[242] (in a different solvent) corresponds to 53% conversion. Thus the experimental agreement between the two sets of workers is quite good. However, whereas some[246] appear to equate the Gill-Hawkins rate constant for total conversion with k_{143}, the Allen-Gavalas model predicts that only 1% of the total conversion proceeds via k_{143}.

Along with dominant disproportionation, a small amount of a mixture of C_{20} products is also formed from thermolysis of neat **65**.[243,246] Franz and coworkers[246] identified these with the help of simplifications of their NMR spectra offered by use of **65**-d_4. They were all formulated as the result of radical additions to **65** of not only **35**, but especially of 2-tetralyl (**100**) and 1,2-dihydro-1-naphthyl (**103**) radicals.

The simultaneous disproportionation and dehydrogenation of **65** in the dilute gas phase at 400°C in a quartz vessel was assigned by Gangwer[219,235] as totally wall-catalyzed, as for **34**. Thermolysis of **65** at 725-825°C in flowing nitrogen carrier was somewhat more rapid than that of **34**, and the complex set of products formed was discussed as arising from disproportionation followed by secondary decomposition of **34**.[225]

Could step 143 serve as the mysterious "radical source" to initiate the chain reactions of tetralin (**34**) under the conditions of Table 16 (Section 10.1.6) if **65** were a trace impurity or were formed in trace quantities by, say, wall reactions?[219] Consider 5 M **34** at 450°C where the rate of formation of **91** is ~3.5 % h^{-1} = 4.9 x 10^{-5} M s^{-1}. Assume **65** accumulated to a level of 10^{-2} M (0.2% conversion); [the equilibrium limit is ~2 x 10^{-2} M (Table 18)]. The rate of step 143 from the Allen-Gavalas estimate[245] would then be ~3.3 x 10^{-8} M s^{-1}, <0.1% of the rate of formation of **91**. While the chain length demanded appears unreasonably long, a modest increase in the value assigned to k_{143} would make this scenario plausible. Further information on the correct value of k_{143} is clearly desirable. Equally worthy of consideration as a

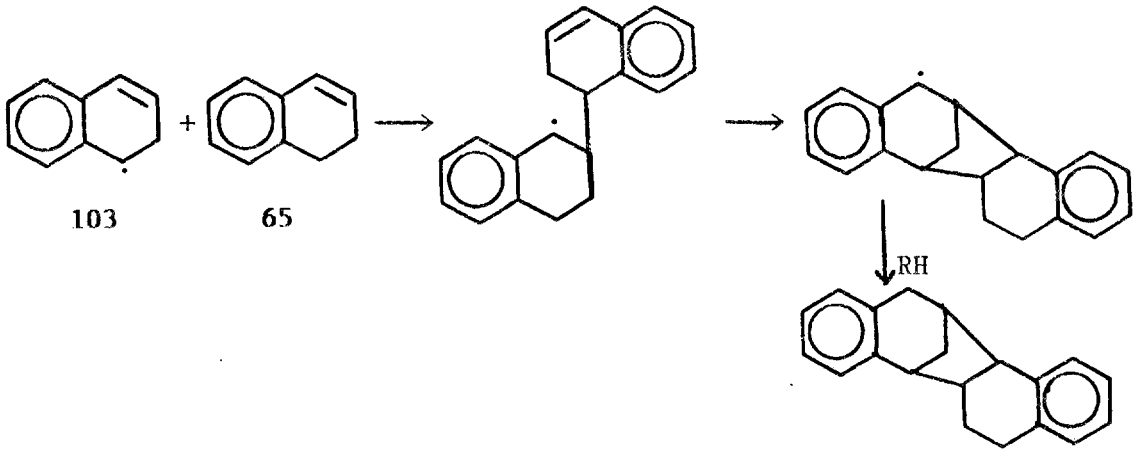

Both endo-2α,7α and exo-2β,7β isomers

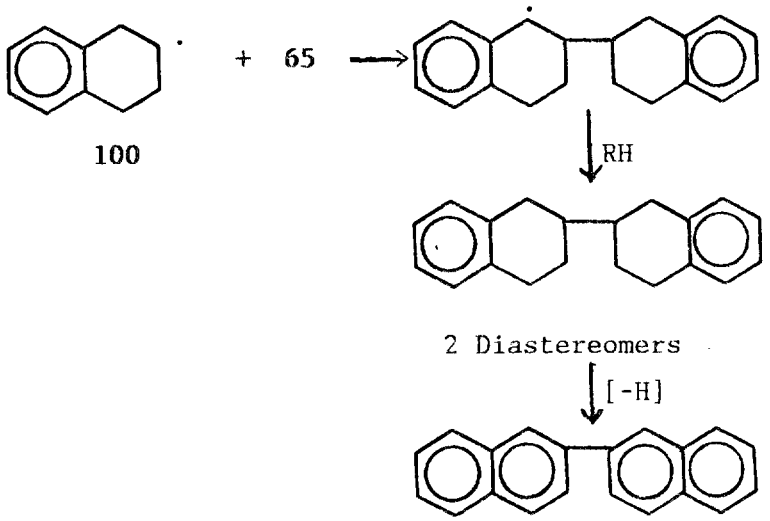

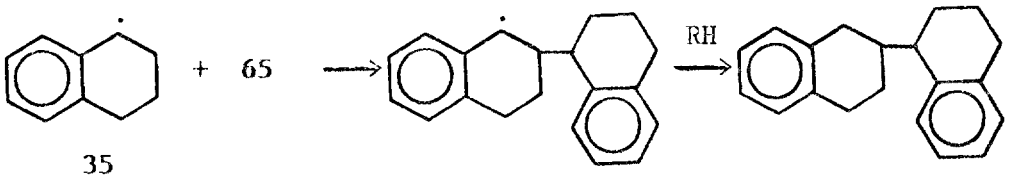

2 Diastereomers

radical source is a scenario involving molecular disproportionation between one molecule of **65** and one of **34** (step 148). The need to break

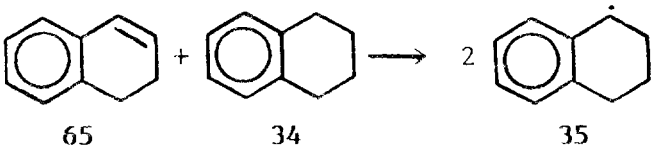

(148)

the C_1-H bond in **34**, which is ~7 kcal mol^{-1} stronger[29,246] than the C_2-H bond in **65**, would decrease k_{148} some 130-fold at 450°C, compared with k_{143}. Inversely, until the level of **65** reached ~1/130 that of **34** (0.8% conversion), step 148 would then be more rapid than step 143. Of course, step 148 is simply the reverse of step 134; i.e., the interaction of two tetralyl radicals need not be totally "terminating" but rather may maintain a low steady-state radical level.

1,4-Dihydronaphthalene (**104**) underwent disproportionation to form a mixture of **34** and **67** at a rate similar to that of **65**, but it also simultaneously isomerized to form **65** in similar amounts;[242,244] conversion of **104** to **65** is the thermodynamically favorable direction.[244] A reasonable path for the isomerization has been offered by Allen and Gavalas:[245]

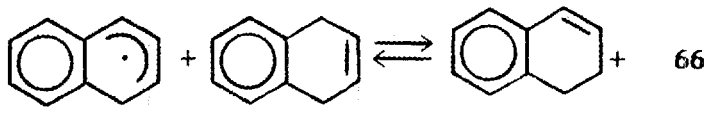

66 **104** **65**

and a chain scheme similar to steps 135 and 144-146 can be written for disproportionation. However, the initiating event deserves further attention since step 149 would be expected to be ~10 kcal mol^{-1} less favorable than step 143 because the unstabilized radical **100** must be formed.

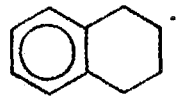

2 **104** ⟶ + **66** (149)

100

10.3 OTHER SIX-MEMBERED-RING HYDROAROMATICS

Cronauer and coworkers[247] heated liquid 1,2,3,4,5,6,7,8-octahydrophenanthrene (**105**) at 450°C, both in the presence and absence of bibenzyl, and observed both dehydrogenation and ring contraction to form several isomers of **106**, in analogy to the behavior of **34**. Similarly,

Collin and coworkers[240] observed both processes for 1,2,3,4,5,6,7,8-octahydroanthracene (**107**) (12% conversion after 1 h at 450°C) and for 1,2,3,4,5,6,7,8,9,10,11,12-dodecahydrotriphenylene (**108**) (30% conversion under the same conditions). In each case, the ratio of ring contraction : dehydrogenation increased with increasing temperature. At 450°C, this ratio was less for **107** (0.7) than for **108** (5).[240] However, the inflections in plots of this ratio vs. temperature,[240] the variations observed among various workers in the analogous ratio for **34** (Table 16), and the uncertainties in the dehydrogenation mechanism (Section 10.1.6) suggest caution in drawing either fundamental mechanistic inferences or coal processing implications.

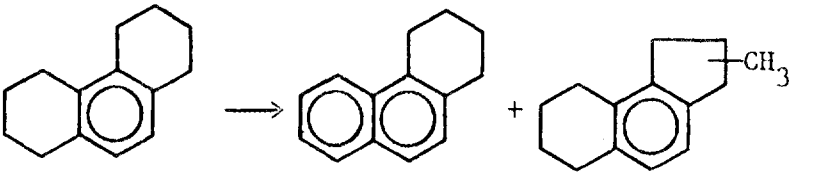

105 **106**

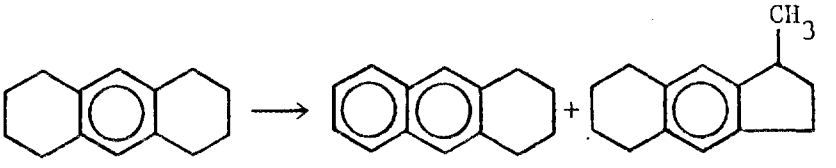

107

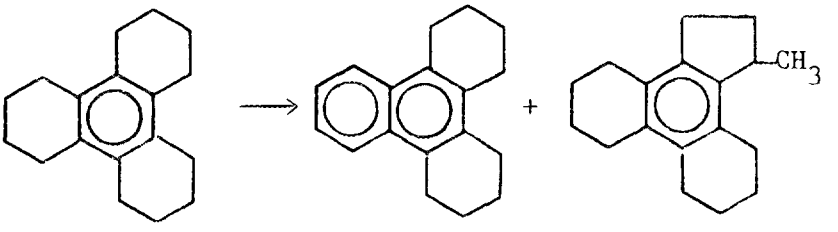

108

10.4 INDANE

Penninger[221] reported kinetics of decomposition of gaseous indane (**109**) at 500°C over the range 0.012-0.432 M in the presence of nitrogen and hydrogen. The major process under nitrogen was dehydrogenation to form indene (**93**) with 1/2-order kinetics. Ring cleavage products toluene

(**18**) and n-propylbenzene (**111**) were formed in much smaller amounts. Not surprisingly in light of the strain destabilization of benzocyclobutene, no ring contraction was observed. The following mechanism was proposed for dehydrogenation:

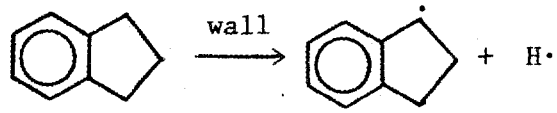

109 **110** (150)

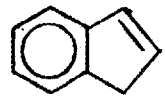

110 ⟶ + H· (151)

93

H· + **109** ⟶ **110** + H_2 (152)

H· + **109** ⟶ $Ph(CH_2)_2CH_2\cdot$ ⟶ C_2H_4 + $PhCH_2\cdot$

112

+**109** ↓ -**110** +**109** ↓ -**110**

$Ph(CH_2)_2CH_3$ $PhCH_3$

111 **18**

2 **110** ⟶ Non-radical products

with $k_{151} << k_{152}[\mathbf{109}]$. Kinetic analysis of the response of rates to hydrogen concentration coupled with the use of isotopic exchange with deuterium led to $k_{150} = 10^{7.9}\exp(-41{,}000/RT)\ s^{-1}$. Penninger recognized such A and E values to be much too low for unimolecular C-H homolysis and therefore proposed this initiation step to be wall-catalyzed. Such conclusions are oversimplified because homolysis cannot be "catalyzed" in the classical sense because its transition state enthalpy, already being at the same level as the products, cannot be lowered further by a "catalyst." Significant wall effects would demand chemisorptive stabilization of the "radical" products. Also, this mechanism predicts that the ratio of **18** : **111** should increase as the concentration of **109** decreases and β-scission of radical **112** is able to compete more effectively; yet

the data showed a virtually constant ratio over a 35-fold variation in concentration. As with **34**, replacement of nitrogen with high-pressure hydrogen markedly accelerated formation of the ring cleavage products.

10.5 BENZOCYCLOBUTENE AND DIMERS

Analogs of highly strained benzocyclobutene (**94**) are unlikely to be present in coal, but we include information on its thermal behavior because of its possible involvement as a product from high-temperature thermolysis of tetralin (Section 10.1.2). Thermolysis of dilute **94** at high temperature gave styrene (**26**). Various labeling experiments[248] defined the following unimolecular pathway:

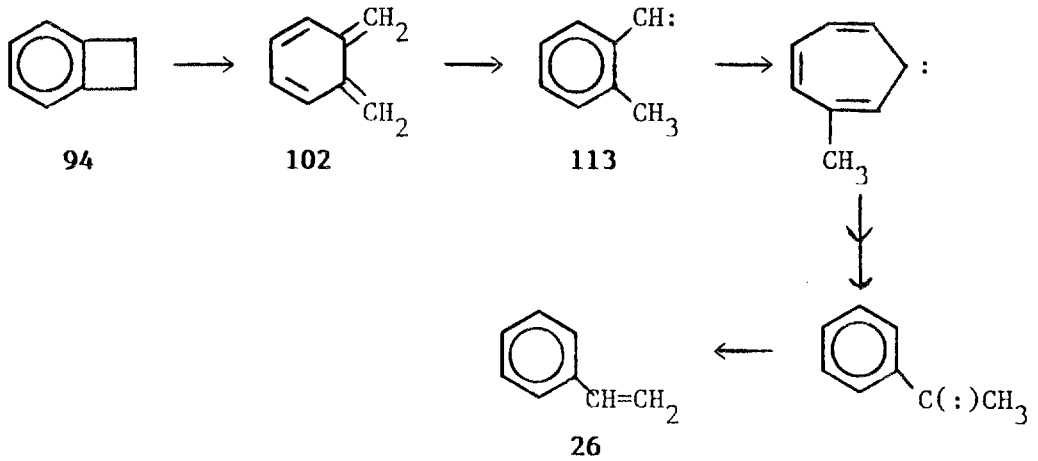

Ring-opened **102** is converted to 2-methylphenylcarbene (**113**) by an unusual intramolecular 1,4-hydrogen transfer step. A series of known reversible phenylcarbene--cycloheptatrienylidene rearrangements then ultimately places the carbene center on a C_2 side-chain from which formation of **26** is expected. Under more concentrated conditions, **102** dimerizes to form, among others, [4+4] dimers. Trahanovsky and Surber[249] have described formation of anthracenes in modest yield from FVP of such dibenzocyclooctadienes at 900-980°C, and the following mechanism was proposed to account for the counterintuitive substitution pattern observed:

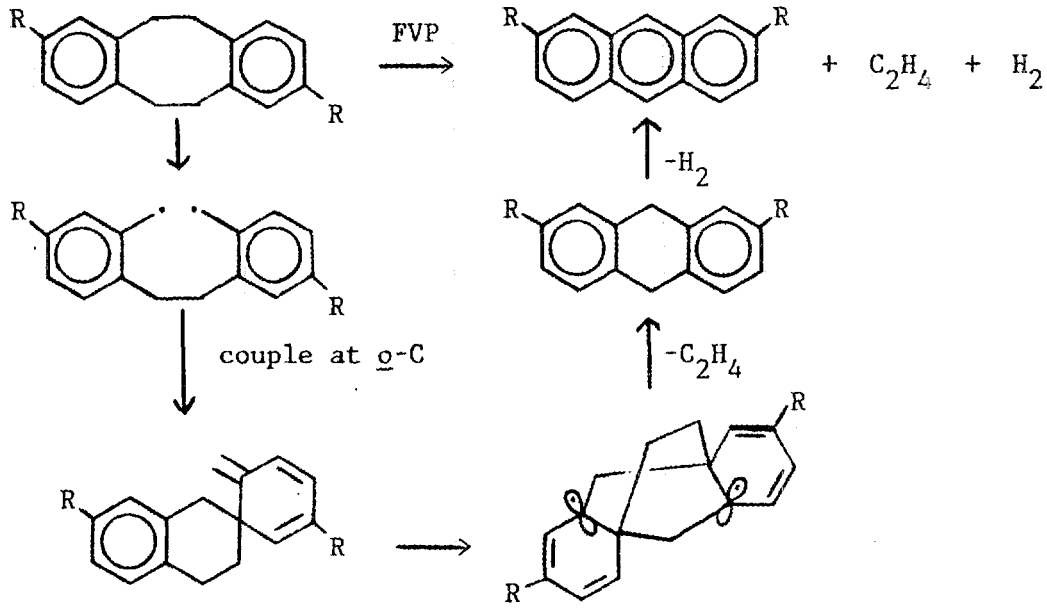

114 **115**

The unusual step is a molecule-induced homolysis between a methylene-cyclohexadiene unit and a benzene ring in intermediate **114** to generate 1,4-diradical **115**, each radical center of which is stabilized as part of a cyclohexadienyl system, from which expulsion of ethylene generates a dihydroanthracene unit.

10.6 HYDROGEN TRANSFER BETWEEN HYDROAROMATICS AND AROMATICS

The facile hydrogen transfer between hydroaromatics and aromatics that occurs in the low-temperature regime is clearly relevant to coal liquefaction, especially to the phenomenon of "hydrogen shuttling" in which certain polycyclic aromatics appear to act as hydrogen-transport agents between hydrogen and coal. Virk and coworkers[201] reported that anthracene (**13**) in 1,4-dihydronaphthalene (**104**) solution was converted to 9,10-dihydroanthracene (**116**) at 300°C some 10 times more rapidly than it was in a corresponding solution in the 1,2-isomer **65**. Yet for analogous hydrogenation of phenanthrene (**15**), which required a temperature of 400°C to achieve comparable conversions, **65** was a more effective hydrogenating agent than **104** by a factor of 1.6. These contrasting results are in accord with predictions based on orbital symmetry considerations for concerted transfer of hydrogen; i.e., the (**13** + **104**) combination is an

allowed ($\sigma_{2s} + \pi_{2s} + \sigma_{2s} + \pi_{2s} + \pi_{2s}$) case and the (**15** + **65**) combination is also allowed ($\sigma_{2s} + \sigma_{2s} + \pi_{2s}$), whereas the inverse cases are disallowed. These results did not, however, withstand further scrutiny.

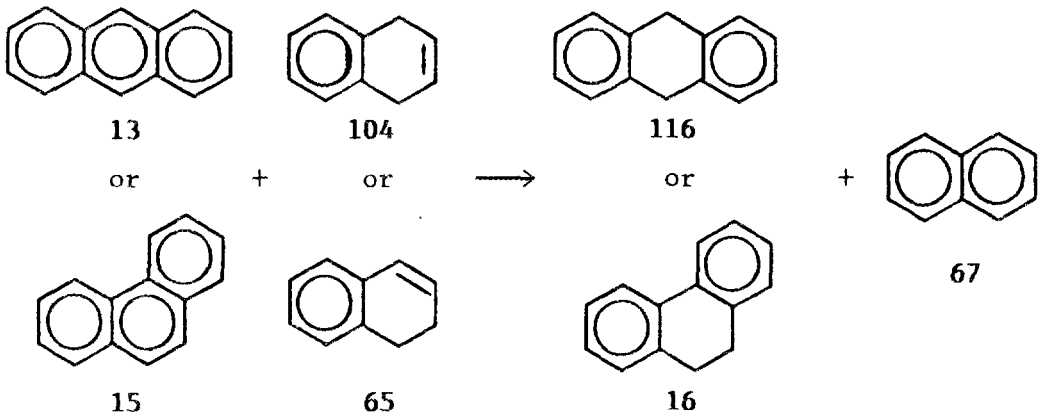

King and Stock[244] were able to reproduce the selectivity reported for **13**. However, this is the less diagnostic case since isomer **104** might be expected to be a more potent hydrogenation agent than **65**, regardless of mechanism, because it is thermodynamically the less stable. However, they could not reproduce the "contrathermodynamic" selectivity for **15**. In fact, they showed that, at the 400°C temperature needed to hydrogenate **15**, disproportionation of **65** and of **104** to form tetralin (**34**) and **67** (Section 10.2) was so rapid that the actual reducing agent must have been largely **34**. Stilbene, which is in the same π_{2s} symmetry class as **15** but is reactive at 300°C, did not show the selectivity predicted by orbital symmetry considerations. Also, hydrogenation of naphthacene by a mixture of **104** and **104**-d_{10} gave significant amounts of d_1 and d_3 products. Similarly, reduction of 9,10-dimethylanthracene by **116** gave both <u>cis</u> and <u>trans</u> dihydro products.[27] Hence these hydrogen transfers must occur in a stepwise, i.e., radical, manner. Although the concerted pathway for hydrogen transfer is "allowed" by orbital symmetry in appropriate cases, more detailed theory shows that it nevertheless has a very high activation barrier.[250]

Stein and coworkers[27] provided a well-behaved example,[27] which gives more insight into the stepwise mechanism, by studying the symmetrical reaction between 9,10-dihydroanthracene (**116**) and

2-ethylanthracene (**117**), where the ethyl group simply serves as a remote label to distinguish the hydrogen donor and acceptor. Second-order kinetics were observed for ratios of **117** : **116** between 0.1 and 10, both neat and diluted up to 100-fold with biphenyl. The following nonchain radical sequence involving molecular disproportionation followed by all possible radical disproportionations was proposed:

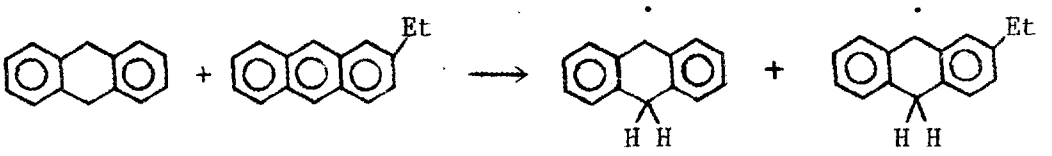

116 **117** **118** **119** (153)

118 + **119** → **116** + **117** (-153)

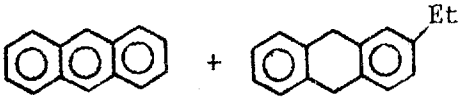

(154)

13 **120**

2 **118** → **13** + **116** (155)

2 **119** → **117** + **120** (156)

for which $k_{exp} = k_{153}/2$ because half of the radical disproportionation events regenerate the starting materials. With the assumption that molecular disproportionation step 153 was rate-determining with no chain amplification, the observed value of $k_{exp} = 10^{9.6}\exp(-36{,}800/RT)\ M^{-1}s^{-1}$ (225-400°C) led to a value of ΔH_f^{o} of the 9,10-dihydro-9-anthryl radical (**118**) which was consistent with existing data.[29] The modest rate increase which was observed when **117** : **116** exceeded 10 was considered to be diagnostic of the onset of radical hydrogen transfer step 157. As

118 + **117** → **13** + **119** (157)

this step begins to compete with steps 154 and 155, k_{exp} will approach k_{153} rather than $k_{153}/2$. The smooth rate decrease, which was observed with initially added anthracene (**13**) product as a competitive hydrogen

acceptor, was attributed to the reversal of model thermoneutral radical hydrogen transfer step 157 and allowed evaluation of k_{-157} at 350°C

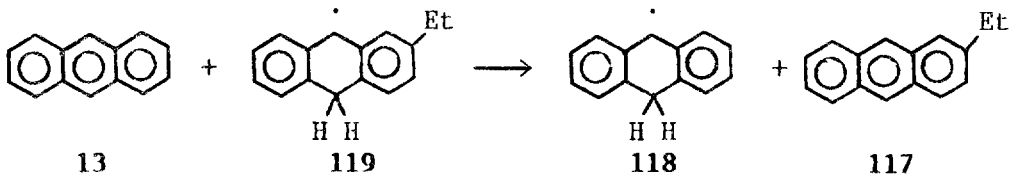

(-157)

which, for an assumed $A_{-157} = 10^{8.5}\ M^{-1}s^{-1}$, led to $E_{-157} = 18.3$ kcal mol^{-1}. Note that this barrier for bimolecular hydrogen atom transfer is indeed significantly less than the endothermicity for complete hydrogen atom expulsion: ΔH_f^{o}(**13**) + ΔH_f^{o}(H·) - ΔH_f^{o}(**118**) = 55.2 + 52.1 - 78.4[27] = 28.9 kcal mol^{-1}. A possible ambiguity remains, however, in that a step such as 157 is kinetically equivalent to and has not been unequivocally distinguished from an addition--hydrogen shift--β-scission sequence 158:[27]

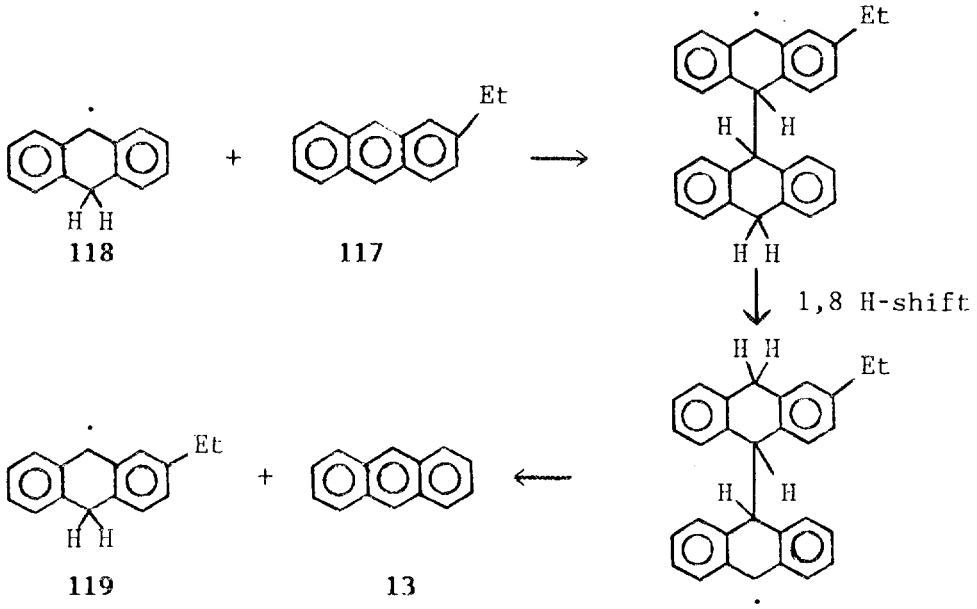

(158)

Apparently molecular disproportion step 153 is rapid enough to establish a concentration of radicals high enough that disproportionation

steps 154-156 dominate product formation, and hydrogen abstraction step 159, which might have led to a chain reaction (see below), does not

$$\mathbf{119} + \mathbf{116} \longrightarrow \mathbf{120} + \mathbf{118} \qquad (159)$$

compete. This situation did not, however, appear true for the exergonic reaction 160 between 9,10-dihydrophenanthrene (**16**) and anthracene (**13**).[27] The product **116** catalyzed the reaction at low conversions but inhibited it at high conversions. To model successfully such complex kinetic behavior[27] required including two initiation steps and a chain sequence for product formation rather than simply disproportionation. Initially

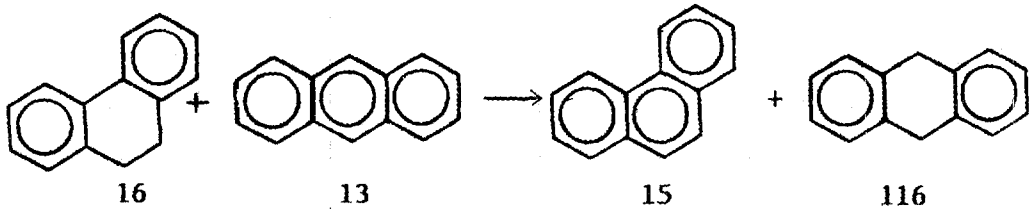

(160)

$$\Delta H^{o}_{298} = -9.3 \text{ kcal mol}^{-1} \text{ (Reference 231)}$$

$$\Delta S^{o}_{298} = 1.4 \text{ cal mol}^{-1} \text{ K}^{-1}$$

$$\Delta G^{o}_{673} \sim -8.4 \text{ kcal mol}^{-1}$$

radicals are formed from the reactants in step 161 with an estimated $k_{161} \sim 3.2 \times 10^{-6}\ M^{-1}s^{-1}$ at 350°C. However, step 162, which involves one

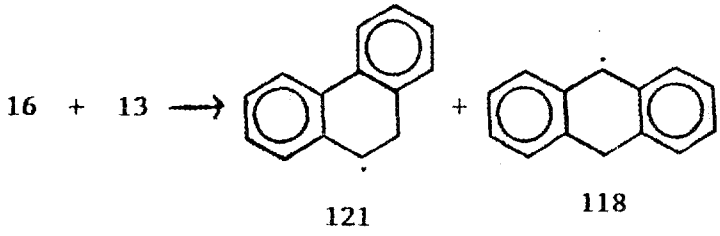

(161)

$$\mathbf{116} + \mathbf{13} \longrightarrow 2\ \mathbf{118} \qquad (162)$$

reactant and one product molecule and which is analogous to step 153, was estimated to be some 250 times more rapid so that it became equally effective at generating radicals at only 0.4% conversion. Product formation was then dominated by hydrogen abstraction step 163, analogous to step 159, and radical hydrogen transfer step 164, analogous to step

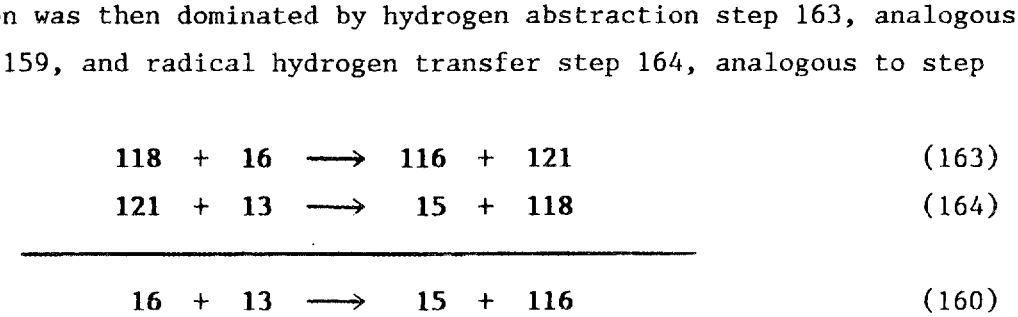

$$\mathbf{118} + \mathbf{16} \longrightarrow \mathbf{116} + \mathbf{121} \qquad (163)$$

$$\mathbf{121} + \mathbf{13} \longrightarrow \mathbf{15} + \mathbf{118} \qquad (164)$$

$$\mathbf{16} + \mathbf{13} \longrightarrow \mathbf{15} + \mathbf{116} \qquad (160)$$

157. The source of these kinetic differences between the (**16** + **13**) and (**116** + **13**) systems could be traced to the greater stability of radical **118**, which profits from double benzylic stabilization, compared with radical **121**. For example, step 164 is some 14 kcal mol^{-1} exothermic[27] while, of course, step 157 is essentially thermoneutral.

11. PHENOLS AND AROMATIC ETHERS

11.1 PHENOL

A significant fraction of the oxygen functionality in native coals occurs as aromatic hydroxyl groups. Additional ones will be formed during coal processing by thermal decomposition of aryl ethers (Sections 5.5, 7.2, 8.2, 11.6, and 11.7). Phenol (**45**) itself reacts only sluggishly in the low-temperature regime.[251,252] King and Stock[156] observed H-D exchange between C-2 and C-4 of phenol and C-1 of tetralin-d_{12} when dense mixtures were heated at 427°C for 4 h, behavior suggestive of radical intermediates, but 90-95% of both reagents survived chemically unchanged. Thermolysis of gaseous **45** does occur readily in the high-temperature regime and gives an extremely complex mixture of products.[253] Braekman-Danheux and Heyvaert[254] and Cypres and Bettens[255] detected 7 gaseous products, over 50 condensable products ranging from cyclopentadiene to benzofluoranthene, and a carbonaceous residue over the range 665-865°C and 2.5 s residence time. The major products at 14% conversion (780°C), in order of decreasing abundance, were carbon monoxide, water, solid residue, hydrogen, benzene (**9**), naphthalene,

methane, dibenzofuran (**71**), indene, and cyclopentadiene (**122**). These groups[254-256] proposed that three competitive stoichiometries were involved:

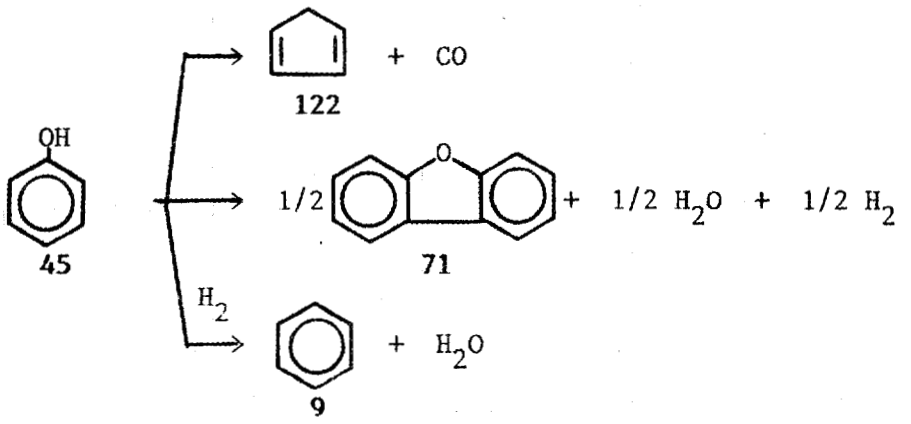

(165)

(166)

(167)

The carbon monoxide derived from **45**-1-^{14}C was labeled, whereas most of the numerous hydrocarbon products were not.[255] In addition, the compositional pattern of these hydrocarbons was very similar to that derived from thermolysis of **122**.[256] Therefore, the first reaction was proposed to be <u>decarbonylation</u> (step 165). Since carbon monoxide is also a typical product of coal pyrolysis, this model reaction deserves attention. Product **71** was considered diagnostic of a separate <u>condensation</u> reaction. Based on tritium labeling results, condensation at the lower end of the temperature range studied was proposed to involve two molecules of **45** with release of water and hydrogen (step 166); however, at higher temperatures, it was proposed to involve one molecule of **45** and one molecule of product **9** with release of two molecules of hydrogen. In contrast to the other hydrocarbon products, the **9** formed from **45**-1-^{14}C was labeled, and therefore a secondary <u>hydrodehydroxylation</u> by hydrogen product was proposed as its source (step 167). In the context of coal processing, hydrodehydroxylation is a generally desirable reaction because it removes oxygen, albeit with consumption of hydrogen; condensation is an undesirable retrograde reaction; and decarbonylation is desirable to the extent that it removes oxygen, but it may be a mixed blessing if reactions of the remaining hydrocarbon fragment lead to heavier final products. Condensation appeared to be favored by lower temperatures[255] and decarbonylation by lower pressures,[256] but the

dependencies of each pathway on temperature and partial pressure of **45** were not unraveled in detail. Voronkov and coworkers[257] also observed **9**, water, carbon monoxide, hydrogen, and methane among the products from thermolysis of **45** at 750°C. However, their claimed high selectivity to form p-terphenyl, along with significant production of carbon dioxide, is unusual and may suggest trace oxygen in the feed.

The Brussels group[255] pictured decarbonylation as proceeding by extrusion of carbon monoxide from the cyclohexadienone tautomer of **45** (step 168); an alternate radical chain based on the known decarbonylation of phenoxy radical (**46**) will be considered below. They did not suggest a mechanism for forming the first C-O or C-C bond during condensation. Their suggested key step in hydrodehydroxylation was displacement by by hydrogen atom, of unspecified origin, on O (step 169). An alternate

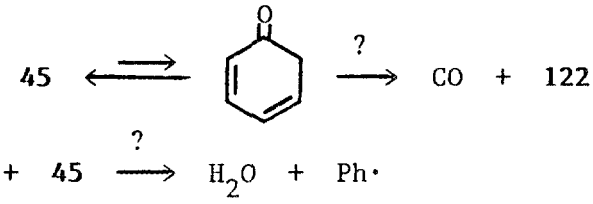

(168)

(169)

ipso aromatic displacement (see below) is more likely because S_H2 reactions at O, while better known than at C, are still not common.[24f] Noting the similarities in thermal sensitivity and thermochemistry between **45** and toluene [D^o(PhO-H) = 86.5 kcal mol^{-1} ~ D^o($PhCH_2$-H) = 88.0 kcal mol^{-1}][20], we suggest that considerations of mechanism for thermolysis of **45** should begin with the well-understood behavior of toluene. Consider steps 170-174, the analogs of steps 33-37 in Section 4.1.1:

$$\mathrm{PhOH} \longrightarrow \mathrm{PhO\cdot} + \mathrm{H\cdot} \qquad (170)$$

45 **46**

$$v\ \mathrm{H\cdot} + v\ \mathbf{45} \longrightarrow v\ \mathrm{H_2} + v\ \mathbf{46} \qquad (171)$$

$$(1 - v)\ \mathrm{H\cdot} + (1 - v)\ \mathbf{45} \longrightarrow (1 - v)\ \mathbf{9} + (1 - v)\ \mathrm{HO\cdot} \qquad (172)$$

$$(1 - v)\ \mathrm{HO\cdot} + (1 - v)\ \mathbf{45} \longrightarrow (1 - v)\ \mathrm{H_2O} + (1 - v)\ \mathbf{46} \qquad (173)$$

$$2\ \mathbf{46} \longrightarrow \mathrm{C_{12}H_{10}O_2} \qquad (174)$$

$$(3 - v)\ \mathbf{45} \longrightarrow \mathrm{C_{12}H_{10}O_2} + (1 - v)\ \mathbf{9} + v\ \mathrm{H_2} + (1 - v)\ \mathrm{H_2O}$$

These steps would rationalize the source of hydrogen atom and the hydrodehydroxylation process directly. They may also rationalize the condensation process <u>if</u> the $C_{12}H_{10}O_2$ "dimer" from combination of **46** ultimately leads to dibenzofuran; we return to this question in Section 11.2. Finally, the decarbonylation process might proceed by a short chain:

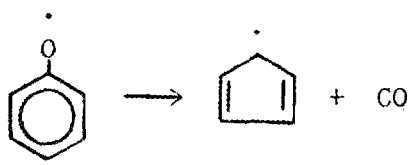

46 **123** (175)

$$\mathbf{123} + \mathbf{45} \longrightarrow \mathbf{122} + \mathbf{46} \qquad (176)$$

$$\mathbf{45} \longrightarrow \mathbf{122} + \mathrm{CO}$$

The extrusion of carbon monoxide from radical **46** to give cyclopentadienyl radical (**123**) is well documented.[258] The reported rate constant[259] of $10^{12.0}\exp(-47{,}700/RT)\ s^{-1}$ corresponds to a lifetime of **46** at 750°C of only 11 ms.

Sakai and Hattori[260] heated gaseous **45** under slightly elevated hydrogen pressure at 600°C for 60 min and reported 40% conversion largely to form the hydrodehydroxylation product **9**, but no search for heavier

products was made. Products formed under 20 MPa hydrogen at 450°C were **9**, cyclohexane, and biphenyl.[261]

11.2 NAPHTHOLS

The naphthols, which are more realistic models than phenol itself for polycyclic phenols, exhibit measurable reactivity in the low-temperature regime. Over 100 years ago, Merz and Weith[262] isolated three neutral products in modest yield from thermolysis of liquid 1-naphthol (**124**) at 350-400°C for 40 h: water, naphthalene, and a $C_{20}H_{12}O$ product (2 **124** - H_2 - H_2O) which ultimately proved[263] to be dinaphtho[1,2-b:2',1'-d]furan (**125**). Neither bis(1-naphthyl) ether nor gases were formed. Hence, in the low-temperature regime, condensation and hydrodehydroxylation appeared to be coupled in some way that did not allow hydrogen to be evolved, whereas decarbonylation did not occur. The demonstrated thermal stability of bis(1-naphthyl) ether[262] (cf. Section 7.2) precludes its being a transient intermediate on the route to furan **125**. A recent study by Poutsma and Dyer[264] showed that each of the three identified products was, in fact, a secondary product. Thermolysis of liquid **124** at 400°C proceeded with an initial rate of ~30% h^{-1}. Extrapolation of product distributions to zero conversion showed that the dominant initial products were 2,2'-binaphthalene-1,1'-diol (**126**) and 1-tetralone (**127**) (along with a much smaller amount of 5,6,7,8-tetrahydro-1-naphthol). Biphenol **126** then rapidly underwent cyclization to form furan **125** and water, while ketone **127** was more slowly hydrogenated further to 1-tetralol (Section 12.2) and thence to a mixture of tetralin and naphthalene, probably by way of dehydration followed by disproportionation of intermediate dihydronaphthalenes (Section 10.2). The fundamental mechanistic questions then concern the mode of regio-selective coupling of two molecules of **124** at the carbon adjacent to the hydroxyl group to form biphenol **126** and the simultaneous transfer of the hydrogen so made available to a third molecule of **124** to reduce it to **127**.

Conversion of **124** in the gas phase was very much slower than in the liquid phase. Also, liquid dilution experiments in m-terphenyl as solvent showed a rapid falloff in rate,[264] corresponding to a formal

kinetic order ~2.5, but no major changes in product composition. Although this non-integral value was not partitioned between the inherent kinetic order and effects of solvent polarity, a kinetic order of at least 2 seems likely. In contrast, dilution with benzophenone (**128**)[265] accelerated the formation of the condensation products (**126** plus **125**) but

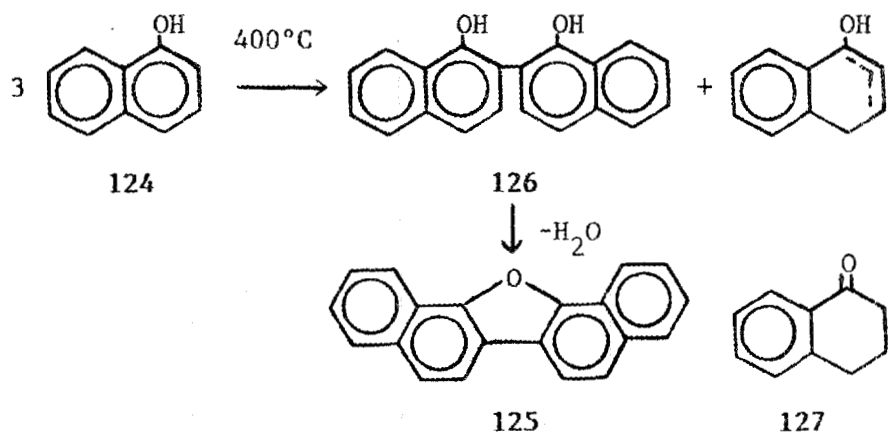

ketone **127** was replaced as product by diphenylmethane (**32**); i.e., reaction 177 was replaced by reaction 178. [The role of **128** as a hydrogen acceptor in discussed in Section 12.1.]

$$2\ \mathbf{124} + 1/2\ Ph_2C{=}O \longrightarrow \mathbf{126} + 1/2\ Ph_2CH_2 + 1/2\ H_2O \quad (178)$$

128 **32**

All mechanisms examined[264] for reaction 177 left unanswered difficulties, but one consisting of steps 179-181 was judged worthy of future consideration. Unimolecular homolysis of the weakest bond in **124** [$D^o(C_{10}H_7O\text{-}H)$ ~ 83 kcal mol^{-1} [264]] would be much too slow at 400°C to be involved. The proposed rate-controlling step 179 is a molecular disproportionation of two molecules of **124** to produce 1-naphthoxy radical (**129**) and the formal hydrogen atom adduct radical **130**. A barrier of ~50 kcal mol^{-1} was estimated by subtracting from $D^o(O\text{-}H)$ an estimate of ~33 kcal mol^{-1} for the exothermicity of adding hydrogen atom to **124**. If $A_{179} \sim 10^{11}\ M^{-1}s^{-1}$, step 179 would then have a rate only 5-fold less than that observed for the overall reaction. Hydrogen abstraction step 180

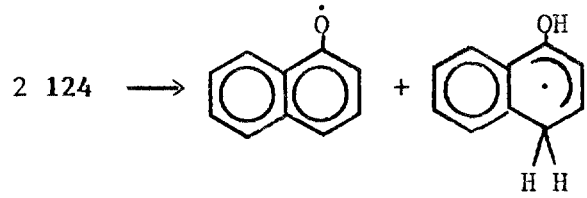

(179)

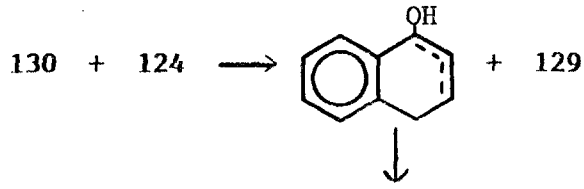

(180)

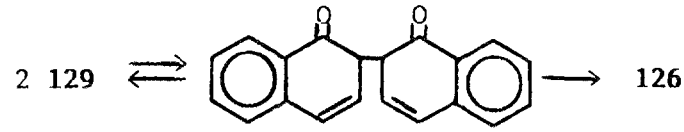

(181)

would then generate the enolic precursor to product **127** and a second radical **129**. Finally, radical coupling of **129** followed by two enolizations would generate the binaphthol **126**. The regiochemistry demanded to form **126** in step 181 (and step 174 more generally) poses an apparent difficulty because radical **129** is normally considered to couple predominantly at C-4, rather than C-2.[266] However, some evidence suggests that under appropriate conditions the initial coupling step of aryloxy radicals to give cyclohexadienones may be reversible compared with rates of subsequent enolization.[267] Other recent evidence[268] suggests that aryloxy radicals need not couple preferentially at the site of maximum spin density,[269] as commonly supposed. Therefore, the regiochemistry of combination of aryloxy radicals and the role of "free" radicals in oxidative coupling of phenols deserves further attention.

If this mechanism is correct, the accelerating effect of benzophenone would follow naturally because it should be a better hydrogen-accepting partner in the molecular disproportionation step 182 than is **124** itself in step 179 because of the high stability of radical **131**.

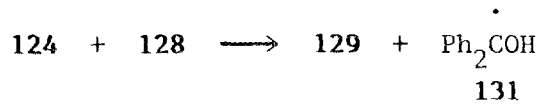

(182)

A possible non-radical ene reaction between **124** and its cyclohexadienone tautomer as the first step was considered,[264] but it created a number of major mechanistic difficulties in subsequent steps.

Parallel thermolysis of liquid 2-naphthol (**132**) proceeded somewhat less rapidly,[264] and the initial product composition was more complex because both C_1-$C_{1'}$ and C_1-$C_{3'}$ bonding occurred to form ultimately two dibenzofurans, the symmetrical [2,1-b:1',2'-d] isomer **133** and the unsymmetrical [2,1-b:2',3'-d] isomer **134**. The observed gradual increase in the C_1-$C_{3'}$: C_1-$C_{1'}$ coupling ratio with increasing conversion is not clearly understood but provides further circumstantial evidence for some form of reversibility along the coupling pathway.

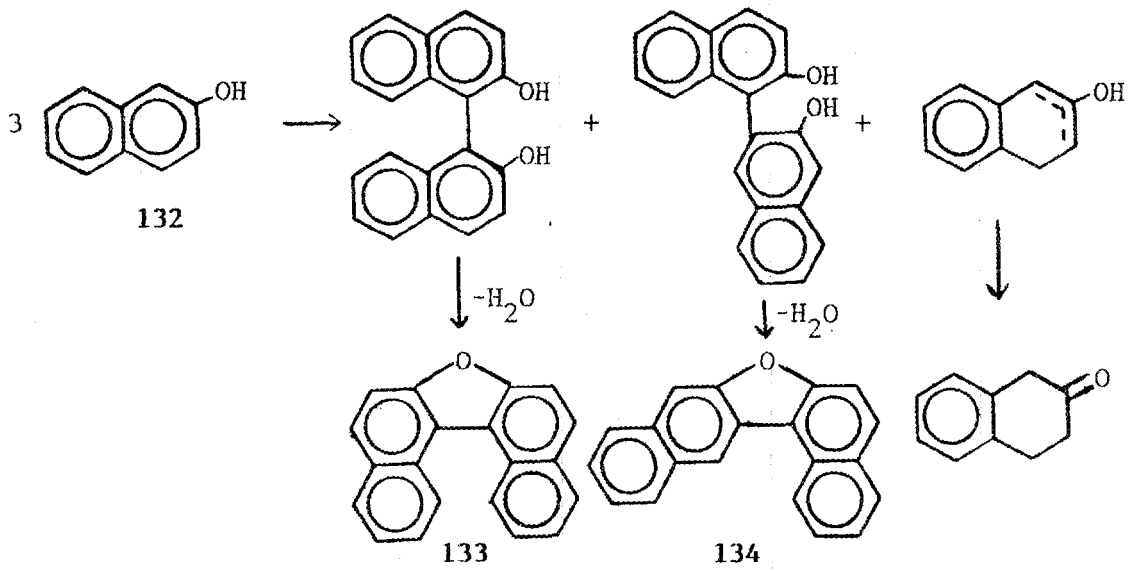

The only product reported by Cronauer's group[13] from heating **124** as a 9.2 mol% solution in tetralin at 400-450°C was naphthalene, but the analytical methods used may not have detected furan **125**. Reactions were not followed to high enough conversion to justify the assignment of first-order kinetics. Comparison with the corresponding rate of consumption of **124** at a similar concentration in m-terphenyl[264] suggests that reaction in tetralin was moderately more rapid. Whereas Cronauer[13] observed 6.5% conversion in 30 min at 450°C, Yao and Kamiya[154] observed only 1.4% conversion for a 1.9 mol% solution of **124** in tetralin--1-methylnaphthalene under high hydrogen pressure. This 4.6-fold decrease in conversion accompanying a 4.8-fold decrease in

concentration is suggestive of second-order kinetics if hydrogen has no kinetic effect. No products were identified.[154] The important question whether hydrogen donor solvents uncouple hydrodehydroxylation from condensation remains unanswered.

Hall[270] heated **124** and **132** under high hydrogen pressure at 400-500°C with no added solvent. Although the analytical methods were limited by modern standards, dinaphthofurans were clearly identified as the major products, along with tetralin and naphthalene. In contrast, working with somewhat lower hydrogen pressure, Schlosberg and Kurs[271] reported that the major products were tetralin, naphthalene, and 1-tetralone, with "dimeric" products being of only minor importance. [Their conversion-vs.-time plot is unusual in that the first half-life at 450°C was achieved in $\lesssim$ 10 min, whereas the second was not yet achieved after 120 min.] Because of the discrepancy between these parallel studies,[270,271] the role of hydrogen in the low-temperature thermolysis of the naphthols also remains ambigous.

Schaden[272] subjected **124** and **132** to the other extreme of high temperature and low pressure, FVP at 900°C and ~3 Pa pressure. The major organic material identified in each case was the decarbonylation product indene (**93**), but the yields were only 5% and 17%, respectively; even smaller amounts of naphthalene (**67**) were formed.

At intermediate temperature and pressure, Bredael and coworkers[273,274] exposed **124** and **132** in nitrogen carrier to several temperatures between 720 and 900°C with a 0.5 s residence time. The only condensable products reported were **67** and **93**; the simpler product mixture, compared with phenol,[254-256] presumably resulted because **93** is much less thermally sensitive than **122**. The gaseous products described were carbon monoxide, water, and hydrogen. The more reactive **132** gave a **93** : **67** ratio ~9 : 1 whereas **124** gave a ratio ~1 : 1. The relevant reactions were written as:

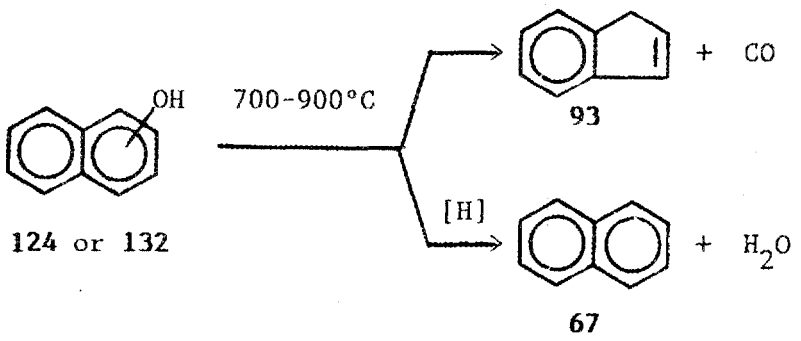

The **93** : carbon monoxide ratios observed were close to unity, particularly after corrections were made for secondary consumption of **93** and for possible interference from the water gas shift reaction [$CO + H_2O$ ---> $H_2 + CO_2$]. The authors[273] again suggested that decarbonylation proceeds through ketonic tautomers and that the more rapid reaction of **132** resulted from an inherently weaker C-(C=O) bond in its ketonic form. Their discussion of the route to **67** did not specify the source of the hydrogen needed for hydrodehydroxylation. In fact, hydrogen was a net product, generally exceeding the amount of water. The simplest explanation appears to be steps analogous to 170-176 coupled with failure to detect heavier, hydrogen-depleted products ("dimers"); in fact, observation of carbonaceous residue was a common feature.[255] A similar study[275] at 700-850°C and a 6-s residence time but with steam as the carrier also described the major products from **124** as hydrogen, carbon monoxide, **67**, and **93**, and from **132** as carbon monoxide, hydrogen, and **93**; again no heavier products were described. In a much earlier study by Hagemann[253] at the somewhat lower temperature of 660°C, not only were carbon monoxide and hydrogen detected, but also a more extensive slate of condensable products was isolated in each case: **67** (5-6%); an oxygen-containing "dimer" (13-14%); and a hydrocarbon "dimer" (5-10%); **93** was not noted. The O-containing product from **124** was assigned as furan **125**; that from **132** was assigned as a dinaphthopyran, but the evidence does not preclude furan **133** or **134**. The heavy hydrocarbons were suggested to be C_{22} rather than C_{20} structures, but the evidence is weak. In summary, whereas each of these studies[253,273-275] suggests competitive decomposition pathways for the naphthols in this intermediate temperature

range, as for **45**, none offers complete enough material balances to specify the exact stoichiometries or to define mechanisms with any certainty.

At the very forcing conditions of 950°C and 1 MPa hydrogen for 5 s, which were sufficient to consume **124** completely, the low yield of carbon monoxide and significant formation of **67**[107] suggest that high-pressure hydrogen can indeed preferentially enhance the hydrodehydroxylation pathway at high temperatures.

11.3 POLYHYDROXYAROMATICS

Some polycyclic aromatic systems in coal, particularly for lower ranks, may well contain more than one hydroxyl group. Model compound data reveal that adding a second hydroxyl group to an aromatic ring increases thermal reactivity markedly as well as increasing the tendency toward retrograde reactions. For example, after 1 h at 400°C, conditions where phenol (**45**) is stable, neat resorcinol (**135**) was 56% consumed;[276] except for a trace of **45**, all the products were nonvolatile. Hence, whatever "dimers" were formed initially must be considerably more reactive than **135** towards further condensation with **135** or themselves. Catechol (**136**) was only slightly less reactive.[276] A clearer view of the early stages of reaction was achieved by McMillen and coworkers[276] by using the even more reactive 1,3-dihydroxynaphthalene (**137**), because its "dimers" were relatively less prone to condense further. The reactivity of **137** could be moderated further by adding the monofunctional m-cresol, which served to "cap" oligomers, and/or hydrogen donor solvents. The major initial product from a 25% solution of **137** in tetralin held at 400°C for 5 min was a trihydroxybinaphthyl, and isomer **138** was assigned as the most likely structure.[276] This material rapidly underwent

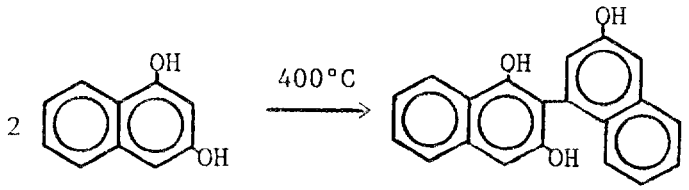

137 **138**

cyclization and dehydrogenation to form a dihydroxydinaphthofuran, which itself oligomerized further.

There is thus a qualitative, not just a quantitative, difference between the thermal reactivity of **137** and 1-naphthol (**124**). Whereas the characteristic process for **124** was coupling by dehydrogenation to give binaphthol **126**, that for **137** was coupling by dehydration. McMillen and coworkers[276] offered a speculative mechanism (steps 183-185). One troublesome feature of the proposed homolytic aromatic substitution by the carbon center of naphthoxy radical **139** at the C-O bond of **137** is that the relative energetics of β-scission suggest that intermediate cyclohexadienyl radical **140** would very much prefer to re-eject the stabilized naphthoxy radical **139** rather than hydroxyl radical. That difficulty might be surmounted if **140** disappeared instead by hydrogen abstraction (step 186) followed by dehydration (and enolization) by a polar mechanism to give product **138**. Another alternative is addition of radical **139** to a small equilibrium concentration of the ketonic tautomer of **137** (step 187) followed by hydrogen abstraction and dehydration. However, the more fundamental unanswered question is why the second hydroxyl group opens such addition pathways for **137** whereas they are unavailable to **124** (or at least are much slower than the pathway starting with probable step 179).

Hagemann[253] noted the tendency of catechol (**136**), resorcinol (**135**), and hydroquinone (**141**) to lose two molecules of carbon monoxide when heated at higher temperatures (650°C) in the gas phase. Sakai and Hattori[260] reported yields of carbon monoxide approaching 200% from static thermolyses in helium diluent at 600°C, behavior indicative of serial decarbonylation (step 188). Product-vs.-time plots indicated that the major detectable initial organic product was butadiene, which then

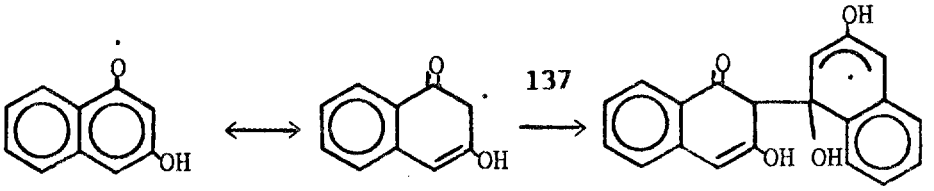

139 140 (183)

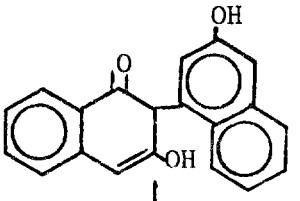

140 + HO· (184)

138

HO· + 137 → H_2O + 139 (185)

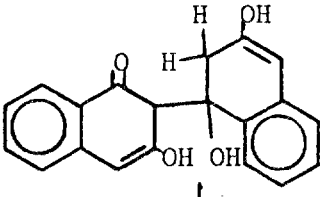

140 + 137 → + 139 (186)

$-H_2O, -H$

138

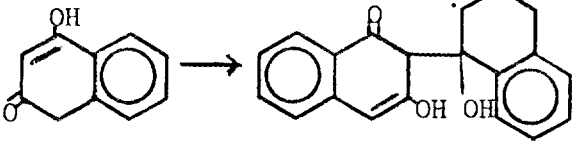

139 + (187)

137

+ 137 - 139

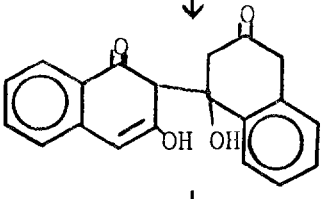

$-H_2O, -H$

138

underwent rapid secondary reactions. The relative rates were **136** : **135** : **141** ~ 15 : 2 : 1; even the least reactive p-isomer was at

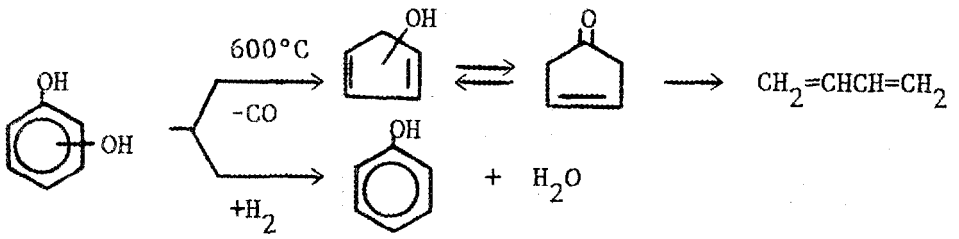

$CH_2{=}CHCH{=}CH_2$ + CO (188)

(189)

45

least 50-fold more reactive towards decarbonylation than phenol (**45**) itself. Replacement of the helium diluent with hydrogen near atmospheric pressure did not alter the decarbonylation process but induced simultaneous hydrodehydroxylation (step 189) to form phenol (**45**). The relative rates of hydrodehydroxylation were more compressed (~4 : 2 : 1), as was the spread between the least reactive **141** and **45**. At 600°C with hydrogen near atmospheric pressure, decarbonylation was more rapid than hydrodehydroxylation for **136**, the two processes were nearly balanced for **141**, and hydrodehydroxylation dominated for **45**; presumably higher pressures of hydrogen would further promote hydrodehydroxylation, but this was not tested.

Schaden[272] subjected several isomeric naphthalenediols to FVP conditions at 900°C and ~3 Pa pressure. Yields of identified products were larger than from the monofunctional naphthols but were still modest, and major losses to heavier products are implied. Among identified reactions, decarbonylation predominated, but hydrodehydroxylation was a persistent side-reaction. The diols with one hydroxyl group in each ring gave largely the corresponding indenols (double bond equilibration in indenes is rapid at these temperatures); for example:

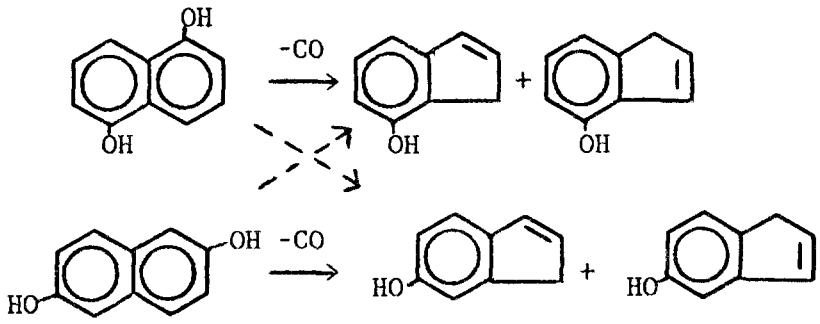

There was also a less dominant process which shifted the position of the remaining hydroxyl group. The 2,3-diol gave 2-indanone and benzocyclobutene, but the 1,4-diol underwent largelydehydrogenation:

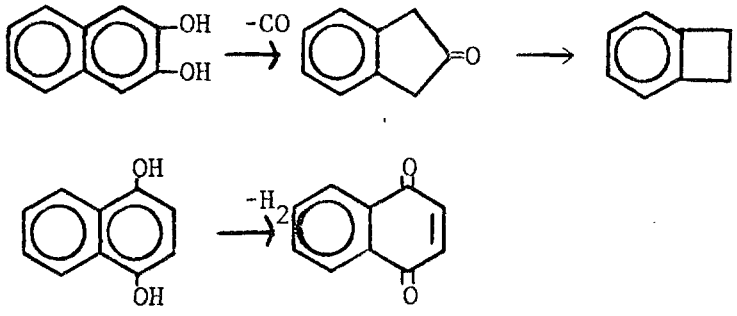

11.4 HOMOLYSIS OF KETONIC TAUTOMERS

Before discussing alkylphenols in Section 11.5, we consider the specific case of benzylphenols because they illustrate an added mechanistic feature. Whereas diphenylmethane is thermally stable in tetralin at 400°C (Section 7.1), introduction of an <u>ortho</u>- (or <u>para</u>-) hydroxy substituent led to 20% (10%) conversion after only 1 h to form toluene and phenol.[12] This enhancement in thermal cracking of hydroxydiphenylmethanes for the <u>ortho</u> and <u>para</u>, but not <u>meta</u>, isomers,[151] to a level even greater than that of bibenzyl (Section 5.1.3), is remarkable since a ring hydroxyl substituent would not be expected to significantly weaken the C-C bond because of the σ-structure of aryl radicals.[277] The role of the hydroxyl group was clarified by McMillen and coworkers.[151] Phenolic form 143, which was estimated to have $D^{o}(Ar\text{-}CH_2) \gtrsim 86$ kcal mol^{-1}, is in

equilibrium with the keto tautomer **143**, which was estimated by thermochemical kinetic methods to have $D^o(C\text{-}C) \sim 47$ kcal mol^{-1} because it can undergo C-C homolysis directly to <u>two</u> resonance-stabilized π-radicals, benzyl (**20**) and phenoxy (**46**). The observed first-order kinetics indicate complete attainment of the enol-ketone equilibrium prior to rate-controlling homolysis so that $k_{exp} = (k_{190}/k_{-190})(k_{191})$. Whereas the

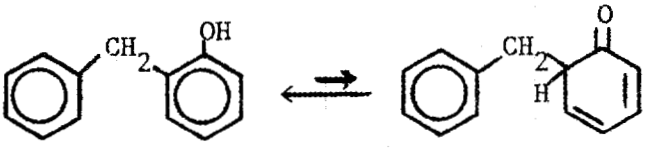

(190)

142 **143**

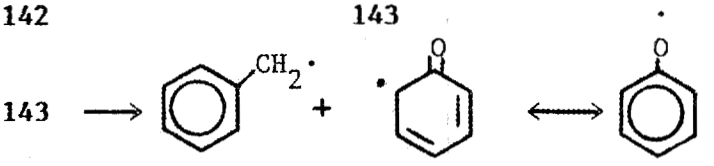

(191)

20 **46**

equilibrium constant K_{190} was estimated to be only $\sim 10^{-6.2}$ at 400°C, the decrease in D^o of $\gtrsim 39$ kcal mol^{-1} would contribute a huge offsetting favorable factor of $\gtrsim 10^{12.7}$.

Thermolysis of diphenyl ether (Section 7.2) was also accelerated by an <u>ortho</u> hydroxy substituent. The absolute size of the effect was less dramatic than for **142**, but it could be enhanced further in this case by added potassium hydroxide or phenols.[151] Therefore, the same reaction scheme was proposed except that the ketonization step, which presumably occurs through ionic intermediates, is slower and thus becomes partially rate-controlling.

11.5 CRESOLS AND ETHYLPHENOLS

The simultaneous presence of a methyl and hydroxyl substituent on the same aromatic ring system in coal is a not unlikely occurrence which can be modeled by the cresols. Phenol (**45**) appears to be somewhat more reactive than toluene at ~700°C.[91,255] Combining the methyl and hydroxyl functionality in the cresols gives a further modest enhancement in thermal reactivity. Data for the cresols, while more extensive than for

45, is, however, more difficult to interpret mechanistically because typical reports describe only high-conversion reactions and extremely complex reaction mixtures that have been only partly speciated. The identified products are typically more hydrogen-rich than cresol, presumably because of formation of heavy carbon-rich residues.

The most complete material balances at the lowest conversions exist in an early study by Jones and Neuworth,[278] who used very short (0.05 s) residence times. The reactivity order at 816°C was ortho (**144**) (14.7% conversion) $\gtrsim$ para (**146**) (12.7%) > meta (**145**) (4.9%). Activation energies near 70 kcal mol^{-1} were observed, with the assumption of first-order kinetics. The molar selectivities to the major products from **144** at 14.7% conversion were:

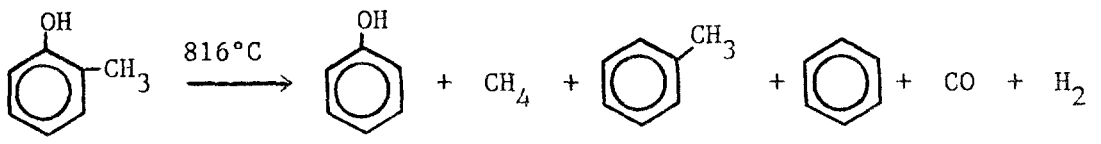

144	**45**		**18**	**9**		
	0.41	0.28	0.23	0.23	0.60	0.44

Formation of phenol (**45**) and methane indicates a hydrodealkylation process, as observed for alkylaromatics (Section 4 and below), whereas formation of toluene (**18**) and water indicates a slightly slower but nevertheless competitive hydrodehydroxylation process, as observed for **45** (Section 11.1). Carbon monoxide signals that ring decarbonylation also occurs, as with **45**. The fate of the corresponding methylcyclopentadiene is unclear, but it may be a source[279] of some of the benzene (**9**) by rearrangement and dehydrogenation. For example, the 1 : 1 ratio of **9** : **18** formed at only 14.7% conversion [this ratio exceeded unity for the other isomers at even lower conversions] provides circumstantial evidence that **9** may be a primary coproduct of decarbonylation rather than simply a secondary hydrogenolysis product of **18** and/or **45**. Even so, the sum of **18** and **45** (0.64) as primary hydrogenolysis products does not leave room for 0.60 more units of C_6 fragments to accompany the carbon monoxide formed. However, because the carrier was steam, some of the carbon

monoxide and hydrogen may have arisen from the water gas reaction with small amounts of carbonaneous residue which deposited in the reactor.

In a study at much higher conversion, Cypres and Bettens[255] compared thermolysis of gaseous **144** and **146** with that of **45** (see Section 11.1) at 780°C and 2.5 s residence time. The conversions achieved, ~75%, ~63%, and ~14%, respectively, indicate the modest rate acceleration provided by the added methyl group. The major products from **144**, in decreasing order of abundance, were **45** > CO > methane > hydrogen > **9** > water > **18** > "solids"; the corresponding order from **146** was qualitatively similar: CO > **45** > methane > **9** > hydrogen > "solids" > water > **18**. The "solids" presumably have served as a net source of hydrogen for the volatile products. A recent set of kinetic data[280] for thermolysis of the individual cresols diluted 1 : 25 with argon at 800-900°C and 1.5-4.5 s residence time is limited to very high conversions, which, at 800°C and 1.5 s, fell in the order **144** (92.6%) $\gtrsim$ **146** (88.2 %) > **145** (68.9%). The gaseous products were CO > methane > hydrogen. Identification of the liquid products, which included **45**, polycyclic aromatics such as methylated naphthalenes, and heavier materials, was fragmentary. The reported kinetics at these high conversions were very complex: 1.5-order for overall disappearance of the cresols; first-order for formation of CO product; and second-order for formation of methane and hydrogen products. Arrhenius expressions were given for each process, and the authors attempted to rationalize mechanistically the unusual observation that E for CO formation from **145** (130 kcal mol^{-1}) was twice that from **144** (64 kcal mol^{-1}). Yet the A factors reported were virtually identical. These derived parameters imply a reactivity ratio for the two isomers of 10^{13}, whereas the tabular data presented show a ratio of ~2. In addition to such experimental inconsistencies, mechanistic proposals included such unlikely events as the formation of naphthalene product by a termolecular reaction between **9** and <u>two</u> $H\dot{C}{=}\dot{C}H$ biradicals. We judge attempts to draw further conclusions from this work[280] unwise. However, we do note that the data again suggest the occurrence of a modest amount of isomerism among the cresol isomers during thermolysis.

In summary, these studies[255,278,280] indicate that thermolysis of cresols in the high-temperature regime involves hydrodemethylation and

somewhat slower hydrodehydroxylation, but the stoichiometric source of hydrogen is unclear. Decarbonylation occurs at a competitive rate, but the fate of the methylcyclopentadienyl fragment is unclear. Firm evidence for the condensation channel, which in this case would give dimethyldibenzofurans, is lacking. To describe more quantitatively the subtle perturbations of the methyl substituent on the phenolic functionality, and vice versa, will require studies at very limited conversions with complete product analyses. It is however interesting historically to note mechanistic proposals for hydrogenolysis made some 35 years ago by Jones and Neuworth[278] in light of newer knowledge (cf. Sections 4.1.1 and 11.1). They suggested initial homolysis of the benzylic C-H bond to give hydrogen atom and a hydroxybenzyl radical; current values of bond energies[20] suggest that homolysis of the phenolic O-H bond would be competitive. They suggested three modes of attack of hydrogen atom on cresol. Homolytic aromatic displacement of the methyl radical would give **45**; this step remains highly probable. Second, S_H2 displacement on oxygen would generate water and a tolyl radical which would rapidly abstract hydrogen from cresol to form **18**; in fact, homolytic aromatic displacement of hydroxyl radical is the more likely process to achieve ultimately the same overall reaction. Third, abstraction of hydrogen from the methyl group would generate hydrogen and another hydroxybenzyl radical; abstraction would, in fact, probably occur preferentially from the hydroxyl group to generate a methylphenoxy radical.

We have implied above that **45** and methane arise mechanistically by homolytic aromatic substitution. However, the behavior of the benzylphenols (Section 11.4) raises the question whether these products might arise from homolysis of a cyclohexadienone tautomer. The only modestly greater reactivity of **144** and **146**, compared with **145**, may well indicate otherwise, but further clarification is needed.

Thermolysis of **144** under FVP conditions at 660°C and $\lesssim$ 0.15 Pa[279] was claimed to give largely **45** and acetone with only traces of **18** and **9**. Not only is the acetone product unprecedented, but also the overall reactivity at such a low temperature and short residence time seems very high when compared with the studies outlined above. The proposed mechanism[279] for acetone formation by termolecular combination of carbon

monoxide and two methyl radicals is unreasonable both statistically and energetically. Under these same FVP conditions, the major reaction of 2,4-xylenol was claimed to be isomerization to the 2,5- and 2,6-isomers at temperatures as low as 400°C. The constant threat of catalytic wall effects in FVP studies may have manifested itself and disguised any purely thermal reactivity.

Long and coworkers[281,282] reported an acceleration of the disappearance of the cresols at 650°C by 3 MPa added excess hydrogen, which plateaued at ~10-fold when the hydrogen : cresol ratio reached 4 : 1. The added hydrogen increased the selectivity to **45** and **18**, at the expense of **9**, and decreased the formation of carbonaceous residue and gas. At these conditions where hydrogenolysis appears to have outpaced the purely thermal reactions, the time required for half-conversion of the most reactive <u>ortho</u> isomer was 16 s and the reactivity ratio was **144** : **146** : **145** = 3.3 : 2.5 : 1.[282] Hydrodemethylation was somewhat more rapid than hydrodehydroxylation: the **45** : **18** ratio was ~3 : 1 from **144**[281] and ~1.5 : 1 from **145**.[282] Kinetic data were fitted to a rate law of the form:

$$-d[\text{cresol}]/dt = k[\text{cresol}][H_2]^{1/2}$$

The half-order dependence on hydrogen was taken as evidence for the involvement of hydrogen atom in the hydrogenolysis reactions (cf. Section 4.1.2). Hydropyrolysis of 2,4-xylenol at 725°C and 1 MPa hydrogen pressure gave 50% conversion after 0.8 s. The comparable amounts of <u>m</u>-xylene, <u>p</u>-cresol, and <u>o</u>-cresol formed indicate that hydrodehydroxylation and hydrodemethylation were competitive.[283]

Zhou and Crynes[284] studied thermolysis of <u>o</u>-ethylphenol (**147**) in the low-temperature, dense-phase regime; a typical conversion under high nitrogen pressure was 0.7% after 100 min at 350°C. The major liquid product was phenol (**45**) with lesser amounts of unidentified heavy products and positional isomers of the starting phenol. The major gaseous product was ethane, although in amounts much less than that of **45**. Rates were expressed as first-order rate constants, but the shape of the product-vs.-time plots suggests distinct autoacceleration. The

authors proposed that **45** resulted largely from homolysis of the Ar-CH_2 bond (step 192), which they felt would be more rapid than that of the CH_2-CH_3 bond (step 193) [**144** was only a trace product]. Because of the σ-character of aryl radicals, the hydroxy substituent would not be expected to weaken the Ar-CH_2 bond significantly, and we expect the reverse, i.e., $k_{193} >> k_{192}$. Nevertheless, neither of these steps appears rapid enough to explain the reactivity observed at 350°C, and we suggest that homolysis of cyclohexadienone tautomer **148** (step 194) should

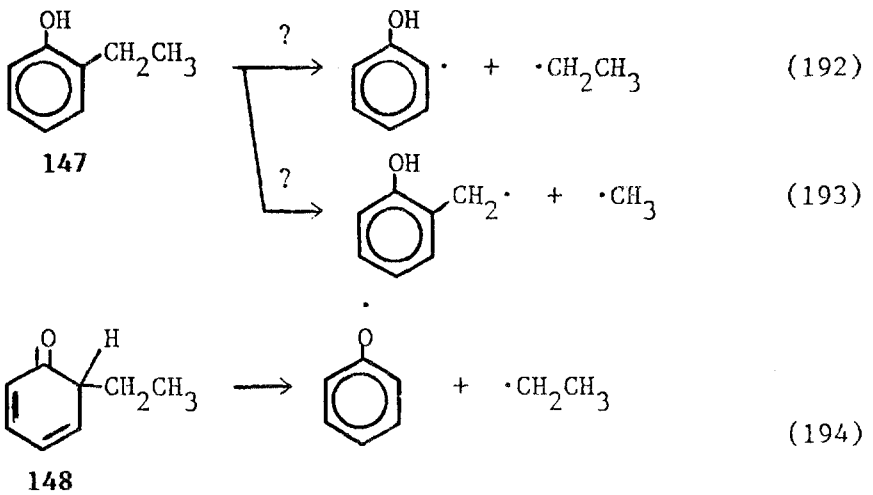

again be considered. The formation of **45** could also, of course, result from a hydrodeethylation step, but the failure of high-pressure hydrogen to accelerate the disappearance of **147**[284] under these low-temperature conditions would seem to mitigate against it. This work provides another example (see above) of the occurrence of positional isomerism during thermolysis of alkylphenols, although the specific mechanisms proposed have no precedent. This group[284,285] also studied the thermal decomposition of all the isomers of ethylphenol in dilute solution in n-dodecane, but results are difficult to interpret mechanistically because the "solvent" was actively decomposing concurrently with the phenols.

11.6 ARYL ALKYL ETHERS

We have already considered the thermal behavior of aryl ethers that model oxygen functionality within the backbone structure of coal: ArOAr' in Section 7.2, $ArOCH_2Ar'$ in Section 5.5, and $ArOCH_2CH_2Ar'$ in Section 8.2. We now turn to alkoxy substituents on aromatic rings. Phenyl alkyl ethers are reactive in the low-temperature regime, in contrast to phenol itself. Klein and Virk[286] found that the disappearance of supercritical phenyl methyl ether (anisole; **149**) was first-order over the range 0.45-3.1 M at 450°C with $k = 10^{12.1}\exp(-51{,}400/RT)\ s^{-1}$ over the range 344-550°C. Vuori and Bredenberg[287,288] found $k = 10^{14.0}\exp(-56{,}600/RT)\ s^{-1}$ but with large error limits because of the small temperature range covered (375-400°C). Evaluated at 450°C, these Arrhenius correlations for neat **149** give k values of $3.6 \times 10^{-4}\ s^{-1}$ [286] ($t_{1/2}$ = 32 min) and $7.8 \times 10^{-4}\ s^{-1}$ [287,288] compared with a one-point value of $2.6 \times 10^{-4}\ s^{-1}$ at ~0.6 M given by Schlosberg and coworkers.[289] While there is thus modest agreement among various groups concerning the experimental rate of thermolysis of **149**, there is less consistency in the descriptions of the products.

Klein and Virk's data[286] at rather low conversion indicate a normalized ratio for the major observed products at 450°C of o-cresol (**144**) : phenol (**45**) : benzene (**9**) : methane : carbon monoxide = 52 : 32 : 6 : 7 : 4; toluene (**18**) (see below) was only a trace product. They suggested the occurrence of three parallel pathways for consumption of **149**, all following first-order kinetics: (1) isomerization to form **144**; (2) formation of methane and **45** [although this involves net consumption of hydrogen and the observed methane : **45** ratio was nearer 0.2 than 1]; and (3) formation of carbon monoxide and **9** [although this involves net release of hydrogen and the observed carbon monoxide : **9** ratio was 0.6 rather than 1]. In contrast, Schlosberg and coworkers[290] made no mention of **144** but specified the major liquid product to be **45** with lesser amounts of benzaldehyde (**79**) and **18**; methane, benzyl alcohol (**150**), **9**, biphenyl, water, carbon monoxide, and heavier materials were also reported but not quantified. The Finnish group[287,288] described the major products as **45**, **150**, and **79** with lesser amounts of **9**, **18**, **144**, **146**,

and "dimers." Major discrepancies thus exist concerning the relative amounts of isomerization of **149** to **144** and of rearrangement to products such as **79** and **150** which contain the Ph-C-O bonding pattern.

The lack of detailed product selectivities as a function of conversion makes a rigorous mechanistic description impossible. However, following the general outlines of Schlosberg and coworkers,[290] we sketch the most probable steps. If we estimate $A = 10^{15}$-10^{16} s^{-1} for homolysis of **149** and take $E \sim D^{o}(PhO\text{-}CH_3) = 63.8$ kcal mol^{-1},[20] we can predict a rate constant for unimolecular homolysis at 400°C of 1.9-19 x 10^{-6} s^{-1}. Klein and Virk[286] observed $k = 25.5 \times 10^{-6}$ s^{-1} for total disappearance of neat **149**, while Vuori and Bredenberg[287,288] observed $k = 41.5 \times 10^{-6}$ s^{-1} for neat **149** and $k = 20.9 \times 10^{-6}$ s^{-1} in tetralin solution. Thus, the observed thermal lability is consistent with C-O homolysis making a stoichiometrically significant contribution to product formation, while the modest deceleration in tetralin[287,288] and the products containing the Ph-C-O bonding pattern suggest a second pathway for decomposition that is induced by hydrogen abstraction. Homolysis would generate phenoxy (**46**) and methyl radicals (step 195); under FVP conditions at 950°C, the production of **46** from **149** has been observed directly by mass spectroscopy.[258] Recombination at carbon (step 196) would generate the cresols, although the large amount and regiochemical preference for **144** reported by Klein and Virk[286] are somewhat surprising. Hydrogen abstraction from **149** would generate **45** and methane (step 197) along with phenoxymethyl radical (**151**). A 1,2-phenyl shift from O to C (see below and Section 5.5) would convert **151** to radical **152** in step 198 and establish the Ph-C bond seen in products **18**, **79**, and **150**. Based on the known facility with which alkoxy radicals abstract hydrogen, radical **152** would be expected largely to produce **150** by exothermic hydrogen abstraction from **149**. Steps 198 and 199 constitute a chain for isomerization of **149** to **150**; however, based on the observations that products containing the Ph-C bond did not completely dominate and that the overall rate was not much greater than expected from the rate of C-O homolysis, the chain length must be $\lesssim 1$, possibly because the predominant radical in the system is the relatively stable **46**. Secondary pathways for converting benzyl

$$\underset{\mathbf{149}}{PhOCH_3} \longrightarrow \underset{\mathbf{46}}{PhO\cdot} + \cdot CH_3 \qquad (195)$$

$$\mathbf{46} + \cdot CH_3 \longrightarrow$$ 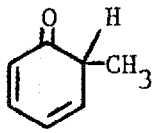 $$\longrightarrow$$ 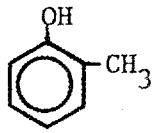 $$(196)$$

(and/or <u>para</u>) **144** (and/or **146**)

$$\mathbf{46}\ (CH_3\cdot) + \mathbf{149} \longrightarrow \underset{\mathbf{45}}{PhOH}\ (CH_4) + \underset{\mathbf{151}}{PhOCH_2\cdot} \qquad (197)$$

$$\mathbf{151} \longrightarrow \underset{\mathbf{152}}{PhCH_2O\cdot} \qquad (198)$$

$$\mathbf{152} + \mathbf{149} \longrightarrow \underset{\mathbf{150}}{PhCH_2OH} + \mathbf{151} \qquad (199)$$

$$2\ \mathbf{150} \longrightarrow \underset{\mathbf{79}}{PhCH{=}O} + \underset{\mathbf{18}}{PhCH_3} + H_2O \qquad (200)$$

$$\mathbf{152} + R\cdot \longrightarrow \mathbf{79} + RH \qquad (201)$$

$$\mathbf{79} \longrightarrow \underset{\mathbf{9}}{PhH} + CO \qquad (202)$$

alcohol to a mixture of **18** and **79** (step 200) and for converting the latter to carbon monoxide and **9** (step 202) are discussed in Section 12.

The conversion of **149** in tetralin under ~4.8 MPa hydrogen pressure after 1 h at 450°C was 56%, and the products were **45** (66%), **18** (15%), and **9** (2%).[195] Note that the excess tetralin did not completely eliminate the induced phenyl shift process (see Section 12.4 for reduction of **150** in tetralin). Nor did added hydrogen introduce a major hydrodemethoxylation route to give **9** and methanol. This process might well occur, however, at the higher temperatures where hydrodehydroxylation of **45** occurs (Section 11.1). Results from a parallel study at 345°C[291] suffered from acceleration by wall effects.[288]

A VLPP study of the next higher homolog, phenyl ethyl ether (**153**), gave kinetic results corresponding to

$$\underset{\mathbf{153}}{PhOCH_2CH_3} \longrightarrow PhO\cdot + \cdot CH_2CH_3 \qquad (203)$$

$k_{203} = 10^{15.3}\exp(-60{,}400/RT)\ s^{-1}$.[292] Extrapolation to 400°C predicts a half-life for homolysis of 4 h, a value in general agreement with the 5% conversion of **153** observed for a solution in tetralin after 1 h at 400°C.[12] Kamiya and coworkers[195] exposed ethyl ether **153** and methyl ether **149** to identical conditions of 1 h at 450°C in tetralin solution under hydrogen pressure. The observed conversions of 89% and 56%, respectively, are in the order expected for the relative rates of steps 203 and 195 based on the relative stabilities of ethyl and methyl radicals. The selectivity to **45** from **153** at this high conversion was 78%.

Collins and coworkers[205,293] heated **153**, labeled separately with ^{14}C in the α and β carbons of the ethyl group, in tetralin for 18 h at 400°C. The major products, normalized to 100%, were **45** (54%), **9** (12%), **18** (11%), ethylbenzene (**25**) (10%), and methylnaphthalenes (11%). The major position of the labeled carbons in products **18** and **25** was as shown:

$$\overset{x}{Ph}O\overset{o}{CH_2}CH_3 \longrightarrow \overset{x}{Ph}CH_3 + \overset{x}{Ph}\overset{o}{CH_2}CH_3$$

A cross-over experiment with **153**-α-^{14}C and p-tolyl ethyl ether demonstrated that the formation of the Ph-C_α bond was an intramolecular process. Thus a 1,2-phenyl shift from O to C in radical **154** (step 204)

$$\mathbf{153} \xrightarrow{R\cdot} \underset{\mathbf{154}}{PhO\overset{\cdot}{C}HCH_3} \longrightarrow \underset{\mathbf{155}}{\cdot OCHPhCH_3} \longrightarrow\!\!\!\!\longrightarrow \underset{\mathbf{25}}{PhCH_2CH_3} \quad (204)$$

was proposed as the key event preceding formation of **25**. [An analogous 1,2-phenyl shift from N to C has been proposed by Stenberg and coworkers[294] to occur during thermolysis of N,N-dimethylaniline.] To rationalize the formation of **18**, an alternate C-C homolysis, followed by step 198, was suggested:

$$\mathbf{153} \longrightarrow \underset{\mathbf{151}}{PhOCH_2\cdot} + \cdot CH_3 \quad (205)$$

However, it is improbable that this bond is weak enough for step 205 to compete with step 203. A more likely scheme involves β-scission of radical **155** and followed by hydrogenation of **79** (Section 12.3):

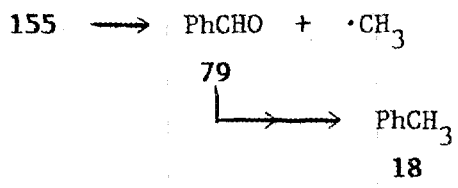

The reactivity of **153** is in accord with rate-limiting homolysis and does not show the added acceleration seen for its β-phenyl derivative **81** (Section 8.2); i.e., a chain elimination process to form **45** and ethylene from **153** does not occur even under condensed phase conditions. Even though D^{o}(C-O) should be essentially the same for the two ethers, presumably the barrier for abstraction of the unactivated prim C_{β}-H in **153** by radical **46** is too great to allow efficient chain propagation, whereas the benzylic activation of the corresponding bond in **81** does allow this. Elimination to form **45** and i-butene does characterize the gas-phase thermolysis of phenyl t-butyl ether at 327-402°C, but a four-center molecular elimination mechanism was proposed.[295] This change in mechanism, specifically for tert ethers, seems general.

Conversions of neat 1-naphthyl methyl ether, 2-naphthyl methyl ether, and **149** after 6 min at 450°C were 67%, 29%, and 9%, respectively.[289] This reactivity order parallels the expected order of resonance stabilization of aryloxy radicals, i.e., 1-naphthoxy > 2-naphthoxy > phenoxy. Characteristic products for each naphthyl ether were the naphthol, the methylnaphthalene, and the naphthaldehyde. Hence, the product-forming steps appear analogous to those for **149**, although more quantitative conclusions cannot be drawn because the incomplete material balances do not allow an adequate separation of homolysis and induced decomposition. A slow interconversion of the two isomeric ethers was also observed.

11.7 HYDROXY- AND METHOXYANISOLES

Finally, we consider the effects of the presence of multiple alkoxy substituents and of mixed alkoxy and hydroxy substituents. Vuori and Bredenberg[288,296] have compared the rates and products of thermolysis of ortho-, meta-, and para-dimethoxybenzenes (**156-158**) and of the corresponding isomeric hydroxyanisoles (**159-161**) at 325-400°C, both neat and diluted 1 : 1 with tetralin. Product data and conversion levels after 60 min at 350°C will be used as the basis of comparison here. The conversions of **156-158** were 8.3, 1.4, and 11.1%, respectively, indicative of a reactivity order p $\gtrsim$ o > m. Parallels to the products formed from anisole (Section 11.6) can be readily seen. The most prevalent product from each was the corresponding isomer of **159-161** (40.4% from **156**, 41.8% from **157**, and 32.3% from **158**) which presumably results from C-O homolysis in step 206 followed by hydrogen abstraction. For **156** and **158**, a second

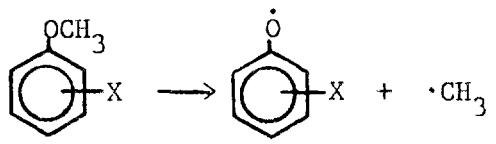

(206)

149 (X = H)
156-158 (X = OCH_3; o, m, p)
159-161 (X = OH; o, m, p)

product class consisted of molecules with a $CH_3OC_6H_4$-R bonding pattern where R = CH_2OH (9.5 and 23.2%), CHO (21.7 and 21.8%), CH_3 (4.9 and 8.1%) and H (8.4 and 11.2%). These rearranged products (44.5% from **156** and 64.3% from **158**) presumably all result from a 1,2-aryl shift, analogous to step 198, in the radical which is formed by hydrogen abstraction from the substrate. Finally, trace amounts of ring-methylated hydroxyanisoles were formed, 4.0% from **156** and 2.8% from **158**, and these presumably result from recombination of radicals formed by C-O homolysis. In contrast, the second most prevalent product class from the m-isomer **157** was ring-methylated resorcinols (38.9%) in which both O-CH_3 bonds were broken and a new C-CH_3 bond was formed. The source of this product at such low conversion is not immediately apparent.

Continuing the comparison of 60-min runs at 350°C,[288,296] we note a change in reactivity order for the isomers of the hydroxyanisoles: o (17.2%) > p (5.6%) > m (3.2%). The major product in each case was again that expected from C-O homolysis, the corresponding dihydroxybenzene: 55.2% from **159**, 51.3% from **160**, and 53.4% from **161**. Hence, this series is better considered mechanistically as hydroxy-perturbed anisoles rather than methoxy-perturbed phenols. For **159** and **161**, the second most prevalent product class, HOC_6H_4-R, again represented aryl shift, but the dominant material had R = CH_3 (18.9% from **159** and 36.7% from **161**). Control thermolyses of the hydroxybenzyl alcohols and hydroxybenzaldehydes showed them to be more reactive than their methoxy analogs. In contrast, the second most prevalent product from **160** was **157**; this conversion does not fit into an obvious mechanistic pattern.

Overall rates of disappearance of **156-161** were all suppressed by factors typically 2-3 fold by added tetralin; selectivities to demethylation products were generally increased. The Arrhenius factors presented[288,296] have large error limits and unexpectedly large variations from isomer to isomer. We choose to focus only on the relative rates of disappearance in tetralin reported for the median temperature of 375°C. These are compared in Table 19 with that of anisole as the parent and should represent an approximation to the relative rates of C-O homolysis in step 206, based on the presumption that the fraction of induced decomposition is rather small and similar in each case. The acceleration by a m-OH or m-OCH_3 substituent is <2-fold, while that by a p-OH, p-OCH_3, or o-OCH_3 substituent is about one order of magnitude. Qualitatively, these effects are consistent with the fact that substitution of an oxy group for hydrogen at radical centers is stabilizing[20] and that phenoxy radicals have positive spin density at the o- and p- but not m-positions. Such substitution in localized methyl radical is stabilizing by some 10 kcal mol^{-1}.[20] A rate acceleration of 10-15 fold at 375°C corresponds to ~3 kcal mol^{-1}. Hence, the quantitative magnitude of the observed substituent effects on step 206, which produces a delocalized phenoxy radical, also appears reasonable. But what then is the source of the additional acceleration of almost another order of magnitude observed specifically for the o-hydroxy substituent in **159**?

Table 19. Thermolyses of Substituted Anisoles in Tetralin at 375°C[a]

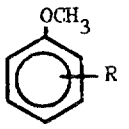

	k_{rel}[b]		
R	ortho	meta	para
H	1.0[c]	1.0[c]	1.0[c]
OH	74	1.5	8.1
OCH_3	12.9[d]	1.6[d]	9.4[d]

[a]Refs. 288 and 296. [b]Apparent first-order rate constant for total disappearance. [c]Anisole. [d]Adjusted for statistical advantage of 2 methoxy groups.

Earlier, Klein and Virk[286] had presented data specifically on thermolysis of neat guaiacol (**159**) at quite low conversions over the ranges 0.46-3.07 M and 250-525°C. They reported a 31-fold acceleration at 375°C over the rate they observed for total disappearance of anisole, compared with the 74-fold acceleration (Table 19) observed in tetralin by Vuori and Bredenberg.[288] They concluded that two parallel decomposition pathways occurred, steps 207 and 208, with

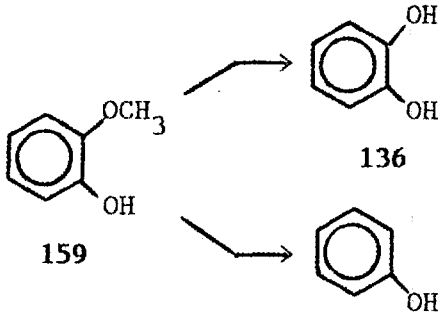

$+ \; CH_4 \quad (-\,2H)$ (207)

$+ \; CO \quad (+\,2H)$ (208)

$k_{207} = 10^{10.9}\exp(-43{,}700/RT)\ s^{-1}$ and $k_{208} = 10^{11.5}\exp(-47{,}400/RT)\ s^{-1}$. Although they observed methane : catechol and carbon monoxide : phenol ratios ~ 1 as demanded by these equations, the ratio k_{207}/k_{208} was considerably greater than unity, e.g. 4.4 at 375°C. The two equations are thus not in hydrogen balance and hence cannot be a complete description of the stoichiometry, let alone the mechanism. They ascribed the enhanced rate for **159** and the increase in its selectivity to form **136** and methane to a concerted six-center elimination (step 209) with presumably rapid secondary hydrogenation of o-quinone (**162**) (Section 12.1), although most of the associated dehydrogenated products from **159** were not identified. Stein[16] did not favor this concerted route because his mass spectral studies of thermolysis of **159** under VLPP conditions revealed methyl radical, but not methane, as a direct unimolecular decomposition product. Unfortunately, this is not directly relevant at ~400°C because, if steps 209 and 210 compete, the latter, which will surely have the higher A factor and therefore also the higher E value, will naturally be favored under high-temperature VLPP

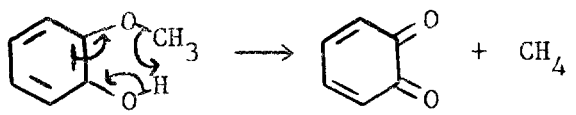

(209)

159 **162**

↓ + 2H

136

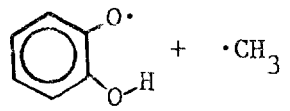

(210)

159 → **163**

conditions. He suggested a possible chain route based on β-scission of radical **164** to account for the rate acceleration:

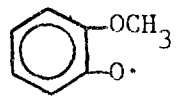

159 + $CH_3\cdot$ → **164**

164 → **162** + $CH_3\cdot$

However, it is not apparent why this route would not then be available to the <u>para</u> isomer **161** as well. Another alternate explanation might be an enhanced C-O homolysis rate because of intramolecular hydrogen bonding stabilization in radical **163** that is not present in **159** itself; hydrogen bonding stabilization of alkoxy radicals is known.[24g] Yet, if there is unusual stability in phenoxy radical **163** provided specifically by the <u>o</u>-hydroxy substituent, it did not manifest itself in the relative rates of hydrogen abstraction from the dihydroxybenzenes by <u>o</u>-allylbenzyl radical which fell in the order <u>p</u> > <u>o</u> > <u>m</u>.[142] ESR measurements of the number of free spins that survived after reaction mixtures were cooled to room temperature[296] are not relevant since this signal must surely result from highly stabilized radicals formed from complex byproducts, not primary radicals along the major mechanistic pathway. We conclude that

the reason for the enhanced thermal lability of **159**, compared with its isomers, has not been uniquely demonstrated.

12. CARBONYL COMPOUNDS

Carbonyl functionality occurs in low-rank coals; also, carbonyl compounds are products from thermolysis of appropriate ethers (Section 8.2 and 11.6). Model studies of thermolysis of carbonyl compounds have highlighted their reduction by hydrogen donor solvents.

12.1 DIARYL KETONES

The typical diaryl ketones benzophenone (**128**)[195,265,297] and fluorenone[297] were reduced to diphenylmethane (**32**) and fluorene, respectively, when heated in hydrogen donor solvents at ~400°C. Choi and Stock[297] have suggested three stages of reaction: (1) hydrogen transfer to produce the alcohol (e.g. **165**) in step 211; (2) equilibration of the alcohol with its ether (e.g. **166**) and water in step 212, via ionic intermediates,; and (3) cracking of the ether to form a mixture of the hydrocarbon product (e.g. **32**) and starting ketone in step 213, by a radical chain analogous to that for dibenzyl ether (Section 8.2). A radical chain is also indicated for the initial step 211 by the marked

$$\underset{\mathbf{128}}{2\ Ph_2C{=}O} + 2\ ArH_2 \longrightarrow \underset{\mathbf{165}}{2\ Ph_2CHOH} + 2\ Ar \qquad (211)$$

$$2\ \mathbf{165} \rightleftharpoons \underset{\mathbf{166}}{Ph_2CHOCHPh_2} + H_2O \qquad (212)$$

$$\mathbf{166} \longrightarrow \underset{\mathbf{32}}{Ph_2CH_2} + \mathbf{128} \qquad (213)$$

$$\mathbf{128} + 2\ ArH_2 \longrightarrow \mathbf{32} + 2\ Ar + H_2O \qquad (214)$$

acceleration by added benzyl phenyl sulfide. However, whether this involves a direct radical hydrogen transfer (step 215) or free hydrogen

$$\mathrm{ArH}\cdot + \mathbf{128} \longrightarrow \mathrm{Ar} + \underset{\mathbf{131}}{\mathrm{Ph_2\dot{C}OH}} \tag{215}$$

$$\mathrm{ArH}\cdot \longrightarrow \mathrm{Ar} + \mathrm{H}\cdot \tag{216}$$

$$\mathrm{H}\cdot + \mathbf{128} \longrightarrow \mathbf{131} \tag{217}$$

$$\mathbf{131} + \mathrm{ArH_2} \longrightarrow \mathbf{165} + \mathrm{ArH}\cdot \tag{218}$$

atom (steps 216 plus 217) is not clear.[297] Nor is the initiating step in the absence of added initiators, although molecular disproportionation (step 219) is worthy of consideration.

$$\mathrm{ArH_2} + \mathbf{128} \longrightarrow \mathrm{ArH}\cdot + \mathbf{131} \tag{219}$$

Raaen and Roark[265] suggested the use of relative rates of reduction of **128** as a measure of the hydrogen donor ability of solvents. For example, extents of conversion to **32** after 90 min at 400°C for various hydrogen donors were 1,2-dihydronaphthalene (28%) > 1,2,3,4-tetrahydroquinoline (21%) $\gtrsim$ 9,10-dihydrophenanthrene (20%) > tetralin (17%) > 9,10-dihydroanthracene (13%) >> decalin (0%). Corresponding values[297] for fluorenone after 60 min at 400°C were 1,2,3,4-tetrahydroquinoline (28%) > 9,10-dihydroanthracene (14%) > 9,10-dihydrophenanthrene (5%) > tetralin (3%) > decalin (0.4%). Unfortunately, in the absence of information on the relative contributions of steps 215 (or 216), 218, and possibly 219 to establishing the observed rate of reduction in reaction 214, the particular mechanistic aspect of "hydrogen donor ability" that is actually being measured in this complex reaction cannot be specified.

Polycyclic quinones dehydrogenate tetralin efficiently at 400°C and give mixtures of the corresponding aromatic hydrocarbon and phenol.[12,298]

12.2 ARYL ALKYL KETONES

The rate of reduction of acetophenone to ethylbenzene was responsive not only to the nature of the hydrogen donor solvent but also to the hydrogen pressure.[195] For example, for dilute solutions in donor solvent : n-dodecane (1 : 7.8) mixtures,[13,182] relative rates of reduction at 412°C for tetralin-nitrogen, 1,2,3,4-tetrahydroquinoline-nitrogen, and

tetralin-10.3 MPa hydrogen were 1 : 4.4 : 9.1. This behavior suggests at least some involvement of hydrogen atom. In the absence of a hydrogen donor solvent, neat acetophenone decomposed at 350-550°C to give a very complex mixture containing benzene, toluene, xylenes, styrene, carbon monoxide, methane, and several other minor products.[286] Although the strength of the C-C bond [$D^o(Ph(C{=}O)-CH_3$ = 81.9 kcal mol^{-1}][20] precludes significant unimolecular homolysis in this low-temperature regime, further rationalization of the observed $k = 10^{10.3}\exp(-50{,}700/RT)\ s^{-1}$ for overall disappearance and details of mechanism are lacking. The reaction in dilute tetralin-n-dodecane[182] was almost 10 times more rapid at 400°C than that in neat acetophenone.[286]

Heating 1-tetralone in hydrogen donor solvents (2,6-dimethyltetralin and/or mesitylene) gave both the reduction product, tetralin, and a dehydration product, naphthalene.[13] Thermolysis of the neat ketone gave tetralin, naphthalene, and 1-naphthol.[299] Cronauer and coworkers[13] suggested that this cyclic ketone might function not only as a hydrogen acceptor but also as a hydrogen donor to generate the 1-naphthol; further details of stoichiometry and mechanism are again lacking.

12.3 BENZALDEHYDE

The products formed from heating benzaldehyde (**79**) in tetralin solution at 350-400°C have been variously described as toluene (at a rate notably greater than that for acetophenone),[13,182] benzene and carbon monoxide,[298] or a mixture of both reduction and decarbonylation.[195] The change from ketonic to aldehydic functionality allowed a new pathway, decarbonylation, to emerge even in hydrogen donor solvents, but the conflicting data do not reveal the factors which control the reduction : decarbonylation ratio. Although the amount of aromatic aldehydes in most coals appears low, they might contribute to the formation of carbon monoxide during pyrolysis by the indirect sequence:

$$ArOCH_2R \longrightarrow ArOCH_2\cdot \longrightarrow ArCHO \longrightarrow CO$$

Decarbonylation of neat **79** followed first-order kinetics at 400°C over the initial concentration range 0.45-3.0 M with

$k = 10^{9.5}\exp(-41{,}500/RT)\ s^{-1}$ over the range 300-500°C,[286] and Klein and Virk suggested a concerted cheletropic expulsion of carbon monoxide (step 220) to rationalize these kinetics. At very high conversions (>90% after 6 min at 450°C), Schlosberg and coworkers[207,290] observed not only carbon monoxide and benzene, but also a complex mixture of heavier liquid products containing, among others, biphenyl, fluorene, benzophenone, and terphenyl. Their reported rate constant at 450°C, $4.8 \times 10^{-3}\ s^{-1}$, is some five times greater than that predicted from the Klein-Virk correlation, and they implicitly assumed the occurrence of a radical mechanism involving decarbonylation of benzoyl radical in step 221. Further mechanistic speculation is not fruitful in the absence of additional data.

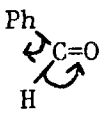

$$\longrightarrow \quad PhH + CO \qquad (220)$$

$$PhC(\cdot)=O \longrightarrow Ph\cdot + CO \qquad (221)$$

12.4 BENZYLIC ALCOHOLS

Heating neat benzhydrol (**165**) at 400°C gave a mixture of diphenylmethane (**32**), benzophenone (**128**), and water:[265,297]

$$\underset{\mathbf{165}}{2\ Ph_2CHOH} \longrightarrow \underset{\mathbf{32}}{Ph_2CH_2} + \underset{\mathbf{128}}{Ph_2C{=}O} + H_2O$$

We have already described the probable mechanism consisting of steps 212 and 213 (Section 12.1).[297] In a hydrogen donor solvent, **128** was further reduced (Section 12.1)[154,265] so that the net stoichiometry was:

$$\mathbf{165} + ArH_2 \longrightarrow \mathbf{32} + Ar + H_2O$$

Benzyl alcohol behaved similarly.[13] Although direct C-O homolysis has been proposed,[13] the strength of the C-O bond

[$D^o(PhCH_2\text{-}OH)$ = 81.2 kcal mol^{-1} [20]] precludes this as a significant participant at 400°C. A mechanism parallel to that for **165** appears more likely.

13. EFFECTS OF HYDROGEN SULFIDE

The well-known ability of hydrogen sulfide to perturb the thermolysis of alkanes[40c,300] arises because it is a reactive hydrogen donor [$D^o(H\text{-}SH)$ = 91.1 kcal mol^{-1}][20] in step 222. This can lead either to acceleration or inhibition, dependent on the relative rate constants for the propagation steps in the unperturbed chain reaction (Section 2). In brief,[300] acceleration requires two conditions to be met: (1) hydrogen abstraction rather than β-scission must be the inherently slow propagation step; and (2) the <u>sum</u> of steps 222 and 223, which together achieve the same result as step 224, must be more rapid than step 224 occurring

$$R\cdot + HSH \longrightarrow RH + \cdot SH \qquad (222)$$

$$HS\cdot + R'H \longrightarrow HSH + R'\cdot \qquad (223)$$

$$\overline{\qquad\qquad\qquad\qquad\qquad\qquad\qquad\qquad}$$

$$R\cdot + R'H \longrightarrow RH + R'\cdot \qquad (224)$$

directly. Under these conditions, hydrogen sulfide can, in effect, catalyze hydrogen transfer. As an example of its high hydrogen donor activity, Rebick[40c] found k_{222}/k_{224} = 164 at 650°C when R· = C_2H_5· and R'H = <u>n</u>-butane. If these two conditions are not met, the dominant result of forming some HS· radicals in step 222 will be additional termination pathways, and overall inhibition is observed. Added hydrogen sulfide can also affect product distributions by converting alkyl radicals, which would normally undergo further β-scission, to alkanes in step 222 and by modifying the ratio of isomeric radicals formed by hydrogen abstraction for the substrate since HS· shows different selectivity from small alkyl radicals and/or hydrogen atom.

Several examples of this accelerating effect of chain reactions by added hydrogen sulfide or thiols have been reported for the key model compounds under discussion. The H-D exchange between diphenylmethane and tetralin-d_{12} at 400°C (Section 10.1.6), which occurs by repetitive

hydrogen abstraction steps, was accelerated by hydrogen sulfide, aliphatic thiols, and aromatic thiols.[200,238] The even greater acceleration of exchange by added diphenyl disulfide or benzyl phenyl sulfide probably resulted largely from added initiation by homolysis of the weak S-S or C-S bonds, but some catalysis of hydrogen transfer by the thiols formed during the initiation process also probably occurred. Similarly, the thermolysis of 1,3-diphenylpropane was accelerated by added thiophenol.[200,238] Since this reaction involves a chain in which hydrogen abstraction is inherently slower than β-scission (Section 8.1), catalysis of hydrogen transfer is again indicated. The presence of an equimolar amount of hydrogen sulfide during thermolysis of bibenzyl as a dense gas at 425°C for 30 min (22% conversion) had negligible effect on the amounts of toluene and stilbene formed but notably increased the amount of 1,1-diphenylethane.[301,302] This rearrangement is yet another case of a chain reaction in which hydrogen abstraction is rate-limiting (Section 5.1.3), and a third example of catalysis of hydrogen transfer is indicated.

A different role of hydrogen sulfide has been observed during thermolysis of compounds containing one-atom linkages (Section 7).[301,303] Whereas the conversion of diphenylmethane as a dense gas in Pyrex vessels was $\lesssim$3% after 1 h at 450°C, addition of a 2.9-fold excess of hydrogen sulfide increased conversion to 14%; the major products were toluene and thiophenol. [Results in a stainless steel vessel were less dramatic, presumably because of consumption of hydrogen sulfide by reaction with

$$\underset{Y = CH_2;\ O}{PhYPh} + H_2S \longrightarrow PhYH + PhSH$$

iron.] This cleavage reaction was largely quenched by added tetralin. Very similar behavior occurred for diphenyl ether which was converted to a mixture of phenol and thiophenol. Stenberg and coworkers[301] proposed that the key step was a homolytic aromatic substitution reaction:

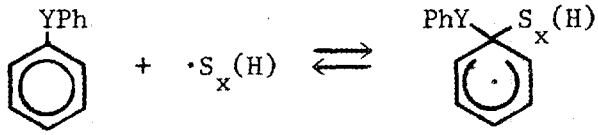

(225)

Because of expected equilibrations among sulfur-containing species, these authors did not attempt to specify uniquely the number of sulfur atoms, x, in the attacking species or the presence or absence of a terminal hydrogen.

With hydrogen sulfide : bibenzyl ratios > 1, not only the extent of phenyl shift (see above) but also that of cleavage to form toluene increased compared with the purely thermal reaction,[301,302] and hydrogen sulfide was considered to be a net hydrogen donor. The mechanism

$$PhCH_2CH_2Ph + H_2S \longrightarrow 2\ PhCH_3 + S$$

proposed was sketchy, but the authors[301] appeared to imply the occurrence of steps such as:

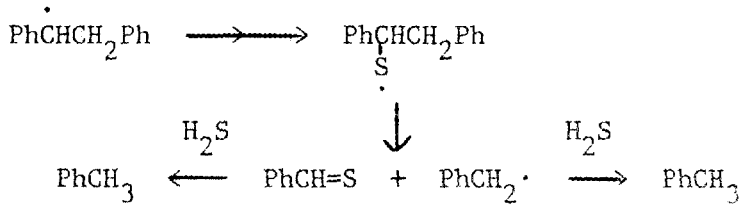

In contrast with the behavior of diphenylmethane (see above), the ipso substitution products, ethylbenzene and thiophenol, were not observed, possibly because the addition step in sequence 225 is highly reversible with as unstable a leaving radical as 2-phenylethyl.

ACKNOWLEDGMENT

Preparation of this review was sponsored by the Division of Chemical Sciences, Office of Basic Energy Sciences, U. S. Department of Energy, under contract DE-AC05-840R21400 with Martin Marietta Energy Systems, Inc.

14. REFERENCES

1. R. A. Meyers, Ed., "Coal Structure," Academic Press: New York, 1982.
2. R. M. Davidson in "Coal Science," M. L. Gorbaty, J. W. Larsen, and I. Wender, Eds., Academic Press: New York, 1982; Vol. 1.
3. M. A. Elliott, Ed., "Chemistry of Coal Utilization," Wiley-Interscience: New York, 1981; Suppl. Vol. 2:
   (a) I. Wender, L. A. Heredy, M. B. Neuworth, and I. G. C. Dryden, Chapter 8;
   (b) J. B. Howard, Chapter 12;
   (c) D. Habermehl, F. Orywal, and H.-D. Beyer, Chapter 6;
   (d) L. Seglin and S. A. Bresler, Chapter 13;
   (e) W. Eisenhut, Chapter 14;
   (f) M. Perch, Chapter 15;
   (g) E. Aristoff, R. W. Rieve, and H. Shalit, Chapter 16;
   (h) D. McNeil, Chapter 17;
   (i) E. Gorin, Chapter 27;
   (j) S. B. Alpert and R. H. Wolk, Chapter 28;
   (k) J. L. Johnson, Chapter 23;
   (l) D. Hebden and H. J. F. Stroud, Chapter 24;
   (m) R. H. Essenhigh, Chapter 19;
   (n) F. J. Ceely and E. L. Daman, Chapter 20.
4. N. Berkowitz, "An Introduction to Coal Technology," Academic Press: New York, 1980.
5. G. R. Gavalas, "Coal Pyrolysis," Elsevier: Amsterdam, 1982.
6. D. D. Whitehurst, T. O. Mitchell, and M. Farcasiu, "Coal Liquefaction," Academic Press: New York, 1980.
7. G. P. Curran, R. T. Struck, and E. Gorin, Ind. Eng. Chem., Proc. Des. Develop., **1967**, 6, 167.
8. W. H. Wiser, Fuel, **1968**, 47, 475.
9. R. C. Neavel, Fuel, **1976**, 55, 237.
10. E. A. Depp, C. M. Stevens, and M. B. Neuworth, Fuel, **1956**, 35, 437; E. A. Depp and M. B. Neuworth, Brennstoff-Chem., **1958**, 39, 90.

11. R. Brücker and G. Kölling, Brennstoff-Chem., **1965**, 46, 41; G. Kölling and D. Hausigk, ibid., **1969**, 50, 8.

12. B. M. Benjamin, V. F. Raaen, P. H. Maupin, L. L. Brown, and C. J. Collins, Fuel, **1978**, 57, 269.

13. D. C. Cronauer, D. M. Jewell, Y. T. Shah, and R. J. Modi, Ind. Eng. Chem., Fundam., **1979**, 18, 153.

14. Y. Kamiya, T. Yao, and S. Oikawa, Amer. Chem. Soc. Symp. Ser., **1980**, 139, 291.

15. D. D. Whitehurst, M. Farcasiu, T. O. Mitchell, and J. J. Dickert, Jr., Electric Power Research Institute Reports AF-252 (1976) and AF-480 (1977).

16. S. E. Stein, Amer. Chem. Soc. Symp. Ser., **1981**, 169, 97.

17. S. E. Stein, in "Chemistry of Coal Conversion," R. H. Schlosberg, Ed., Plenum Press: New York, 1985; Chp. 2.

18. E. Hedaya, Accts. Chem. Res., **1969**, 2, 367.

19. D. M. Golden, G. N. Spokes, and S. W. Benson, Angew. Chem., Int. Edn. Engl., **1973**, 12, 534.

20. D. F. McMillen and D. M. Golden, Ann. Rev. Phys. Chem., **1982**, 33, 493.

21. W. Tsang, J. Amer. Chem. Soc., **1985**, 107, 2872.

22. S. W. Benson and R. Shaw, J. Amer. Chem. Soc., **1967**, 89, 5351.

23. S. W. Benson and R. Shaw, J. Chem. Phys., **1967**, 47, 4052.

24. J. K. Kochi, Ed., "Free Radicals," Wiley: New York, 1973; 2 Vols.:
    (a) M. J. Perkins, Chapter 16;
    (b) J. A. Kerr, Chapter 1;
    (c) J. W. Wilt, Chapter 8;
    (d) T. Koenig and H. Fischer, Chapter 4;
    (e) G. A. Russell, Chapter 7;
    (f) M. L. Poutsma, Chapter 14;
    (g) J. C. Martin, Chapter 20.

25. J. O. Metzger, Angew. Chem., Int. Edn. Engl., **1986**, 25, 80.

26. D. F. McMillen, R. Malhotra, S.-J. Chang, and S. E. Nigenda, Preprints, Div. Fuel Chem., Amer. Chem. Soc., **1985**, 30(4), 297, 334.

27. R. Billmers, L. L. Griffith, and S. E. Stein, J. Phys. Chem., **1986**, 90, 517; Preprints, Div. Fuel Chem., Amer. Chem. Soc., **1985**, 30(4), 283.

28. S. W. Benson, Int. J. Chem. Kinetics, **1980**, 12, 755.

29. S. W. Benson, "Thermochemical Kinetics," Wiley-Interscience: New York, 1976.

30. D. R. Stull, E. F. Westrum, Jr., and G. C. Sinke, "The Chemical Thermodynamics of Organic Compounds," Wiley: New York, 1969.

31. J. D. Cox and G. Pilcher, "Thermochemistry of Organic and Organometallic Compounds," Academic Press: London, 1970.

32. S. E. Stein, J. Amer. Chem. Soc., **1981**, 103, 5685.

33. B. M. Ladanyi and J. T. Hynes, J. Amer. Chem. Soc., **1986**, 108, 585; J. T. Hynes, Ann. Rev. Phys. Chem., **1985**, 36, 573.

34. F. O. Rice and K. K. Rice, "The Aliphatic Free Radicals," Johns Hopkins Press: Baltimore, 1935; Chp. 7; A. Kossiakoff and F. O. Rice, J. Amer. Chem. Soc., **1943**, 65, 590.

35. D. A. Leathard and J. H. Purnell, Ann. Rev. Phys. Chem., **1970**, 21, 197.

36. K. J. Laidler and L. F. Loucks in "Comprehensive Chemical Kinetics," C. H. Bamford and C. F. H. Tipper, Eds., Vol. 5, Elsevier: Amsterdam, 1972.

37. D. L. Allara and D. Edelson, Int. J. Chem. Kinetics, **1975**, 7, 479.

38. K. H. Ebert, H. J. Ederer, and G. Isbarn, Angew. Chem., Int. Edn. Engl., **1980**, 19, 333.

39. K. M. Sundaram and G. F. Froment, Ind. Eng. Chem., Fundam., **1978**, 17, 174.

40. W. A. Pryor, Ed., "Frontiers of Free Radical Chemistry," Academic Press: New York, 1980:
(a) J. N. Bradley, pp. 73-92;
(b) J. H. Purnell, pp. 93-116;
(c) C. Rebick, pp. 117-138.

41. T. J. Ford, Ind. Eng. Chem., Fundam., **1986**, 25, 240.

42. P. Zhou and B. L. Crynes, Ind. Eng. Chem., Proc. Des. Develop., **1986**, 25, 508.

43. J. Burgess, R. D. W. Kemmitt, N. Morton, C. T. Mortimer, and M. P. Wilkinson, J. Organometal. Chem., **1980**, 191, 477.

44. R. E. Miller and S. E. Stein, J. Phys. Chem., **1981**, 85, 580.

45. D. J. Coleman and G. Pilcher, Trans. Faraday Soc., **1966**, 62, 821; A. G. Osborn and D. W. Scott, J. Chem. Thermodynamics, **1980**, 12, 429; E. Morawetz, J. Chem. Thermodynamics, **1972**, 4, 455.

46. A. L. Castlehaus, P. R. Marriott, and D. Griller, J. Amer. Chem. Soc., **1981**, 103, 4262.

47. J.-R. Cao and M. H. Back, Int. J. Chem. Kinetics, **1984**, 16, 961.

48. E. Ranzi, M. Dente, S. Pierucci, and G. Biardi, Ind. Eng. Chem., Fundam., **1983**, 22, 132.

49. J.-R. Cao and M. H. Back, J. Phys. Chem., **1984**, 88, 3074.

50. D. L. Baulch and J. Duxbury, Combust. Flame, **1980**, 37, 313.

51. M. L. Poutsma and S. R. Schaffer, J. Phys. Chem., **1973**, 77, 158.

52. M. Murata and S. Saito, J. Chem. Eng. Japan, **1974**, 7, 389.

53. V. Illés, I. Pleszkáts, and L. Szepesy, Acta Chim. (Budapest), **1973**, 79, 259.

54. F. E. Imbert and R. M. Marshall, Int. J. Chem. Kinetics, **1987**, 19, 81.

55. K. H. Ebert, H. J. Ederer, and G. Isbarn, Int. J. Chem. Kinetics, **1983**, 15, 475.

56. A. Dombi and P. Huhn, Int. J. Chem. Kinetics, **1986**, 18, 227, 241; A. Dombi, I. Horvath, and P. Huhn, Int. J. Chem. Kinetics, **1986**, 18, 255.

57. G. W. Harris and J. N. Pitts, J. Chem. Phys., **1982**, 77, 3995; K. Sugawara, K. Okazaki, and S. Sato, Bull. Chem. Soc. Japan, 1981, 54, 2872.

58. K. N. Houk, M. N. Paddon-Row, D. C. Spellmeyer, N. G. Rondan, and S. Nagase, J. Org. Chem., **1986**, 51, 2874.

59. B. M. Fabuss, J. O. Smith, and C. N. Satterfield, Adv. Petr. Chem. Refin., **1964**, 9, 179.

60. B. Blouri, F. Hamdan, and D. Herault, Ind. Eng. Chem., Proc. Des. Develop., **1985**, 24, 30.

61. Y. V. Kissin, Preprints, Div. Petr. Chem., Amer. Chem. Soc., 1985, 30, 652.

62. P. D. Pacey and J. H. Wimalasena, J. Phys. Chem., **1984**, 88, 5657.

63. W. Tsang, Int. J. Chem. Kinetics, **1978**, 10, 821.

64. R. Dasgupta and B. R. Maiti, Ind. Eng. Chem., Proc. Des. Develop., **1986**. 25, 381.

65. R. Louw and H. J. Lucas, Recl. Trav. Chim. Pays-Bas, **1973**, 92, 55.

66. C. T. Brooks, S. J. Peacock, and B. G. Reuben, J. Chem. Soc., Faraday I, **1979**, 75, 652.

67. S. E. Stein and V. P. Senthilnathan, Preprints, Div. Petr. Chem., Amer. Chem. Soc., **1986**, 31(4), 848.

68. R. Louw, J. H. M. Dijks, and P. Mulder, Recl. Trav. Chim. Pays-Bas, **1984**, 103, 271.

69. S. E. Stein, Carbon, **1981**, 19, 421.

70. J. H. Kiefer, L. J. Mizerka, M. R. Patel, and H.-C. Wei, J. Phys. Chem., **1985**, 89, 2013.

71. V. Subba Rao and G. B. Skinner, J. Phys. Chem., **1984**, 88, 5990.

72. M. B. Colket, III, Preprints, Div. Fuel. Chem., Amer. Chem. Soc., **1986**, 31(2), 98.

73. J. M. Nicovich and A. R. Ravishankara, J. Phys. Chem., **1984**, 88, 2534.

74. J. J. Madison and R. M. Roberts, Ind. Eng. Chem., **1958**, 50, 237.

75. A. J. Sharkey, Jr., J. L. Shultz, and R. A. Friedel, Carbon, **1966**, 4, 365.

76. M. Zander, Fuel, **1986**, 65, 1019.

77. I. C. Lewis and T. Edstrom, J. Org. Chem., **1963**, 28, 2050.

78. W. C. Herndon, Tetrahedron, **1982**, 38, 1389.

79. S. E. Stein, R. L. Brown, L. L. Griffith, and M. Manka, Preprints, Div. Fuel Chem., Amer. Chem. Soc., **1984**, 29(2), 42.

80. P. W. Whang, F. Dachille, and P. L. Walker, Jr., High Temp.-High Press., **1974**, 6, 127.

81. I. Mochida and H. Marsh, Fuel, **1979**, 58, 626; E. Fitzer, K. Mueller, and W. Schaefer in "Chemistry and Physics of Carbon," P. L. Walker, Jr., Ed., Vol. 7, Marcel Dekker: New York, 1971; I. C. Lewis and L. S. Singer, in "Chemistry and Physics of Carbon," P. L. Walker, Jr., Ed., Vol. 17, Marcel Dekker: New York, 1981.

82. R. A. Greinke and I. C. Lewis, Carbon, **1984**, 22, 305.

83. I. C. Lewis and L. S. Singer, Preprints, Div. Petr. Chem., Amer. Chem. Soc., **1986**, 31(4), 834.

84. B. M. Benjamin, E. W. Hagaman, V. F. Raaen, and C. J. Collins, Fuel, **1979**, 58, 386.

85. L. T. Scott, Accounts Chem. Res., **1982**, 15, 52.

86. M. J. S. Dewar and K. M. Merz, Jr., J. Amer. Chem. Soc., **1986**, 108, 5146.

87. R. Cypres and B. Bettens, Fuel, **1986**, 65, 507.

88. M. Szwarc, J. Chem. Phys., **1948**, 16, 128.

89. H. Blades, A. T. Blades, and E. W. R. Steacie, Can. J. Chem., **1954**, 32, 298.

90. M. Takahasi, Bull. Chem. Soc. Japan, **1960**, 33, 801, 808.

91. S. J. Price, Can. J. Chem., **1962**, 40, 1310.

92. C. T. Brooks, C. P. R. Cummins, and S. J. Peacock, Trans. Faraday Soc., **1971**, 67, 3265.

93. G. M. Badger and T. M. Spotswood, J. Chem. Soc., **1960**, 4420.

94. C. D. Hurd and A. R. Macon, J. Amer. Chem. Soc., **1962**, 84, 4524.

95. L. A. Errede and J. P. Cassidy, J. Amer. Chem. Soc., **1960**, 82, 3653.

96. M. F. R. Mulcahy and M. R. Pethard, Aust. J. Chem., **1963**, 16, 527.

97. V. Subba Rao and G. B. Skinner, J. Phys. Chem., **1984**, 88, 4362.

98. R. D. Smith, J. Phys. Chem., **1979**, 83, 1553.

99. S. W. Benson and J. H. Buss, J. Phys. Chem., **1957**, 61, 104.

100. D. A. Robaugh, W. Tsang, A. Fahr, and S. E. Stein, Ber. Bunsenges. Phys. Chem., **1986**, 90, 77.

101. D. Robaugh and W. Tsang, J. Phys. Chem., **1986**, 90, 4159.

102. M. Cher, C. S. Hollingsworth, and F. Sicilio, J. Phys. Chem., **1966**, 70, 877.

103. A. T. Blades and E. W. R. Steacie, Can. J. Chem., **1954**, 32, 1142.

104. J. G. Burr, R. A. Meyer, and J. D. Strong, J. Amer. Chem. Soc., **1964**, 86, 3846.

105. M. Lehni, H. Schuh, and H. Fischer, Int. J. Chem. Kinetics, **1979**, 11, 705.

106. W.-D. Gräber and K. J. Hüttinger, Fuel, **1982**, 61, 505.

107. P. F. Nelson and K. J. Hüttinger, Fuel, **1986**, 65, 354.

108. R. I. Silsby and E. W. Sawyer, J. Appl. Chem., **1956**, 6, 347.

109. S. E. Shull and A. N. Hixson, Ind. Eng. Chem., Proc. Des. Develop., **1966**, 5, 146.

110. W. D. Betts, F. Popper, and R. I. Silsby, J. Appl. Chem., **1957**, 7, 497.

111. J. R. Schaefgen, J. Polym. Sci., **1955**, 15, 203.

112. S. M. Lee in "Kirk-Othmer Encyclopedia of Chemical Technology," Vol. 24, Wiley-Interscience: New York, 1984; p. 744.

113. K. Schroeder, B. Bockrath, and G. Keldsen, Preprints, Div. Petr. Chem., Amer. Chem. Soc., **1986**, 31(3), 752.

114. M. Szwarc, J. Chem. Phys., **1949**, 17, 431.

115. H. G. Davis, Int. J. Chem. Kinetics, **1983**, 15, 469.

116. K. H. Ebert, H. J. Ederer, and P. S. Schmidt, Amer. Chem. Soc. Symp. Ser., **1978**, 65, 313.

117. W. D. Clark and S. J. Price, Can. J. Chem., **1970**, 48, 1059.

118. C. W. P. Crowne, V. J. Grigulis, and J. J. Throssell, Trans. Faraday Soc., **1969**, 65, 1051.

119. G. L. Estaban, J. A. Kerr, and A. F. Trotman-Dickenson, J. Chem. Soc., **1963**, 3873.

120. L. J. Mizerka and J. H. Kiefer, Int. J. Chem. Kinetics, **1986**, 18, 363.

121. D. F. McMillen, P. L. Trevor, and D. M. Golden, J. Amer. Chem. Soc., **1980**, 102, 7400.

122. D. A. Robaugh and S. E. Stein, Int. J. Chem. Kinetics, **1981**, 13, 445.

123. M. L. Poutsma and C. W. Dyer, J. Org. Chem., **1982**, 47, 4903.

124. J. H. Lee, J. V. Michael, W. A. Payne, and L. J. Stief, J. Amer. Chem. Soc., **1978**, 68, 1817.

125. S. Nagase, T. Fueno, and K. Morokuma, J. Amer. Chem. Soc., **1979**, 101, 5849.

126. P. E. Savage and M. T. Klein, Preprints, Div. Petr. Chem., Amer. Chem. Soc., **1985**, 30, 642.

127. G. W. Mushrush and R. N. Hazlett, Ind. Eng. Chem., Fundam., **1984**, 23, 288.

128. M. L. Poutsma, Fuel, **1980**, 59, 335.

129. F. P. Petrocelli and M. T. Klein, Macromolecules, **1984**, 17, 161.

130. M. J. Gibian and R. C. Corley, J. Amer. Chem. Soc., **1972**, 94, 4178.

131. C. Horrex and S. E. Miles, Disc. Faraday Soc., **1951**, 10, 187.

132. B. Bockrath, E. Bittner, and J. McGrew, J. Amer. Chem. Soc., **1984**, 106, 135.

133. Y. Sato, T. Yamakawa, R. Onishi, H. Kameyama, and A. Amano, J. Japan Petrol. Inst., **1978**, 21, 110.

134. S. E. Stein, D. A. Robaugh, A. D. Alfieri, and R. E. Miller, J. Amer. Chem. Soc., **1982**, 104, 6567.

135. H. E. van den Bergh and A. B. Callear, Trans. Faraday Soc., **1970**, 66, 2681.

136. H. Zeldes and R. Livingston, Fuel, **1982**, 61, 1254.

137. R. Livingston, H. Zeldes, and M. S. Conradi, J. Amer. Chem. Soc., **1979**, 101, 4312.

138. D. Duprez, M. Bastick, and J. Bastick, Bull. Soc. Chim. France, **1972**, 2583.

139. Y. Sekiguchi and K. J. Klabunde, Fuel Process Tech., **1981**, 4, 73.

140. J. W. Sweeting and J. F. K. Wilshire, Aust. J. Chem., **1962**, 15, 89.

141. R. A. Jackson and D. W. O'Neill, Chem. Comm., **1969**, 1210.

142. J. A. Franz, M. S. Alnajjar, R. D. Barrows, D. L. Kaisaki, D. M. Camaioni, and N. K. Suleman, J. Org. Chem., **1986**, 51, 1446.

143. B. Bockrath, E. W. Bittner, and T. C. Marecic, J. Org. Chem., **1986**, 51, 15.

144. R. Louw and J. J. Bunk, Recl. Trav. Chim. Pays-Bas, **1983**, 102, 119.

145. R. E. Miller and S. E. Stein, Preprints, Div. Fuel Chem., Amer. Chem. Soc., **1979**, 24(3), 271.

146. W. Rickatson and T. S. Stevens, J. Chem. Soc., **1963**, 3960.

147. E. J. Hamilton, Jr. and H. Fischer, Helv. Chim. Acta, **1973**, 56, 795.

148. A. C. Buchanan, III, T. D. J. Dunstan, E. C. Douglas, and M. L. Poutsma, J. Amer. Chem. Soc., **1986**, 108, 7703.

149. B. M. Benjamin, M. J. Michalczyk, and M. C. Woody, Preprints, Fuels and Petrochem. Div., Amer. Inst. Chem. Eng., **1980**, 1, 366.

150. D. C. Cronauer, D. M. Jewell, Y. T. Shah, and K. A. Kueser, Ind. Eng. Chem., Fundam., **1978**, 17, 291.

151. D. F. McMillen, W. C. Ogier, and D. S. Ross, J. Org. Chem., **1981**, 46, 3322.

152. K. R. Brower, J. Org. Chem., **1980**, 45, 1004.

153. J. Pajak and K. R. Brower, J. Org. Chem., **1985**, 50, 2210.

154. T. Yao and Y. Kamiya, Bull. Chem. Soc. Japan, **1979**, 52, 492.

155. Y. Sato and T. Yamakawa, Ind. Eng. Chem., Fundam., **1985**, 24, 12.

156. H.-H. King and L. M. Stock, Fuel, **1982**, 61, 1172; H.-H. King and L. M. Stock, Fuel, **1984**, 63, 811.

157. F. Mondragon and K. Ouchi, Fuel, **1984**, 63, 973.

158. L. W. Vernon, Fuel, **1980**, 59, 102.

159. J. G. Burr and I. Javeri, Fuel, **1984**, 63, 854.

160. P. S. Virk, Fuel, **1979**, 58, 149.

161. S. E. Stein, Fuel, **1980**, 59, 900.

162. (a) J. D. Unruh and G. J. Gleicher, J. Amer. Chem. Soc., **1971**, 93, 2008;

(b) R. B. Roark, J. M. Roberts, D. W. Croom, and R. D. Gilliom, J. Org. Chem., **1972**, 37, 2042.

163. W. C. Herndon, J. Org. Chem., **1981**, 46, 2119.

164. S. E. Stein and D. M. Golden, J. Org. Chem., **1977**, 42, 839.

165. Y. Sato, Fuel, **1979**, 58, 318.

166. D. E. Robaugh and S. E. Stein, J. Amer. Chem. Soc., **1986**, 108, 3224.

167. M. J. Manka, R. L. Brown, and S. E. Stein, J. Phys. Chem., **1985**, 89, 5421.

168. M. J. Rossi, D. F. McMillen, and D. M. Golden, J. Phys. Chem., **1984**, 88, 5031.

169. C. Rüchardt and H.-D. Beckhaus, Angew. Chem., Int. Edn. Engl., **1980**, 19, 429.

170. J. J. deVlieger, J. W. de Leeuw, A. P. G. Kieboom, and H. van Bekkum, Recl., J. Roy. Neth. Chem. Soc., **1984**, 103, 203.

171. F. M. Elkobaisi and W. J. Hickinbottom, J. Chem. Soc., **1959**, 1873.

172. R. H. Schlosberg, W. H. Davis, Jr., and T. R. Ashe, Fuel, **1981**, 60, 201.

173. S. Ozawa, K. Sasaki, and Y. Ogino, Fuel, **1986**, 65, 707.

174. D. Meyer, D. Nicole, and J. J. Delpuech, Fuel Process. Tech., **1986**, 12, 255.

175. A. I. Scott, Quart. Rev., **1965**, 19 u, 1; E. R. Altwicker, Chem. Rev., **1967**, 67, 475.

176. A. M. de P. Nicholas and D. R. Arnold, Can. J. Chem., **1984**, 62, 1850.

177. E. S. Huyser and R. M. Van Scoy, J. Org. Chem., **1968**, 33, 3524.

178. A. E. Abdel-Rahman and A. A. Abdel-Wahab, Indian J. Chem., **1979**, 18B, 402.

179. M. S. Alnajjar and J. A. Franz, Preprints, Div. Fuel Chem., Amer. Chem. Soc., **1986**, 31(1), 287.

180. F. A. Davis, T. W. Panunto, S. B. Awad, R. L. Billmers, and T. G. Squires, J. Org. Chem., **1984**, 49, 1228.

181. T. M. Ignasiak and O. P. Strausz, Fuel, **1979**, 57, 617.

182. S. V. Panvelker, Y. T. Shah, and D. C. Cronauer, Ind. Eng. Chem. Fundam., **1982**, 21, 236.

183. B. Fixari, V. Abi-Khers, and P. Le Perchec, Nouv. J. Chim., **1984**, 8, 177.

184. M. A. Abraham and M. T. Klein, Ind. Eng. Chem., Prod. Res. Dev., **1985**, 24, 300; Preprints, Div. Fuel. Chem., Amer. Chem. Soc., **1985**, 30(3), 88.

185. M. Z. A. Badr and H. A. H. El-Sherief, Indian J. Chem., **1974**, 12, 1067.

186. D. W. Carson and B. S. Ignasiak, Fuel, **1980**, 59, 757.

187. J. A. Franz, N. K. Suleman, and M. S. Alnajjar, J. Org. Chem., **1986**, 51, 19.

188. J. A. Franz, R. D. Barrows, and D. M. Camaioni, Preprints, Div. Fuel Chem., Amer. Chem. Soc., **1983**, 28(5), 77.

189. B. Fixari and P. le Perchec, Nouv. J. Chim., **1984**, 8, 171.

190. T. Gäumann and J.-M. Rayroux, Helv. Chim. Acta, **1962**, 45, 1563.

191. M. Lutz, J. Chim. Phys., **1969**, 66, 365.

192. E. K. Fields and S. Meyerson, J. Org. Chem., **1969**, 34, 4168.

193. S. E. Stein, Amer. Chem. Soc. Symp. Ser., **1981**, 169, 97.

194. D. T. Allen and G. R. Gavalas, Fuel, **1984**, 63, 586.

195. Y. Kamiya, S. Nagae, and S. Oikawa, Fuel, **1983**, 62, 30.

196. P. J. Cassidy, P. A. Hertan, W. R. Jackson, F. P. Larkins, and D. Rash, Fuel, **1982**, 61, 939.

197. Y. Kamiya, E. Ogata, K. Goto, and T. Nomi, Fuel, **1986**, 65, 587.

198. R. K. Sharma, K. P. Raman, and B. Miller, Fuel, **1986**, 65, 738.

199. K. S. Medepalli and Y. K. Kao, Chem. Eng. Comm., **1981**, 8, 269.

200. C. B. Huang and L. M. Stock, Preprints, Div. Fuel Chem., Amer. Chem. Soc., **1982**, 27(3-4), 28.

201. P. S. Virk, D. H. Bass, C. P. Eppig, and D. J. Ekpenyong, Amer. Chem. Soc. Symp. Ser. 139, **1980**, Chp. 19.

202. A. T. Blades and H. S. Sandhu, Inter. J. Chem. Kinetics, **1971**, 3, 187; W. Tsang, ibid., **1973**, 5, 929; C. Rebick, Adv. Chem. Ser., **1979**, 183, 1.

203. K. E. Gilbert and J. J. Gajewski, J. Org. Chem., **1982**, 47, 4899.

204. K. E. Gilbert, J. Org. Chem., **1984**, 49, 6.

205. C. J. Collins, V. F. Raaen, B. M. Benjamin, P. H. Maupin, and W. H. Roark, J. Amer. Chem. Soc., **1979**, 101, 5009.

206. R. Livingston and H. Zeldes, J. Phys. Chem., **1983**, 87, 1086.

207. R. H. Schlosberg, T. R. Ashe, R. J. Pancirov, and M. Donaldson, Fuel, **1981**, 60, 155.

208. M. M. O'Malley, M. A. Bennett, M. B. Simmons, E. D. Thompson, and M. T. Klein, Fuel, **1985**, 64, 1027.

209. M. T. Klein and P. S. Virk, Ind. Eng. Chem., Fundam., **1983**, 22, 35.

210. M. Z. A. Badr, M. M. Aly, H. A. H. El-Sherief, and A. E. A. Rahaman, J. Appl. Chem. Biotechnol., **1977**, 27, 291.

211. M.-H. Hung and L. M. Stock, Fuel, **1982**, 61, 1161.

212. R. J. Hooper, H. A. J. Battaerd, and D. G. Evans, Fuel, **1979**, 58, 132.

213. J. J. de Vlieger, A. P. G. Kieboom, and H. van Bekkum, Fuel, **1984**, 63, 334.

214. R. G. Mallinson, K. C. Chao, and R. A. Greenkorn, Preprints, Div. Fuel. Chem., Amer. Chem. Soc., **1980**, 25(4), 120.

215. W. P. McPherson, N. R. Foster, D. W. Hastings, J. R. Kalman, and T. D. Gilbert, Fuel, **1985**, 64, 457.

216. W. M. Reed, A. R. Tarrer, J. A. Guin, C. W. Curtis, and D. Gary, Preprints, Div. Fuel Chem., Amer. Chem. Soc., **1984**, 29(5), 83.

217. R. I. McNeil, D. C. Cronauer, and D. C. Young, Proc. Int. Conf. Coal Sci., Dusseldorf, 1981, 410.

218. P. B. Comita, M. R. Berman, C. B. Moore, and R. G. Bergman, J. Phys. Chem., **1981**, 85, 3266.

219. T. Gangwer, D. MacKenzie, and S. Casano, J. Phys. Chem., **1979**, 83, 2013.

220. A. G. Loudon, A. Maccoll, and S. K. Wong, J. Chem. Soc. (B), **1970**, 1733.

221. J. M. L. Penninger, Int. J. Chem. Kinetics, **1982**, 14, 761.

222. K. Takahashi and Y. Ogino, Fuel, **1981**, 60, 975.

223. L. B. Trushkova, R. Z. Magaril, N. V. Korzun, and R. A. Bulatov, Russ. J. Phys. Chem., **1980**, 54, 1062; N. V. Korzun and L. V. Trushkova, Kinetics Catal., **1985**, 26, 195.

224. W. Hillebrand, W. Hodek, and G. Kölling, Fuel, **1984**, 63, 756.

225. P. Bredael and T. H. Vinh, Fuel, **1979**, 58, 211; R. Cyprés and P. Bredael, Fuel Process. Tech., **1980**, 3, 297.

226. W. S. Trahanovsky and K. E. Swenson, J. Org. Chem., **1981**, 46, 2984.

227. M. Bajus and J. Baxa, Coll. Czech. Chem. Comm., **1982**, 47, 1838.

228. G. M. Badger and R. W. L. Kimber, J. Chem. Soc., **1960**, 266; G. M. Badger, R. W. L. Kimber, and J. Novotny, Aust. J. Chem., **1962**, 15, 616.

229. J. M. L. Penninger and H. W. Slotboom, Recl. Trav. Chim. Pays-Bas, **1973**, 92, 513, 1089.

230. B. M. Benjamin, Fuel, **1978**, 57, 378.

231. R. Shaw, D. M. Golden, and S. W. Benson, J. Phys. Chem., **1977**, 81, 1716.

232. J. A. Franz and D. M. Camaioni, Fuel, **1980**, 59, 803.

233. J. A. Franz and D. M. Camaioni, J. Org. Chem., **1980**, 45, 5247.

234. J. A. Franz, R. D. Barrows, and D. M. Camaioni, J. Amer. Chem. Soc., **1984**, 106, 3964.

235. T. Gangwer, Proc. Int. Conf. Coal Sci., Dusseldorf, 1981, 422.

236. M. J. Manka and S. E. Stein, J. Phys. Chem., **1984**, 88, 5914.

237. H.-H. King and L. M. Stock, Fuel, **1980**, 59, 447; H.-H. King and L. M. Stock, Fuel, **1982**, 61, 257.

238. L. M. Stock, J. E. Duran, C.-B. Huang, V. R. Srinivas, and R. S. Willis, Fuel, **1986**, 65, 754.

239. T. C. Brown, K. D. King, and T. T. Nguyen, J. Phys. Chem., **1986**, 90, 419.

240. P. J. Collin, T. D. Gilbert, H. Rottendorf, and M. A. Wilson, Fuel, **1985**, 64, 1280.

241. N. V. Korzun, R. Z. Magaril, L. V. Trushkova, and O. V. Chunikhina, Petr. Chem. USSR, **1980**, 20, 186.

242. G. B. Gill, S. Hawkins, and P. H. Gore, J. Chem. Soc., Chem. Comm., **1974**, 742.

243. A. Heesing and W. Müllers, Chem. Ber., **1980**, 113, 9.

244. H.-H. King and L. M. Stock, Fuel, **1981**, 60, 748.

245. D. T. Allen and G. R. Gavalas, Int. J. Chem. Kinetics, **1983**, 15, 219.

246. J. A. Franz, D. M. Camaioni, R. R. Beishline, and D. K. Dalling, J. Org. Chem., **1984**, 49, 3563.

247. D. C. Cronauer, D. M. Jewell, Y. T. Shah, R. J. Modi, and K. S. Seshadri, Ind. Eng. Chem., Fundam., **1979**, 18, 368.

248. O. L. Chapman and U.-P. E. Tsou, J. Amer. Chem. Soc., **1984**, 106, 7974; W. S. Trahanovsky and M. E. Scribner, J. Amer. Chem. Soc., **1984**, 106, 7976.

249. W. S. Trahanovsky and B. W. Surber, J. Amer. Chem. Soc., **1985**, 107, 4995.

250. D. F. Feller, M. W. Schmidt, and K. Ruedenberg, J. Amer. Chem. Soc., **1982**, 104, 960.

251. L. R. Herndon and E. E. Reid, J. Amer. Chem. Soc., **1928**, 50, 3066.

252. E. Briner, J. Bron-Stalet, and H. Paillard, Helv. Chim. Acta, **1932**, 15, 619.

253. A. Hagemann, Z. Angew. Chem., **1929**, 42, 355, 503.

254. C. Braekman-Danheux and A. Heyvaert, Ann. Mines Belg., **1972**, 37.

255. R. Cypres and B. Bettens, Tetrahedron, **1974**, 30, 1253; **1975**, 31, 359.

256. R. Spielman and C. A. Cramers, Chromatographia, **1972**, 5, 295.

257. M. G. Voronkov, E. N. Deryagina, E. N. Sukhomazova, and L. J. Klochkova, J. Org. Chem. USSR, **1975**, 11, 1116.

258. R. F. Pottie and F. P. Lossing, J. Amer. Chem. Soc., **1963**, 85, 269; E. Hedaya, M. E. Kent, D. W. McNeil, F. P. Lossing, and T. McAllister, Tetrahedron Lett., **1968**, 3415.

259. C.-Y. Lin and M. C. Lin, Int. J. Chem. Kinetics, **1985**, 17, 1025.

260. T. Sakai and M. Hattori, Chem. Lett., **1976**, 1153.

261. C. M. Cawley, Research (London), **1948**, 1, 553.

262. V. Merz and W. Weith, Ber., **1881**, 14, 187.

263. G. R. Clemo, J. G. Cockburn, and R. Spence, J. Chem. Soc., **1931**, 1265.

264. M. L. Poutsma and C. W. Dyer, J. Org. Chem., **1982**, 47, 3367.

265. V. F. Raaen and W. H. Roark, Fuel, **1978**, 57, 650.

266. Y. S. Chauhan and K. B. L. Mathur, Indian J. Chem., **1975**, 13, 38; H. Musso in "Oxidative Coupling of Phenols," W. I. Taylor and A. R. Battersby, Eds.; Marcel Dekker: New York, 1967; Chp. 1.

267. L. R. Mahoney and S. A. Wiener, J. Amer. Chem. Soc., **1972**, 94, 585.

268. D. R. Armstrong, C. Cameron, D. C. Nonhebel, and P. G. Perkins, J. Chem. Soc., Perkin Trans. II, **1983**, 563; D. R. Armstrong, R. J. Breckenridge, C. Cameron, D. C. Nonhebel, P. L. Pauson, and P. G. Perkins, Tetrahedron Lett., **1983**, 24, 1071.

269. W. T. Dixon, W. E. J. Foster, and D. Murphy, J. Chem. Soc., Perkin Trans. II, **1973**, 2124.

270. C. C. Hall, Fuel, **1933**, 12, 419.

271. R. H. Schlosberg and A. Kurs, Preprints, Div. Fuel Chem., Amer. Chem. Soc., **1985**, 30(1), 360; J. Org. Chem., **1984**, 49, 3032.

272. G. Schaden, Liebigs Ann. Chem., **1978**, 559.

273. P. Bredael, T. H. Vinh, and C. Braekman-Danheux, Fuel, **1983**, 62, 1193.

274. R. Cypres, Preprints, Div. Fuel Chem., Amer. Chem. Soc., **1981**, 26(3), 44.

275. H. T. Raudsepp and H. E. Raudsepp, Tr. Tallin. Politekh. Inst. Ser. A, **1967**, No. 254, 35.

276. D. F. McMillen, S.-J. Chang, S. E. Nigenda, and R. Malhotra, Preprints, Div. Fuel Chem., Amer. Chem. Soc., **1985**, 30(4), 414.

277. P. H. Kasai, P. A. Clark, and E. B. Whipple, J. Amer. Chem. Soc., **1970**, 92, 2640; R. P. Johnson, J. Org. Chem., **1984**, 49, 4857; J. Pacansky and D. W. Brown, J. Phys. Chem., **1983**, 81, 1553.

278. B. W. Jones and M. B. Neuworth, Ind. Eng. Chem., **1952**. 44, 2872.

279. C. Braekman-Danheux, C. Delaunois, and N. C. Quyen, Fuel Process. Tech., **1977**. 1, 57.

280. V. V. Platonov, L.N. Ivleva, O. A. Klyavina, and E. E. Prokof'ev, Solid Fuel Chem., **1981**, 15(5), 84; V. V. Platonov, O. A. Klyavina, E. E. Prokof'ev, and L. N. Ivleva, ibid., **1981**, 15(6), 96.

281. G. L. Wells and R. Long, Ind. Eng. Chem., Proc. Des. Develop., **1962**, 1, 73.

282. G. A. Davies and R. Long, J. Appl. Chem., **1965**, 15, 117.

283. R. Cypres, C. Braekman-Danheux, and A. Progneaux, Fuel, **1986**, 65, 1300.

284. P. Zhou and B. L. Crynes, Ind. Eng. Chem., Proc. Des. Develop., **1986**, 25, 898.

285. P. Zhou and B. L. Crynes, Ind. Eng. Chem., Proc. Des. Develop., **1986**, 25, 767.

286. M. T. Klein and P. S. Virk, Preprints, Div. Fuel Chem., Amer. Chem. Soc., **1980**, 25(4), 180.

287. A. Vuori, T. Karinen, and J. B. Bredenberg, Finn. Chem. Lett., **1984**, 89; Chem. Abstr., **1985**, 102, 116367.

288. A. I. Vuori and J. B. Bredenberg, Preprints, Div. Fuel Chem., Amer. Chem. Soc., **1985**, 30(1), 366.

289. R. H. Schlosberg, G. D. Dupre, A. Kurs, P. F. Szajowski, T. R. Ashe, and R. J. Pancirov, Liquid Fuels Tech., **1983**, 1, 115.

290. R. H. Schlosberg, P. F. Szajowski, G. D. Dupre, J. A. Danik, A. Kurs, T. R. Ashe, and W. N. Olmstead, Fuel, **1983**, 62, 690.

291. J. B. Bredenberg and R. Ceylan, Fuel, **1983**, 62, 342.

292. A. J. Colussi, F. Zabel, and S. W. Benson, Int. J. Chem. Kinetics, **1977**, 9, 161.

293. C. J. Collins, W. H. Roark, V. F. Raaen, and B. M. Benjamin, J. Amer. Chem. Soc., **1979**, 101, 1877.

294. V. I. Stenberg, V. R. Srinivas, R. J. Baltisberger, and N. F. Woolsey, J. Org. Chem., **1983**, 48, 1107.

295. N. J. Daly, S. A. Robertson, and L. P. Steele, Aust. J. Chem., **1981**, 34, 343.

296. A. Vuori, Fuel, **1986**, 65, 1575.

297. C. Choi and L. M. Stock, J. Org. Chem., **1984**, 49, 2871.

298. K. R. Brower, Fuel, **1977**, 56, 245.

299. R. H. Schlosberg, A. Kurs, G. D. Dupre, and R. J. Pancirov, Preprints, Div. Fuel Chem., Amer. Chem. Soc., **1985**, 30(1), 379.

300. F. Baronnet and M. Niclause, Ind. Eng. Chem., Fundam., **1986**, 25, 9.

301. R. D. Hei, P. G. Sweeny, and V. I. Stenberg, Fuel, **1986**, 65, 577.

302. V. I. Stenberg and R. D. Hei, J. Org. Chem., **1985**, 50, 1810.

303. V. I. Stenberg and P. G. Sweeny, Ind. Eng. Chem., Fundam., **1986**, 25, 735.

15. FIGURE CAPTIONS

Figure 1--Rate constants for gas-phase homolysis of the central C-C bond in bibenzyl (k_{55}) vs. temperature. Line 1: Arrhenius correlation of Stein and coworkers (Reference 134) based on tetralin-carrier technique. Line 2: Arrhenius correlation of Sato and coworkers (Reference 133) based on tetralin-carrier technique. Line 3: Arrhenius correlation of Petrocelli and Klein (Reference 129) based on rate of formation of toluene with biphenyl diluent. Line 4: Arrhenius correlation of Horrex and Miles (Reference 131) based on rate of formation of toluene. Line 5: Arrhenius correlation of Klabunde (Reference 139) based on rate of disappearance of bibenzyl. Line 6: Rate constants of Louw and Bunk (Reference 144) based on rate of formation of p-methylbibenzyl with p,p'-dimethylbibenzyl diluent. Line 7: Extrapolation of average of lines 1 and 2. Circles: "One-point" rate constants of Poutsma (Reference 128) based on rate of formation of toluene. Square: Rate constant of Livingston and Zeldes (Reference 136) based on ESR assay for benzyl radical in equilibrium with bibenzyl. Triangle: Rate constant of Stein and coworkers (Reference 134) based on VLPP data.

Figure 2--Rate constants for liquid-phase homolysis of the central C-C bond in bibenzyl (k_{55}) vs. temperature. Line 1: Arrhenius correlation of Sato and coworkers (Reference 133) based on tetralin-carrier technique. Line 2: Arrhenius correlation of McMillen and coworkers

(Reference 151) based on tetralin-carrier technique. Line 3: Arrhenius correlation of Stein and coworkers (Reference 134) based on tetralin-carrier technique. Line 4: Arrhenius correlation of Brower (Reference 152) based on rate of formation of toluene at elevated pressure. Line 5: Arrhenius correlation of Cronauer and coworkers (Reference 150) based on hydrogen donor-carrier technique.
Line 6: Arrhenius correlation of Stein and coworkers (Reference 134) in the gas phase based on tetralin-carrier technique (see Figure 1).

Figure 3--Estimated free-energy profile for interconversion of $C_{10}H_{11}\cdot$ radicals. Free-energy levels for radicals based on estimates of $\Delta H^{o}_{f,298}$ and S^{o}_{298} from Reference 234; $\Delta G^{o}_{673} \sim \Delta H^{o}_{298} - (673)\Delta S^{o}_{298}$; i.e., no corrections attempted for $\langle \Delta C_p^{o} \rangle$ terms which are small and tend to cancel. Free-energy levels for transition states based on the following rate constants:
k(**98** ---> **35**) = $10^{11.3}\exp(-9{,}400/RT)\ s^{-1}$ (Reference 234);
k(**98** ---> **97**) = $10^{10.6}\exp(-7{,}300/RT)\ s^{-1}$ (Reference 234);
k(**97** ---> **100**) = $10^{11.8}\exp(-14{,}900/RT)\ s^{-1}$ (Reference 234);
k(**57** ---> **100**) = $10^{11.1}\exp(-18{,}300/RT)\ s^{-1}$ (Reference 187);
k(**57** ---> **58**) = $10^{11.1}\exp(-16{,}300/RT)\ s^{-1}$ (Reference 187). The dotted connection between radicals **35** and **100** represents bimolecular hydrogen abstraction from tetralin with $k_{131} \sim 10^{9.2}\exp(-20{,}100/RT)\ M^{-1}s^{-1}$ (Reference 123) and [tetralin] = 5 M.

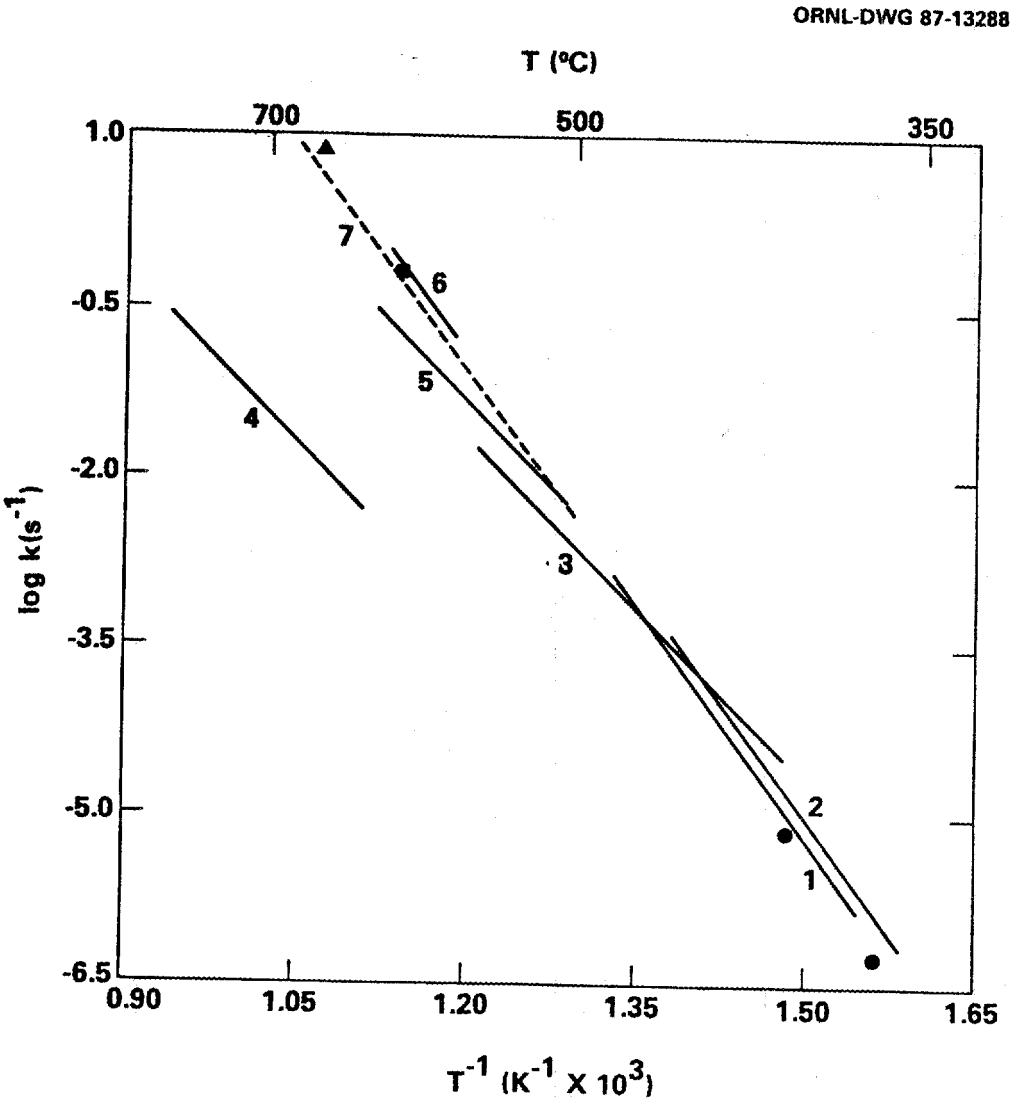
ORNL-DWG 87-13288
T (°C)
700
500
350
1.0
-0.5
-2.0
-3.5
-5.0
-6.5
log k(s^{-1})
0.90
1.05
1.20
1.35
1.50
1.65
T^{-1} (K^{-1} X 10^{3})
1
2
3
4
5
6
7

FIGURE 1

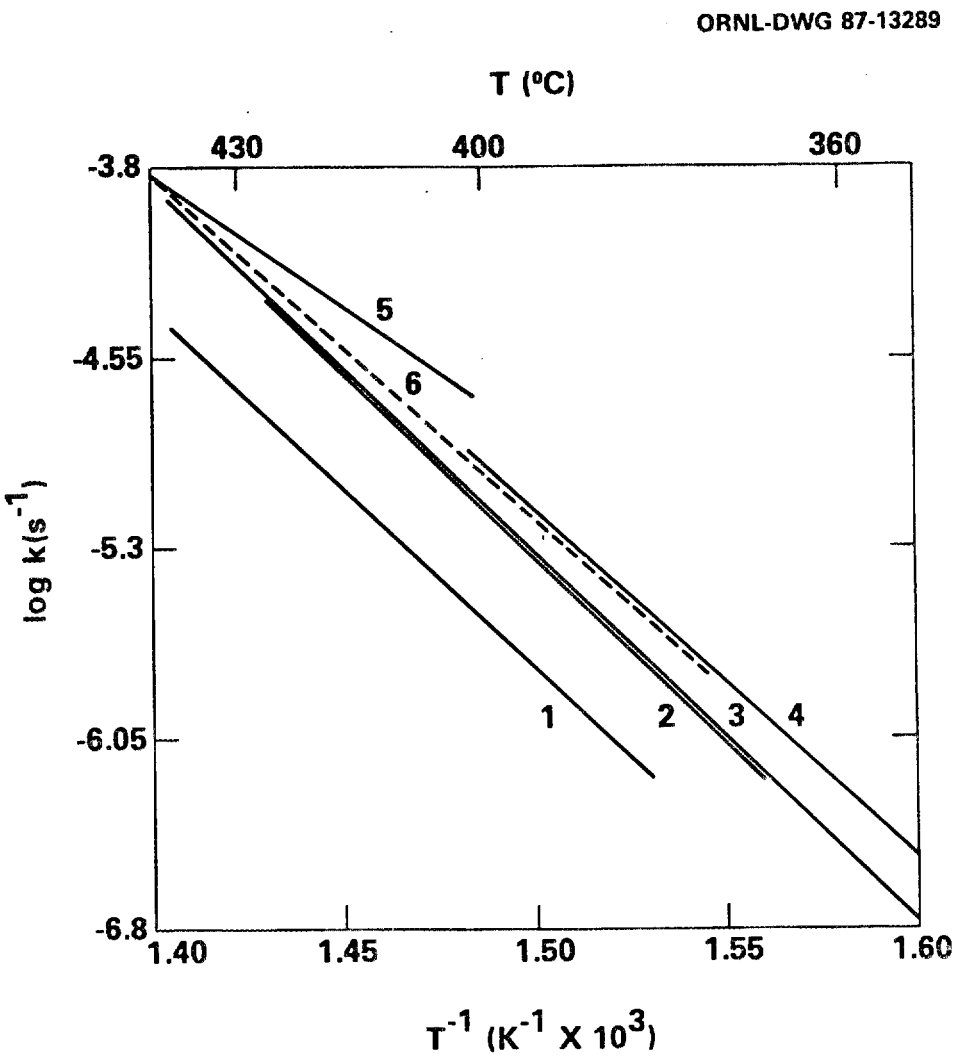
ORNL-DWG 87-13289
T (°C)
430
400
360
-3.8
-4.55
-5.3
-6.05
-6.8
log k(s^{-1})
5
6
1
2
3
4
1.40
1.45
1.50
1.55
1.60
T^{-1} (K^{-1} X 10^{3})

FIGURE 2

ORNL-DWG 87-13290

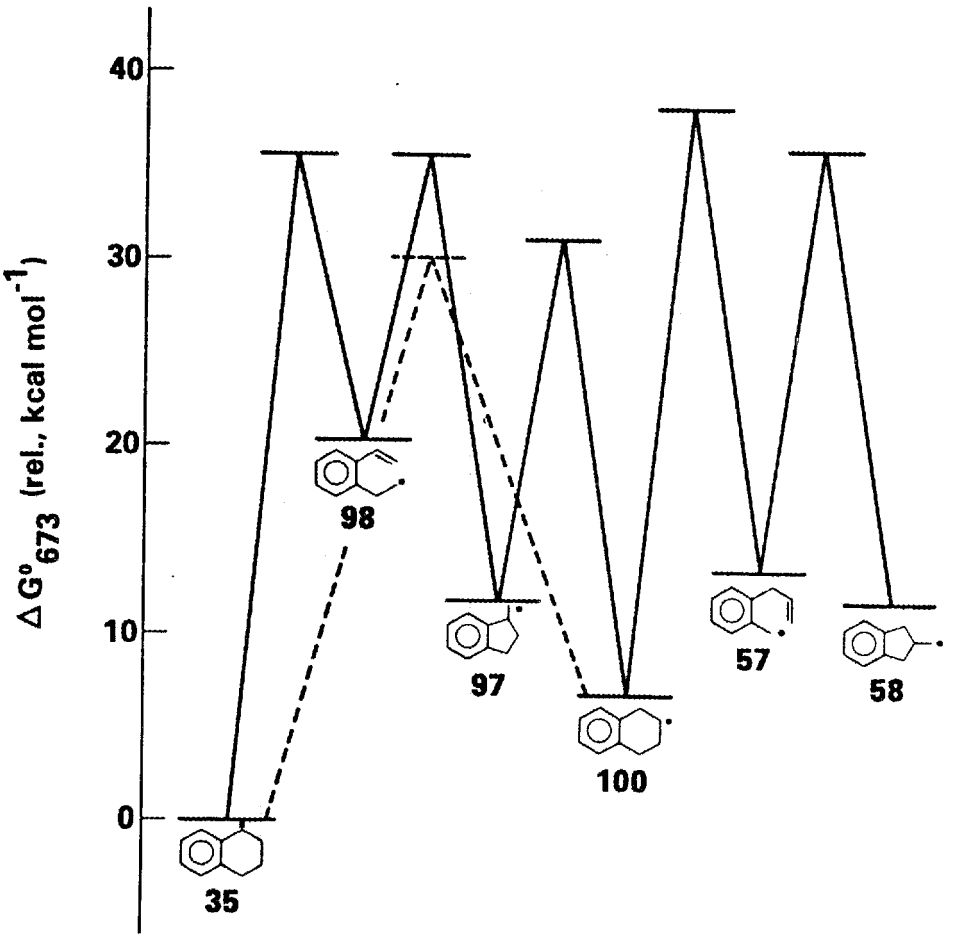

FIGURE 3

INTERNAL DISTRIBUTION

1-15. M. L. Poutsma
16. A. C. Buchanan
17. P. F. Britt
18. A. Zucker
19-20. Central Research Library
21-22. Laboratory Records
23. Laboratory Records, ORNL R.C.
24. ORNL Patent Section
25. ORNL Y-12 Technical Library
Document Reference Section

EXTERNAL DISTRIBUTION

26. Office of Assistant Manager for Energy Research and Development, DOE-ORO, P. O. Box E, Oak Ridge, TN 37831
27-57. Technical Information Center, Oak Ridge, TN 37831